

## Doctoral Program in Optical Engineering

Doctoral Thesis

# STRUCTURAL AND FUNCTIONAL MACULAR INTER-OCULAR ASYMMETRY IN PATIENTS WITH HIGH MYOPIA

Ph.D. Candidate

**Zeyad A. Alzaben**

Directed by:

Dr. Genís Cardona (Department of Optics and Optometry, UPC)

Dr. Miguel Zapata (Department of Ophthalmology, Vall d'Hebron  
Hospital)

Terrassa, Maig 2018





Curs acadèmic:

## Acta de qualificació de tesi doctoral

Nom i cognoms  
Zeyad A. Alzaben

Programa de doctorat  
Enginyeria Òptica

Unitat estructural responsable del programa  
Òptica i Optometria

## Resolució del Tribunal

Reunit el Tribunal designat a l'efecte, el doctorand exposa el tema de la seva tesi doctoral titulada  
STRUCTURAL AND FUNCTIONAL MACULAR INTER-OCULAR ASYMMETRY IN PATIENTS  
WITH HIGH MYOPIA

Acabada la lectura i després de donar resposta a les qüestions formulades pels membres titulars del tribunal, aquest atorga la qualificació:

NO APTE       APROVAT       NOTABLE        
EXCEL·LENT

(Nom, cognoms i signatura)		(Nom, cognoms i signatura)	
President/a		Secretari/ària	
(Nom, cognoms i signatura)	(Nom, cognoms i signatura)	(Nom, cognoms i signatura)	
Vocal	Vocal	Vocal	

\_\_\_\_\_, \_\_\_\_\_ d'/de \_\_\_\_\_ de \_\_\_\_\_

El resultat de l'escrutini dels vots emesos pels membres titulars del tribunal, efectuat per la Comissió Permanent de l'Escola de Doctorat, atorga la MENCIÓ CUM LAUDE:

SÍ       NO

(Nom, cognoms i signatura)		(Nom, cognoms i signatura)	
President/a de la Comissió Permanent de l'Escola de Doctorat		Secretari/ària de la Comissió Permanent de l'Escola de Doctorat	

Barcelona, \_\_\_\_\_ d'/de \_\_\_\_\_ de \_\_\_\_\_



## Summary

*Background and Purpose:* Retinal evaluation performed in the optometry clinic allows optometrists to track the prognosis of retinal disease and to assess anatomical and functional changes related to age and pathological and non-pathological conditions. The purpose of this research was to investigate the normal range of inter-ocular asymmetry in retinal and choroidal thickness and in retinal sensitivity high myopia without ocular fundus manifestations and to determine the relationship between inter-ocular asymmetry and refractive error.

*Methods:* Forty-three patients ( $35.07 \pm 13.31$  years) with high myopia, and 45 healthy participants ( $39.9 \pm 14.1$  years) were administered an ocular coherence tomography and a microperimetry examination to determine retinal and choroidal thickness and retinal sensitivity at the foveal region and at 1, 2 and 3 mm, nasally, temporally, superiorly and inferiorly. Absolute inter-ocular differences were calculated to determine the normal range of asymmetry, in 95% confidence intervals.

*Results:* The choroid was thinner in the myopic group at all explored locations (all  $p < 0.05$ ), with larger absolute inter-ocular differences in most of the choroidal locations under evaluation (all  $p < 0.05$ ). Similarly, retinal sensitivity was reduced in the myopic group, although statistically significant differences were only encountered at the subfoveal location ( $p = 0.001$ ). Retinal sensitivity asymmetry was found to increase with refractive error.

*Conclusion:* The expanded range of retinal and choroidal thickness, as well as retinal sensitivity asymmetry found in high myopia in the absence of disease is of relevance when exploring these patients for early signs of ocular pathology.



## Resumen

*Fundamento y objetivos:* La evaluación de la retina que se realiza en la clínica optométrica permite a los optometristas evaluar el estado de la retina y explorar los cambios funcionales y anatómicos asociados a la edad y a condiciones patológicas y no patológicas. El objetivo de la presente tesis era investigar el rango normal de asimetría inter-ocular en espesor retiniano y corioideo y en sensibilidad retiniana en pacientes con miopía alta sin manifestaciones oculares y determinar la posible asociación entre asimetría y error refractivo.

*Métodos:* Cuarenta y tres pacientes ( $35.07 \pm 13.31$  años) con miopía alta y 45 participantes sanos ( $39.9 \pm 14.1$  años) siguieron un examen con tomografía de coherencia óptica y microperimetría para determinar el espesor de la retina y la coroides y la sensibilidad en retina en la zona foveal y a 1, 2 y 3 mm, en los cuadrantes nasal, temporal, superior e inferior. Se calcularon las diferencias inter-oculares absolutas para determinar el rango normal de asimetría, y los intervalos de confianza al 95%.

*Resultados:* La coroides presento mayor delgadez en el grupo de miopes en todas las zonas sometidas a examen (todas las  $p < 0.05$ ), con mayores diferencias absolutas en términos de asimetría en la mayoría de las zonas exploradas ( $p < 0.05$ ). Igualmente, la sensibilidad retiniana se encontró reducida en el grupo miope, si bien sólo se hallaron diferencias estadísticas en la zona subfoveal ( $p = 0.001$ ). La asimetría en sensibilidad retiniana aumentaba con el error refractivo.

*Conclusiones:* El rango extendido en asimetría en espesor de retina y coroides y en sensibilidad retiniana hallado en miopía alta sin afectación ocular es muy relevante en el momento de explorar estos pacientes para la detección de los primeros signos de patología ocular.





## Acknowledgements

I am honored by the help that I received from my advisors Dr. Genis Cardona and Dr. Miguel Zapata. My advisors helped me in the content writing that made my research to be more informative and full of insight.

Thanks for the help from the clinic personnel at Optipunt Zaben Eye Clinic for aiding in collecting the data that I really required for my research. I am grateful for the voluntary support that they offered. I will be forever grateful.

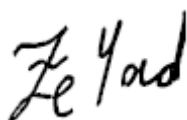
I would also like to express my gratitude to my lecturers Dana N. Koff, Izdihar Alsalman, Mayy Bakkar, Suha Abu Saif, Samah, Abu Mokh, and Areej Otum who ensured that I acquired the right skills that helped me to get to the Bachelor level and through to the Doctorate level.

I cannot also fail to thank my esteemed team in Spain who were industrious in equipping me with competent skills in the Doctorate level: Aurora Torrents, Eulalia Sánchez, Montserrat Morató, Vanesa Budi, Mónica Hernández, Ferran Casals, Dr. Xavier Corretger, Dr. Sanchez Dalmau, the other partners in the Hospital Clínic de Barcelona, and to Dr. Begoña Coco Martin at IOBA.

Moreover, I also want to appreciate the help and compassion that my family members, coordinators, and friends offered to me throughout the period of my dissertation. I was humbled by the motivation of my ever cheerful friends, to Hala Abulwafa, Ayman Bsharat and Osama Ben Zaid who were with me through thick and thin. I would also like to thank Dr. Ahmad Zaben, an ally who was resourceful, giving me the best and the most conducive environment for carrying out my research.

Thanks to Dr. Miguel J. Maldonado, who qualified my skills as a scientific researcher throughout the difficult times in my research. Furthermore, my special thanks go to my former teacher Fatiha Assaf who offered me excellent guidance throughout my research. My deepest gratitude to my close relatives for their love and care, my parents, my sisters Alia & Basmalah, my uncles and my grandparents.

Thanks to All.

A handwritten signature in black ink that reads "Ze Yad". The letters are stylized and cursive.



## List of abbreviations

3D: Three Dimensions	IR: Infrared
ARMD: Age-Related Macular Degeneration	IS: Interior Segment
asb: apostilb	ISNT: Inferior, Superior, Nasal, and Temporal
BCEA: Bivariate Contour Ellipse Area	LASEK: Laser Epithelial Keratomileusis
CCD: Charge - Coupled Device	LASIK: Laser-Assisted In Situ Keratomileusis
cd: candles	LCD: Liquid Crystal Display
CDR or C/D: Cup Disc Ratio	LDF: Laser Doppler Flowmeter
CDVA: Best Distance Corrected Visual Acuity	logMAR: logarithm of the Minimum Angle of Resolution
CS: Central Sensitivity	MAIA: Macular Integrity Assessment
D: Diopter	MP1: Microperimeter-1
dB: decibel	NQ: Nasal Quadrant
EDI: Enhanced Depth Imaging	OCT: Optical Coherence Tomography
ELM: External Limiting Membrane	OD: Oculus Dexter
EPILASIK: Epipolis Laser In Situ Keratomileusis	OFDI: Optical Frequency Domain Imaging
ETDRS: Early Treatment Diabetic Retinopathy Study	ONL: Outer Nuclear Layer
FD: Fourier Domain	OPL: Outer Plexiform Layer
GCL: Ganglion Cells Layer	OS: Oculus Sinister
ICGA: Indocyanine Green Angiography	P1: first point of fixation
ILM: Internal Limiting Membrane	P2: second point of fixation
IML: Intermediate Line	perc.: percentile
INL: Internal Nuclear Membrane	PRK: PhotoRefractive Keratectomy
IPL: Internal Plexiform Layer	PRLs: Preferred Retinal Loci
IQ: Inferior Quadrant	

Rho: Spearman coefficient of correlation

RNFL: Retinal Nerve Fibres Layer

RPE: Retinal Pigmented Epithelium

S1: Sensitivity at the first ring

S2: Sensitivity at the second ring

S3: Sensitivity at the third ring

SAP: Standard Automated Perimetry

SD: Standard Deviation

SE: Spherical Equivalent

SLO: Scanning Laser Ophthalmoscope

SPSS: Statistical Package for the Social Sciences

SQ: Superior Quadrant

t: thickness

TD: Time Domain

TQ: Temporal Quadrant

TSLO: Tracking Scanning Laser Ophthalmoscope

V: version

VA: Visual Acuity

Z: Wilcoxon coefficient



## Contents

1. Information relating to the thesis .....	8
2. Introduction .....	9
3. State of the art .....	13
3.1 High Myopia .....	13
3.1.1 Definition.....	13
3.1.2 Epidemiology.....	14
3.1.3 Physiopathology.....	15
3.1.4 Clinical Characteristics of pathological myopia.....	16
3.1.5 Treatment .....	21
3.2 Optical Coherence Tomography (OCT).....	23
3.2.1 Fundamental Concepts. The macula.....	23
3.2.2 History .....	27
3.2.3 Physical Basis.....	27
3.2.4 Types of OCT .....	29
3.2.5 Clinical Protocols of the OCT.....	35
3.2.6 Measuring the Ocular Fundus Parameters Using OCT.....	35
3.3 Microperimeter (Fundus Related Perimeter).....	55
3.3.1 Fundamental Concepts .....	55
3.3.2 History .....	56
3.3.3 Physical Bases in Brief .....	56
3.3.4 Types of microperimeter.....	58
3.3.5 Microperimetry Measurements.....	59
3.3.6 Microperimeter Evaluation in Association with OCT .....	62
4. Objectives, Justification and Hypotheses.....	65
4.1 General Objective.....	65
4.2 Specific Objectives.....	66
5. Material and Methods.....	71
5.1 Patients.....	71
5.2 Methodology and Instrumentation.....	72
5.2.1 Optical Coherence Tomography .....	74
5.2.2 MAIA™ Microperimeter (Macular Integrity Assessment) .....	78

5.3 Statistical Analysis .....	85
6. Results and Discussion .....	87
6.1. Measuring retinal thickness asymmetry using SD-OCT in normal patients: .....	87
6.2. Measuring choroidal thickness in normal patients using the enhanced depth imaging (EDI) technique of the SD – OCT:.....	97
6.3. Exploring retinal (macular) sensitivity differences between both eyes in normal patients:.....	102
6.4 Measuring retinal thickness asymmetry using SD-OCT in patients with high myopia.....	108
6.5 Measuring choroidal thickness in patients with high myopia using the enhanced depth imaging (EDI) technique of SD – OCT:.....	116
6.6 Exploring the inter-ocular asymmetry of macular sensitivity in patients with high myopia:.....	123
6.7 Analysing the relationship between structural and functional changes in patients with high myopia:.....	131
7. CONCLUSIONS .....	137
8. Future Research .....	141
9. Works Derived From the Thesis .....	143
10. References.....	145
11. Annexes.....	167

## 1. Information relating to the thesis

- Title of the thesis

**Structural and functional macular inter-ocular asymmetry in patients with high myopia**

- Ph.D. Candidate

**Zeyad A. Alzaben**

- Thesis directors

**Dr. Genís Cardona Torradeflot** (Department of Optics and Optometry, Universitat Politècnica de Catalunya)

**Dr. Miguel Zapata Victori** (Department of Ophthalmology, Vall d'Hebron Hospital)

- Institution

**Universitat Politècnica de Catalunya (UPC)**

- Dedication

**Full-time**







## 2. Introduction

A comprehensive evaluation of vision should not only include the routine optometric assessment commonly conducted by eye care practitioners. In addition, tests such as retinal evaluation, visual field examination and retinal sensitivity exploration should also be performed and the corresponding inter-ocular differences should be assessed and compared with functional vision (Takahashi et al., 2012).

The choroid is a connective tissue or layer that is located between the sclera and the retina and is considered the main vascular layer of the eye. The main function of the choroid is nourishment of the fundus or posterior pole. The choroid is connected anteriorly with the ciliary body and posteriorly with the edges of the optic nerve. Choroidal appraisal using ocular coherence tomography (OCT), particularly using enhanced depth imaging technique or EDI, has been an emerging investigative topic for the past couple of years. Researchers have devoted efforts to study choroidal thickness in normal eyes, in addition to the thickness of the choroid in some progressive pathological ocular conditions such as in cases of pathological myopia (Benmerzouga Mahfoudi et al., 2015).

However, among these studies conducted on the choroid, only one study was devoted to exploring the physiological asymmetries and variations of choroidal thickness seen in normal patients (Ruiz-Medrano et al, 2015). As far as we know, no previous research has been conducted to evaluate the variations and asymmetries of choroidal thickness seen in patients affected with high myopia.

**High myopia** is a condition with significant social and economic consequences (Saw et al., 2005). When it leads to pathological myopia it is considered one of the main causes of blindness in the developed countries, mainly affecting young adults at working age (Gallego-Pinazo and Díaz-Llopis, 2011; Wong et al., 2014).

High myopia is associated with diverse structural changes in the eye, including thinning of both the retina and the choroid (Flores-Moreno et al., 2013; Honjo et al., 2015; Ikuno and Tano, 2009; Kawaguchi et al., 2014; Michalewski et al., 2014; Ohno-Matsui and Yoshida, 2015; Vincent et al., 2013; Wong et al., 2015).

However, the relationship between these structural changes, eye functionality and changes in vision in these patients is still unclear (El Matri et al., 2012; El Matri et al., 2013; Flores-Moreno et al., 2013; Zaben et al., 2015). Thus, from a clinical perspective, understanding the nature and degree of association between morphological changes and retinal function in patients with high myopia is of vital importance since these elements can affect the course of the condition and play a key role in its treatment.

Since the introduction of high-resolution OCT, a number of studies have analyzed retinal and choroidal thickness in normal patients (Adhi et al., 2014; Branchini et al., 2013; Hirata et al., 2011; Karapetyan et al., 2016; Matsuo et al., 2013; Nagasawa et al., 2013; Park and Oh, 2013; Rossou et al., 2014; Ruiz-Medrano et al., 2015; Spaide et al., 2008; Tuncer et al., 2015; Wang et al., 2015), and in patients with macular alterations such as retinitis pigmentosa (Battu et al., 2015), glaucoma (Dagliesh et al., 2015; Um et al., 2012), diabetes (Virgili et al., 2015), and age-related macular degeneration (Miyake and Tsunoda, 2015; Van Bol and Rasquin, 2014), but few researches have been conducted on patients with high or pathological myopia (Chen et al., 2012; Nishida et al., 2012).

The most predictive factors of visual acuity in patients affected by high myopia without any macular pathology have been described as: subfoveal choroidal thickness, mean macular choroidal thickness and external retinal thickness (Flores-Moreno et al., 2013; Nishida et al., 2012).

Likewise, few studies have assessed retinal sensitivity of patients with highly myopic eyes; in fact, at the time of writing this thesis the only published research on the correlation between functional and morphological parameters in high myopia consists of preliminary studies presented at various meetings (Alluwimi et al., 2014; Choi et al., 2014; Field et al., 2014; Yamashita et al., 2014; Zaben et al, 2015). Indeed, the standard visual function assessment is routinely conducted using simple visual tests, such as the visual acuity test, and other psychophysical tests, such as the Amsler grid test to evaluate central vision. Other tests to determine the health of the macular area are contrast sensitivity, electroretinography, electro-oculography, and visual evoked potentials (VEP). However, in order to assess the correlation between the functional and structural changes in the retina in health and disease microperimetry is an excellent new tool (Zaben et al, 2015). In effect, fundus - related perimetry (microperimetry) is capable of quantitative assessment of the visual field sensitivity at any point of the retinal surface with a direct imaging of the fundus. For this purpose, it employs an infrared camera and perimetric testing techniques to track the stimulus, thus overcoming the non - foveal fixation problem. Also, this technique may be used in cases of poor fixation stability (Battaglia Parod et al., 2015).

The **main goal of this study** was to investigate **inter-ocular asymmetries** in retinal and choroidal thickness in the macular area and to evaluate the correlation between choroidal thickness and macular sensitivity, as measured with the aid of a microperimeter, in eyes of patients with high myopia, and to compare the results with those of a sample of age-matched healthy eyes. In addition, the association between functional and anatomical inter-ocular asymmetry and refractive error was explored to determine whether the same range of normality commonly accepted for normal patients may also be considered valid in high myopia.



### **3. State of the art**

In this chapter we will describe high myopia, its epidemiology, and the most common clinical complications associated with the condition. Also, the instrumentation employed to explore the anatomical and functional parameters of the retina and choroid will be introduced and the correlation between anatomical and functional parameters will be briefly discussed in the case of patients with high myopia.

#### **3.1 High Myopia**

##### **3.1.1 Definition**

High myopia is characterized by a progressive elongation of the anterior-posterior axis of the eye after its full growth, subsequently leading to anatomical changes in the sclera, choroid and retina, resulting in a significant thinning in these ocular structures. The refractive error in high myopia is by definition above 6.00 dioptres, and the axial length of the eye is more than 26 mm (Chen et al., 2012; Ohno-Matsui and Yoshida, 2015; Saw et al., 2005; Wong et al., 2015).

Besides the term 'High Myopia', there are some other terms that are used to describe the condition, such as 'Degenerative' or 'pathological' myopia, which is an eye condition that may lead to many complications and ending up with visual loss (Maduka Okafor et al., 2009; Saw, 2006). Degenerative myopia, as the name implies, leads to degenerative changes in the posterior pole of the eye such as the formation of epiretinal membranes, retinal detachment, macular holes, lacquer cracks, choroidal neovascularization, posterior staphyloma, Fuchs spots, and macular atrophy, by which the visual acuity of patients suffering from the condition is drastically reduced (Flores-Moreno et al., 2013). Likewise, the term "Myopic retinopathy" refers to the degeneration seen in chorioretinal tissues secondary to the elongation and changes in axial length associated to

pathological myopia (Takahashi et al., 2012). Also, pathological myopia is considered the main cause of blindness or low vision in children.

### 3.1.2 Epidemiology

Overall, myopia affects around 1.600 million people worldwide (Figure 3.1) and Spain is no exception, with a percentage of myopia that reached 20-30% of the population in 2011 (Gallego-Pinazo and Díaz-Llopis, 2011; Wong et al., 2014). In turn, myopia is a major ocular problem among children in India (Saxena et al., 2015), amongst other countries, particularly those of South-East Asia, with many cases progressing to pathological myopia (Table 3.1). While the pathogenesis of myopia remains unclear, some co-factors that may play role in its apparition and progression are: genetics, prolonged near work and lack of outdoor activities (Ostadimoghaddam et al., 2014).

The epidemiology of pathological myopia was explored in the study of Wong (Wong et al., 2014). These authors, who concluded that the impact on the visual function of this condition is unclear, noted a higher prevalence among the Chinese population.

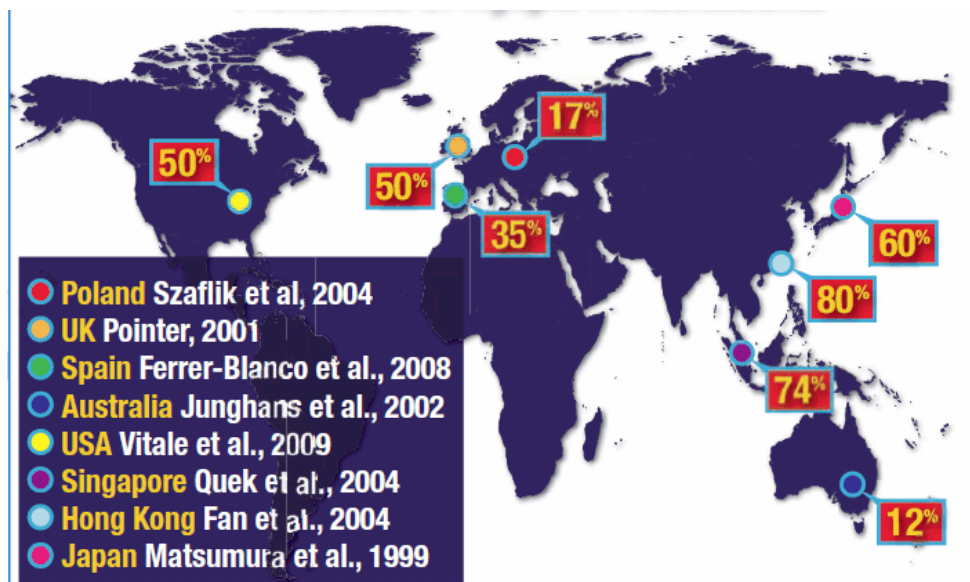


Figure 3.1 Prevalence of myopia in adolescents (From: [www.meniconamerica.com](http://www.meniconamerica.com))



Population	Prevalence of pathological myopia
Urban Australia	0.93%
China	3.10%
Japan	1.74%
Netherlands	0.11%
Palestine	0.03%
USA	0.05%
Italia	0.47%
Spain	0.96%

**Table 3.1** Prevalence of pathological myopia in the general population (Neelam et al., 2012)

The prevalence of pathological myopia in the Spanish population for the year 2011 was 2-3% (943.016 – 1.414.525 individuals) with 1.75 % of them from Catalunya. Of these, 16.9% had an ONCE affiliation.

### 3.1.3 Physiopathology

There is a lack of understanding of the pathophysiology and pathogenesis associated with the changes seen in the macular area and around it in patients with degenerative myopia. As of today, two theories have been adopted by scientists to try to explain the physiopathology of degenerative myopia:

- **The biomechanical theory:** in which the degenerative changes seen in myopia are caused by the excessive elongation of the eye, accompanied by a progressive extension of the posterior pole, presence of a myopic crescent, choroidal thinning, and posterior staphyloma (Bell, 1993; Dirani et al., 2006 ; McBrien et al., 2009).
- **The hereditary (degenerative) theory:** in which, due to highly determined genetics, all choroidal and retinal changes follow a similar process and progression to that observed in cases of choroidal and retinal atrophy. Genetic predisposition is the predominant factor that causes most of the

pathological changes seen in the sclera (Rydzanicz et al., 2011). Choriorretinal degeneration is considered the fourth leading cause of blindness worldwide (Young, 2004).

### **3.1.4 Clinical Characteristics of pathological myopia**

Pathological myopia is associated with secondary changes that affect the sclera, retina, optic nerve head, and choroid, in addition to the fact that it leads to maculopathy, which is the main cause of visual loss associated with this condition (Alkabes et al., 2013; Henaine-Berra et al., 2013; Koh et al., 2013; Nakano et al., 2013; Samarawickrama et al., 2011). It must be stressed, however, that not all patients with high myopia will progress to pathological myopia, and that it remains undisclosed the actual mechanism leading from the former to the later in certain patients.

#### **3.1.4.1 Clinical Signs and Complications**

The **clinical signs** that are detected in the fundus of patients with pathological myopia include: (Benmerzouga Mahfoudi et al., 2015; García-Ben et al., 2014)

- **Myopic cone:** it shows as a myopic optic disc that is inclined and obliquely shaped; the nasal zone has an elevated border and the temporal border is surrounded by a concentric area of pigmentation which gives rise to the term myopic cone or temporal crescent and enables examiners to see the internal surface of the sclera (see **Figure 3.2**). It must be noted that in pathological myopia the choroid must be extended to a point very close to the temporal margin of the optic nerve to form the retinal pigmented epithelium (RPE).

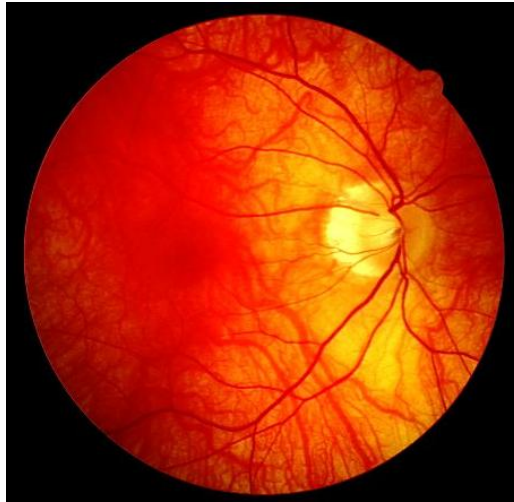


**Figure 3.2** Myopic cone (From: [www1.appstate.edu](http://www1.appstate.edu))

- **Tigroid fundus appearance:** it is caused by diffuse attenuation of the retinal pigmented epithelium that is accompanied by visible main choroidal vessels (**Figure 3.3**).

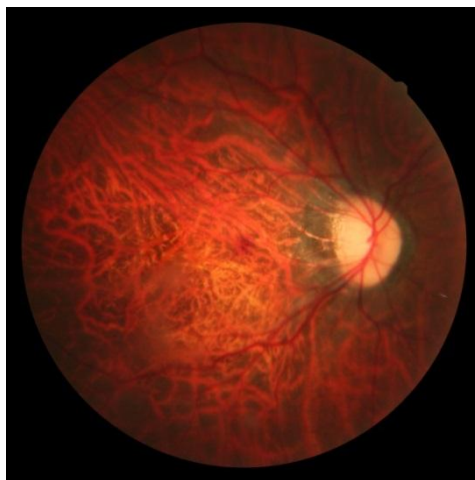


**Figure 3.3** Tigroid fundus in degenerative myopia (From: [usa.nidek.com](http://usa.nidek.com))

- **Focal chorioretinal atrophy:** it is characterized by the progressive visibility of the main blood vessels of the choroid. The sclera, the choroid and the retinal pigmented epithelium show great thinning, generally in the inferior part of the fundus.

- **Lacquer cracks:** it consists of breakages in the RPE – Bruch membrane and choriocapillary membrane complex, which are characterized by fine yellowish coloured irregular lines (**Figure 3.4**).

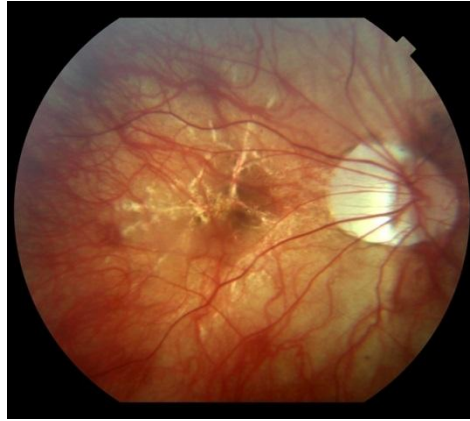


**Figure 3.4** Lacquer cracks (From: imagebank.asrs.org)

- **Myopic sub-retinal neovascular membrane:** it is one of the complications of degenerative myopia that is formed as a result of the presence of lacquer cracks.
- **Nummular sub-retinal haemorrhage:** it may lead to Fuchs spots, which are elevated pigmented lesions, circular in shape and considered as the end products of macular haemorrhages after being absorbed in the retina.

On the other hand, the most frequent **complications** of pathological myopia are: (Chebil et al., 2014; Gómez-Resca et al., 2014)

- **Staphyloma:** it is caused by the extension of the globe and ocular structures, leading to scleral thinning, affecting the posterior pole. It is associated with macular holes (**Figure 3.5**).



**Figure 3.5** Posterior staphyloma (From: [www.kellogg.umich.edu](http://www.kellogg.umich.edu))

- **Rhegmatogenous retinal detachment**: it is associated with the liquefaction of the vitreous, lattice degeneration, macular holes, and occasionally giant retinal tears (**Figure 3.6**).



**Figure 3.6** Rhegmatogenous retinal detachment (From: [dro.hs.columbia.edu](http://dro.hs.columbia.edu))

- **Retinoschisis**: it consists of retinal splitting in two locations. The first separation is produced at the level of the external plexiform layer, while retinal detachment occurs between the retinal neuroepithelial layer and the RPE layer, without the formation or presence of a macular hole (**Figure 3.7**). The vitreous traction in this case can lead to posterior staphyloma, secondary to pathological myopia.

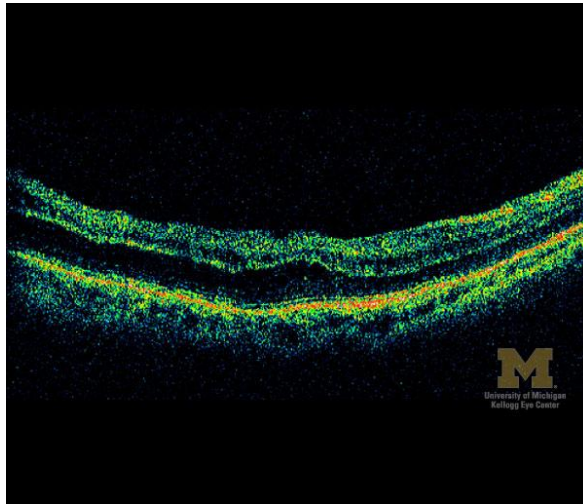


**Figure 3.7** Retinoschisis (From: [www.kellogg.umich.edu](http://www.kellogg.umich.edu))

- **Peripapillary detachment**: it is an asymptomatic orange to yellow elevation of the RPE at the inferior margin of the myopic cone.

#### **3.1.4.2 Symptoms**

Pathological myopia may be associated with one or various of the following symptoms:

- **Decreased visual acuity**, although there was a long-term study which deduced that pathological myopic patients undergoing laser treatment showed no further drop in visual acuity for at least two years following their treatment (Tano, 2002).
- **Scotomas**, or partial loss of vision, which are more common in the superior-nasal quadrant of the visual field among patients with retinopathy (Browning and Lee, 2015).
- **Metamorphopsia**: it occurs as a result of changes in the effective axial length of the eye, leading to distortion in the image perceived. This is considered as one of the main symptoms of pathological myopia (Simunovic, 2015).

- **Decreased nocturnal vision** that occurs consequently with myopia, in which there is a reduction in contrast sensitivity, associated with asthenopia, under low illumination conditions (Gaucher et al., 2007; Lee et al., 2005; Maalej et al., 2014; Morgan et al., 2012).

### **3.1.5 Treatment**

The treatment of pathological myopia aims at improving functional vision, as well as at slowing down the overall progression (Albou-Ganem et al., 2015; Nakagawa et al., 2000; Shen et al., 2015; Qian and Jiang, 2010).

Myopic patients need optical corrections to see clearly, either through the use of a divergent (negative) ophthalmic lens, contact lens, or intraocular lens, to bring the retinal image into focus. Also, other methods of correction consist in reforming the corneal curvature with a laser beam, throughout various surgical refractive procedures such as PRK, LASIK, LASEK, or EPILASIK (Silva, 2012).

The main objective of treatment, however, aims at stopping the progression of posterior staphyloma, thus to try and prevent the loss of vision associated with the condition. However, up to the present date there is no effective treatment to completely prevent or reverse vision loss in patients who suffer from pathological myopia. It must be noted, however, that, as mentioned above, not all patients with high myopia develop pathological myopia.

In particular, in small children, topical atropine has been proved to efficiently delay or slow down the progression and the changes seen in the axial length of the eye. However, there is an increase risk from the light rays which enter the dilated pupil to cause damage to the lens and the retina, so when considering side effects, most patients tend to avoid this method of treatment.

Other attempts at slowing down the progression of the axial elongation and growth of the globe have employed peripheral defocusing techniques (Atchison, 2014; Benavente-Pérez et al., 2014). Alternative recent approaches include

photodynamic therapy, intravitreal injection of antiangiogenic drugs, Pegaptanib sodium injection, Ranibizumab injection and Bevacizumab injection, amongst others.

To conclude this section, **Figure 3.8** displays a summary of the various aspects of pathological myopia discussed above.

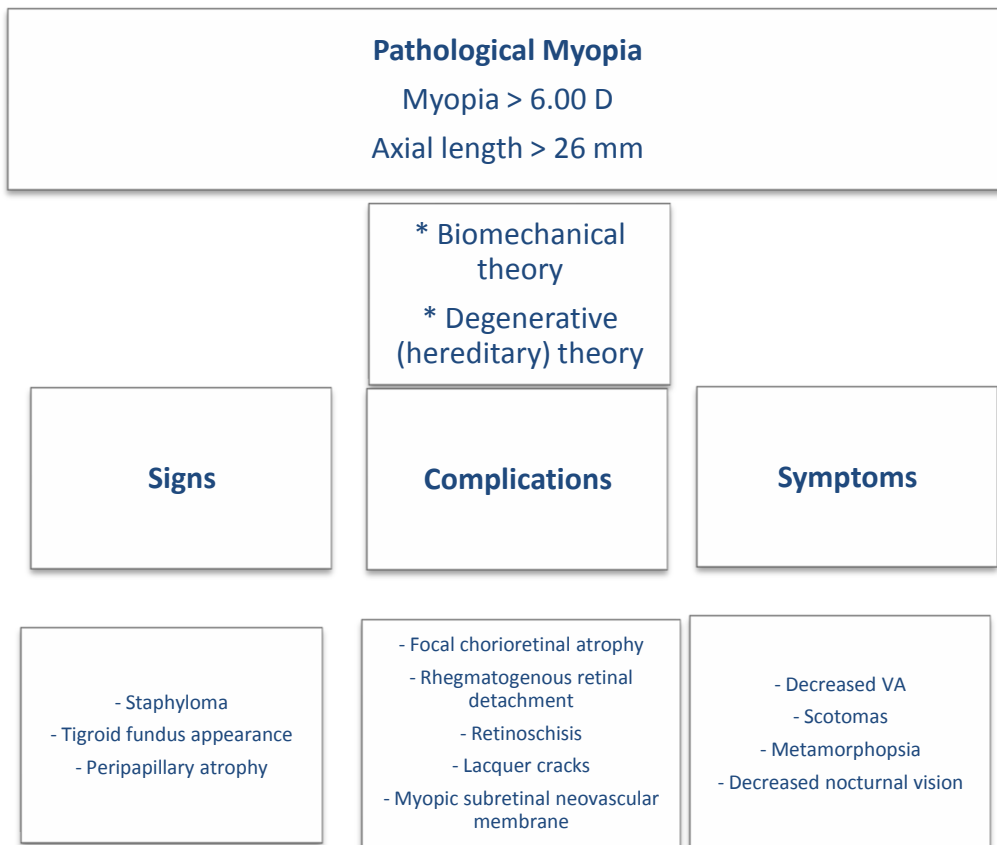


**Figure 3.8** Summary of pathological myopia concepts



## 3.2 Optical Coherence Tomography (OCT)

### 3.2.1 Fundamental Concepts. The macula.

Optical Coherence Tomography is used to assess retinal thickness, specifically at the macula. It is a very useful technique in a clinical setting to diagnose, manage and follow up different ocular pathologies, including progressive myopia (Scott et al., 2000), diabetic retinopathy, macular oedema, retinal dystrophies, macular holes, age-related maculopathy, etc. (Miyake and Tsunoda, 2015; Van Bol and Rasquin, 2014; Virgili et al., 2015).

The macula is the retinal area that is situated at the posterior pole of the eye. It is located temporal to the optic nerve and between the temporal (superior and inferior) arcades. It is approximately 5.5 mm in diameter. The macula covers 20° from the point of fixation of the central visual field. Half of its components consist of ganglion cells, which have central receptive fields that are smaller in size when compared to those in the periphery of the retina.

In turn, the fovea is approximately 1.5 mm in diameter and has a thickness of about 350 microns. It is located central to the macula (see [Figure 3.9](#)) (Chui et al., 2014; Kee et al., 2006).

The fovea has the maximum concentration of cone photoreceptors, but lacks rods and is hexagonal in shape. The macula, specifically at the fovea, has a distinctive, yellowish coloured appearance that is acquired from the presence of xanthophyll carotenoids and zeaxanthin pigments, which can also clearly be seen in the Henle fibre layer, which is entirely made out of cone axons. This pigment prevents the photoreceptors from absorbing the shorter wavelengths of blue light, thus protecting the area from oxidative damage.

In the centre of the fovea there is a minute avascular structure called the foveola, which is 350 microns in diameter, 170 microns in thickness and contains only cone photoreceptors that are easily identifiable by their elongated, thin, external segments (Rajavi et al., 2014; Tenlik et al., 2015).

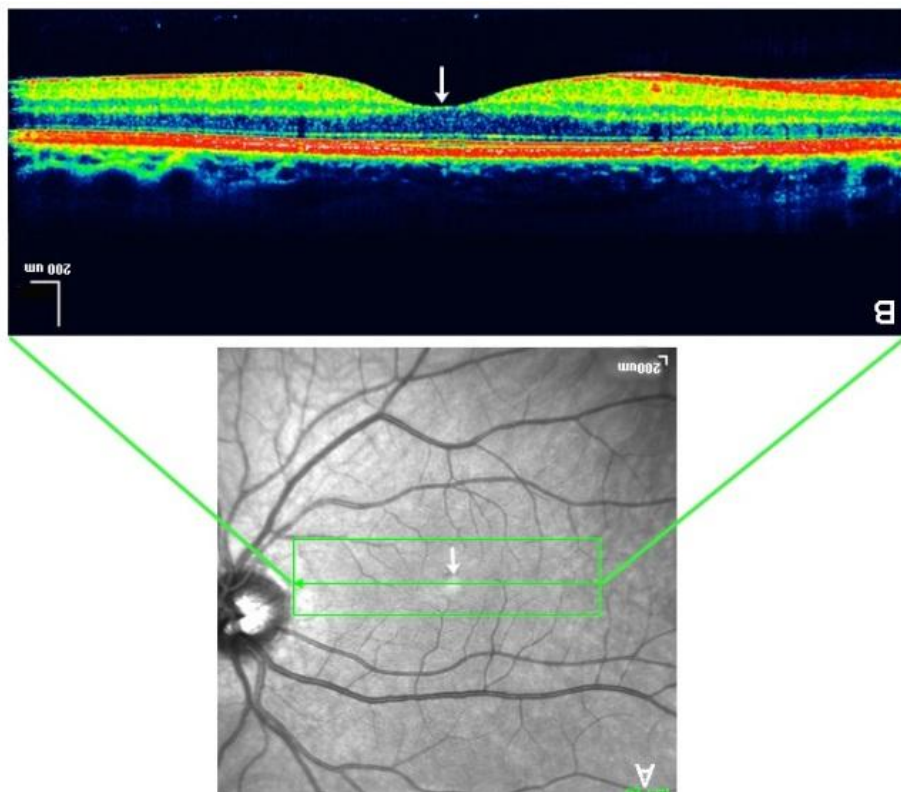


**Figure 3.9** Normal macular area as seen with OCT (From: [webvision.med.utah.edu](http://webvision.med.utah.edu))

The Henle fibre layer consists of cone axons, which are conveyed together in a radial manner to reach the external plexiform layer of the retina. As a result of the displacement of the internal layers of the retina, a depression in the macula is formed which represents the fovea mentioned above. The axial incident light falls down only on the cone photoreceptors found in the macula, specifically the fovea. This anatomical area (depression) in the macula increases its susceptibility for the accumulation of liquids and lipids in cases of macular oedema (see [Figure 3.10](#)) (Zhu et al., 2014).

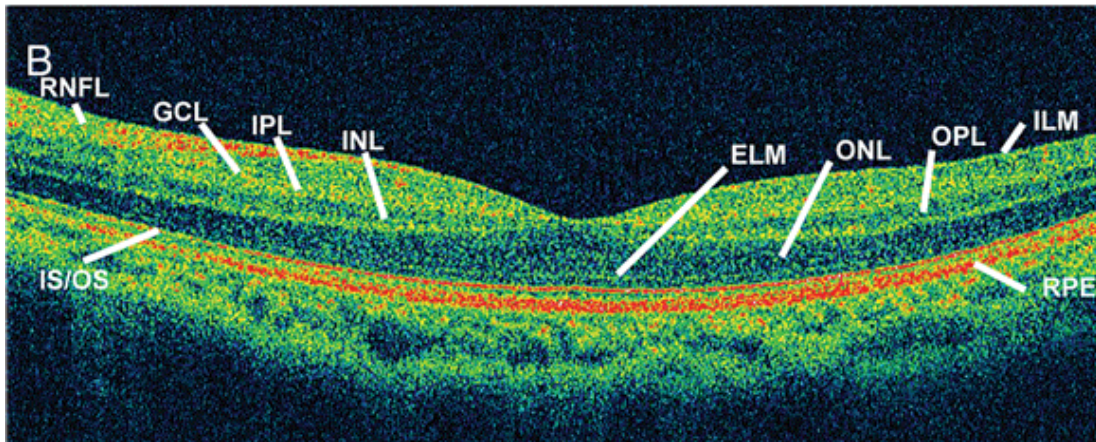


**Figure 3.10** Image obtained with OCT showing all retinal layers. ILM: Internal Limiting Membrane, RNFL: Retinal Nerve Fibres Layer, GCL: Ganglion Cells Layer, IPL: Internal Plexiform Layer, INL: Internal Nuclear Membrane, ELM: External Limiting Membrane, OPL: Outer Plexiform Layer, ONL: Outer Nuclear Layer, RPE: Retinal Pigmented Epithelium, and IS/OS: Internal Segments / Outer Segments of the photoreceptors.

The OCT is an advanced instrument that can analyse different regions or locations in the retina by its scanning ability. It can section images of ocular tissues and help diagnose and follow up any diseases with signs present in the anterior and posterior segments of the eye (Alasil et al., 2013; Knight et al., 2012; Varma et al., 2003).

The OCT utilizes light in the range of infrared wavelengths to obtain a resolution that is equal to 5-10 microns. It scans ocular tissues in a sectional manner depending on the type of OCT being used, through non-dilated pupils of 2.25 – 3.37 mm in diameter. That is, it is a non-invasive real-time method.

In order to understand OCT principles, some fundamental concepts need to be described first:

**A – Scan:** it is a one dimensional form scan, used in ophthalmology to measure the axial length of the eye, which is very effective in calculating the power of the intraocular lens implants in cataract surgery (Yang et al., 2014).

**B – Scan:** it is used to produce two dimensional scans of different ocular structures, mainly to inspect lesions in the posterior segment of the eye. It may also be employed to monitor ocular pathologies such as cataracts, retinal detachment, vitreous disorders, etc. (Aironi and Gandage, 2009).

**Light coherence:** it is the ability of light to produce interference effects, based on the phase-relationship at different locations and in the specific time between two sinusoidal waves of light.

**Low coherence interferometry:** it is an optical technique used to localize the object precisely in an axial position by measuring the delay in time of its echo, which is the technique adopted in optical biopsy and in the OCT (Zhu et al., 2012).

**Spatial resolution:** it determines the clarity of an image ( Liu et al., 2013; Winter et al., 2014).

**Axial resolution:** it is the ability to differentiate between two objects which lie on the same axis.

Albeit the numerous advantages of the OCT retinal imaging system, the technology still has a series of limitations and difficulties: (Arevalo et al., 2009; Chhablani et al., 2014)

1. Incorrect acquisition of retinal image.
2. Incorrect identification of internal and external retina.
3. Degraded image scanning.
4. High sensitivity to ocular movements.
5. Errors induced by opacities in the vitreous.
6. Misalignments.

### 3.2.2 History

The first OCT released for the retina was introduced in 1990 by the Fujimoto team, with the primary results of device efficiency being published in 1991 by D. Huang. The OCT was then enhanced in 1997 by Carl Zeiss and A. Fercher, who performed their first analytical assessment of the images from a diseased retina in 1995. The third generation of this instrument was developed in 2002 and was known as “Stratus OCT” by Zeiss (Carmen A., 2012; Gabriele et al., 2011; Huang et al., 1991; Zysk et al., 2007).

### 3.2.3 Physical Basis

The principles of OCT are based on the ability of the device to capture cross-sectional images of an object with infrared-light (820 nm) in high resolution. The low-coherence interferometry approach measures the difference in reflectivity between the target and the reference beam.

The interferometry part of the instrument consists of a beam splitter, light source and two mirrors. So, as the light source hits the beam splitter, the light follows two pathways. The reflected beam returning from the ocular fundus then recombines with the other beam and interference occurs, depending on the actual distance followed by each light path. Interference patterns are then recorded on a special detector ( [Figure 3.11](#)).

The colours of the retinal images obtained by the OCT are based on the reflectivity of each retinal tissue, giving examiners a tool to detect any abnormality in the image ( [Figure 3.12](#)). Retinal reflectivity of OCT maps is interpreted as follows: (van Velthoven et al., 2007)

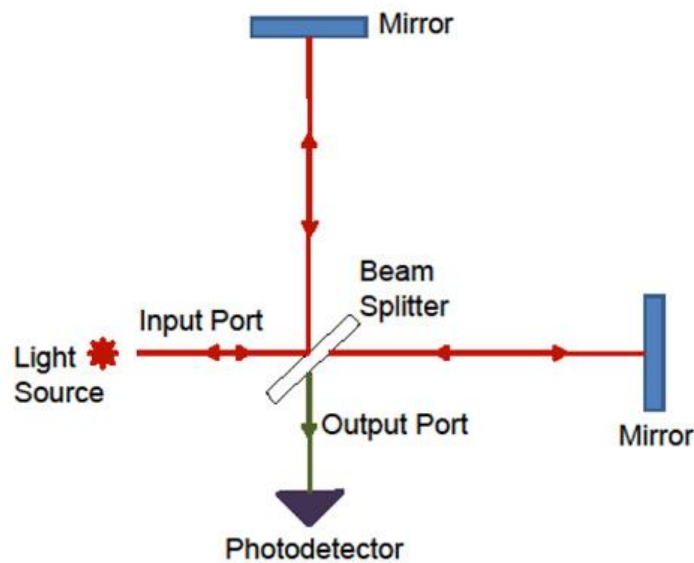


**Figure 3.11** Michelson interferometry  
(From: [www.learner.org](http://www.learner.org))

- The high reflectivity of retinal tissues such as the RPE/ Choriocapillary complex, interior/exterior junction of photoreceptors segment, retinal nerve fibres layer (RNFL) and blood vessels is represented by a red colour.
- The moderate reflectivity of retinal tissues is represented by a yellow-green colour, such as the colour seen in the external limiting membrane (ELM), outer plexiform layer (OPL) and internal plexiform layer (IPL).
- The low reflectivity of retinal tissues such as the outer nuclear layer (ONL), internal nuclear layer (INL) and ganglion cell layer (GCL) is represented by a blue colour.
- Tissues without reflectivity, such as in the vitreous cavity or in cases of a sub-retinal oedema are represented by a black colour.



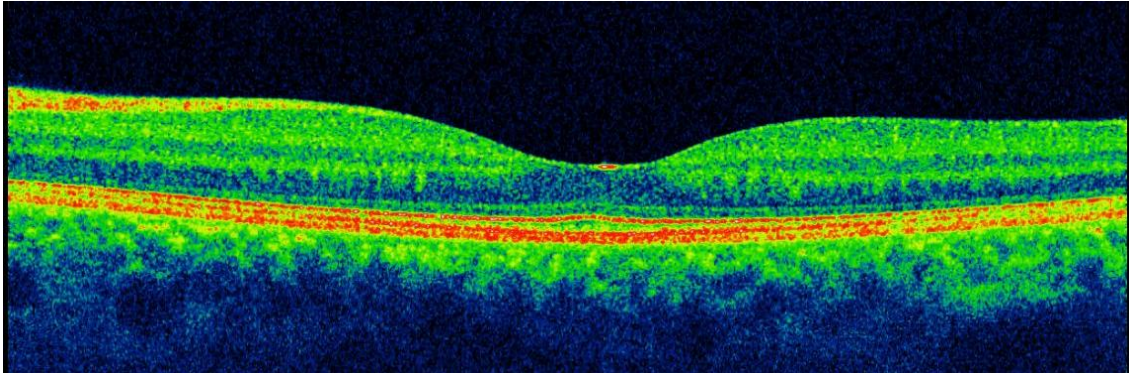


**Figure 3.12** View of the normal macula using spectral domain OCT approach

### 3.2.4 Types of OCT

#### 3.2.4.1 Time-Domain Optical Coherence Tomography (TD-OCT)

Devices based on TD obtain two dimensional images of a scanned tissue, producing A-scans that are gradually captured over time, while representing the reflectivity profile by moving the reference mirror of the interferometer before generating B-scans, as a cross-sectional image. They require a minimal pupil size of 3.2 mm. An example of this instrument is the “Stratus type OCT”, integrated by Zeiss Meditec.

#### 3.2.4.2 Spectral-Domain Optical Coherence Tomography (SD-OCT)

In this type of OCT the depth information is generated and transformed from frequency domain, without using the reference mirror needed for time domain. Thus, images are captured very rapidly, approximately 60 times faster than TD-OCT, while providing high axial resolution. In addition, this type of OCT is capable of reducing the noise at the moment of image acquisition by using two methods when scanning the area targeted in the test: (Adhi and Duker, 2013)

- **Fourier-domain (FD) OCT:** A-scans are obtained by a CCD camera (Charge-Coupled Device) using a wavelength of 840 nm.
- **Swept-source OCT:** it utilizes a longer wavelength at 1050 nm in order to overcome the scattering effect produced by the RPE. In addition, it employs photo-detectors instead of a CCD camera to increase the resolution of the device to around 1 micron, having twice the velocity of FD-OCT up to a 100 thousand A-scans/second. Thus, this device is considered superior and much faster when compared to B-scans.

One of the most commonly employed models of SD-OCT is the 3D OCT-2000 (Topcon, Inc.) (**Figure 3.13**). This is an FD-OCT model with a super luminescent diode light at a wavelength of 840 nm and a scanning speed of 18 thousand cuts/second. The axial and transverse resolution lengths are 6 mm (5 microns) and 20 mm (< 20 microns), respectively, while scanning of the retina is achieved in a box-manner scan, line-scan, radial-scan, and circular-scan in a 3.3 mm diameter pupil.

It must be highlighted that this device may be employed to scan the macula, obtaining 3 dimensional images, using the 512 x 128 protocol (128 line of horizontal scan with 512 A-scans). This instrument will be described and covered in more depth **later on** in section **5.2.1**, as it was the device employed in this study.





**Figure 3.13** Topcon 3D OCT - 2000

Not aiming at exhaustivity, other types of OCT commercially available are:

1. **Spectralis OCT** (Heidelberg Engineering)

This instrument employs confocal scanning laser ophthalmoscopy to examine the optic nerve. The device is designed to acquire 3 dimensional images of the posterior pole including the optic nerve head, with the assistance of a 670 nm diode laser, using two oscillating mirrors to redirect the beam in the x and y axis, perpendicular to Z-axis (optic axis) to obtain 15° x 15° two dimensional images, which are reflected from the retina and utilized by a luminance detector. The axial and transverse resolutions are 300 and 10 microns, respectively. The minimum pupil diameter required to be able to use this device is 2.5 mm (**Figure 3.14**).



**Figure 3.14** Heidelberg engineering OCT (From: [www.optometricmanagement.com](http://www.optometricmanagement.com))

## 2. Cirrus HD-OCT (Zeiss)

This device captures retinal images in real time using SLO (Scanning Laser Ophthalmoscope) with a wavelength of 840 nm, an axial resolution of 5 microns and a capturing velocity of 27 thousand A-scans/second throughout a minimum pupil diameter of 2 mm (**Figure 3.15**).



**Figure 3.15** Cirrus HD-OCT (From: [www.medilexonline.com](http://www.medilexonline.com))

### 3. iVue

This is a portable spectral domain optical coherence tomographer that scans the anterior and posterior segments of the eye in high resolution (5 microns), using A-scan in a rate of 26 thousand A-scan/second, with a traverse resolution of 15 microns, and a wavelength of 840 nm. It requires a minimum pupil diameter of 2.5 mm, while providing a 21° field of view (**Figure 3.16**).



**Figure 3.16** iVue OCT (From: [optovue.com](http://optovue.com))

### 4. Optos OCT SLO

This instrument uses a super luminescent diode source of light with a wavelength of 830 nm, providing an axial resolution of less than 6 microns, a transverse resolution of 20 microns and a 29° field of view (**Figure 3.17**).



**Figure 3.17** Optos OCT SLO (From: [www.medgadget.com](http://www.medgadget.com))

5. **DRI OCT Triton (plus)** – Topcon

This device is based on Swept-Source technology. It uses a wavelength of 1050 nm, with a scanning velocity of 100 thousand A-Scans/second. This instrument offers the possibility of using a monochrome camera for fluorescein angiography. (See **Figure 3.18**)



**Figure 3.18** DRI SS-OCT Triton (plus) – Topcon

(From: [www.topcon-medical.co.uk](http://www.topcon-medical.co.uk))

OCT type	Wavelength (nm)	A-Scans / second (thousand)	Minimum required pupil diameter (mm)	Axial resolution (microns)	Transversal resolution (microns)	Field of view
<b>3D OCT-2000</b>	840	18	3.30	5	<20	45°
<b>Spectralis</b>	670	40	2.50	300	10	15° x 15°
<b>Cirrus HD</b>	840	27	2.00	5	-	-
<b>iVue</b>	840	26	2.50	5	15	21°
<b>Optos</b>	830	-	-	< 6	20	29°
<b>DRI - Triton</b>	1050	100	2.00	-	-	30°

**Table 3.2** Summary of the main characteristics of various OCT devices

### 3.2.5 Clinical Protocols of the OCT

All types of OCTs are mainly used to visualize the retina in order for examiners to automatically explore the fovea and the optic disc, using 3 different protocols:

- **Macular box protocol**, which captures 3-D images of the macula to measure the thickness and volume of this area.
- **Raster line**, which is a B-scan that explores retinal areas rapidly and in high definition.
- **Optic nerve protocol**, which in general emphasizes on glaucomatous features of the optic cup and disc.

### 3.2.6 Measuring the Ocular Fundus Parameters Using OCT

The evaluation of the posterior pole including the retina and the choroid is critical to provide full eye health care needed for patients. This assessment is needed to diagnose, manage, and follow up various ocular conditions, such as: Diabetic retinopathy, macular oedema, macular holes, age-related maculopathy, etc. (Wolf-Schnurrbusch et al., 2009).

#### 3.2.6.1 Measuring the Retinal Thickness Using Spectral - Domain OCT

Optical coherence tomography provides vital information including anatomical details of both the retina and the macula, with a colour coded scale according to the reflectivity of the various retinal tissues.

##### 3.2.6.1.1 Retinal Images in Normal Eyes Using OCT

The measurement of retinal thickness using OCT varies from one model of OCT to the other (time-domain versus spectral-domain), due to differences in the way the outer boundaries of the retina are interpreted (**Figure 3.19**). Nowadays, however, the SD-OCT is considered superior to the TD-OCT (Grover et al., 2010; Seibold et al., 2010; Shin and Cho, 2011).

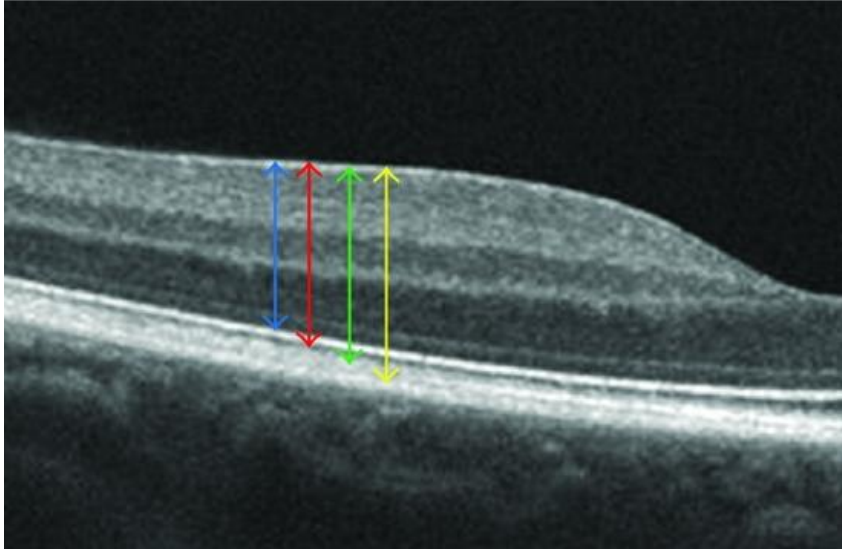


**Figure 3.19** Retinal thickness boundaries using different types of OCT (From: [www.hindawi.com/journals](http://www.hindawi.com/journals))

In the image, the external/internal retinal boundaries can be clearly seen as captured by different types of OCTs: the blue arrow representing the boundary between the internal limiting membrane (ILM) and the internal/external segment junction of the photoreceptors, as seen with a Stratus OCT, while the red arrow demonstrates the boundary between the ILM and the outer segment of the photoreceptors/RPE junction using SD OCT. Similarly, the green arrow shows the boundary between ILM and Verhoeff's membrane using Cirrus OCT, and the yellow arrow displays the retinal boundary between the ILM and Bruch's membrane using Spectralis OCT (Bentaleb-Machkour et al., 2012). Verhoeff's membrane (also known as the intermediate line, or IML) is the site in which the tips of the outer segment of the cone photoreceptors are covered by microvilli (Yamada et al., 2009).

The time-domain optical coherence tomography is able to visualize the retinal nerve fibres layer (RNFL) and the internal/external plexiform layers, but it is incapable of visualizing the RPE, the internal/external retinal layers and the

junction between the outer and the inner segments of the photoreceptors in subjects with ocular pathologies (Rahimy et al., 2013). On the other hand, by using spectral-domain optical coherence tomography the differences between ganglion cells layer (GCL), the interior plexiform layer (IPL), the interior nuclear layer, the external plexiform layer, the external nuclear layer, the external limiting membrane, the internal segment of the photoreceptors, the external segment of photoreceptor, the RPE and Bruch's membrane are easily distinguished ( Krebs et al., 2011; Lim et al., 2014). Thus, TD and SD OCTs should not be considered as interchangeable devices (Vizzeri et al., 2009).

Normal OCT maps include the analysis of the central macular thickness and the macular thickness in the 9 sectors of the ETDRS macular map (Early Treatment Diabetic Retinopathy Study) (Figure 3.20 and 3.21) (Hong et al., 2015; Liu et al., 2011; Song et al., 2010).

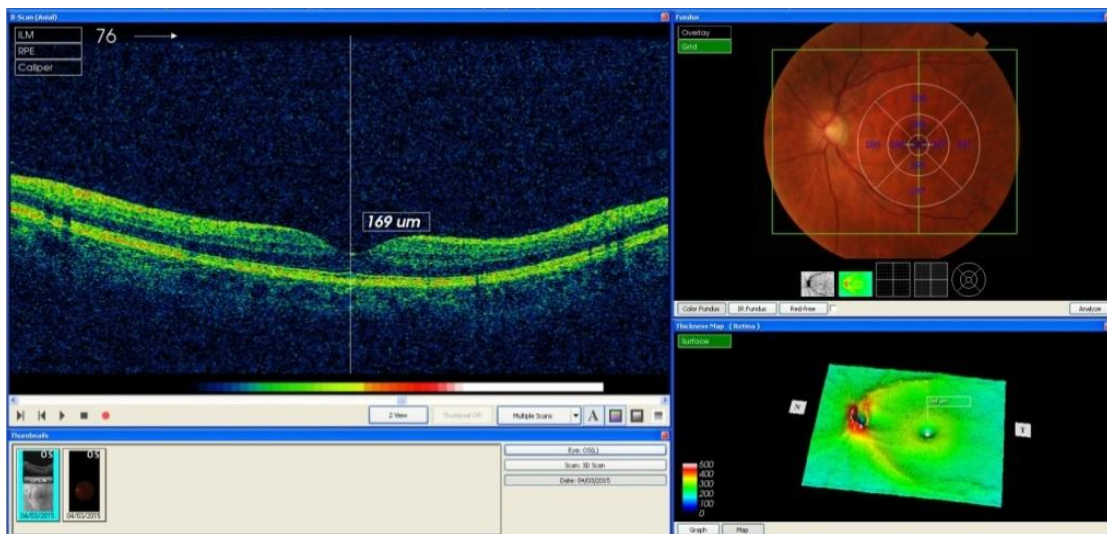


**Figure 3.20** Macula in patient with high myopia. At top right: ETDRS macular map (From: OptRetina)

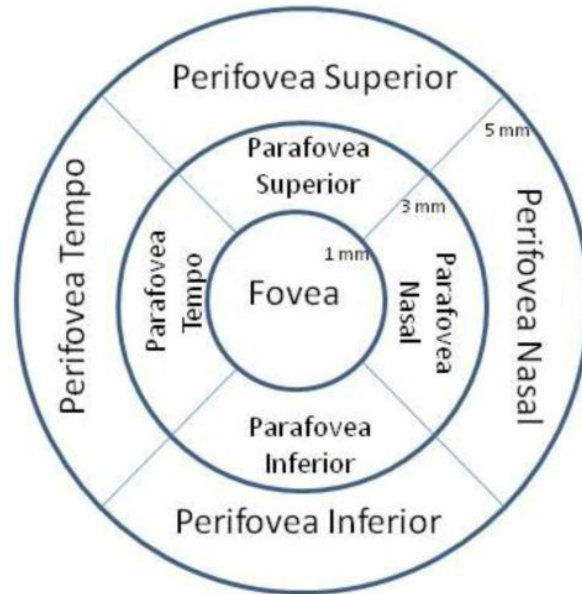


**Figure 3.21** Contour of normal macular area explored by the OCT (From: [www.mdpi.com](http://www.mdpi.com))

Previous studies in healthy subjects have shown an obvious reduction in macular thickness mainly in the central (1 mm diameter) region of the macula and an increased thickness in the para-foveal (3 mm diameter) region, followed by a further reduction in thickness in the peri-foveal part (5 mm diameter) area of the macula (Richer et al., 2012). When divided into four quadrants, retinal thickness measurements obtained from previous studies have shown variations: Nasal quadrant (NQ) > superior quadrant (SQ) > inferior quadrant (IQ) > temporal quadrant (TQ) (LoDuca et al., 2010; Sull et al., 2010; Wang et al., 2012; Zainab Bentaleb-Machkour et al., 2012).

It may be noted, however, that average central macular thickness results vary widely depending on the type of OCT device being used for the measurement. With the OCT-2000 3-D device used in this study, the average central macular thickness in normal subjects was found to be 231  $\mu\text{m}$  (Mehreen et al., 2012). In addition, gender and age also influence macular thickness values. Gender related differences in macular thickness were reported in some of the previous studies, where macular thickness was higher in males than in females, with significant



correlations between the age of normal healthy individuals and macular thickness (Adhi et al., 2012). Also, there is an association between African-American ethnicity and a lower than average foveal thickness (Kashani et al., 2010). This ethnicity is also associated with less progression in axial length growth with age (Hyman et al., 2005).

#### ***3.2.6.1.2 Retinal Image Captured in High and Pathological Myopia Using OCT***

In myopia, a relationship has been observed between the degree of myopic refractive error and retinal thickness, in which as the degree of myopia increases, retinal thickness decreases, especially using the Stratus type OCT (Liu et al., 2014). In a study by Song et al., (2014), which was conducted in Qilu Hospital (Shandong University, China), researchers noted that in high myopia average foveal thickness increased, but that macular thickness in the inner and outer regions decreases. These authors also found that females had higher average foveal thickness, and decreased macular thickness, when compared to males.

Other studies have found that the retina was thicker in patients with high myopia at the fovea and the foveola, and thinner in the inner/outer macular area, with a smaller number of cells at the macula (Wu, et al., 2008). In patients with degenerative myopia, there is a significant decrement in choroidal thickness and in the thickness of the photoreceptors layer in the para-foveal area (Chen et al., 2012). The loss of visual acuity in high myopia is related to the changes seen in sub-foveal choroidal thickness, which is decreased in correlation with the age of the individual and the degree of myopia (Ho et al., 2013).

Similarly, Wu et al described a reduction in the thickness of the macular area in young adults with high myopia, when compared with normal healthy eyes (Wu et al., 2008). Other authors have noted that the average macular retinal thickness of the fovea did not vary with the presence of myopia, while the total volume and the retinal thickness of the para-foveal areas were reduced with an increase in the degree of myopia (Lim and Chun, 2013).

The enhanced depth imaging (EDI) technology using SD-OCT enables examiners to explore the following clinical features in patients with high or degenerative myopia (**Figure 3.22**):

- Elongation of the anterior-posterior axis of the eye.
- The temporal crescent and the oblique optic nerve head.
- Vitreous humour.
- Epiretinal membrane.
- Arteriolar sclerosis.
- EPR thinning.
- Chorioretinal atrophies.
- Lacquer cracks.
- Posterior staphyloma.

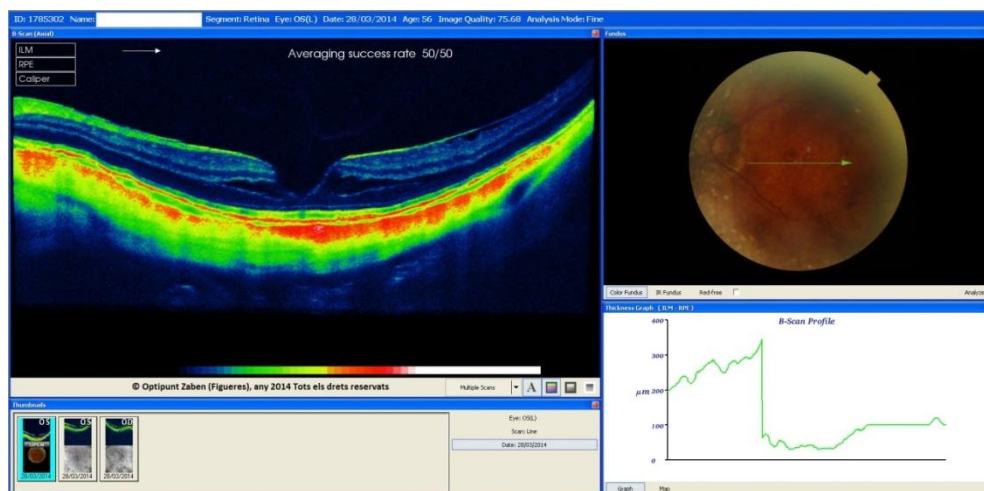


**Figure 3.22** Left eye with pathological myopic macula (From: OptRetina)

### **3.2.6.1.3 Retinal Image Captured in Different Ocular Pathologies Using OCT**

The main application of the OCT device is to check, evaluate, diagnose and follow up macular conditions, such as: Macular edema, macular holes, central serous chorioretinopathy, and age-related macular degeneration, in addition to optic

nerve assessment (Wojtkowski et al., 2009). Some of these applications are discussed next to illustrate the usefulness of this device:

Regarding **age-related macular degeneration (ARMD)**, the OCT device is useful to differentiate between the different types of ARMD and to determine the type of drusen located underneath the hyper-reflective line that represents the RPE layer. Thus, the drusen of the dry type of ARMD are localized below this line as small elevated obscured gaps, forming a geographic atrophy of the RPE, which leads to an ocular condition known as pigmented epithelial detachment (PED) that is accompanied with choroidal neovascularization. However, in the wet type of ARMD the drusen are located above the hyper-reflective line forming an ocular condition known as neuroepithelial detachment (NED) that usually results in the presence of abnormal sub-retinal fluid (Castillo et al., 2014; Gregori et al., 2014) (**Figure 3.23, Figure 3.24, and Figure 3.25**).

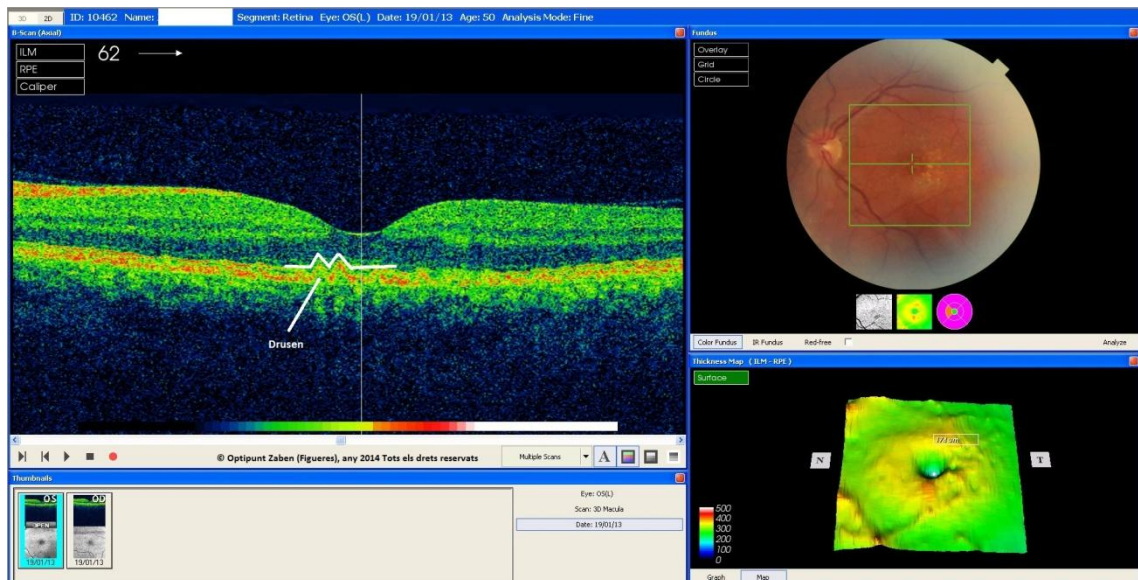


**Figure 3.23** Early ARMD maps (Taken by: The OptRetina)

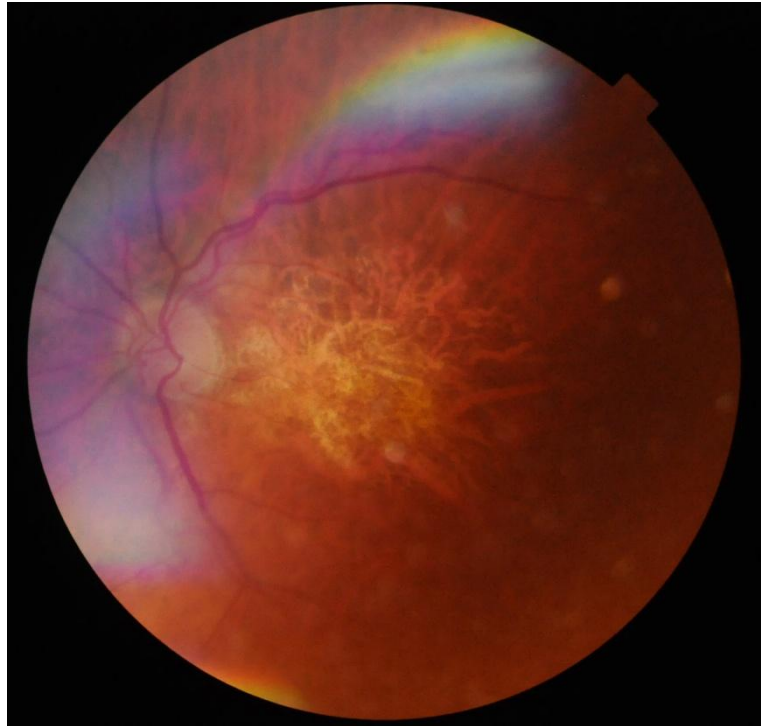


Figure 3.24 Atrophic ARMD (Taken by: The OptRetina)

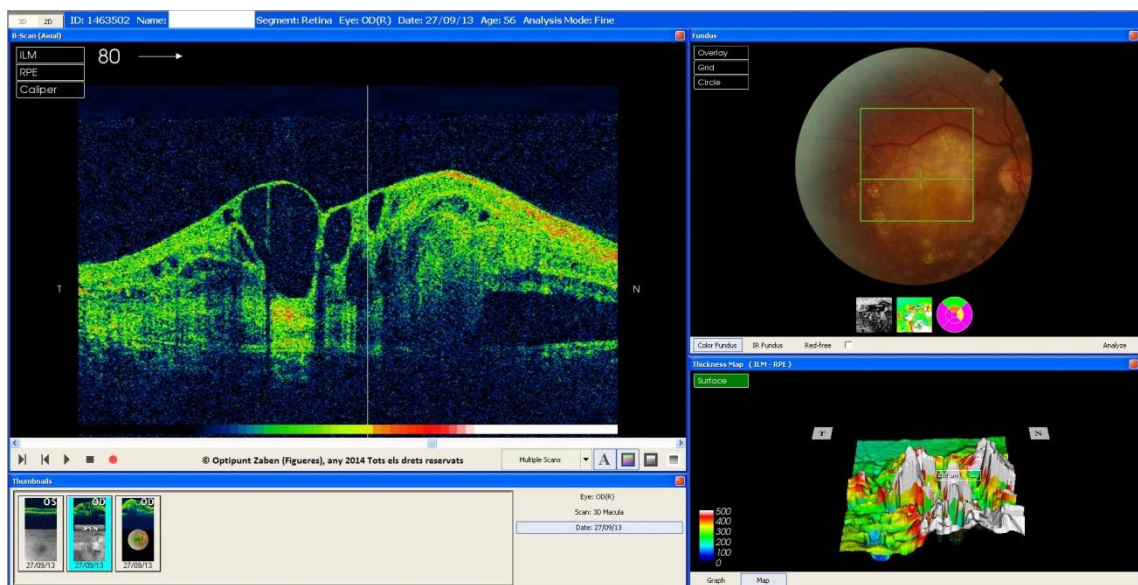
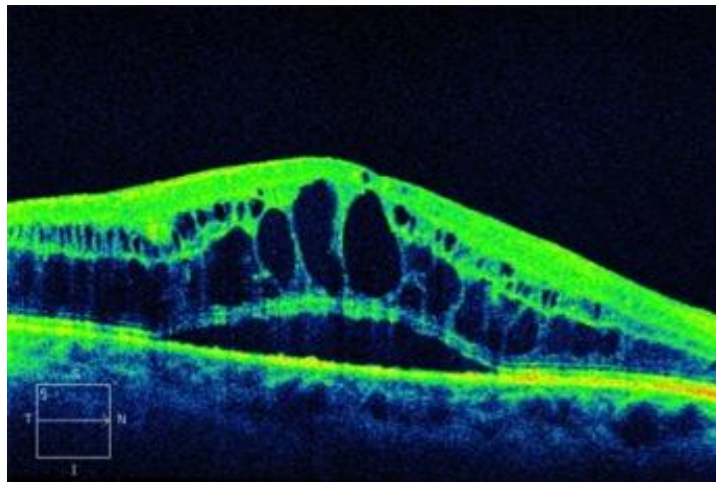


Figure 3.25 Wet exudative type of ARMD maps in the late stage (Taken by: The OptRetina)

OCT assessment is also essential for the early diagnosis of **macular edema** in clinical practice, where there is an increased retinal thickness due to the pressure exerted upward by sub-retinal fluids, which accumulate forming cystic shape gaps, such as in diabetic retinopathy (**Figure 3.26**). Besides, the device is a promising tool in the monitoring and following up of patients undergoing different macular therapeutic procedures or treatments (Koleva-Georgieva and Sivkova, 2010).



**Figure 3.26** Macular edema in diabetic retinopathy (Taken from: [www.drbrendancronin.com.au](http://www.drbrendancronin.com.au))

The OCT scan of a **macular hole** is characterized by symmetrical borders, where the depth of the hole reaches the RPE, and with the visibility of hyaloid detachments (Keane and Sadda, 2011; Ooto et al., 2014) (**Figure 3.27**).



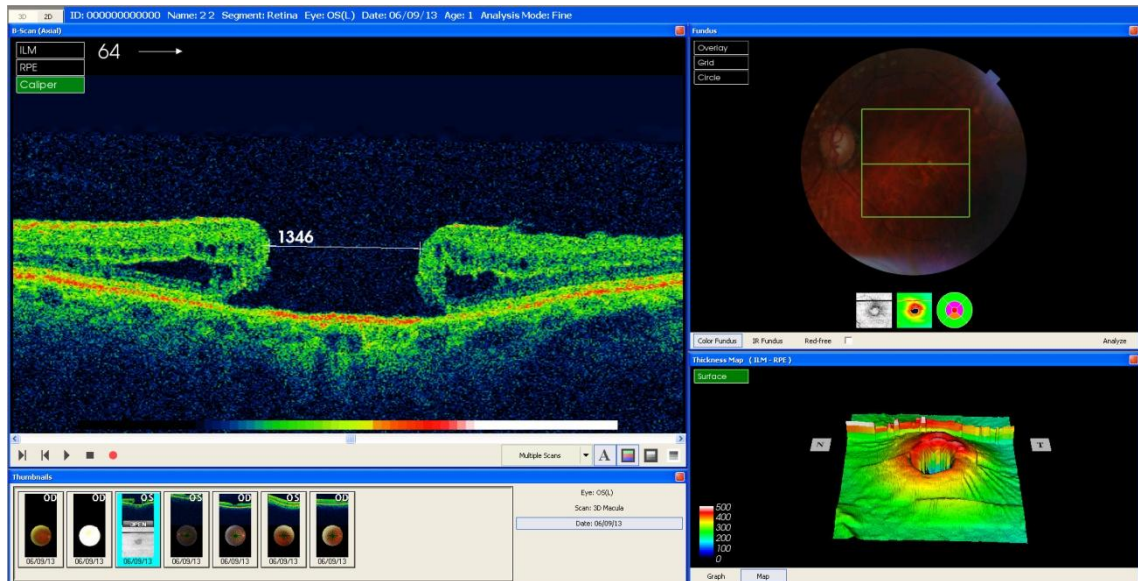


**Figure 3.27** The map of a full-thickness macular hole (Taken by: The OptRetina)

Vitreous traction at the level of the fovea leads to a **lamellar type of macular hole**, which may have asymmetrical borders and may not reach the level of the photoreceptors. The vision in these patients is usually preserved (**Figure 3.28**).

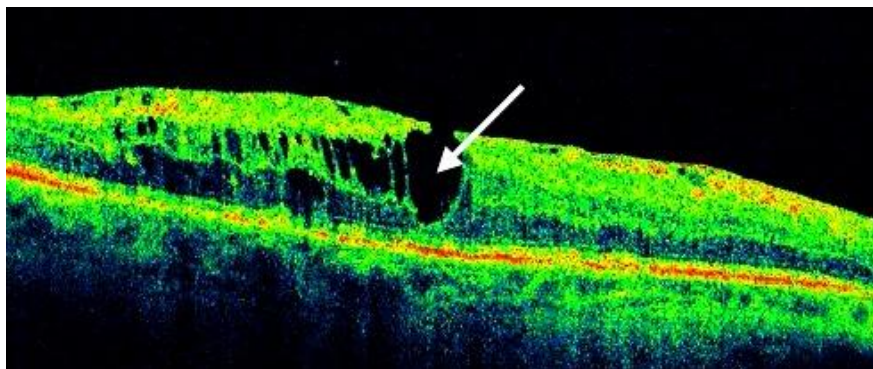


**Figure 3.28** Map of a lamellar macular hole (Taken from: [www.liv.ac.uk](http://www.liv.ac.uk))

Finally, another type of macular hole is called **pseudo-macular hole**, which occurs due to the presence of an epi-retinal membrane at the level of the fovea, altering foveal contour. It is characterized by a small diameter, symmetrical borders hole that does not reach the outer retinal layer, mainly located at the fovea (Borgia and Badalà, 2003) (**Figure 3.29**).

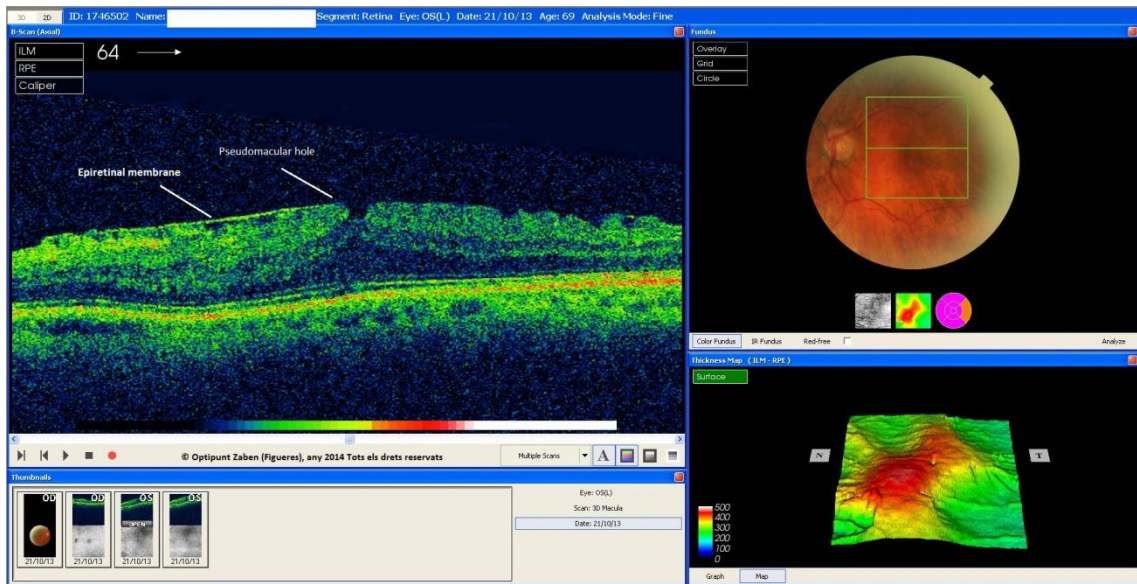


**Figure 3.29** Map of a Pseudo-macular hole (Taken by: The OptRetina)

**Epi-retinal membrane** is a membrane that covers the retina, shown in the OCT scan as an increased retinal thickness at the level of fovea: it is a proliferation and condensation of the posterior hyaloid, which consists of an avascular fibrocellular tissue overlaying the surface of the retina, leading eventually to a foveal-RPE separation (Muraoka et al., 2015) (**Figure 3.30**).

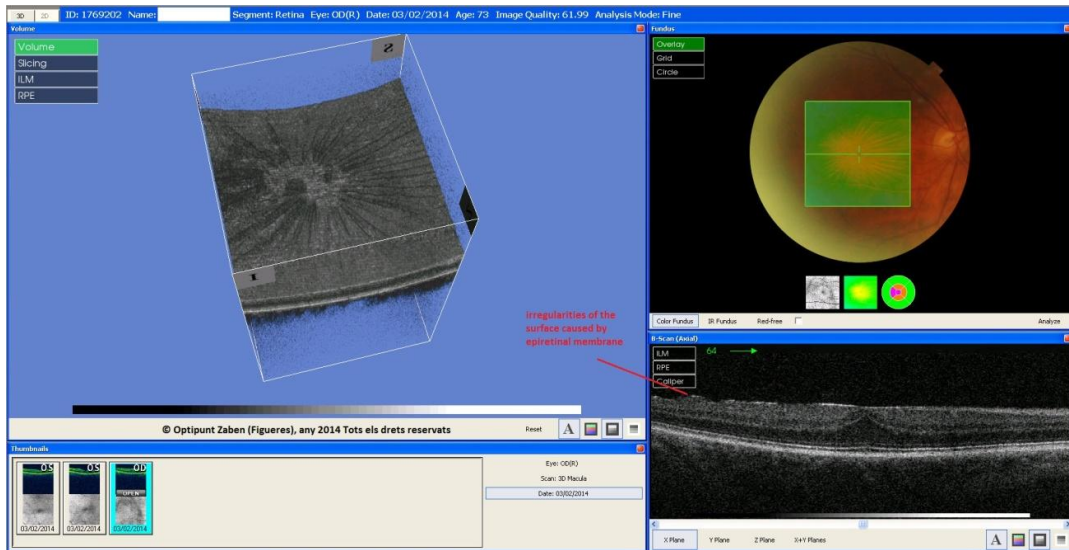


**Figure 3.30** Map of an epi-retinal membrane (Take by: The OptRetina)

The OCT device has also been shown to be useful and effective in the management and treatment of patients who suffer from **central serous chorioretinopathy** (Figure 3.31). This self-limiting condition is typically found in men in their 30s and 50s and is highly associated with heavy weight lifting, corticosteroids use, or chronic stress, and is seen in the OCT maps as an abnormal thickened retina (Ricketti et al., 2015).

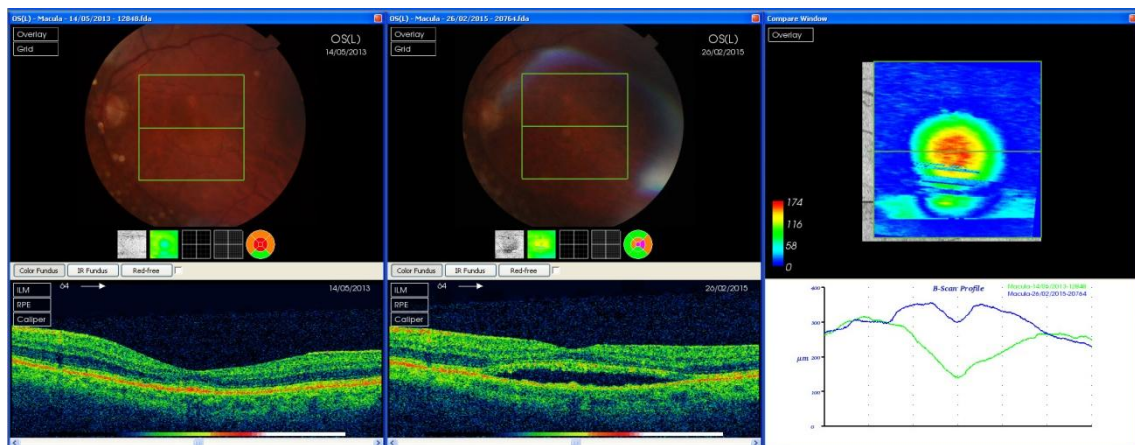


**Figure 3.31** Central serous chorioretinopathy (Taken by: The OptRetina)



### 3.2.6.2 Measuring Choroidal Thickness Using Spectral - Domain OCT

The main function of the choroid, a pigmented vascular structure that extends from the ora serrata (0.10 - 0.15 mm in thickness) to the optic nerve (0.22 mm in thickness), is to nourish the external parts of the retina. Any disruption in the conduction of oxygen from the choroid to the retina may lead to age-related macular degeneration. Besides, the choroid also contains secretory cells, which are involved in the vascularization process and in the growth of other structures such as the sclera (i.e. growth factor secretion). The choroidal limits are shown in [figure 3.32](#) (Maul et al., 2011; Regatieri et al., 2012).

The choroid has also a thermoregulation function and plays a key role in the focusing modulations of the eye, which aids in placing the image in front or behind the retina by adjusting its thickness at the level of the central retina (Nickla and Wallman, 2010).

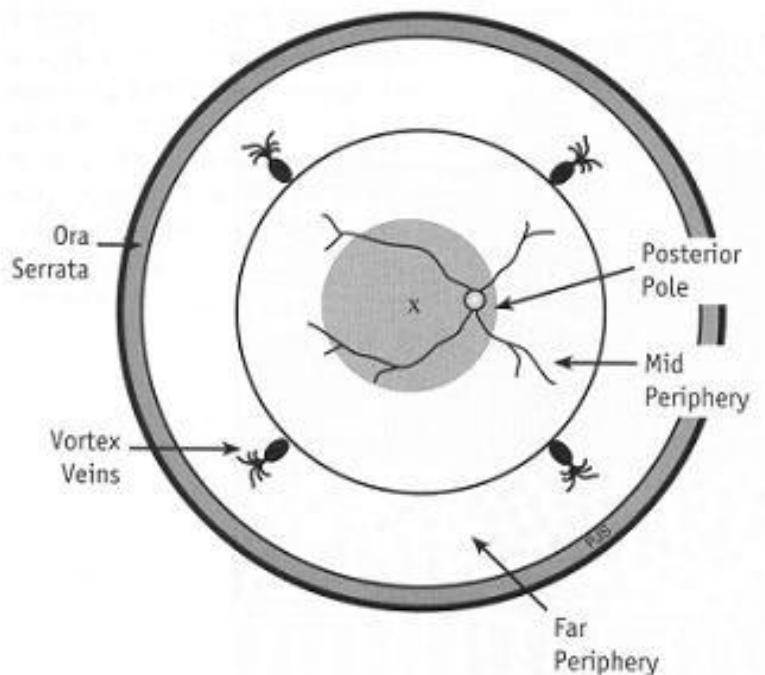


**Figure 3.32** Choroidal limits (From: [www.cybersight.org](http://www.cybersight.org))

The choroidal layers are: (Figure 3.33)

1. Epichoroid (Haller's layer), the outermost layer.
2. Vascular layer (Sattler's layer).
3. Choriocapillaris.
4. Bruch membrane, the innermost layer.

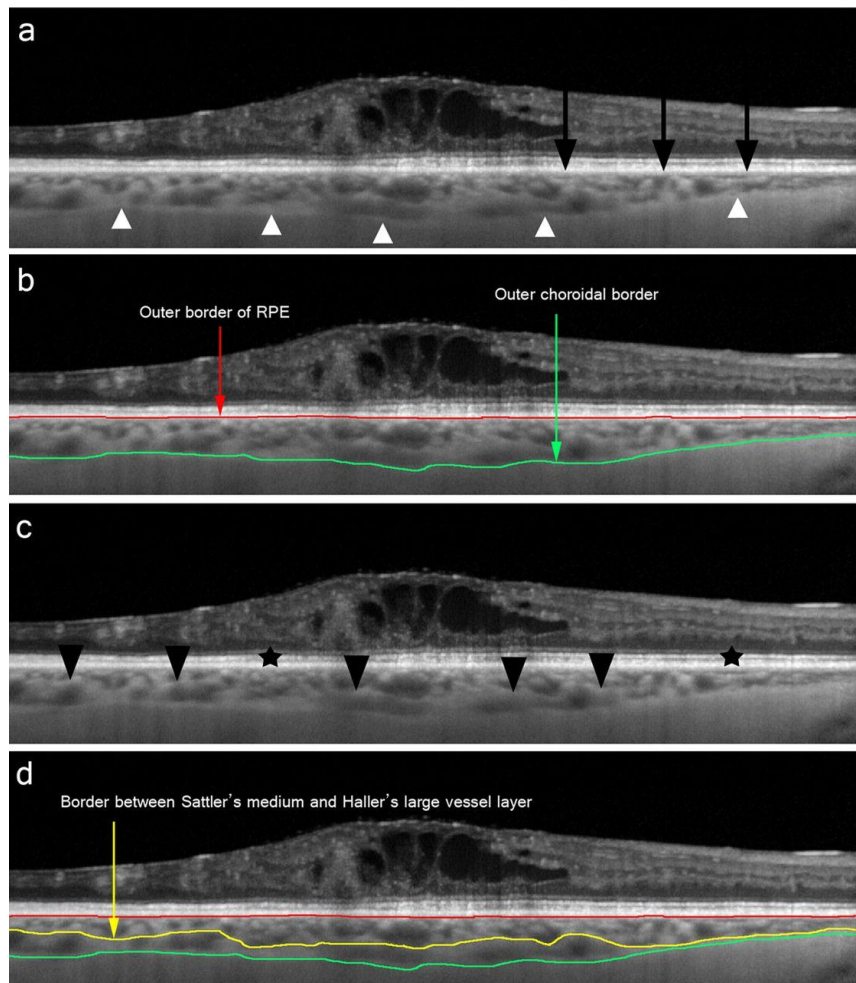


**Figure 3.33** Choroidal layers and segmentation B-scan OCT (From: [www.iovs.org](http://www.iovs.org)) (Sim et al., n.d.)

Choroidal thickness varies in pathological conditions depending on the severity of the macular oedema associated with the disease, as in cases of diabetic retinopathy (Hua et al., 2013; Kim et al., 2013), and also in ARMD, central serous chorioretinopathy and other retinal conditions.

There are many methods for the inspection and detection of any abnormality in the choroid, such as:

1. **Indocyanine green angiography (ICGA)**: it is used for the visualization of choroidal blood vessels and blood flow below the RPE layer of the retina, from the posterior pole to peripheral retina. ICGA is very helpful in cases of choroidal neovascularization, particularly in patients with ARMD (Nicolò et al., 2012; Yannuzzi, 2011) and polypoidal choroidal vasculopathy (Gomi and Tano, 2008).
2. **Fluorescein angiography**: it is a test requiring the injection of fluorescein dye, which is then stimulated by a blue light with a wavelength between 460-490 nm. However, for choroidal examination this test is limited by light scattering and absorption from the RPE layer of the retina (Chhablani et al., 2015).
3. **Ultrasonography**: it is a slightly invasive evaluating tool (it requires contact with the cornea) based on B-scans and ultrasound at 10 MHz. In normal patients, however, it is difficult to differentiate between the overlying retina and the sclera using this technique and in high myopic patients, choroidal thickness is less than what the B-scan's resolution is able to detect (Khetan et al., 2014; Spaide et al., 2013). Even when the image is finally captured, retinal choroidal thickness is commonly overestimated (Singh et al., 2015).
4. **Laser Doppler Flowmeter (LDF)**: it is used to measure the perfusion of red blood cells in the optic nerve head and sub-foveal choroid by projecting a flickering stimulus at the fovea, which is based on Schlieren's principle (Geiser et al., 2013). Blood pressure and heart rate must be stabilized prior to LDF measurements for the examiner to precisely report any glaucomatous damage or any retinal circulation defects (Riva et al., 2010).

5. **Spectral domain optical coherence tomography (SD-OCT):** This device, previously described, enables examiners to visualize the choroid at transverse sections and to check the posterior pole for any possible diseases. In particular, the EDI technique has enabled examiners to measure sub-foveal choroidal thickness (**Figure 3.34**), which decreases with time in patients with high myopia (Phasukkijwatana et al., 2014). EDI offers a three-dimensional visualization of the choroid, providing valuable anatomical information (Invernizzi et al., 2015; Lavers and Zambarakji, 2014; Turan-Vural et al., 2015).

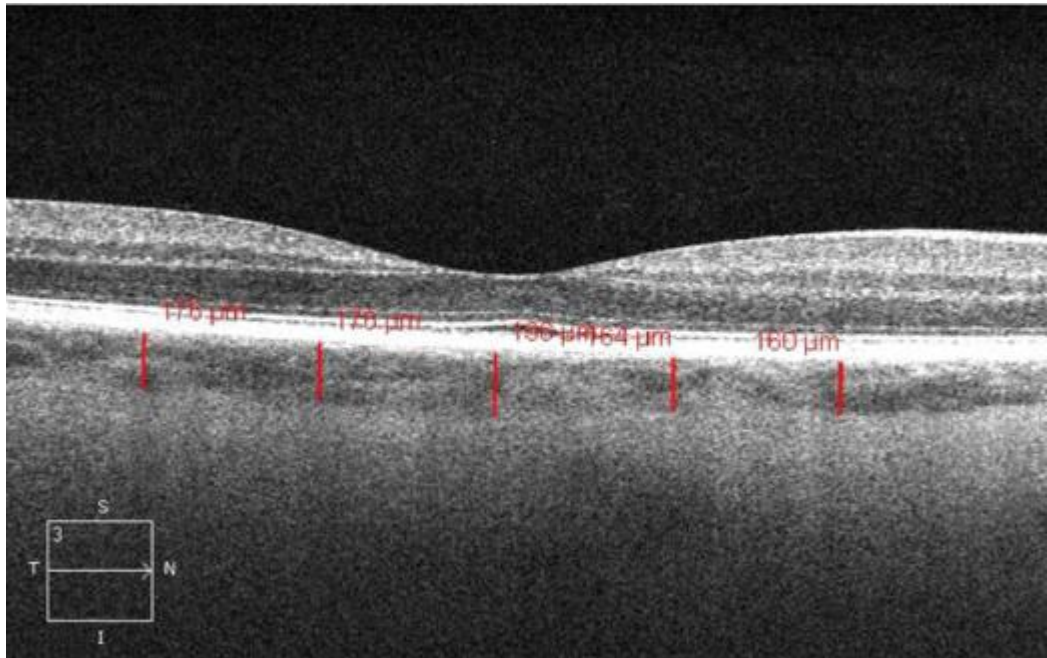


**Figure 3.34** Sub-foveal choroidal thickness using EDI-OCT centrally and at 1 and 2 mm nasally and temporally (From: [www.springer.com](http://www.springer.com))

#### **3.2.6.2.1. Choroidal Thickness in Normal Eyes**

Previous studies have evaluated choroidal thickness in normal eyes using the EDI-OCT device (Li et al., 2012). In the study of Margolis's group, for example, the authors report that the sub-foveal choroidal thickness has a negative correlation with age, with a 1.56 μm reduction per year in the fovea and 1.34 μm per year at

3 mm nasally from the fovea (i.e. over the age of 80, the human eye has lost one third of its sub-foveal choroidal thickness). Similarly, the Fujiwara group concluded that for every 10 years of age among normal Japanese subjects, the sub-foveal choroidal thickness was decreased by 20  $\mu\text{m}$ , and that choroidal thickness was mainly influenced by the type and amount of refractive error in healthy individuals (Fujiwara et al., 2012). In turn, Tanabe and co-workers found that a normal healthy eye has an anatomical feature located inferior to the optic disc, which is considered the thinnest spot in the choroid. This area is easily affected by hypoxia and any elevation in intraocular pressure (Tanabe et al., 2012). Overall, the thickness of the choroid is reduced in the nasal macula more than in the sub-foveal area and it is at its thinnest in the peripapillary area, (Margolis and Spaide, 2009) (Figure 3.35). Good visual acuity is strictly associated with a thick sub-foveal choroidal layer (Shao et al., 2014).

The effect of gender on choroidal thickness at the posterior pole in normal eyes was explored in a sample of volunteers less than 70 years old. The authors concluded that choroidal thickness in males was greater than in females (Zeng et al., 2012).

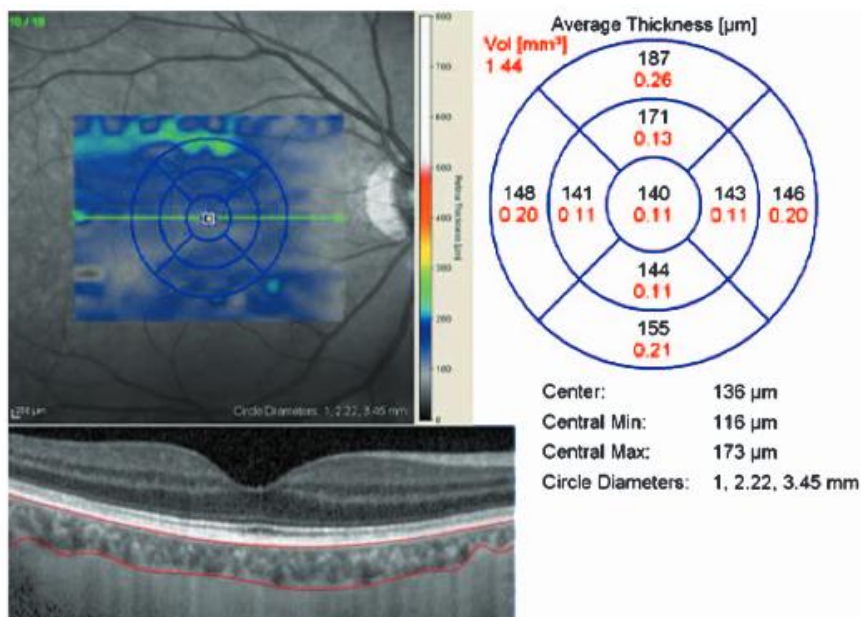


**Figure 3.35** Choroidal thickness and volume in the 9 sectors of the ETDRS map at the central 3.45 mm region (From: www.pubmed.com) (Noori et al., 2012)

Regarding refractive error a strong relationship between choroidal thickness and the type and amount of refractive error has been described, with emmetropic eyes having the thickest choroid, with the highest thickness detected in the temporal and the superior quadrants, followed by the inferior and finally the nasal quadrant. It may be worth noting that, as described above, the opposite is seen in the retina, with the nasal quadrant of the retina being the thickest part and the temporal quadrant the thinnest (Tan et al., 2014).

Values of choroidal thickness have also been observed to vary with ethnicity. In effect, Ozdogan and co-workers measured choroidal thickness in the sub-foveal area of normal Turkish subjects, obtaining values of  $280.23 \mu\text{m} \pm 81.15 \mu\text{m}$ , with a range of 124-527  $\mu\text{m}$  (Ozdogan et al., 2014). Similarly, the research group of Chhablani found that the choroid is thickest sub-foveally and is thinnest nasally in a sample of healthy Indian subjects (Chhablani et al., 2014). In turn, in normal, healthy Korean eyes the temporal choroidal area was the thickest, with a mean of sub-foveal choroidal thickness of  $270.8 \mu\text{m} \pm 51 \mu\text{m}$  in the horizontal scan and  $275.0 \mu\text{m} \pm 49 \mu\text{m}$  in the vertical scan (Shin et al., 2012). Also, an study conducted on a sample of normal southern Thai subjects described mean sub-foveal choroidal thickness of  $279.4 \mu\text{m} \pm 75.49 \mu\text{m}$ , values that were found to be negatively correlated with ocular axial length (with a 14.59  $\mu\text{m}$  decrease in thickness for each 1 mm of axial length increment) and also with age (with 2.67  $\mu\text{m}$  decrease in thickness per year) (Jirarattanasopa et al., 2014). Finally, a study conducted in healthy Chinese subjects revealed a thicker sub-foveal area of the choroid, and a reduction in thickness of the choroid of 5.40 microns per year (Ding et al., 2011).

Interestingly, two studies about diurnal variations of choroidal thickness have revealed that the choroid is thicker in the morning than at night, as measured with the SD – OCT (Osmanbasoglu et al., 2013; Tan et al., 2012).

### 3.2.6.2.2 Choroidal Thickness in Highly Myopic Eyes

Histological investigations have revealed a reduction in retinal thickness, with an increase in scleral thickness caused by the elongation of the anterior-posterior axis of the eye (Mwanza et al., 2011). When compared to healthy, normal eyes, patients with high myopia showed a reduction in thickness of the choroid in all macular areas (Gupta et al., 2014; Read et al., 2013), and the choroid was thicker in patients with pathological myopia at the fovea when compared to the nasal parts of the choroid, and thinner than at the superior parts (Ohsugi et al., 2013).

In his study, Fujiwara and colleagues (Fujiwara et al., 2009) concluded that the mean sub-foveal thickness of the choroid was  $93.2 \mu\text{m} \pm 62.5 \mu\text{m}$ , while suggesting a progressive thinning in the choroid with age (12.7  $\mu\text{m}$  decrease for every 10 years of age), as well as with the severity of myopia (8.7  $\mu\text{m}$  decrease in choroidal thickness with each diopter of refractive error). Interestingly, the change of choroidal thickness was found to be a best indicator of the prognosis of pathological myopia than the change in retinal thickness (Ikuno and Tano, 2009). (Figure 3.36 and 3.37).

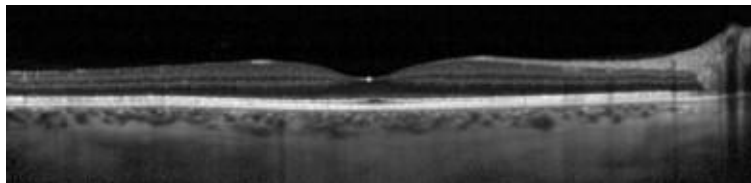


**Figure 3.36** Sub-foveal choroidal thickness of 233  $\mu\text{m}$  in a normal 55 years old male (From: Fujiwara et al., 2009)

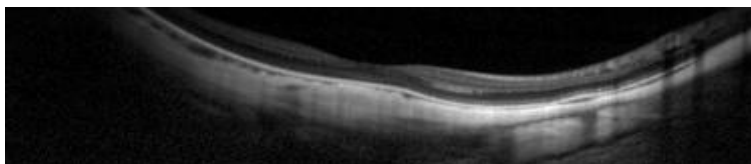


**Figure 3.37** Sub-foveal choroidal thickness of 23  $\mu\text{m}$  in an eye with -20.00 D in a 27 years old female (From: Fujiwara et al., 2009)



### **3.2.6.2.3 Choroidal Thickness in Different Ocular Pathologies**

Given that the main function of the choroid is to metabolically supply the external parts of the retina, including the photoreceptors layer, extreme choroidal thinning and loss of choroidal vascular tissue can lead to photoreceptors damage and functional vision loss (Mrejen and Spaide, 2013). Measuring choroidal thickness using the EDI technique is useful to differentiate between ARDM and central serous chorio-retinopathy. Choroidal thickness is decreased in patients with geographic retinal atrophy secondary to ARMD when compared to patients with normal eyes of the same age (Lindner et al., 2015).

The thickness of the choroid is altered in the presence of an epi-retinal membrane (Michalewska et al., 2015). However, Shao and co-workers investigated sub-foveal choroidal thickness in diabetic retinopathy, describing an increase in thickness with time in certain races, regardless of having any pathological condition, such as in normal healthy eyes of patients coming from a Chinese background, leading the authors to suggest the absence of any correlation between the development of diabetes and choroidal thickness in these patients (Shao et al., 2014a).

Another condition in which choroidal involvement is currently under investigation is glaucoma. Thus, patients with normal tension glaucoma (NTG), or primary-open angle glaucoma (POAG), showed no differences in choroidal thickness when compared to normal eyes (Mwanza et al., 2011). A recent study also failed to discover any difference between POAG and normal eyes, but found a significant difference between normal eyes and NTG, with thinner choroids in these particular patients (Park et al., 2014).

Finally, sub-retinal fluid is present in both Vogt-Koyanagi-Harada disease and in acute central serous chorioretinopathy, leading to changes in the choroid (Lin et al., 2014).



### **3.3 Microperimeter (Fundus Related Perimeter)**

#### **3.3.1 Fundamental Concepts**

Common tests to assess the functional vision of the macula are visual acuity, Amsler grid, reading speed and contrast sensitivity. Although many of these tests have limitations, reading speed and contrast sensitivity are still valuable tests that offer examiners an overview of the improvement in visual function after medical intervention (Hazel et al., 2000; Nguyen et al., 2009).

Microperimetry is a relatively new technique that has proved to be superior to many of the previous tests used to assess the health status of the macula. The residual vision that remains after the loss in macular function is represented by scotomal characteristics, preferred retinal loci (PRLs) and changes in oculomotor control. Therefore, microperimetry allows examiners to estimate the impact and complications seen in retinal and macular diseases or to assess the effect of any ocular intervention on the retina (Markowitz and Reyes, 2013).

Thus, the main uses of microperimetry are to:

- Evaluate glaucomatous damage and the residual function of vision in a diseased eye.
- Evaluate visual function in normal subjects.

Previously, functional vision was assessed with different tests, such as the confrontational visual field test, Amsler grid and Tangent screen test, in addition to Standard Automated Perimetry (SAP). Comparatively, SAP is a commonly used method in ophthalmic assessment, which is not devoid of clinical limitations (Turalba and Grosskreutz, 2010): the grey grid offers low reliability, especially in patients with cataract, as the results are represented with shades of grey that can be confused with glaucomatous damage (Alencar and Medeiros, 2011).

In patients with central visual field loss, it is always better to assess the functional central vision using proper testing methods and techniques, while simultaneously monitoring the retina to obtain precise measurements. This can only be achieved with fundus related perimetry, which enables examiners to record the stimulus presented at each specific point of the retina and to correct any fixation problem or any changes that may be seen in the central vision (Nguyen et al., 2007). Microperimetry provides examiners with retinal sensitivity maps that display differences in luminance intensity at various locations in the examined retina.

### **3.3.2 History**

The first fundus related microperimeter was the “Scanning Laser Ophthalmoscope” (SLO-101) microperimeter (Rodenstock, Munich), which was used to evaluate the functional vision in the macula with a fixation protocol to test the foveal or extrafoveal areas of the retina. In this device, the stability of fixation was described qualitatively rather than quantitatively (Dunbar et al., 2010). Forthwith, Nidek MP1 microperimeter was commercially available for examiners in 2002, which allowed automated eye tracking at the same retinal loci using an infrared camera of the fundus with a resolution of 768 x 576 pixels and a 45° visual field (Chen et al., 2009; Chen et al., 2011).

### **3.3.3 Physical Bases in Brief**

This microperimeter employs a collimated laser to project energy on the retina. During this, the light beam goes through vertical and horizontal scanning mirrors in order to obtain a correct alignment ([Figure 3.38](#)). The microperimeter incorporates a Charge-Coupled Device (CCD) camera and a Shark-Hartmann wavefront sensor. To compensate for any eye movement during the test, the device utilizes a phase-stabilized optical image with an optical frequency domain imaging (OFDI) system and a Tracking Scanning Laser Ophthalmoscope (TSLO)

(Vienola et al., 2012). Different ocular structures may be observed by using different light wavelengths. For example, with green light at 540 nm it is possible to explore retinal vasculature and the nerve fibre layer, whereas with light at 780 nm and by changing to confocal mode, more profound structures such as choroid vasculature may be assessed.

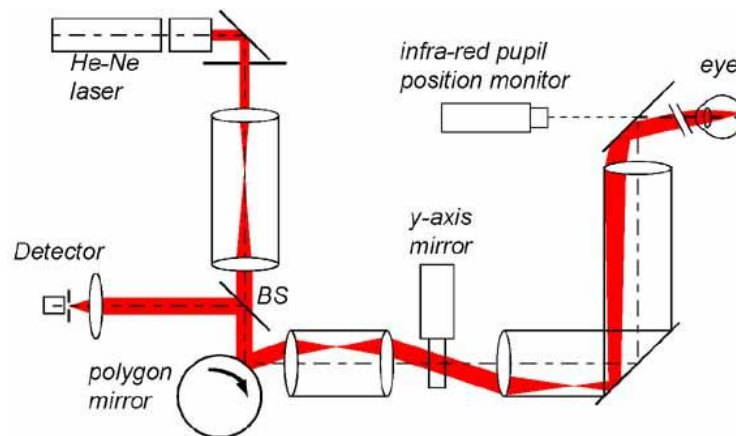


Figure 3.38 SLO (From: [www.roorda.vision.berkeley.edu](http://www.roorda.vision.berkeley.edu))

Some of the most notable features of an automated microperimetry are:

- High resolution of up to 10 stimuli/ degree.
- Short duration of testing as microperimetry, retinography and assessment of stability of fixation are conducted simultaneously.
- Quantification of retinal sensitivity.
- Automated eye tracking.
- Scotometry (detection of areas with absolute or partial loss of visual function).
- Peripapillary microperimetry to follow-up glaucomatous cases.

### **3.3.4 Types of microperimeter**

Several types of microperimeters are commercially available:

#### **1. MP-1 microperimeter**

Manufactured by Nidek Technologies in 2002, Italy, this device consists of an infrared (IR) camera that captures the retinal image while stimuli are presented on an LCD screen. There is also a conventional camera to obtain coloured retinal images, in addition to various visual field patterns.

Consequently, this device may reflect each stimulus at a specific area, modifying the size of the stimulus and fixation point. The normal range of retinal sensitivity from 0-20 dB may be explored, which is equivalent to the retinal sensitivity values of 14-34 dB obtained with the Humphrey perimeter (Wu et al., 2014). Vujosevic and co-workers reported microperimetry to be relatively good in patients with retinal fixation abnormalities secondary to the presence of diabetic macular oedema, due to its ability to precisely locate the point of fixation and the corresponding fixation stability (Vujosevic et al., 2008).

The MP-1 model has a maximum luminance of 3183 cd/m<sup>2</sup> and the dimmest stimulus is only 1% of the brightest target intensity (Crossland et al., 2012; Rohrschneider et al., 2008). Measurements with the MP-1 do not require pupil dilation except in extreme cases.

#### **2. OCT – SLO (OPKO, Miami, Florida, USA)**

This instrument combines the function of OCT with a microperimeter. It requires no pupil dilatation, gives high quality retinal images, and the dimmest stimulus is 2% of the brightest target intensity.

### 3. MAIA™ Microperimeter

This microperimeter captures retinal images with a field of view of 36° X 36° and a resolution of 1024 X 1024 pixels, which penetrates 25 microns into the retina utilizing a light source of infrared super luminance at 850 nm.

Moreover, using this model with a standard perimetry testing of the macula at 10° over a 20° X 20° visual field, the device projects images at a speed of 25 femtoseconds and a working distance of 30 mm. The MAIA™ uses a stimulus size of Goldmann III, which corresponds to a background luminance of 4 cd/m<sup>2</sup>, as well as, a dynamic range of stimuli of 36 dB and a maximum luminance of 1000 cd/m<sup>2</sup>.

MAIA™ requires a minimum pupil diameter of 2.5 mm and may conduct good measurements in the refractive error range from -15.00 to +10.00 D (contact lenses are used for the evaluation of patients beyond this range). This instrument was used in this study and will be described **in further** detail in the methodology section **5.2.2**.

A summary of the characteristics of the different microperimeters is presented on **Table 3.3**.

	Fixation stimulus size	Test stimulus size	Duration	Field of view	Eye tracking
<b>SLO - 101 Microperimeter</b>	-	Goldmann III	-	Central 10°, and 36° total	Manual
<b>Nidek MP1</b>	2°	Goldmann III	200 ms	Central 20°, and 45° total	Automated
<b>MAIA™</b>	-	Goldmann III	37 stimuli in 2 min (fast exam), 4 levels fixed in 3 min, and full threshold 4-2 in 6 min	36° x 36° of fundus imaging, 30° x 30° of perimetry projection, 20° centrally	Automated

**Table 3.3** Types and characteristics of three commercially available microperimeters

### 3.3.5 Microperimetry measurements

Microperimetry is employed to correlate structural and functional characteristics of the ocular fundus.

#### 3.3.5.1 Microperimetry in Normal Patients

A microperimeter may be employed for the following tasks:

- Detecting the presence of central retinopathies.
- Monitoring functional vision in patients with ARMD or diabetic maculopathy.
- Detecting any reduction of function that results from an absolute scotoma.
- Assessing the integrity of different fundus structures, mainly the macula, to track the prognosis of these ocular conditions.

**Figure 3.39** shows a map of a normal macula with the corresponding retinal sensitivity of 37 points.

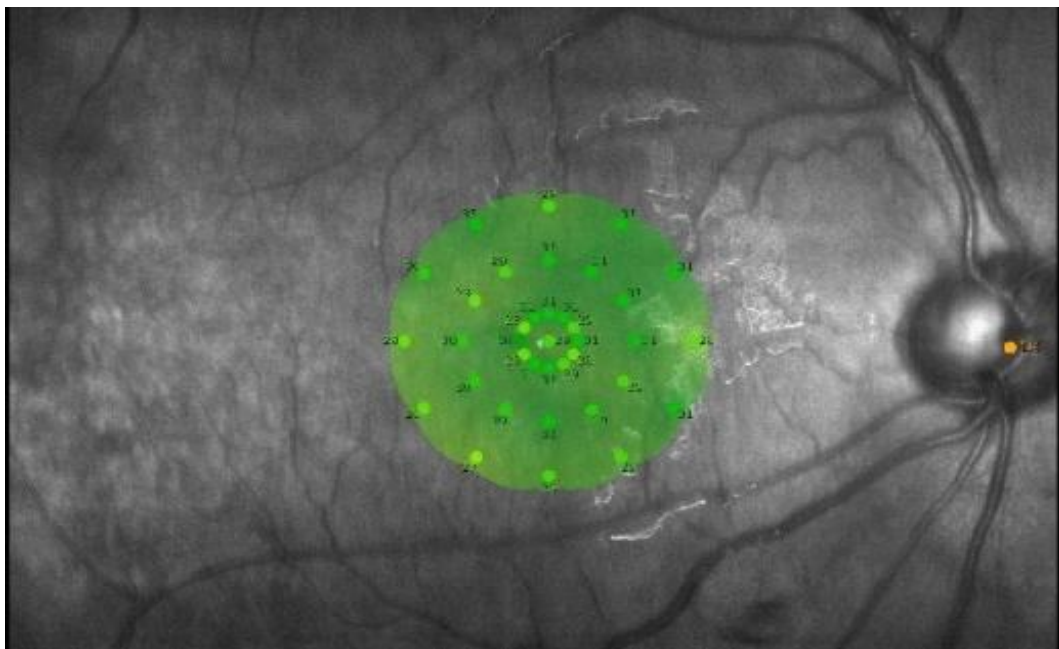


**Figure 3.39** Macular retinal sensitivity in a normal patient

### 3.3.5.2 Microperimetry in Patients with High Myopia

The OCT provides detailed information about the morphological changes and complications seen in the retina of patients with high and pathological myopia. Likewise, microperimetry offers examiners with detailed information of the functional aspects of the retina. Indeed, the earlier the detection of retinal pigmented epithelial atrophy and of choroidal thinning, the earlier the diagnosis of degenerative myopia. Correspondingly, dense absolute scotomas representing atrophic areas are best detected using a microperimeter, due to the stable and fixed extrafoveal fixation these patients have. **Figure 3.40** shows a macular sensitivity map of a patient with pathological myopia in which the black dots represent areas of non-functional vision, or scotomas. Also, the other coloured dots indicate that a higher level of stimulus intensity was required to elicit a response from the patient.

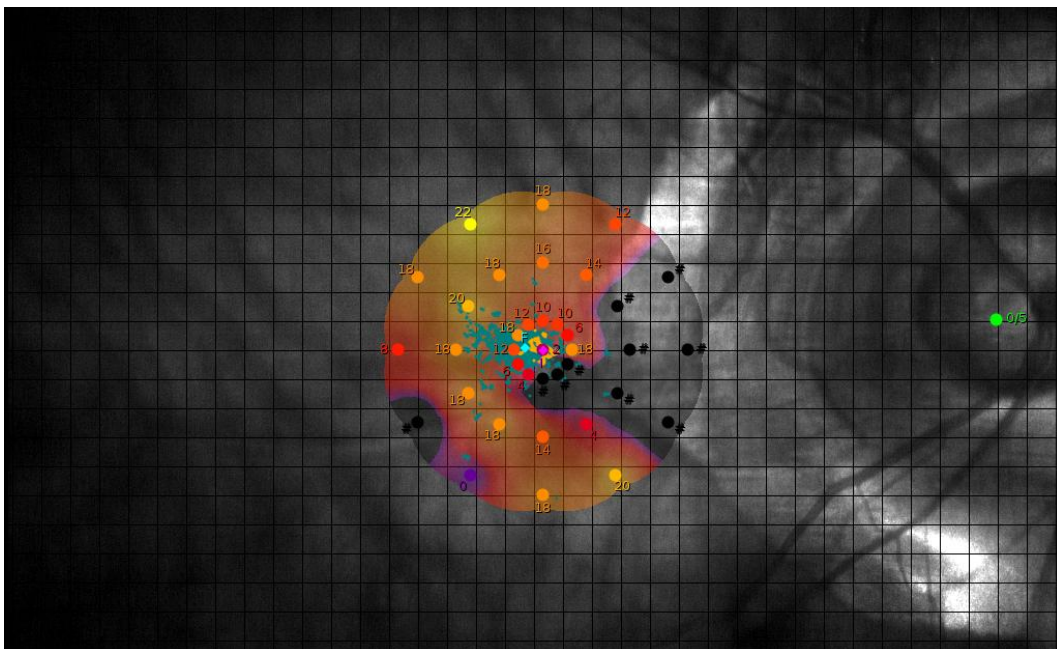


**Figure 3.40** Macular retinal sensitivity of a patient with pathological myopia, in which the black dots represent scotomas

### 3.3.6 Microperimeter Evaluation in Association with OCT

Few researchers have explored retinal sensitivity and anatomical changes in patients with high myopia. In effect, in a recent study of Zaben and co-workers (Zaben et al., 2015) the authors explored retinal sensitivity and choroidal thickness at the macula in patients with high myopia. These authors assessed choroidal thickness (structural evaluation) and retinal sensitivity. An assessment of the macular area of 10 degrees in diameter with a 36-point strategy and duration of stimulus of 200 ms in 5 minutes was performed on each eye. In addition, choroidal thickness measurements were obtained using a 3D – OCT 2000 device with a 6 X 6 protocol (512 X 128). The authors described a significant positive correlation between retinal sensitivity and choroidal thickness, with retinal sensitivity being significantly reduced (Compare [Figure 3.41](#) and [Figure 3.42](#) to note the relationship between the two exploratory methods).

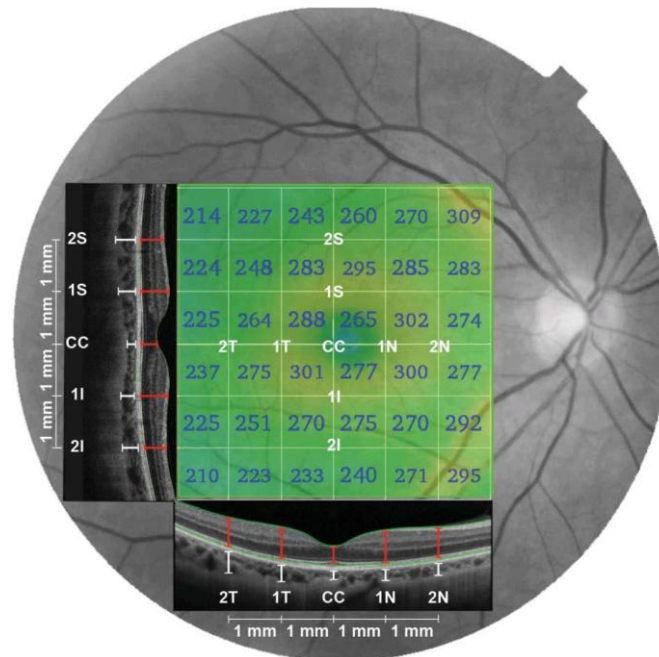


**Figure 3.41** Choroidal thickness using OCT at the centre of the macula, and at 1 mm and 2 mm away from the macula of patient with pathological myopia (superior, inferior, nasally and temporally) (From: zaben et al., 2015)



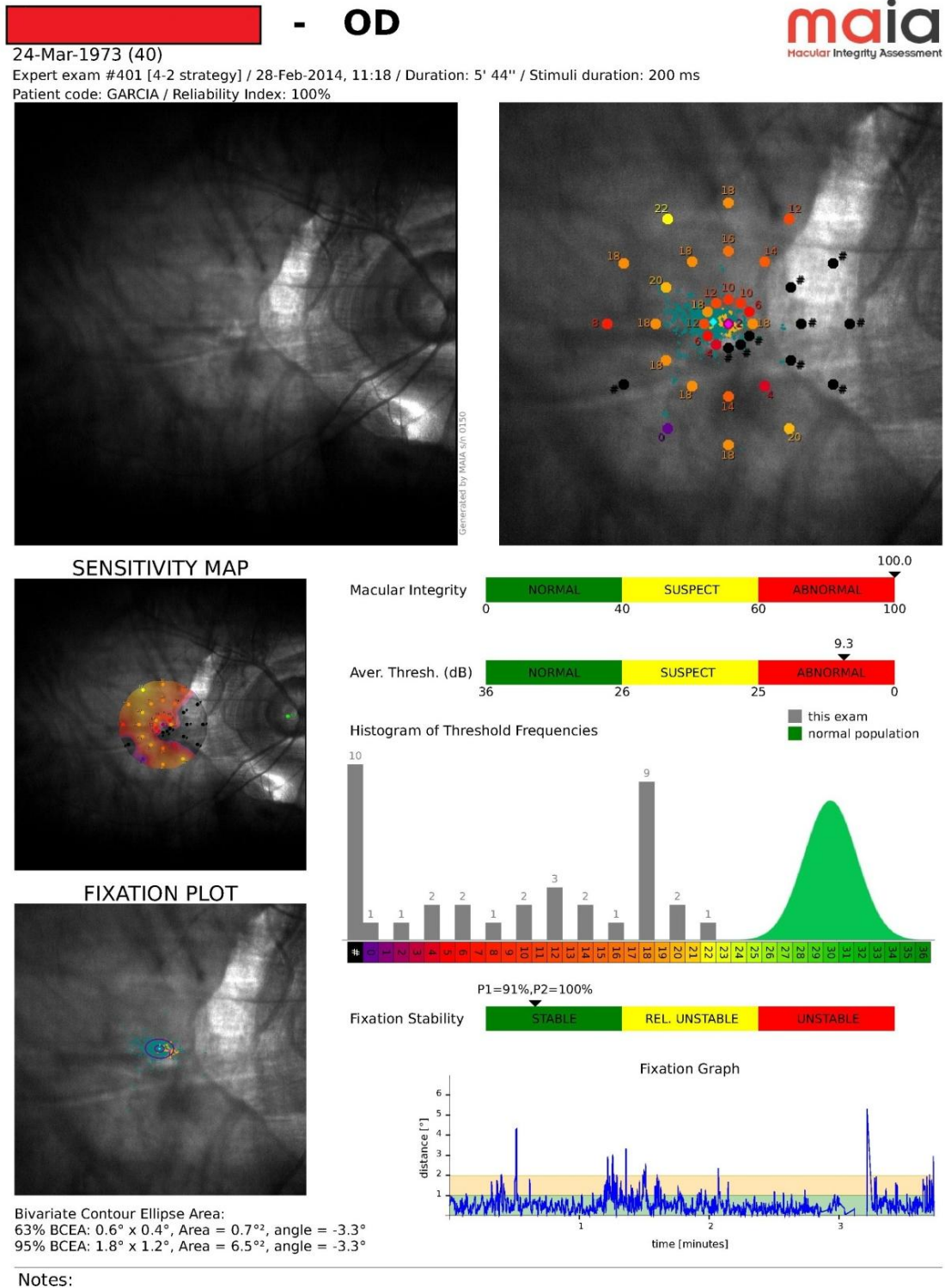


Figure 3.42 Expert exam microperimetry (MAIA™) of the same patient



## **4. Objectives, Justification and Hypotheses**

### **4.1 General Objective**

The general objective of this thesis is:

**To evaluate the relationship between anatomical (using OCT) and functional (using microperimetry) inter-ocular asymmetry of both retina and choroid in patients with high myopia.**

High myopia and its complications in pathological myopia, such as glaucoma, cataract, retinal detachment and macular degeneration, are some of the leading causes of blindness and low vision in industrialized countries.

However, the mechanisms related to the pathological changes that accompany the disease and lead to the thinning seen in the retina and choroid which results in a drop in visual function are not clear. Therefore, it is critical to be able to detect and understand the structural and functional changes to better describe high myopia to aid examiners to evaluate these retinal alterations, to determine the possible progression towards pathological myopia and to manage the condition.

In consequence, the main aim of this study was to gain a better understanding of retinal function in patients affected with high myopia. This objective was approached through precise retinal sensitivity analysis using a microperimeter, jointly with accurate exploration of retinal structures using an SD – OCT, and by assessing the range and correlation between the values of inter-ocular asymmetry in the corresponding anatomical and functional parameters and refractive error. It was the hypothesis of the study that inter-ocular asymmetry would be different according to refractive error.

Several specific objectives derive from the general objective of the present study:

## 4.2 Specific Objectives

### 1. **Measuring retinal thickness asymmetry using SD-OCT in normal patients:**

several studies have explored the normal range of inter-ocular asymmetry in healthy patients. Understanding normality is essential to better interpret the outcomes in high myopia. However, results from these studies describe an incomplete map of normal retinal asymmetry, as outcomes are influenced by several characteristics of the patients such as age, gender and ethnicity, as well as by the device employed for retinal analysis. In particular, as far as we know, the SD-OCT has not been used to explore the normal range of inter-ocular asymmetry in retinal thickness in Caucasian young adults. In short, we aimed at gaining a complete understanding of normal structural asymmetry in health and then to proceed with the myopic group. For that reason, a diagnostic clinical method was designed, using the scanning protocol of the OCT for the optic nerve, retinal nerve fibres layer (RNFL), and macular region, to explore the physiological asymmetry in a sample of young healthy adults between the ages of 12 and 23 years and a spherical equivalent that ranged from -3.00 to +4.00 D. In addition, an aged- and gender-matched control group was also explored to be able to compare retinal thickness asymmetry with that of the high myopia group.

### 2. **Measuring choroidal thickness in normal patients using the enhanced depth imaging (EDI) technique of the SD – OCT:**

Although the OCT has been employed to measure retinal thickness in various locations, there is a lack of evidence regarding choroidal thickness asymmetry in normal patients, although some authors have referred to the anatomical structure and physiological asymmetry in blood flow that reaches the right and left eyes, due to the deficiency and inconsistency of blood originating in and travelling from the aortic arch to the eye, leading to a higher thickness of the choroid in the nasal part of the right than the left eye (Hayreh and Zimmerman, 2014; Ruiz-Medrano et al., 2015; Sohrab et al., 2012). Previous studies remarked the importance of well-

understanding choroidal thickness among normal, healthy eyes (Herrera et al., 2015). With the present study we aimed at providing further information in this relatively new area of research. These results were then interpreted in the light of those found in patients with high myopia.

**3. Exploring retinal (macular) sensitivity differences between both eyes in normal patients:** previous research has revealed a negative correlation between age and retinal macular sensitivity in healthy eyes (Ismail et al., 2015; Shah and Chalam, 2009). Microperimetry has been used in cases of age-related macular degeneration (Alexander et al., 2012) and lamellar macular holes (Parravano et al., 2013). Fujiwara and co-workers determined the normal values of retinal sensitivity with macular integrity assessment (MAIA™) and described the key role of age and axial length in the reduction of retinal sensitivity (Fujiwara et al., 2014). Similar results were obtained by Qin et al with the MP-1 (Qin et al., 2010). The present research on the residual visual function in normal patients using microperimetry was aimed at further exploring the normal range of inter-ocular asymmetry in retinal sensitivity and, by using the same instrument and research protocol, to allow for a better comparison with the results obtained in patients with high myopia.

**4. Measuring retinal thickness asymmetry using SD-OCT in patients with high myopia:** as noted above, previous studies have explored retinal thickness asymmetry with the SD-OCT in normal patients, and in those with glaucoma (Kochendörfer et al., 2014; Seo et al., 2012; Yamada et al., 2014). In the present study we aimed at detecting any structural changes in patients with high myopia using an SD – OCT and at determining the range of inter-ocular difference in this condition and the relationship between inter-ocular asymmetry and refractive error. Several locations of the retina were explored to determine retinal

thickness: macula at the centre and away from the centre at 1 mm, 2 mm, and 3 mm (nasally, temporally, superiorly, and inferiorly) respectively. As far as our literature research has revealed, this study may be considered the first to explore retinal thickness asymmetry in patients with high myopia using the SD – OCT.

**5. Measuring choroidal thickness in patients with high myopia using the enhanced depth imaging (EDI) technique of SD – OCT:** previous research has also described the relevance of understanding key aspects of choroidal thickness in association with some ocular conditions such as age-related macular degeneration (Thorell et al., 2015), anisometropic and strabismic amblyopia (Aygit et al., 2015), primary open-angle glaucoma (Sullivan-Mee et al., 2013; Toprak et al., 2015), Usher syndrome (Colombo et al., 2015), retinitis pigmentosa (Dhoot et al., 2013), diabetic retinopathy (Zhu et al., 2015), high myopic glaucoma (Chebil et al., 2015), and high and pathological myopia (Gupta et al., 2015; Harb et al., 2015; Lee et al., 2015; Zaben et al., 2015). However, the asymmetry in macular choroidal thickness has not been previously explored in patients with high myopia. In the present research, we investigated asymmetries in choroidal thickness in different macular regions and away from the centre at 1 mm, 2 mm and 3 mm (nasally, and temporally). The relationship between asymmetry and refractive error was also explored.

**6. Exploring the inter-ocular asymmetry of macular sensitivity in patients with high myopia:** high myopia may lead to structural alterations in the eyes, such as scleral ectasia, and posterior staphyloma secondary to progressive elongation of the ocular axial length, as well as to the reduction of choroidal thickness. These changes may affect and reduce visual function by altering retinal sensitivity. The main aim of our investigation was to evaluate any asymmetries in macular sensitivity in myopia to determine whether these differences could be

considered as key features in the future diagnosis of this condition. As far as we know, only one previous study explored macular sensitivity in high myopia (Zaben et al, 2015), and no attempt has been conducted to determine inter-ocular asymmetry in these patients or to explore the association between asymmetry and refractive error.

**7. Analysing the relationship between structural and functional changes in patients with high myopia:** the relationship between macular choroidal thickness and retinal sensitivity in highly myopic subjects has been previously explored with the EDI technique of the OCT and the MP-1 microperimeter, evidencing a reduced macular thickness in association with decreased retinal sensitivity (Parravano et al., 2014). Also, the mentioned recent study of Zaben and co-workers (Zaben et al., 2015) described the correlation between retinal sensitivity and choroidal thickness using MAIA™ in patients with high myopia. However, no previous attempt to investigate the association between asymmetry in retinal sensitivity and the corresponding asymmetry in macular and choroidal thickness, or that between asymmetry and refractive error, has been conducted with the SD-OCT and the MAIA™ microperimeter.

The addition of an aged and gender matched control group of healthy subjects, as described in the specific objectives 1 to 3, was very relevant to further understanding any asymmetry in retinal sensitivity and/or choroidal thickness encountered in high myopia. It must be noted that the control group was examined following exactly the same protocol, and instrumentation, as the high myopia group. These methods and instrumentation are the topic of the next section.





## 5. Material and Methods

### 5.1 Patients

This study was conducted between April 2014 and June 2016. Patients were recruited from those attending a busy optometric clinic (Optipunt Zaben, Figueras) for routine visual examination. The present study included a sample of patients affected by high myopia and a corresponding sample of age and gender matched normal patients as a control group.

The following are the **inclusion/exclusion criteria** defined for this study:

- For the objective of exploring the asymmetry of retinal thickness using OCT in normal patients (specific objective 1) the inclusion criteria were age from 12 to 23 years, a spherical equivalent of between +4.00 D and -3.00 D, best corrected monocular distance visual acuity  $\geq 0.0$  logMAR (20/20) and intraocular pressure  $< 21$  mmHg. Participants with a history of ocular trauma or pathology, ocular or refractive surgery, diabetes mellitus and those without central fixation were excluded from the study, as were those with anisometropia  $\geq 0.5$  D or axial length differences larger than 0.3 mm.
- The inclusion criteria for the control group for the measurement of normal inter-ocular asymmetry in retinal function and retinal and choroidal structures (specific objectives 1 to 3) was the same, with the only exception that this group was age and gender matched to the group with high myopia described next.
- Finally, the inclusion criterion for patients with high myopia (specific objectives 4 to 6) was spherical equivalent of  $\geq -6.00$  D. Patients with pathological myopia were excluded from the study, that is, patients with choroidal neovascularization secondary to myopia, as were those with any disease that may lead to an alteration of the macular area, those with any ocular media opacity, existence of glaucoma and those with amblyopia. Patients were also excluded if they did not sign the informed

consent or if they failed to understand the requirements of the test or were unable to cooperate.

All patients were informed of the purpose of the study (parents were informed in case patients were underage) and were given written brochures with information related to the examination and tests. Consent forms were signed regarding the specifics of the examination and the right to analyse all collected data collected in future researches, while assuring all participants of the confidentiality treatment of all personal details (see [Annex I](#)). The study was conducted in accordance and respect to the Declaration of Helsinki tenets of 1975 (as revised in Tokyo in 2004) and received the approval of the **Ethical Review Board of the Hospital Universitario Mútua de Terrassa**.

## 5.2 Methodology and Instrumentation

In order to be able to fulfil the main objective of the study, typical instruments that are found in any optometric practice were employed for routine visual examination, including a retinoscope, a CV.5000 Digital phoropter (Topcon), a digital slit-lamp (Topcon), an air-puff tonometer (Topcon KR.1), a KR.1 Auto Kerato Refractometre (Topcon) and a logarithmic visual acuity chart ETDRS (Early Treatment Diabetic Retinopathy Study).

In addition, the following equipment, which will be described below, was used for retinal and choroid assessment:

- 3D OCT-2000 Optical Coherence Tomography – Topcon (software
- version 8.00)
- Microperimeter – Topcon

On the first visit, a general optometric/ophthalmological case history was recorded from all patients, including demographical information concerning

name, sex, age, general medical history, family history of glaucoma, history of frequent headaches, previous or current systemic treatment (corticosteroids, chloroquine phosphate, etc.).

Next, patients were administered a comprehensive visual assessment and examination to determine their eligibility for the study, according to the inclusion/exclusion criteria described above. Retinoscopy was conducted to determine the amount and type of refractive error. Then the best corrected visual acuity for distance vision was measured with an ETDRS test (Lighthouse International), which is a retro-illuminated box presented at a distance of 4 meters. Visual acuity data was measured and recorded in logMAR notation (logarithm of the minimum angle of resolution).

Furthermore, the integrity of ocular structures was evaluated using a slit-lamp. The following ocular structures were examined: eyelids, sclera, conjunctiva, cornea, tear film and crystalline lens of each eye. Clear ocular media was required for the correct acquisition of ocular fundus images and sensitivity assessment.

Finally, a non-invasive air-puff tonometer (Topcon KR-1), which requires no direct contact with the eye, was used to measure intraocular pressure. Cut-off value of normality for intraocular pressure was <21 mmHg.

In addition, all the images of the ocular fundus captured with the OCT were sent to a medical team of 8 ophthalmologists for diagnosis and recommendations. This feedback is commonly available within 48 hours via Telemedicine (**OptRetina**). The team of ophthalmologists in OptRetina are: Dr. Miguel A. Zapata (co-director of this thesis), Dr. Alejandro Fonollosa, Dr. Gabriel Arcos, Dr. Sergio Copete, Dr. Maximino Abrales, Dr. Christina Klais, Dr. Flores-Moreno, and Dr. Rafael Bueno (From: [www.optretina.com/en/medical-team](http://www.optretina.com/en/medical-team)). (**Figure 5.1**)

**opt retina**

**OPTIPUNT**  
ZABEN

### INFORME OPTOMÉTRICO Y CRIBADO PARA PREVENCIÓN DE LA CEGUERA

Cribado de las enfermedades de la retina central realizado mediante cámara no midriática por oftalmólogos especialistas en retina.  
El presente informe ha sido evaluado por el Dr. Gabriel Arcos con número de colegiado 44939.

¿Sabía que según la Organización Mundial de Salud el 80% de las cegueras son completamente evitables si se detectan a tiempo?

**DATOS GENERALES**

**Nombre:** [REDACTED] **Diabetes:** No  
**Sexo:** Mujer **Edad:** 74  
**Centro:** Optipunt Figueres **Fecha consulta:** 03/03/2015

**EXAMEN OPTOMÉTRICO**

**AV OD:** 0.6 **AV OI:** 0.6  
**EJE:** 85° **CIL:** -0.50 **ESF:** +1.25 **AD:** 3.00 **EJE:** ° **CIL:** **ESF:** +1.25 **AD:** 3.00  
**Presión intraocular OD:** 14 **Presión intraocular OI:** 13

**ANAMNESIS**

**CONSEJOS PARA MIRAR POR SU VISIÓN**

Siga una alimentación equilibrada rica en vitaminas y ácidos grasos omega 3

Compruebe

IS PARA LA PREVENCIÓN DE LA CEGUERA

Figure 5.1 OptRetina service

### 5.2.1 Optical Coherence Tomography

The OCT device was used in this study to evaluate the variations of retinal and choroidal thickness in the macular area in highly myopic patients and in normal subjects.

Thickness values in different parts of the fundus and the precise volume of the macula were recorded using the built-in software of the SD – OCT instrument. Measurements were conducted with the vitreous-mode, a cube of 512 X 128 and the macular protocol for 3D – OCT – 2000, as well as the choroidal-mode for choroidal assessment. All measurements of the OCT device were taken by the same examiner.

The macular cube of 512 X 128 protocol (**Figure 5.2**) performs 512 cuts of horizontal B-scans with 128 A-scans per cut over an area of 6 X 6 mm, providing a thickness map containing concentric sectors that define the nine regions of the macular map. The average thickness of all points within the interior ring of a 1 mm in diameter was defined as the central retinal thickness (central subfield thickness), and the same also applies to macular volume measurements.

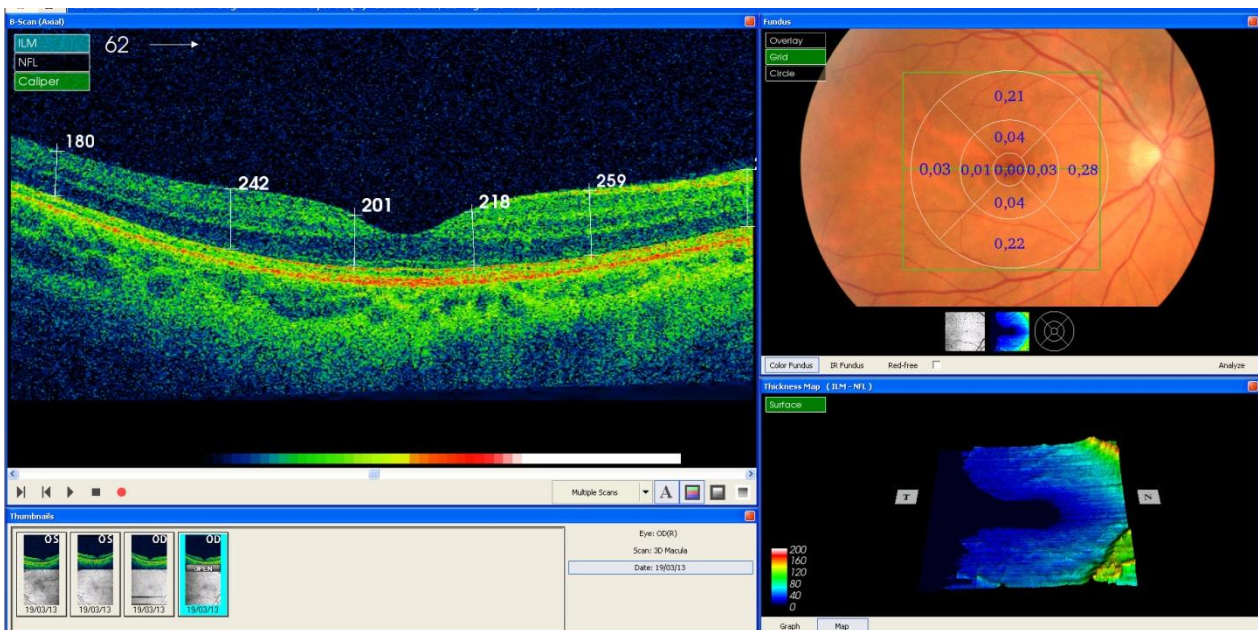


**Figure 5.2** OCT scan of the macula and the corresponding results

The macular volume and average thickness values were calculated by internal algorithms of the 3D-OCT-2000. In this study, the macular cube protocol was considered normal only in cases that:

1. Showed no retinal alterations.
2. The signal strength was greater than 70%.
3. Was centred adequately at the fovea.

Next, the optic disc cube of 512 X 128 protocol was used (Figure 5.3). The scan was adjusted automatically to the size of the optic disc as close as possible to the disc margin while avoiding crossing to the border of the optic nerve at any point.

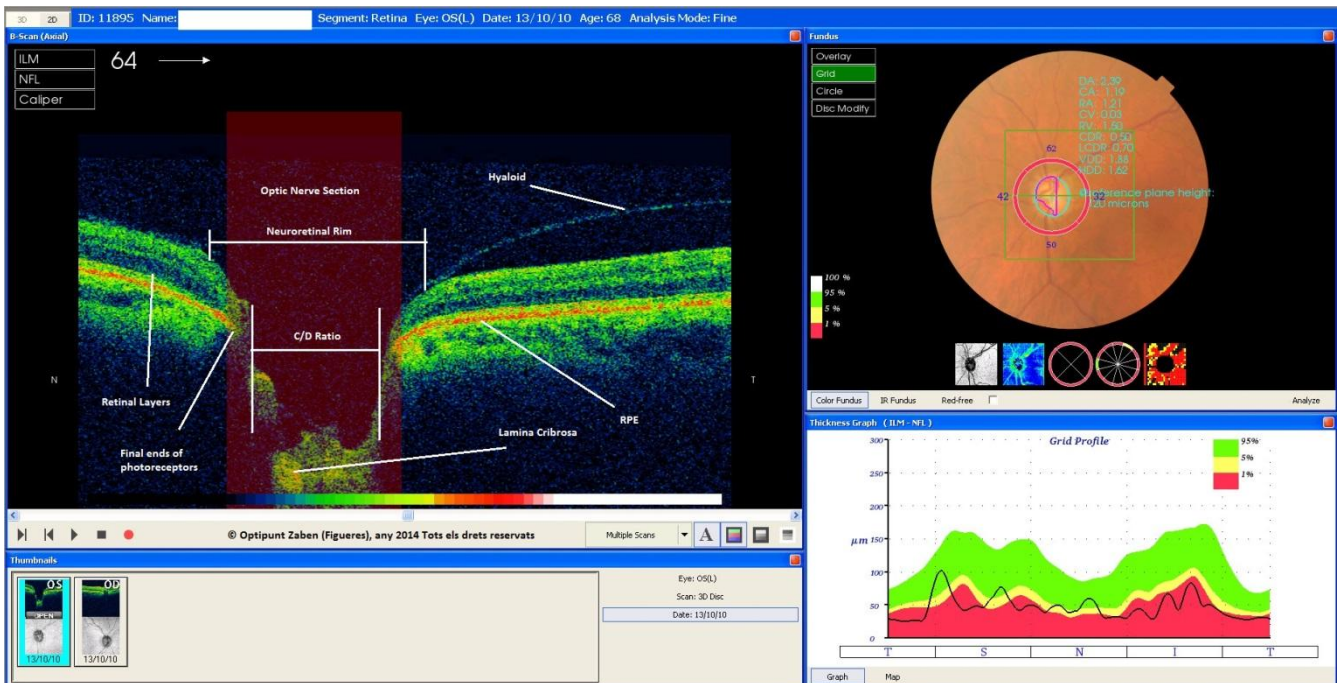


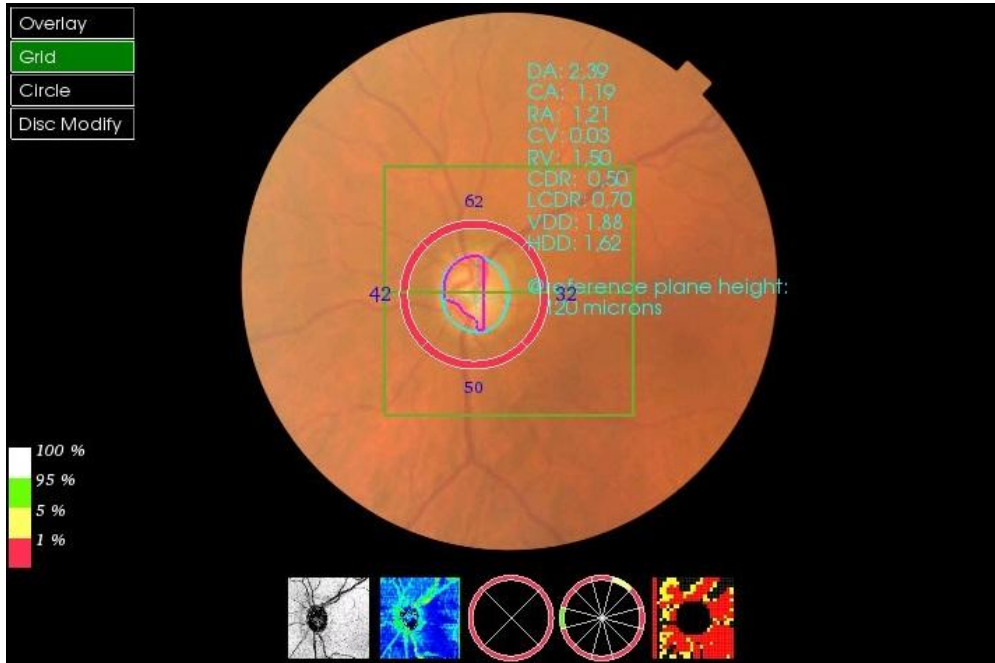
Figure 5.3 OCT scan of the optic nerve head and the corresponding results

Figure 5.4 displays an image of the cup using the OCT software. The inner pink circle was automatically detected. The region between the disc (green line) and the cup margin represents the neuroretinal rim area ( $\text{mm}^2$ ), whereas the cup area ( $\text{mm}^2$ ) corresponds to the region inside cup margin. The summation of these areas is the total disc area ( $\text{mm}^2$ ), and the square root of the cup to disc ratio area is what determines the C/D ratio.

Measurements of the RNFL thickness were obtained using the “automated software measurement analysis protocol”. To ensure good image quality, scans were discarded in cases where excessive eye movement and excessive blinking were present or in cases where the device produced decentred or out of focus images.



Finally, choroidal thickness at the centre, and at 1 mm, 2 mm and 3 mm (nasally, superiorly, temporally, and inferiorly) was measured manually using the corresponding software. (See [Figure 5.5](#))



**Figure 5.4** OCT scan of the optic nerve showing the C/D ratio

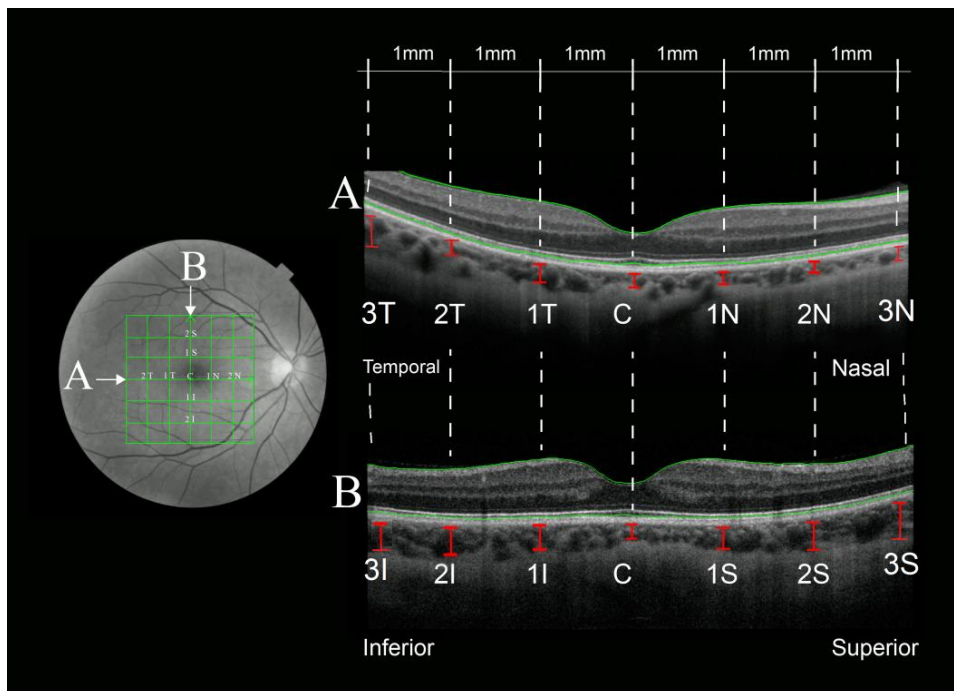


**Figure 5.5** Retinal and choroidal thickness with the OCT

### 5.2.2 MAIA™ Microperimeter (Macular Integrity Assessment)

This examination was performed under mesopic conditions (approximately 5 cd/m<sup>2</sup>) without the need for pupil dilation. First, a “Fast exam” was conducted, which offered a rapid assessment (2-3 minutes for each eye) of macular sensitivity and fixation stability (Figure 5.6).

Then, the threshold of macular sensitivity and fixation stability tests were assessed in the central 10 ° (in diameter) of the macula using the “Expert exam”. It must be noted that each 1° corresponds to 300 microns, that is, 10° = 3000 microns, which covers the whole macula. The test employed a strategy of 36 stimuli, with stimulus duration of 200 ms. The “Expert exam” mode required 5 minutes per eye (Figure 5.7).

The colour coded scale (Figure 5.8) used by the MAIA microperimeter is as follows:

- **Green, normal:** Represents a retinal sensitivity equal or over an stimulus intensity of 27 dB (27 dB corresponds to the 90 percentile of normal values)
- **Yellow, suspect:** Represents a retinal sensitivity between an stimulus intensity of 27 and 26 dB (26 dB corresponds to the 97 percentile of normal values)
- **Red, abnormal:** Represents the inability of the patient to detect an stimuli of 26 dB



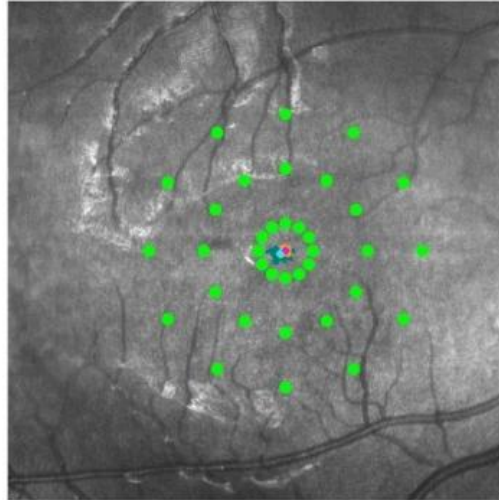
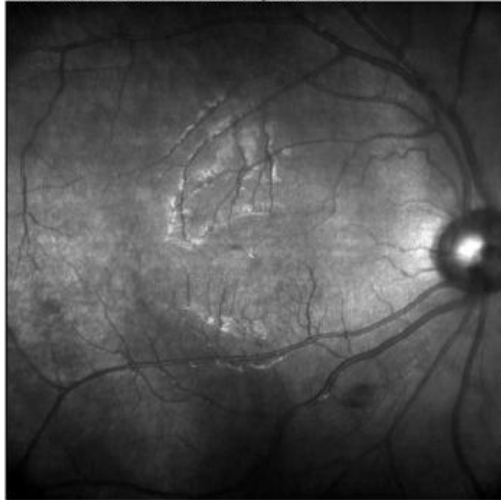
- OD



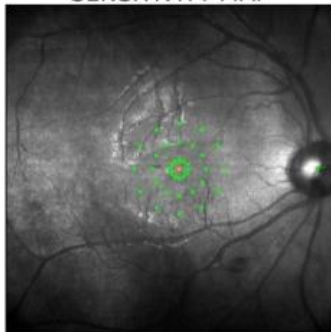
09-May-1991 (23)

Fast exam #458 / 25-Mar-2015, 10:35 / Duration: 1' 46" / Stimuli duration: 200 ms

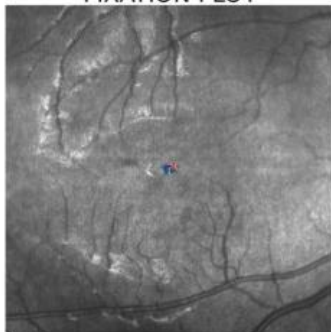
Patient code: 1741102 / Reliability Index: 100%



SENSITIVITY MAP



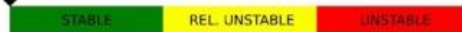
FIXATION PLOT



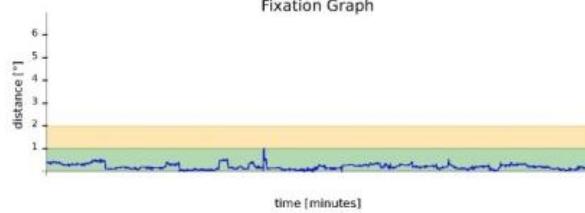
Macular Integrity



Fixation Stability



Fixation Graph



Bivariate Contour Ellipse Area:  
 63% BCEA: 0.2° x 0.1°, Area = 0.1°<sup>2</sup>, angle = -3.4°  
 95% BCEA: 0.6° x 0.3°, Area = 0.6°<sup>2</sup>, angle = -3.4°

Notes:

Figure 5.6 Fast exam microperimetry (MAIA™) in a normal subject

optipunt eye clinic

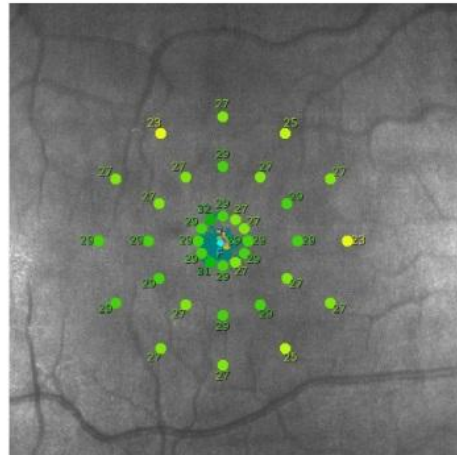
- OD



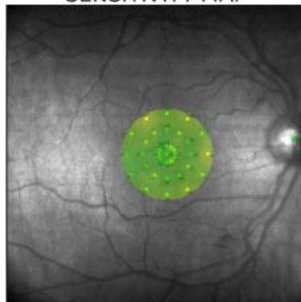
15-May-1993 (22)

Expert exam #551 [4-2 strategy] / 18-Jul-2015, 16:49 / Duration: 5' 55" / Stimuli duration: 200 ms

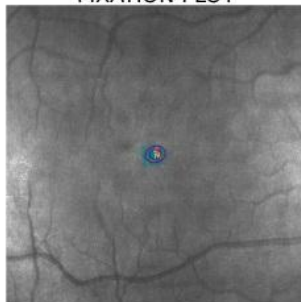
Patient code: 1821702 / Fixation Losses: 0%



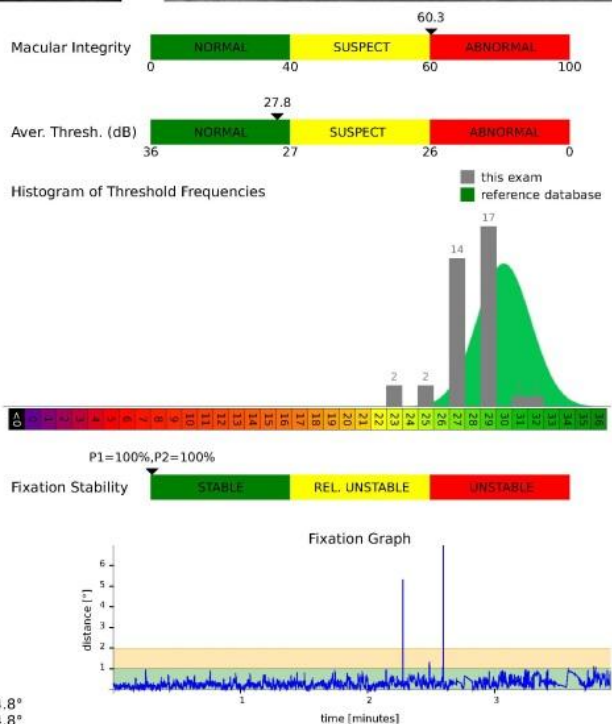
SENSITIVITY MAP



FIXATION PLOT



Bivariate Contour Ellipse Area:  
63% BCEA: 0.7°x0.6°, Area = 0.3°², angle = 14.8°  
95% BCEA: 1.2°x1.0°, Area = 0.9°², angle = 14.8°



Notes:

**Figure 5.7** Expert exam printout (MAIA™) in a normal subject: the top left represents the scanning laser ophthalmoscope (SLO) image of the fundus; the top right represents sensitivity values and preferred retinal loci (PRL); the histogram shows threshold values in grey compared with the normal distribution in green

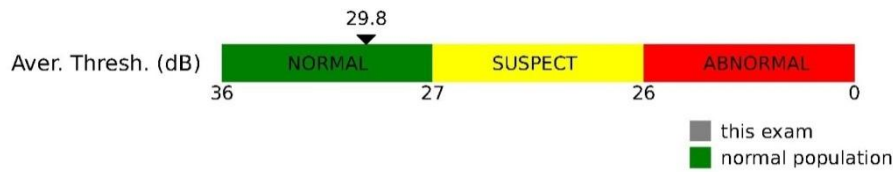


**Figure 5.8** Retinal sensitivity in normal macula (colour code scale)

Similarly, the fixation stability index (**Figure 5.9**) follows the classification:

- **Stable:** If there is more than 75% spread in fixation points within the inner circle (fixation ring of 2° in diameter).
- **Relatively unstable:** If there is more than 75% spread in fixation points within the outer circle (fixation ring of 4° in diameter) and less than 75% spread in fixation points in the inner circle (fixation ring of 2° in diameter).
- **Unstable:** If there is less than 75% spread of fixation points within the outer circle (fixation ring of 4° in diameter).

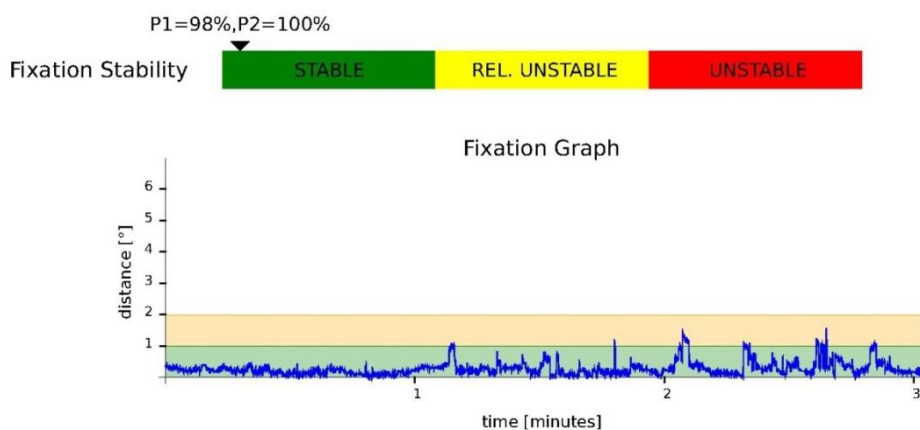


**Figure 5.9** Fixation stability scale in a normal subject that represents P1 (inner ring of 2° in diameter) and P2 (outer ring 4° in diameter), while in this case the fixation was maintained on the central 1° during 98% of the examination time.

In addition, the instrument offers the **fixation plot**, a quantitative indicator of fixation stability in which the position of each fixation point is represented and is calculated in an elliptical area using the Bivariate Contour Ellipse Area (BCEA) method, providing a fixation stability value with decreased values denoting stable fixation. The automatic calculation of the elliptical area to quantify fixation stability is an exclusive feature of MAIA™ (Crossland et al., 2004). (**Figure 5.10**)

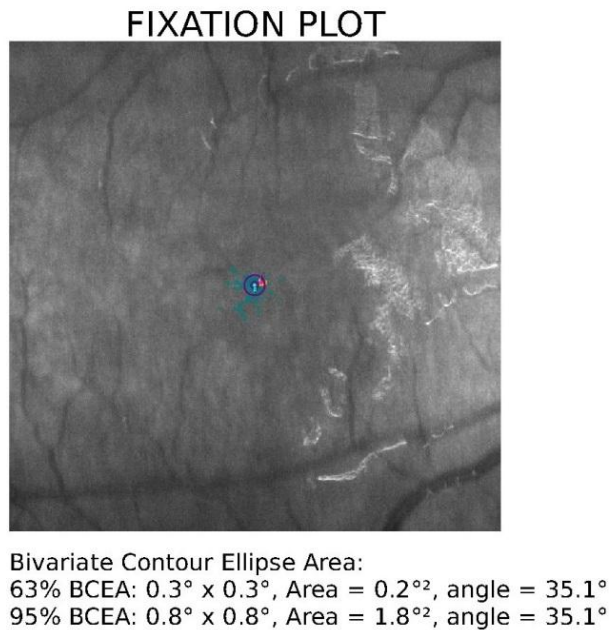


**Figure 5.10** Fixation points over  $2^{\circ}$  and  $4^{\circ}$  diameter rings in a normal subject

Finally, the **macular integrity index** indicates whether the threshold values are normal, suspicious, or abnormal (**Figure 5.11**) in reference to age-corrected paired-normative data.

- **Green:** normal intensity.
- **Yellow:** within to 2 standard deviations of normality.
- **Red:** within to 3 standard deviations of normality.

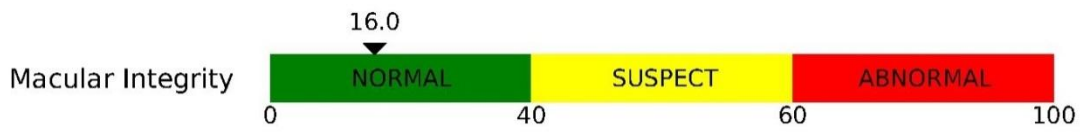


**Figure 5.11** Macular integrity index in a normal subject

As an example, **Figure 5.12** shows a retinal sensitivity map of a normal subject.

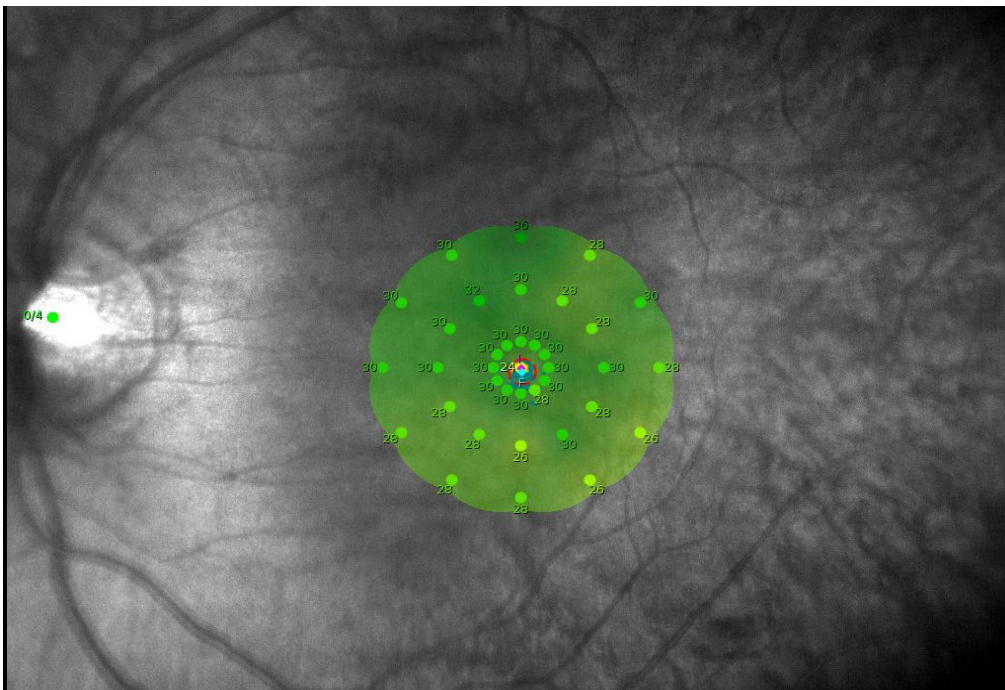


**Figure 5.12** Retinal sensitivity in a normal macula: the red circle represents the fixation point to which the patient must look during the test, with a number at the centre denoting central sensitivity (CS); the first ring represents the sensitivity at 1° (the average is S1); the second ring represents the sensitivity at 3° (S2), and the third ring represents the sensitivity at 5° (S3). Interpretation of the figure enables examiners to detect scotomas. The green dot at the centre of the optic nerve represents the blind spot.



For the purpose of the present study (general objective and specific objective 7), structural (anatomical) and functional (retinal sensitivity) characteristics were assessed in the same, that is, corresponding areas of the retina (**Figure 5.13**).

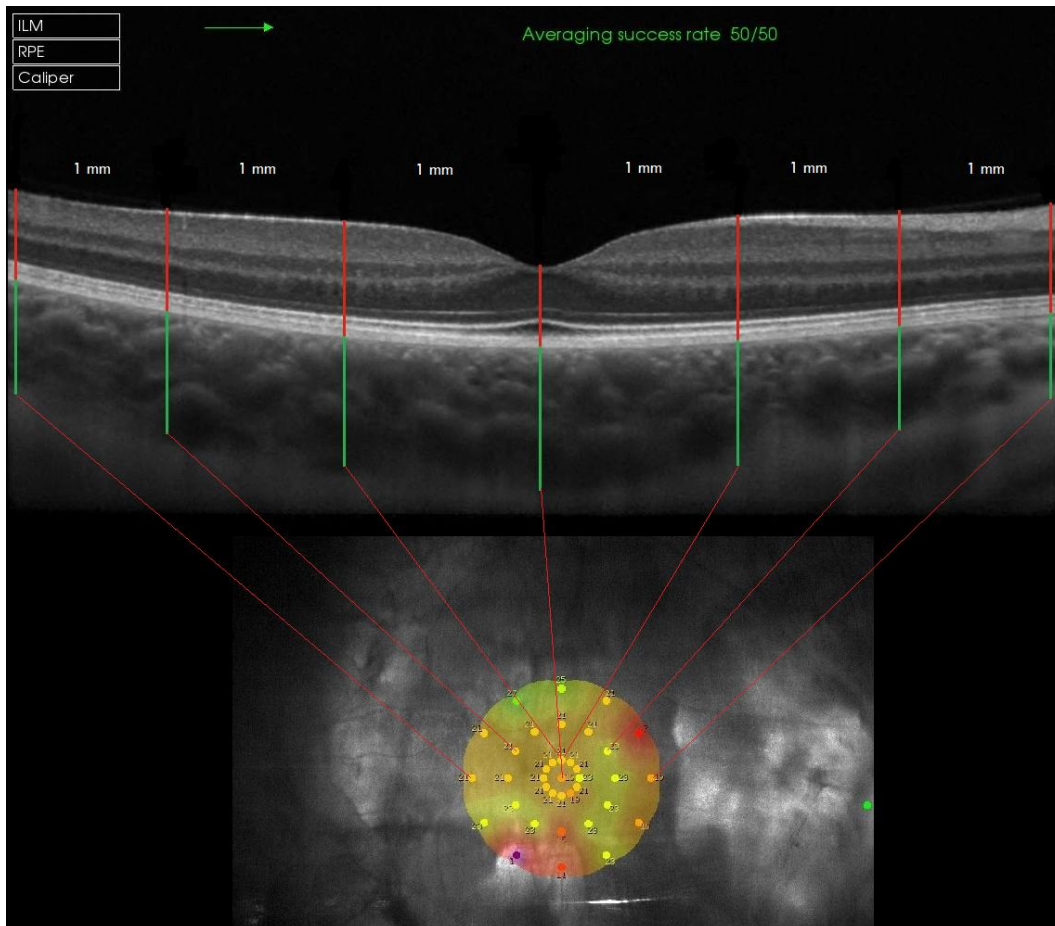


**Figure 5.13** The structural and functional macular assessment

### 5.3 Statistical Analysis

Statistical analysis was conducted with the statistical package IBM SPSS, V. 19 (IBM, Inc, USA) for Windows. Data was compiled in an Excel file, which allowed for basic statistical exploration, and later was transferred to SPSS for statistical analysis.

All data was examined for normality with the Kolmogorov-Smirnov test to determine the type of statistical approach required for data analysis (parametric or non-parametric tests). Descriptive statistics were employed to summarize our results of the various fundus parameters under study, as well as of the resulting inter-ocular differences. Therefore, either mean and standard deviation (SD) or median and interquartile range (IR) was presented. Besides, the 2.5<sup>th</sup> and 97.5<sup>th</sup> percentiles were calculated to define the thresholds for normal inter-ocular asymmetry of the various anatomical and functional parameters.

Inferential statistics were conducted with the Student t-test for matched pairs when comparing data from right and left eyes or with the Student t-test for unmatched pairs if data belongs to different study groups (such as control and high myopia groups). If data did not follow a Gaussian distribution, the corresponding Wilcoxon and Mann-Whitney tests were used instead.

Finally, in order to investigate the possible associations among the various parameters under study, particularly between structural and functional data and between asymmetry and refractive error, the Pearson or the Spearman correlation tests were employed. Correlations were defined as weak, moderate or strong if  $r$  (rho) is between 0.4 and 0.6, between 0.6 and 0.8 and greater than 0.8, respectively. A p-value <0.05 was considered as the threshold for statistical significance.





## 6. Results and Discussion

In this Chapter we will summarize and discuss the main findings of the present research. We will structure the presentation following the specific objectives described in [Chapter 4](#) of this thesis.

### 6.1. Measuring retinal thickness asymmetry using SD-OCT in normal patients:

Aiming at gaining a complete understanding of normal structural asymmetry in non-pathological myopia, and given the lack of studies exploring the physiological asymmetry in young patients, a sample of young adults between the ages of 12 and 23 years and a spherical equivalent that ranged from -3.00 to +4.00 D was selected.

#### *Demographics, refraction and visual acuity of young adults*

Thirty-seven subjects (23 females; 14 males) participated in this study, with an age of  $17.4 \pm 3.5$  years (mean  $\pm$  SD), ranging from 12 to 23 years. [Table 6.1](#) shows a summary of spherical equivalent (SE) and distance corrected visual acuity (CDVA) of right (OD) and left (OS) eyes. No statistically significant inter-ocular differences were found in these parameters.

Parameter	Mean	Median	Interquartile range	Z	p
CDVA (logMAR) OD	0.025	0.000	0.05	-1.342	0.180
CDVA (logMAR) OS	0.021	0.000	0.05		
SE OD (D)	-1.33	-1.00	2.50	-1.297	0.195
SE OS (D)	-1.23	-1.00	2.50		

**Table 6.1** Study sample corrected distance visual acuity (CDVA) (logMAR) and spherical equivalent (SE) (D) for right (OD) and left (OS) eyes. Data is presented as mean, median and interquartile range. The Wilcoxon test was used to assess inter-ocular differences (Z and p values are shown).

*Retinal parameters of young adults*

**Table 6.2** presents a summary of RNFL, macular and disc parameters for both eyes. Statistically significant differences were found between right and left eye in mean RNFL thickness (median values of 102  $\mu\text{m}$  in OD and 104  $\mu\text{m}$  in OS,  $p = 0.003$ ), superior quadrant RNFL thickness (125  $\mu\text{m}$  in OD and 130  $\mu\text{m}$  in OS,  $p = 0.008$ ) and central macular thickness (183  $\mu\text{m}$  in OD and 200  $\mu\text{m}$  in OS,  $p = 0.039$ ). No statistically significant differences were found between both eyes in the rest of retinal parameters under study. In both eyes, RNFL was thicker in the inferior quadrant, followed by the superior, nasal and temporal quadrants (ISNT).

Inter-ocular differences in retinal parameters are shown in **Table 6.3**, which also displays the 95% limits of difference in terms of the 2.5<sup>th</sup> and 97.5<sup>th</sup> percentiles. It may be noted that disc parameters were very symmetrical, with a median difference of 0.025  $\text{mm}^2$  in disc diameter, 0.04  $\text{mm}^2$  in rim area and 0.02 in CDR.

Parameter	Mean	Median	Interquartile range	Z	p
Mean RNFL th. OD ( $\mu\text{m}$ )	102.81	102.00	11.50	-2.959	<b>0.003</b>
Mean RNFL th. OS ( $\mu\text{m}$ )	104.51	104.00	10.00		
S RNFL th. OD ( $\mu\text{m}$ )	124.05	125.00	21.00	-2.658	<b>0.008</b>
S RNFL th. OS ( $\mu\text{m}$ )	128.40	130.00	20.50		
I RNFL th. OD ( $\mu\text{m}$ )	130.18	134.00	18.50	-1.528	0.126
I RNFL th. OS ( $\mu\text{m}$ )	132.75	135.00	19.00		
N RNFL th. OD ( $\mu\text{m}$ )	82.081	84.00	21.50	-0.340	0.734
N RNFL th. OS ( $\mu\text{m}$ )	82.72	80.00	21.00		
T RNFL th. OD ( $\mu\text{m}$ )	74.75	75.00	8.50	-0.961	0.337
T RNFL th. OS ( $\mu\text{m}$ )	74.21	73.00	12.50		
Rim area OD ( $\text{mm}^2$ )	1.88	1.89	0.54	-0.664	0.507
Rim area OS ( $\text{mm}^2$ )	1.92	1.93	0.58		
Disc area OD ( $\text{mm}^2$ )	2.45	2.49	0.57	-1.430	0.153
Disc area OS ( $\text{mm}^2$ )	2.48	2.47	0.57		
CDR OD	0.22	0.21	0.18	-1.318	0.187
CDR OS	0.24	0.24	0.18		
Central macular th. OD ( $\mu\text{m}$ )	194.73	183.00	26.00	-2.067	<b>0.039</b>
Central macular th. OS ( $\mu\text{m}$ )	200.03	200.00	30.00		
Macular Vol. OD ( $\text{mm}^3$ )	7.75	7.72	0.48	-0.574	0.566
Macular Vol. OS ( $\text{mm}^3$ )	7.75	7.75	0.55		
Mean macular th. OD ( $\mu\text{m}$ )	274.21	273.50	17.05	-0.558	0.577
Mean macular th. OS ( $\mu\text{m}$ )	274.35	274.20	19.55		

**Table 6.2** Summary of RNFL, macular and disc parameters for both eyes (RNFL: retinal nerve fibre layer; th: thickness; OD: right eye; OS: left eye, S: superior; I: inferior; N: nasal; T: temporal; CDR: cup to disc ratio; Vol: volume)

Parameter differences (OD-OS)	Mean	Median	Interquartile range	2.5 <sup>th</sup> perc.	97.5 <sup>th</sup> perc.
<b>Mean RNFL th. (<math>\mu\text{m}</math>)</b>	-1.70	-1.00	4.00	-9.00	6.00
<b>S RNFL th. (<math>\mu\text{m}</math>)</b>	-4.35	-4.00	9.50	-28.00	9.00
<b>I RNFL th. (<math>\mu\text{m}</math>)</b>	-2.56	-2.00	10.00	-25.00	14.00
<b>N RNFL th. (<math>\mu\text{m}</math>)</b>	-0.64	-2.00	14.50	-20.00	18.00
<b>T RNFL th. (<math>\mu\text{m}</math>)</b>	0.54	2.00	6.50	-13.00	12.00
<b>Rim area (<math>\text{mm}^2</math>)</b>	-0.04	-0.04	0.29	-1.01	0.35
<b>Disc area (<math>\text{mm}^2</math>)</b>	-0.03	-0.09	0.38	-1.20	2.07
<b>CDR</b>	-0.02	-0.02	0.10	-0.28	0.12
<b>Central macular th. (<math>\mu\text{m}</math>)</b>	-5.30	-9.00	21.00	-39.00	29.00
<b>Macular Vol. (<math>\text{mm}^3</math>)</b>	-0.00	0.00	0.13	-0.33	0.46
<b>Mean macular th. (<math>\mu\text{m}</math>)</b>	-0.13	0.00	4.45	-11.80	16.10

**Table 6.3** Inter-ocular difference in retinal parameters (right eye - left eye). Data is presented as mean, median and interquartile range. Limits of difference are shown as the 2.5<sup>th</sup> and 97.5<sup>th</sup> percentiles. (RNFL: retinal nerve fibre layer; th: thickness; OD: right eye; OS: left eye, S: superior; I: inferior; N: nasal; T: temporal; CDR: cup to disc ratio; Vol: volume)

Overall, our measured absolute retinal parameter values are in agreement with those reported in previous studies, with small discrepancies accounting for the characteristics of each specific study population (age, ethnicity, etc.) and device employed for retinal exploration (time-domain OCT, spectral-domain OCT), as well as to the actual scan protocol (standard, fast, etc.) that was applied. In particular, in both eyes RNFL thickness follows the documented ISNT rule, with the thickest and thinner values corresponding to the inferior and temporal quadrants, respectively (Dave and Shah, 2015).

Statistically significant differences were found between the right and left eyes in mean and superior quadrant RNFL thickness, with larger thickness values in the left eye in both instances. Regarding mean RNFL thickness, these findings are in disagreement with previous reports in which either no significant inter-ocular difference was found (Altemir et al., 2013; Larsson et al., 2011; Huynh et al., 2007; Hong et al., 2015) or the right eye was found to present thicker mean RNFL thickness values than the left (Mwanza et al., 2011; Budenz, 2008; Park et al., 2005). It must be noted that our 2.5<sup>th</sup> and 97.5<sup>th</sup> percentiles of inter-ocular

difference tolerance limits of  $-9.00 \mu\text{m}$  and  $6.00 \mu\text{m}$  are lower than those reported in Caucasian children by Altemir et al ( $-12.00 \mu\text{m}$  and  $13.00 \mu\text{m}$ ) (Altemir et al., 2013) and Huynh et al ( $-16.00 \mu\text{m}$  and  $17.00 \mu\text{m}$ ) (Huynh et al., 2007), and in Korean adults by Park et al ( $-19.11 \mu\text{m}$  and  $25.61 \mu\text{m}$ ) (Park et al., 2005), although the latter two studies were conducted with an earlier OCT version. In contrast, our findings are comparable with those of Hong et al ( $-8.14 \mu\text{m}$  and  $8.00 \mu\text{m}$ ), in a sample of adults, also of Korean ethnicity (Hong et al., 2015). The narrow limits of tolerance range in mean RNFL thickness which was found in the present sample of patients may be explained by our strict inclusion/exclusion criteria with reference to inter-ocular differences in refractive error and/or axial length. In effect, the importance of taking into consideration refractive error differences when assessing physiological asymmetry was evidenced by the statistically significant, albeit weak, correlation which was encountered between refractive error and mean RNFL thickness in both eyes ( $\rho = 0.401$ ;  $p = 0.014$  in OD and  $\rho = 0.379$ ;  $p = 0.021$  in OS).

Interestingly, statistically significant differences were encountered between males and females in both age (median of 19 years in males versus 15 years in females,  $p = 0.018$ ) and in mean RNFL thickness in the right eye (median of  $106 \mu\text{m}$  in males versus  $99 \mu\text{m}$  in females,  $p = 0.020$ ), but not in the left eye, even though no correlation was uncovered between age and mean RNFL thickness, hence dismissing the possible confounding effect of age on this finding. No clear consensus exists in the literature about the actual influence of age and gender on both absolute parameters and inter-ocular asymmetry. Thus, while some authors failed to observe any association between age and retinal parameters (Larsson et al., 2011; Salchow et al., 2006), other authors reported a decrease of  $2 \mu\text{m}$  per decade in mean RNFL thickness (Budenz et al., 2007), resulting in increased inter-ocular asymmetry (Budenz, 2008). Similarly, Turk et al (2012) described a statistically significant difference between boys and girls in RNFL in the inferior quadrant, although other authors failed to encounter any influence of gender on retinal parameters (Larsson et al., 2011; Budenz et al., 2007).

Discrepancies were more manifest in the quadrant per quadrant RNFL thickness analysis of inter-ocular asymmetry, in which a statistically significant difference between right and left eyes was found in the superior quadrant, with 95% limits of tolerance of  $-28.00 \mu\text{m}$  and  $9 \mu\text{m}$ . In effect, whereas previous authors also noted thicker RNFL values in the left eye in the superior quadrant (Altemir et al., 2013; Mawanza et al., 2011; Huynh et al., 2007; Hong et al., 2015), the same authors described other quadrant asymmetries, with nasal and temporal quadrants in the right eye commonly presenting thicker RNFL values than in the left eye. On the contrary, our findings did not reveal significant inter-ocular differences in nasal, temporal and inferior quadrants.

In agreement with previous studies reporting good symmetry for mean macular thickness (Sullivan-Mee et al., 2013), no statistically significant inter-ocular difference was found in this parameter. In contrast, central macular thickness was found to present with statistically significant inter-ocular differences, with larger values in the left eye and 95% tolerance limits at  $-39.00 \mu\text{m}$  and  $29.00 \mu\text{m}$ . Both Altemir et al (2013) and Huynh et al (2007) failed to report significant differences in central macular thickness, although their 95% tolerance limits were not dissimilar to those found in the present research, with values of  $-17.60 \mu\text{m}$  and  $23.20 \mu\text{m}$  and of  $-22.00 \mu\text{m}$  and  $22.00 \mu\text{m}$ , respectively. It is worth mentioning, to approximate an explanation for this discrepancy, that macular thickness and volume are also highly sensitive to ethnicity, both in adults and in children (Huynh et al., 2006; El-Dairi et al., 2009).

In addition to this particular age group, **the normal asymmetry in the control group of age- and gender-matched normal patients was explored** to allow for a better comparison with the myopia group.

*Demographics, refraction and visual acuity of the control group*

Forty-five subjects (23 females; 22 males) were enrolled in the control group, with an age of  $39.9 \pm 14.1$  years, ranging from 16 to 68 years. **Table 6.4** presents a summary of SE and CDVA of both eyes. No statistically significant inter-ocular differences were found in these parameters.

Parameter	Mean	Median	Interquartile range	Z	p
CDVA (logMAR) OD	0.019	0.000	0.000	-0.816	0.414
CDVA (logMAR) OS	0.016	0.000	0.000		
SE OD (D)	-0.22	0.00	1.00	-0.346	0.730
SE OS (D)	-0.21	0.00	0.75		

**Table 6.4** Study sample corrected distance visual acuity (CDVA) (logMAR) and spherical equivalent (SE) (D) for right (OD) and left (OS) eyes for the control group. Data is presented as mean, median and interquartile range. The Wilcoxon test was used to assess interocular differences (Z and p values are shown).

*Retinal parameters of the control group*

With the inclusion of an age- and gender-matched group of healthy subjects we aimed at further understanding the occurrence of any asymmetry in retinal and/or choroidal structures and functions encountered in high myopia.

**Table 6.5** presents a summary of RNFL and macular parameters for both eyes. Statistically significant differences were found between right and left eye in the macular regions at 1 mm nasally (mean values of 309.29  $\mu\text{m}$  in OD and 295.26  $\mu\text{m}$  in OS,  $p = 0.015$ ), 2 mm nasally (mean values of 294.54  $\mu\text{m}$  in OD and 264.31  $\mu\text{m}$  in OS,  $p < 0.001$ ), 3 mm nasally (mean values of 267.94  $\mu\text{m}$  in OD and 233.20

$\mu\text{m}$  in OS,  $p < 0.001$ ), 1 mm temporally (mean values of 291.57  $\mu\text{m}$  in OD and 313.14  $\mu\text{m}$  in OS,  $p = 0.001$ ), 2 mm temporally (mean values of 263.69  $\mu\text{m}$  in OD and 302.06  $\mu\text{m}$  in OS,  $p < 0.001$ ), and 3 mm temporally (mean values of 227.26  $\mu\text{m}$  in OD and 270.43  $\mu\text{m}$  in OS,  $p < 0.001$ ). No other statistically significant differences were found between both eyes in the control group.

Parameter	OD		OS		t	p
	Mean	SD	Mean	SD		
Central RNFL th. ( $\mu\text{m}$ )	187.51	17.31	186.83	25.16	0.18	0.860
1 mm N RNFL th. ( $\mu\text{m}$ )	309.29	37.97	295.26	20.17	2.56	<b>0.015</b>
2 mm N RNFL th. ( $\mu\text{m}$ )	294.54	26.10	264.31	16.88	6.12	<b>&lt;0.001</b>
3 mm N RNFL th. ( $\mu\text{m}$ )	267.94	18.27	233.20	16.88	10.80	<b>&lt;0.001</b>
1 mm T RNFL th. ( $\mu\text{m}$ )	291.57	33.84	313.14	25.84	-3.73	<b>0.001</b>
2 mm T RNFL th. ( $\mu\text{m}$ )	263.69	25.95	302.06	15.49	-8.43	<b>&lt;0.001</b>
3 mm T RNFL th. ( $\mu\text{m}$ )	227.26	14.74	270.43	15.85	-13.52	<b>&lt;0.001</b>
1 mm S RNFL th. ( $\mu\text{m}$ )	316.00	22.57	318.54	22.06	-0.94	0.356
2 mm S RNFL th. ( $\mu\text{m}$ )	283.31	15.09	277.74	33.63	0.99	0.327
3 mm S RNFL th. ( $\mu\text{m}$ )	256.09	21.43	255.60	16.31	0.13	0.897
1 mm I RNFL th. ( $\mu\text{m}$ )	312.46	18.74	314.00	18.88	-0.72	0.475
2 mm I RNFL th. ( $\mu\text{m}$ )	273.20	17.30	271.51	13.99	0.64	0.529
3 mm I RNFL th. ( $\mu\text{m}$ )	239.31	14.79	244.86	24.70	-1.34	0.188
1 mm Mean RNFL th. ( $\mu\text{m}$ )	307.36	22.64	310.26	20.44	-1.06	0.298
2 mm Mean RNFL th. ( $\mu\text{m}$ )	278.71	16.32	278.93	13.46	-0.08	0.938
3 mm Mean RNFL th. ( $\mu\text{m}$ )	247.68	13.52	251.04	13.23	-1.77	0.09
Central macular th. ( $\mu\text{m}$ )	200.03	33.36	197.57	21.42	0.65	0.518
Macular Vol. ( $\text{mm}^3$ )	7.88	0.35	7.91	0.33	-0.71	0.484
Mean macular th. ( $\mu\text{m}$ )	277.87	12.98	278.60	14.30	-0.34	0.732

**Table 6.5** Summary of RNFL and macular parameters for both eyes for the control group. The t-test for matched pairs was used for statistical analysis (t and p values are shown). (RNFL: retinal nerve fibre layer; th: thickness; OD: right eye; OS: left eye, S: superior; I: inferior; N: nasal; T: temporal; Vol: volume)

Inter-ocular differences in retinal parameters are shown in **Table 6.6**, which also displays the 95% limits of difference in terms of the 2.5<sup>th</sup> and 97.5<sup>th</sup> percentiles.

Parameter differences (OD-OS)	Mean	SD	2.5 <sup>th</sup> perc.	97.5 <sup>th</sup> perc.
Central RNFL th. ( $\mu\text{m}$ )	0.69	22.89	-105.00	52.00
1 mm N RNFL th. ( $\mu\text{m}$ )	14.03	32.48	-160.00	45.00
2 mm N RNFL th. ( $\mu\text{m}$ )	30.23	29.22	-107.00	93.00
3 mm N RNFL th. ( $\mu\text{m}$ )	34.74	19.03	-15.00	83.00
1 mm T RNFL th. ( $\mu\text{m}$ )	-21.57	34.20	-189.00	74.00
2 mm T RNFL th. ( $\mu\text{m}$ )	-38.37	26.92	-165.00	00
3 mm T RNFL th. ( $\mu\text{m}$ )	-43.17	18.90	-92.00	26.00
1 mm S RNFL th. ( $\mu\text{m}$ )	-2.54	16.07	-70.00	41.00
2 mm S RNFL th. ( $\mu\text{m}$ )	5.57	33.11	-37.00	176.00
3 mm S RNFL th. ( $\mu\text{m}$ )	0.49	22.02	-44.00	106.00
1 mm I RNFL th. ( $\mu\text{m}$ )	-1.54	12.62	-28.00	35.00
2 mm I RNFL th. ( $\mu\text{m}$ )	1.69	15.66	-50.00	41.00
3 mm I RNFL th. ( $\mu\text{m}$ )	-5.54	24.40	-84.00	60.00
1 mm Mean RNFL th. ( $\mu\text{m}$ )	-2.90	16.22	-78.25	31.00
2 mm Mean RNFL th. ( $\mu\text{m}$ )	-0.22	16.69	-73.00	37.50
3 mm Mean RNFL th. ( $\mu\text{m}$ )	-3.37	11.24	-21.00	35.00
Central macular th. ( $\mu\text{m}$ )	2.46	22.26	-74.00	58.00
Macular Vol. ( $\text{mm}^3$ )	-0.04	0.30	-1.31	0.46
Mean macular th. ( $\mu\text{m}$ )	-0.72	12.33	-46.70	34.70

**Table 6.6** Inter-ocular difference in retinal parameters (right eye - left eye) for the control group. Data is presented as mean  $\pm$  SD. Limits of difference are shown as the 2.5<sup>th</sup> and 97.5<sup>th</sup> percentiles. (RNFL: retinal nerve fibre layer; th: thickness; OD: right eye; OS: left eye, S: superior; I: inferior; N: nasal; T: temporal; Vol: volume)

As seen in **Table 6.5**, The RNFL was thicker at 1 mm followed by 2 mm and 3 mm, that is, RNFL is thicker towards the centre of the macula and is progressively thinner towards the periphery. Besides, within each peripheral ring location, the distribution of RNFL thickness in the four quadrants does not follow the same pattern (See **Figure 6.1**), with further differences between eyes in this distribution of thickness. Indeed, at 1 mm and right eye, the superior quadrant is thicker, followed by the inferior, nasal and temporal quadrants (SINT). Conversely, the order for the left eye at 1 mm is SITN. At the 2 and 3 mm rings the thickness order at the different quadrants is NSIT for the right eye and TSIN for the left eye. It interesting to mention that whereas the nasal quadrant is always thinner in the left eye, the temporal quadrant is always thinner at the right eye, irrespective of the distance from the centre of the macula. In



agreement with previous research of Wu et al (2008), who explored normal eyes at 3 mm and at 6 mm in the four quadrants around the centre of the macula, the retina progressively thins towards the periphery.

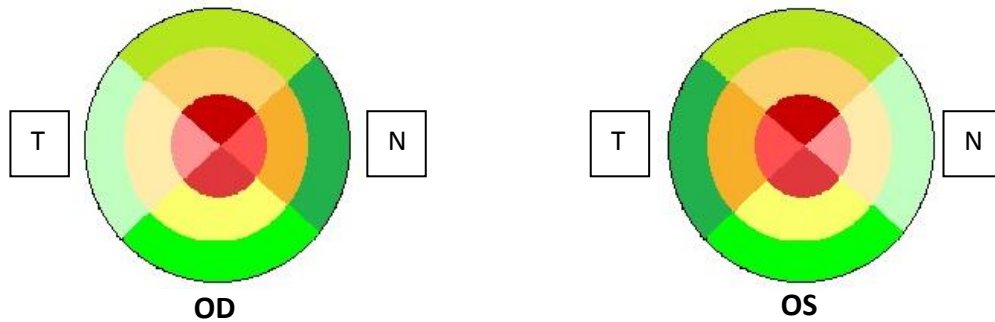


**Figure 6.1** The distribution of RNFL thickness in the four quadrants in control group. Within each peripheral ring location, darker colours denote thicker areas.

In general, our measured absolute retinal parameter values are in agreement with the values presented by previous researchers, although differences in population characteristics (age, ethnicity, etc.) and devices (time-domain OCT, spectral-domain OCT) preclude further comparisons.

It must be noted that our 2.5<sup>th</sup> and 97.5<sup>th</sup> percentiles of inter-ocular difference tolerance limits in mean RNFL thickness of  $-105 \mu\text{m}$  and  $52 \mu\text{m}$  are higher than those reported in Caucasian children by Altemir et al ( $-12.00 \mu\text{m}$  and  $13.00 \mu\text{m}$ ) (Altemir et al., 2013) and Huynh et al ( $-16.00 \mu\text{m}$  and  $17.00 \mu\text{m}$ ) (Huynh et al., 2007), and in Korean adults by Park et al ( $-19.11 \mu\text{m}$  and  $25.61 \mu\text{m}$ ) (Park et al., 2005), and Hong et al ( $-8.14 \mu\text{m}$  and  $8.00 \mu\text{m}$ ) (Hong et al., 2015). The wide limits of tolerance range which were found in the present sample of patients may be explained by the differences in the age of the participants between the various studies, as age may affect both absolute parameters and inter-ocular asymmetry. This was firstly reported by Budenz et al (2007), with the authors describing a decrease of  $2 \mu\text{m}$  per decade in mean RNFL thickness. However, these findings

may be interpreted with caution, as no correlation was uncovered between age and any of the retinal parameters under study in the present sample of patients.

In agreement with the previous studies reporting good symmetry for mean macular thickness (Sullivan-Mee et al., 2013), no statistically significant inter-ocular difference was found in this parameter. Finally, no statistically significant differences were found between males and females in any of the parameters under evaluation.

## 6.2. Measuring choroidal thickness in normal patients using the enhanced depth imaging (EDI) technique of the SD – OCT:

In this section we will present the results of choroidal asymmetry in the control group of age- and gender-matched normal patients.

First, **Table 6.7** displays a summary of the various choroidal parameters for both eyes, including, central choroidal thickness, thickness at each quadrant for each of the three peripheral rings and average thickness of each of these rings.

Parameter	OD		OS		t	p
	Mean	SD	Mean	SD		
Central choroidal th. ( $\mu\text{m}$ )	307.31	13.77	309.80	18.12	-0.717	0.478
1 mm N choroidal th. ( $\mu\text{m}$ )	277.03	13.74	278.06	13.97	6.612	<b>&lt;0.001</b>
1 mm T choroidal th. ( $\mu\text{m}$ )	252.51	16.20	254.23	17.61	-0.433	0.668
1 mm S choroidal th. ( $\mu\text{m}$ )	212.74	19.14	214.70	24.13	-0.396	0.695
1 mm I choroidal th. ( $\mu\text{m}$ )	285.60	11.32	290.71	14.75	-1.514	0.139
2 mm N choroidal th. ( $\mu\text{m}$ )	263.77	10.64	268.91	15.52	-1.650	0.108
2 mm T choroidal th. ( $\mu\text{m}$ )	224.20	14.61	231.09	14.30	-2.616	<b>0.013</b>
2 mm S choroidal th. ( $\mu\text{m}$ )	301.60	20.52	304.40	18.57	-0.699	0.489
2 mm I choroidal th. ( $\mu\text{m}$ )	259.00	14.45	256.71	18.62	0.569	0.573
3 mm N choroidal th. ( $\mu\text{m}$ )	219.26	17.20	221.60	19.55	-0.686	0.497
3 mm T choroidal th. ( $\mu\text{m}$ )	296.23	13.19	296.89	17.52	-0.172	0.865
3 mm S choroidal th. ( $\mu\text{m}$ )	254.83	13.54	255.66	17.33	-0.222	0.826
3 mm I choroidal th. ( $\mu\text{m}$ )	221.63	17.95	216.34	13.82	1.545	0.132
1 mm mean choroidal th. ( $\mu\text{m}$ )	290.14	10.58	292.54	11.60	-0.954	0.347
2 mm mean choroidal th. ( $\mu\text{m}$ )	257.55	8.86	258.90	9.87	-0.621	0.539
3 mm mean choroidal th. ( $\mu\text{m}$ )	219.48	11.61	220.96	13.41	-0.822	0.417

**Table 6.7** Summary of choroidal parameters for both eyes for the control group. The t-test for matched pairs was used for statistical analysis (t and p values are shown). (th: thickness; OD: right eye; OS: left eye, S: superior; I: inferior; N: nasal; T: temporal)

Statistically significant differences were found between right and left eye in the macular regions away from the centre at 1 mm nasally (mean values of 277.03  $\mu\text{m}$  in OD and 278.06  $\mu\text{m}$  in OS,  $p < 0.001$ ), and 2 mm temporally (mean values of 224.20  $\mu\text{m}$  in OD and 231.09  $\mu\text{m}$  in OS,  $p = 0.013$ ). No statistically significant

differences were found between both eyes in the rest of choroidal parameters under study.

In both eyes, in average the choroidal was thicker at the 1 mm ring (mean values of 290.14  $\mu\text{m}$  in OD and 292.54  $\mu\text{m}$  in OS), followed by 2 mm (mean values of 257.55  $\mu\text{m}$  in OD and 258.90  $\mu\text{m}$  in OS), then 3 mm (mean values of 219.48  $\mu\text{m}$  in OD and 220.96  $\mu\text{m}$  in OS).

Besides, as seen in [Table 6.7](#), the choroid was thicker at the centre of the macula in both eyes, followed by 2 mm at the superior quadrant and 3 mm at the inferior quadrant at the left eye. Although the distribution of choroidal thickness in the four quadrants does not follow the same pattern, within each distance and eye, the order of the choroidal thickness at 1 mm was the same for both eyes, with the inferior quadrant being thicker, followed by the nasal, temporal and superior quadrants (INTS). As we move away from the centre of the macula, the order for the right eye at 2 mm is SNIT, and TSIN at 3 mm and for the left eye the order is SNIT and TSNI at 2 and 3 mm, respectively (see [Figure 6.2](#)) It is interesting to mention that, at the 2 mm ring in both eyes, the superior quadrant is always thicker and the temporal quadrant is always thinner.

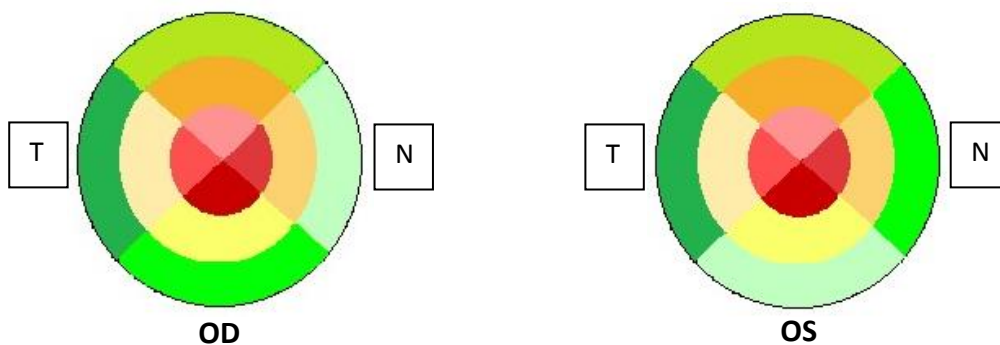


**Figure 6.2** The distribution of choroidal thickness in the four quadrants in control group. Within each peripheral ring location, darker colours denote thicker areas.

In agreement with previous studies reporting the differences in choroidal thickness between the various quadrants (Ding et al., 2011), our findings revealed thicker values at the temporal than at the nasal quadrant only at the 3 mm ring. Overall, the other findings are in agreement with those reported in the literature (Ruiz-Medrano et al., 2015; Tuncer et al., 2015). Nevertheless, as noted above when exploring retinal parameters, discrepancies in choroidal measurements may be explained by different population characteristics (age, ethnicity, etc.) and device employed in this study (EDI technique using choroidal mode, or built-in software of Triton OCT).

Statistically significant differences in choroidal thickness were found between the right and left eyes in the macular regions away from the centre at 1 mm, and 2 mm temporally. Regarding mean choroidal thickness, our findings showing larger values in the left than in the right eye are in disagreement with previous research (Hayreh and Zimmerman, 2014; Ruiz-Medrano et al., 2015; Sohrab et al., 2012), although these differences were not statistically significant. For instance, in the study of Ruiz-Medrano et al (2015), including seventy subjects (40 females; 30 males) with an age of  $25.4 \pm 19.9$  years, ranging from 4 to 75 years, the authors reported that the mean macular nasal choroidal thickness was higher in the right eye than in the left eye (OD:  $228.11 \mu\text{m} \pm 69.23$ ; OS:  $212.27 \mu\text{m} \pm 62.71$ ) and that the mean macular temporal choroidal thickness was lower in the right eye than in the left eye (OD:  $292.02 \mu\text{m} \pm 63.68$ ; OS:  $294.15 \mu\text{m} \pm 54.69$ ). The authors concluded that choroidal thickness was thicker in the right eye in each individual location at the nasal quadrant for males and females except for females at 1 mm nasally, where differences were not statistically significant.

Other authors, such as, Ikuno et al (2010), who investigated seventy-nine normal eyes from 43 patients with an age of  $39.4 \pm 16.0$  years, ranging from 23 to 88 years, using a Prototype 1060-nm HP-OCT, described significantly different subfoveal choroidal thickness than nasal and temporal choroidal thickness (in

addition, the temporal choroid was always thicker than the nasal choroid). Besides, Margolis and Spaide (2009), using an EDI-OCT in thirty normal patients (54 eyes) with a mean age of 50.4 years, ranging from 19 to 85 years (16 males and 14 females), described nasal choroidal thickness values of  $145 \pm 57 \mu\text{m}$  at the 3 mm ring from the fovea, while mean subfoveal choroidal thickness was of  $287 \pm 29 \mu\text{m}$ .

A summary of the inter-ocular differences in choroidal parameters is shown in **Table 6.8**, also showing the 95% limits of difference in terms of the 2.5th and 97.5th percentiles. As far as our literature review has revealed, few authors have explored inter-ocular differences in choroidal thickness. For instance, Chen et al (2012) explored this anatomical structure in fifty normal subjects ranging from 30 to 50 years (mean of 38 years), using an EDI-OCT. The authors reported 2.5th and 97.5th percentiles of inter-ocular difference tolerance limits of  $0.38 \mu\text{m}$  and  $135.13 \mu\text{m}$  for the foveal choroidal thickness.

Parameter differences (OD-OS)	Mean	SD	2.5 <sup>th</sup> perc.	97.5 <sup>th</sup> perc.
Central choroidal th. ( $\mu\text{m}$ )	-2.49	20.52	-72.00	39.00
1 mm N choroidal th. ( $\mu\text{m}$ )	-1.03	19.66	-59.00	42.00
1 mm T choroidal th. ( $\mu\text{m}$ )	-1.71	23.41	-54.00	57.00
1 mm S choroidal th. ( $\mu\text{m}$ )	-1.94	29.03	-65.00	102.00
1 mm I choroidal th. ( $\mu\text{m}$ )	-5.11	19.99	-57.00	37.00
2 mm N choroidal th. ( $\mu\text{m}$ )	-5.14	18.44	-55.00	34.00
2 mm T choroidal th. ( $\mu\text{m}$ )	-6.89	15.57	-48.00	21.00
2 mm S choroidal th. ( $\mu\text{m}$ )	-2.80	23.70	-52.00	37.00
2 mm I choroidal th. ( $\mu\text{m}$ )	2.29	23.77	-45.00	43.00
3 mm N choroidal th. ( $\mu\text{m}$ )	-2.34	20.19	-39.00	41.00
3 mm T choroidal th. ( $\mu\text{m}$ )	-0.66	22.62	-47.00	59.00
3 mm S choroidal th. ( $\mu\text{m}$ )	-0.83	22.11	-37.00	59.00
3 mm I choroidal th. ( $\mu\text{m}$ )	5.29	20.24	-32.00	46.00
1 mm mean choroidal th. ( $\mu\text{m}$ )	-2.40	14.86	-35.00	33.25
2 mm mean choroidal th. ( $\mu\text{m}$ )	-1.35	12.86	-31.75	22.75
3 mm mean choroidal th. ( $\mu\text{m}$ )	-1.47	10.62	-20.50	19.00

**Table 6.8** Inter-ocular difference in choroidal parameters (right eye - left eye) for the control group. Data is presented as mean  $\pm$  SD. Limits of difference are shown as the 2.5<sup>th</sup> and 97.5<sup>th</sup> percentiles. (th: thickness; OD: right eye; OS: left eye, S: superior; I: inferior; N: nasal; T: temporal)

In the present study, none of the choroidal parameters under evaluation were correlated with age. This finding is in contradiction with the work of Margolis and Spaide (2009) in which there was a negative correlation between the age and the choroidal thickness at all points measured.

Finally, our results did not evidence any statistically significant difference in choroidal parameters between males and females in the control group. These findings are in disagreement with a large study including 620 eyes of 310 healthy volunteers with no ophthalmic disease history, including 152 males and 158 females subgrouped according to their ages (Zeng et al., 2012). These authors reported thicker choroidal values for males than females, leading them to suggest a possible explanation for the gender predilection of macular diseases, such as, central serous chorioretinopathy and idiopathic macular hole.

Both discrepancies regarding age and gender may be explained by the particular characteristics of the present sample of patients, which aimed at matching the sample of patients from the myopia group. Therefore, any comparisons with previous research may be approached with caution.

### 6.3. Exploring retinal (macular) sensitivity differences between both eyes in normal patients:

In this section we will summarize and discuss our finding regarding macular sensitivity, that is, visual function, in normal patients, also exploring the normal range of inter-ocular asymmetry in retinal sensitivity.

First, **Table 6.9** displays a summary of the retinal sensitivity parameters for both eyes including central sensitivity and sensitivity at each quadrant for each of the three peripheral rings, as well as mean overall sensitivity and mean sensitivity for each of these rings.

Parameter	OD		OS		t	p
	Mean	SD	Mean	SD		
<b>Central sensitivity (dB)</b>	27.74	2.51	28.09	2.36	-0.760	0.452
<b>1 mm N sensitivity (dB)</b>	27.42	1.86	28.16	1.64	-2.252	<b>0.031</b>
<b>1 mm T sensitivity (dB)</b>	28.37	1.79	28.78	1.63	-1.313	0.198
<b>1 mm S sensitivity (dB)</b>	28.51	2.14	29.07	1.70	-1.700	0.098
<b>1 mm I sensitivity (dB)</b>	27.98	1.96	28.34	1.55	-1.010	0.320
<b>2 mm N sensitivity (dB)</b>	28.03	2.10	28.48	1.26	-1.488	0.146
<b>2 mm T sensitivity (dB)</b>	27.31	1.62	27.75	1.58	-1.633	0.112
<b>2 mm S sensitivity (dB)</b>	27.44	2.24	28.41	1.52	-3.164	<b>0.003</b>
<b>2 mm I sensitivity (dB)</b>	27.69	2.10	28.30	1.30	-1.980	0.056
<b>3 mm N sensitivity (dB)</b>	26.91	1.79	27.78	1.28	-3.350	<b>0.002</b>
<b>3 mm T sensitivity (dB)</b>	26.54	1.92	26.74	1.70	-0.642	0.525
<b>3 mm S sensitivity (dB)</b>	26.69	2.07	27.66	1.52	-3.281	<b>0.002</b>
<b>3 mm I sensitivity (dB)</b>	26.84	1.97	27.55	1.71	-2.866	<b>0.007</b>
<b>1 mm mean sensitivity (dB)</b>	28.04	1.71	28.56	1.46	-2.049	<b>0.048</b>
<b>2 mm mean sensitivity (dB)</b>	27.72	1.91	28.24	1.21	-2.127	<b>0.041</b>
<b>3 mm mean sensitivity (dB)</b>	26.70	1.72	27.43	1.29	-3.356	<b>0.002</b>
<b>Mean Sensitivity (dB)</b>	27.50	1.71	28.07	1.25	-2.831	<b>0.008</b>

**Table 6.9** Summary of retinal sensitivity for both eyes for the control group. The t-test for matched pairs was used for statistical analysis (t and p values are shown). (OD: right eye; OS: left eye, S: superior; I: inferior; N: nasal; T: temporal)



Several statistically significant differences were found between right and left eye in the macular region (mean values of 27.50 dB in OD and 28.07 dB in OS,  $p = 0.008$ ) and away from the centre at several peripheral locations. In all instances the left eye was found to have higher sensitivity than the right eye (larger values in dB). Mean macular sensitivity values gradually decreased towards the periphery, with the lower retinal sensitivity at the 3 mm ring and temporal quadrant in both eyes (mean values 26.54 dB in OD and 26.74 dB in OS), while the higher retinal sensitivity was found at 1 mm in the superior quadrant for both eyes (mean values 28.51 dB in OD and 29.07 dB in OS).

As seen in [Table 6.9](#), the retinal sensitivity in the four quadrants does not follow the same pattern, within each peripheral ring and eye. Thus, at 1 mm and for both eyes higher sensitivity values were found at the superior quadrant, followed by the temporal, inferior and nasal quadrants (STIN). However, at the 2 and 3 mm rings, retinal sensitivity was NIST for the right eye and NSIT for the left eye. It may be observed that the nasal quadrant is always more sensitive at 2 and 3 mm in both eyes, whereas temporal quadrant is always less sensitive (see [Figure 6.3](#)).

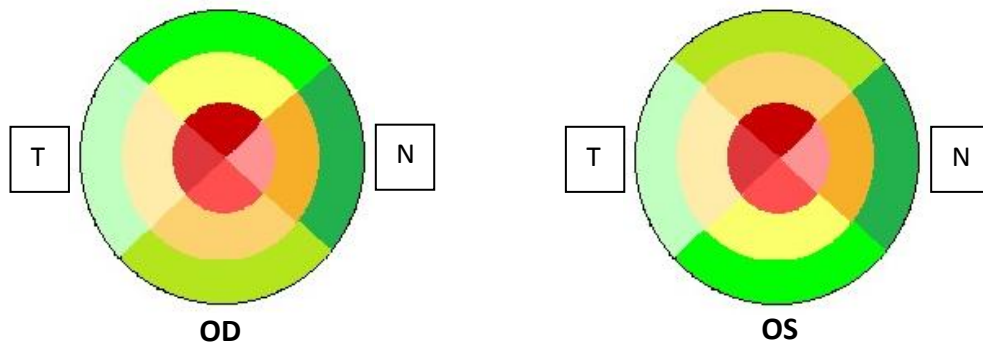


**Figure 6.3** The distribution of retinal sensitivity in the four quadrants in control group. Within each peripheral ring location, darker colours denote thicker areas.

Few studies have explored the retinal sensitivity of normal patients, and, as far as we know, there are no studies assessing the asymmetry of retinal sensitivity in normal subjects. To cite some of these studies, Springer et al. (2005) reported

mean sensitivity values of  $15.5 \pm 0.8$  dB (range of 13.0 – 17.1 dB). Similarly, Parodi et al. (2015) assessed 25 healthy subjects with two microperimeters, MP1 and MAIA™, documenting values of mean sensitivity of the retina of  $28.52 \pm 1.12$  dB as measured by MAIA™. The authors reported that the MAIA™ microperimeter provided a more accurate characterization of visual function than the MP1, especially in cases of high and low retinal sensitivity. Furthermore, Fujiwara et al. (2014) explored the retinal sensitivity in 120 normal Japanese subjects of a wide age range (mean 43.1 years old) using a MAIA™ microperimeter. The authors found that the central sensitivity was significantly lower than the surrounding stimulus positions at 1 degree, 3 degrees, and 5 degrees (26.4 dB, 28.9 dB, 28.7 dB, and 27.8 dB, respectively). These results are partially in agreement with our findings, in which maximum sensitivity was found at 1 mm instead of at the centre of the retina.

A summary of the inter-ocular differences in retinal sensitivity parameters is shown in **Table 6.10**, also showing the 95% limits of difference in terms of the 2.5th and 97.5th percentiles.

Parameter differences (OD-OS)	Mean	SD	2.5 <sup>th</sup> perc.	97.5 <sup>th</sup> perc.
<b>Central sensitivity (dB)</b>	-0.34	2.67	-5.00	8.00
<b>1 mm N sensitivity (dB)</b>	-0.74	1.94	-4.30	2.70
<b>1 mm T sensitivity (dB)</b>	-0.41	1.84	-3.30	2.60
<b>1 mm S sensitivity (dB)</b>	-0.57	1.97	-6.00	3.60
<b>1 mm I sensitivity (dB)</b>	-0.36	2.11	-4.00	6.00
<b>2 mm N sensitivity (dB)</b>	-0.47	1.77	-6.00	3.70
<b>2 mm T sensitivity (dB)</b>	-0.44	1.60	-4.00	2.00
<b>2 mm S sensitivity (dB)</b>	-0.97	1.82	-5.30	2.70
<b>2 mm I sensitivity (dB)</b>	-0.62	1.84	-4.70	2.70
<b>3 mm N sensitivity (dB)</b>	-0.87	1.53	-4.70	1.30
<b>3 mm T sensitivity (dB)</b>	-0.20	1.87	-6.00	4.70
<b>3 mm S sensitivity (dB)</b>	-0.98	1.76	-4.70	2.30
<b>3 mm I sensitivity (dB)</b>	-0.71	1.47	-4.00	1.40
<b>1 mm mean sensitivity (dB)</b>	-0.52	1.50	-4.00	4.00
<b>2 mm mean sensitivity (dB)</b>	-0.51	1.43	-4.20	1.70
<b>3 mm mean sensitivity (dB)</b>	-0.76	1.34	-4.50	1.70
<b>Mean Sensitivity (dB)</b>	-0.60	1.26	-4.20	2.30

**Table 6.10** Inter-ocular difference in retinal sensitivity (right eye - left eye) for the control group. Data is presented as mean  $\pm$  SD. Limits of difference are shown as the 2.5<sup>th</sup> and 97.5<sup>th</sup> percentiles. (OD: right eye; OS: left eye, S: superior; I: inferior; N: nasal; T: temporal)

Finally, we explored the possible correlation of retinal sensitivity with age. The results of this analysis are shown in [Table 6.11](#).

Parameter correlated with age	OD		OS	
	Pearson Correlation (r)	p	Pearson Correlation (r)	p
Central sensitivity (dB)	-0.333	0.050	-0.303	0.077
1 mm N sensitivity (dB)	-0.316	0.064	-0.497	<b>0.002</b>
1 mm T sensitivity (dB)	-0.306	0.074	-0.504	<b>0.002</b>
1 mm S sensitivity (dB)	-0.444	<b>0.008</b>	-0.403	<b>0.016</b>
1 mm I sensitivity (dB)	-0.208	0.231	-0.302	0.078
2 mm N sensitivity (dB)	-0.377	<b>0.026</b>	-0.481	<b>0.003</b>
2 mm T sensitivity (dB)	-0.352	0.038	-0.338	<b>0.047</b>
2 mm S sensitivity (dB)	-0.256	0.138	-0.474	<b>0.004</b>
2 mm I sensitivity (dB)	-0.637	<b>&lt;0.001</b>	-0.434	<b>0.009</b>
3 mm N sensitivity (dB)	-0.346	<b>0.042</b>	-0.295	0.085
3 mm T sensitivity (dB)	-0.345	<b>0.042</b>	-0.283	0.100
3 mm S sensitivity (dB)	-0.293	0.088	-0.346	<b>0.042</b>
3 mm I sensitivity (dB)	-0.377	<b>0.026</b>	0.496	<b>0.002</b>
1 mm mean sensitivity (dB)	-0.352	<b>0.038</b>	-0.519	<b>0.001</b>
2 mm mean sensitivity (dB)	-0.411	<b>0.014</b>	-0.500	<b>0.002</b>
3 mm mean sensitivity (dB)	-0.347	<b>0.041</b>	-0.435	<b>0.009</b>
Mean Sensitivity (dB)	-0.412	<b>0.014</b>	-0.514	<b>0.002</b>

**Table 6.11** Correlation between age and retinal sensitivity parameters for the control group. (OD: right eye; OS: left eye, S: superior; I: inferior; N: nasal; T: temporal)

Statistically significant weak to moderate negative correlations were found between retinal sensitivity at the various locations and age, with slight differences between both eyes. Retinal sensitivity was found to decrease with age (see [Figure 6.4](#) and [6.5](#)).

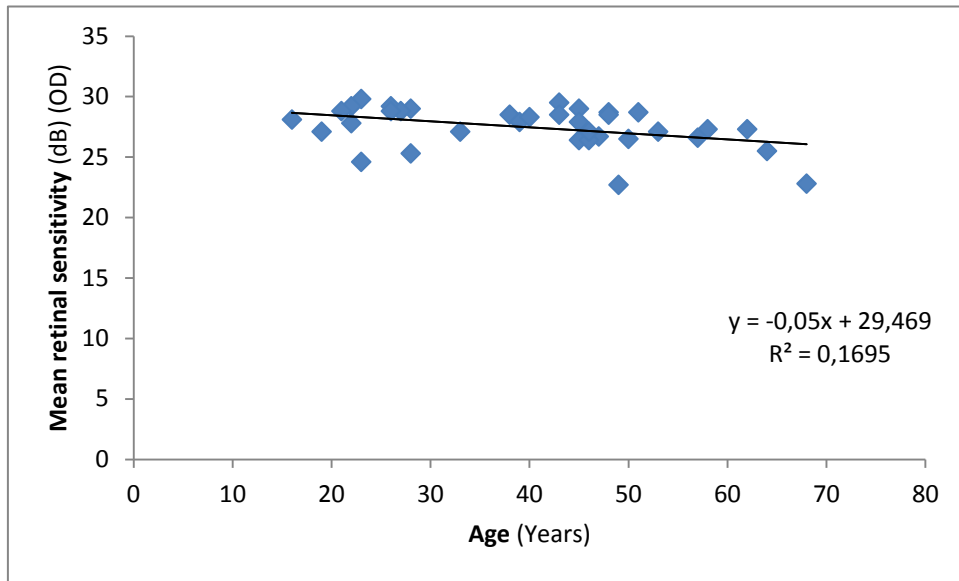


**Figure 6.4** The linear regression between the mean retinal sensitivity of right eye (OD) and age (regression equation and  $R^2$  values are shown)

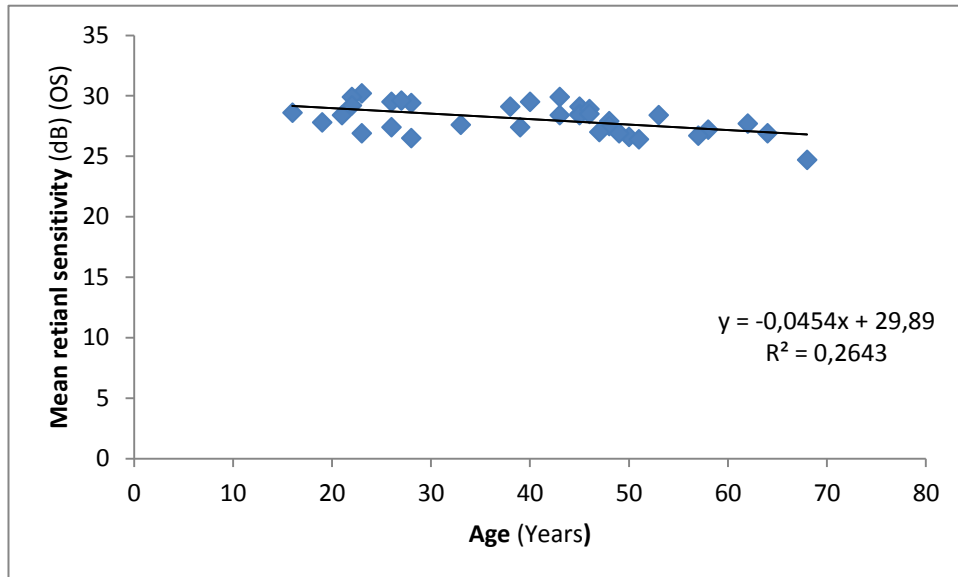


**Figure 6.5** The linear regression between the mean retinal sensitivity of left eye (OS) and age (regression equation and  $R^2$  values are shown)

These results are in agreement with the previously described study by Fujiwara et al. (2014), in which the authors reported central sensitivity values of 28.9 dB for subjects under 20 years, 27.2 dB for subjects between 20 and 60 years, and 24.50 dB for subjects over 60 years. Average sensitivity values in the present study were 29.6 dB for subjects under 20 years, 28.7 dB for subjects between 20 and 60 years, and 26.3 dB for subjects over 60 years. The results show a correlation of sensitivity with age in which retinal sensitivity gradually decreases by approximately 0.6 dB every 10 years ( $p = 0.01$ ). Similarly, Shah and Chalam (2009), in a study in which the authors assessed 37 healthy subjects using the MP-1 microperimeter, encountered a gradual decrement every year by approximately 0.344% and 0.122 % at 2 and 4 eccentricity degrees, respectively. These findings are in agreement with our regression analysis results, the correlation of the mean retinal sensitivity with age has a gradual decrement by approximately 0.17% every year for the right eye ( $p=0.014$ ), and by 0.26% every year for the left eye ( $p=0.002$ ), that is, about 0.5 dB every 10 years.

Finally, no statistically significant differences were found between males and females in retinal sensitivity parameters in the control group. These results are in agreement with the studies of Sabates et al. (2011) and of Shah and Chalam (2009), in which the authors described no effect of either gender or ethnicity on the retinal sensitivity.

## 6.4 Measuring retinal thickness asymmetry using SD-OCT in patients with high myopia

### *Demographics, refraction and visual acuity of the myopic group*

Forty-three subjects (15 females; 28 males) were enrolled in the myopic group, with an age of  $35.07 \pm 13.31$  years, ranging from 13 to 60 years. **Table 6.12** presents a summary of SE and CDVA of both eyes. No statistically significant inter-ocular differences were found in these parameters.

Parameter	Mean	Median	Interquartile range	Z	p
CDVA (logMAR) OD	0.057	0.022	0.097	0.000	1.000
CDVA (logMAR) OS	0.057	0.022	0.097		
SE OD (D)	-9.05	-8.00	2.75	-0.189	0.850
SE OS (D)	-9.03	-8.00	2.00		

**Table 6.12** Study sample corrected distance visual acuity (CDVA) (logMAR) and spherical equivalent (SE) (D) for right (OD) and left (OS) eyes for the myopic group. Data is presented as mean, median and interquartile range. The Wilcoxon test was used to assess interocular differences (Z and p values are shown).

### *Retinal parameters of the myopic group*

With the inclusion of subjects affected by high myopia we aimed at further understanding the occurrence of any asymmetry in retinal and/or choroidal structures and functions encountered in high myopia.

**Table 6.13** presents a summary of RNFL and macular parameters for both eyes. Statistically significant differences were found at the nasal quadrant between right and left eyes at the 3 macular regions, as well as at the 2 and 3 mm rings at the temporal quadrant, and in central macular thickness (mean values of 205.20

$\mu\text{m}$  in OD and  $192.65 \mu\text{m}$  in OS,  $p = 0.016$ ). No other statistically significant differences were found between both eyes in the myopic group.

Parameter	OD		OS		t	p
	Mean	SD	Mean	SD		
Central RNFL th. ( $\mu\text{m}$ )	192.45	20.70	188.94	20.98	1.627	0.111
1 mm N RNFL th. ( $\mu\text{m}$ )	312.34	14.68	302.05	20.75	3.661	<b>0.001</b>
2 mm N RNFL th. ( $\mu\text{m}$ )	284.43	18.31	270.95	28.30	3.622	<b>0.001</b>
3 mm N RNFL th. ( $\mu\text{m}$ )	262.98	36.40	228.30	25.05	5.227	<b>&lt;0.001</b>
1 mm T RNFL th. ( $\mu\text{m}$ )	294.71	22.82	295.21	21.15	-0.145	0.886
2 mm T RNFL th. ( $\mu\text{m}$ )	255.40	23.66	264.21	24.07	-2.163	<b>0.036</b>
3 mm T RNFL th. ( $\mu\text{m}$ )	231.60	67.18	260.67	36.40	-2.429	<b>0.020</b>
1 mm S RNFL th. ( $\mu\text{m}$ )	310.90	17.71	311.36	18.44	-0.155	0.877
2 mm S RNFL th. ( $\mu\text{m}$ )	274.66	17.05	269.24	17.13	1.801	0.079
3 mm S RNFL th. ( $\mu\text{m}$ )	245.16	20.20	239.44	31.11	1.111	0.273
1 mm I RNFL th. ( $\mu\text{m}$ )	298.14	31.07	305.44	16.76	-1.478	0.147
2 mm I RNFL th. ( $\mu\text{m}$ )	263.07	25.19	258.93	23.67	0.984	0.331
3 mm I RNFL th. ( $\mu\text{m}$ )	235.15	31.72	233.77	24.37	0.281	0.780
1 mm Mean RNFL th. ( $\mu\text{m}$ )	304.04	17.16	303.53	16.88	0.195	0.846
2 mm Mean RNFL th. ( $\mu\text{m}$ )	269.40	14.78	265.85	16.88	1.639	0.109
3 mm Mean RNFL th. ( $\mu\text{m}$ )	243.75	16.80	240.57	16.21	0.964	0.341
Central macular th. ( $\mu\text{m}$ )	205.20	33.33	192.65	31.17	2.502	<b>0.016</b>
Macular Vol. ( $\text{mm}^3$ )	7.58	0.46	7.50	0.59	1.358	0.182
Mean macular th. ( $\mu\text{m}$ )	267.57	17.20	262.94	27.62	1.265	0.213

**Table 6.13** Summary of RNFL and macular parameters for both eyes for the myopic group. The t-test for matched pairs was used for statistical analysis (t and p values are shown). (RNFL: retinal nerve fibre layer; th: thickness; OD: right eye; OS: left eye, S: superior; I: inferior; N: nasal; T: temporal; Vol: volume)

As seen in **Table 6.13**, the RNFL of the right eye is thinner only at the 3 mm ring. Besides, within each distance and eye, the distribution of RNFL thickness in the four quadrants does not follow the same pattern (see **Figure 6.6**). Thus, whereas the thickness order at the different quadrants remains constant for the right eye (NSIT), the order for the left eye at 1 mm is SINT, at 2 mm is NSTI, and at 3 mm is TSIN. In this regards, the nasal quadrant is always thicker in the right eye, whereas the temporal quadrant is always thicker at the left eye, irrespective of the distance from the centre of the macula.

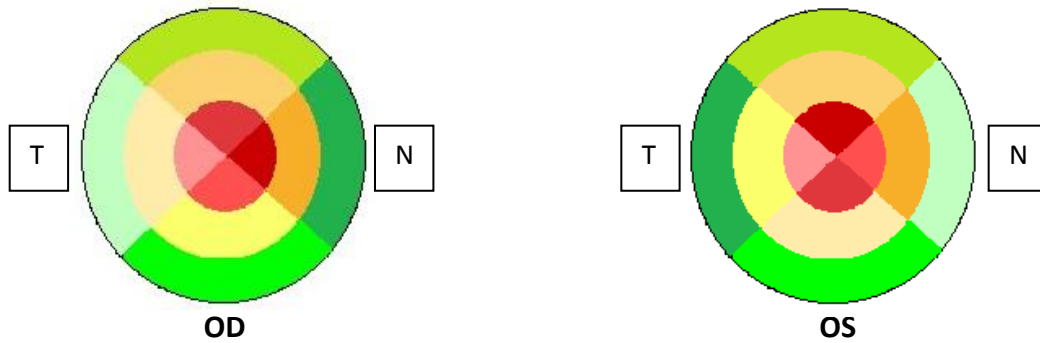


**Figure 6.6** The distribution of RNFL thickness in the four quadrants in myopic group. Within each peripheral ring location, darker colours denote thicker areas.

In the study of Jin et al. (2016) the authors reported retinal and choroidal thickness of 276 children aged 7 to 13 years and with different refractive errors, and they described retinal thinning in the myopic group, as compared with the emmetropic and hyperopic groups, at the superior parafoveal areas ( $p < 0.05$ ). Furthermore, Liu et al. (2015) explored the macular thickness profiles in 30 young patients with refractive errors ranging from +0.50 to -10.25 D, reporting lower values of macular thickness in the peripheral regions. Similarly, Lee et al. (2015) investigated the RNFL thickness in 201 myopic, hyperopic, and emmetropic patients. Once differences in age had been adjusted, the authors observed that myopes had a thinner RNFL than the other 2 groups (all  $p < 0.001$ ), but there was no RNFL thickness difference between the emmetropic and hyperopic groups.

Inter-ocular differences in retinal parameters for the myopic group are shown in **Table 6.14**, which also displays the 95% limits of difference in terms of the 2.5<sup>th</sup> and 97.5<sup>th</sup> percentiles. Regarding these inter-ocular differences, our 2.5<sup>th</sup> and 97.5<sup>th</sup> percentiles of inter-ocular difference tolerance limits in central RNFL thickness of -26.40  $\mu\text{m}$  and 53.40  $\mu\text{m}$  are higher than those reported in other studies, although no previous research, as far as we know, has explored inter-ocular asymmetry in high myopia. Thus, for instance, previous research assessed



glaucomatous eyes (Kochendörfer et al., 2014) or localized retinal nerve fibre layer defects (RNFLD) (Seo et al., 2012).

Parameter differences (OD-OS)	Mean	SD	2.5 <sup>th</sup> perc.	97.5 <sup>th</sup> perc.
Central RNFL th. ( $\mu\text{m}$ )	3.51	14.16	-26.40	53.40
1 mm N RNFL th. ( $\mu\text{m}$ )	10.29	18.43	-22.00	88.35
2 mm N RNFL th. ( $\mu\text{m}$ )	13.48	24.40	-13.95	91.50
3 mm N RNFL th. ( $\mu\text{m}$ )	34.67	43.50	-83.00	177.90
1 mm T RNFL th. ( $\mu\text{m}$ )	-0.50	22.69	-35.30	90.55
2 mm T RNFL th. ( $\mu\text{m}$ )	-8.81	26.72	-92.45	60.35
3 mm T RNFL th. ( $\mu\text{m}$ )	-29.07	78.49	-105.90	383.90
1 mm S RNFL th. ( $\mu\text{m}$ )	-0.47	19.65	-38.45	79.10
2 mm S RNFL th. ( $\mu\text{m}$ )	5.42	19.73	-35.60	68.10
3 mm S RNFL th. ( $\mu\text{m}$ )	5.72	33.76	-79.50	125.80
1 mm I RNFL th. ( $\mu\text{m}$ )	-7.30	32.40	-120.85	67.85
2 mm I RNFL th. ( $\mu\text{m}$ )	4.14	27.58	-94.30	55.65
3 mm I RNFL th. ( $\mu\text{m}$ )	1.38	32.26	-105.10	92.10
1 mm Mean RNFL th. ( $\mu\text{m}$ )	0.51	17.31	-34.20	72.51
2 mm Mean RNFL th. ( $\mu\text{m}$ )	3.55	14.22	-35.65	62.39
3 mm Mean RNFL th. ( $\mu\text{m}$ )	3.18	21.62	-41.59	90.80
Central macular th. ( $\mu\text{m}$ )	12.55	32.89	-50.15	109.90
Macular Vol. ( $\text{mm}^3$ )	0.09	0.42	-1.20	1.77
Mean macular th. ( $\mu\text{m}$ )	4.63	23.10	-44.59	107.23

**Table 6.14** Inter-ocular difference in retinal sensitivity (right eye - left eye) for the myopic group. Data is presented as mean  $\pm$  SD. Limits of difference are shown as the 2.5<sup>th</sup> and 97.5<sup>th</sup> percentiles. (OD: right eye; OS: left eye, S: superior; I: inferior; N: nasal; T: temporal)

Finally, statistically significant differences were found between males and females in several peripheral regions, as well as, in the average macular thickness of the right eye, and in the macular volume of the right eye. These findings are partially in agreement with a large study including 193 eyes of myopic volunteers ( $-4.57 \pm 3.52$  D) aged between 18 to 49, to assess the retinal thickness association with spherical equivalent, age and gender (Li et al., 2016). The authors reported that variations in thickness of the central areas were affected by both gender and axial length, while in the outer regions thickness was

affected only by axial length. It must be noted, however, that refractive error of these patients is not comparable with the one of the patients included in the present study.

In addition, the correlation between the absolute values of inter-ocular asymmetry (that is, without considering the laterality of the asymmetry) and the degree of refractive error (taken as the mean of both eyes) was explored. Statistically significant correlations were found between mean refractive error and absolute inter-ocular thickness asymmetry at the centre of the retina (see [Figure 6.7](#)) ( $r=-0.56$ ;  $p<0.001$ ), at the first ring and inferior quadrant ( $r=-0.36$ ;  $p=0.012$ ) and at the second ring and temporal quadrant ( $r=-0.45$ ;  $p=0.002$ ). These findings suggest that as myopia increases, the level of asymmetry also increases, being this association particularly relevant at the centre of the retina. It may be noted, however, that many of the data points of [Figure 6.7](#) are clustered at levels of myopia between -6D and -10D, thus warranting further investigation to verify this association.

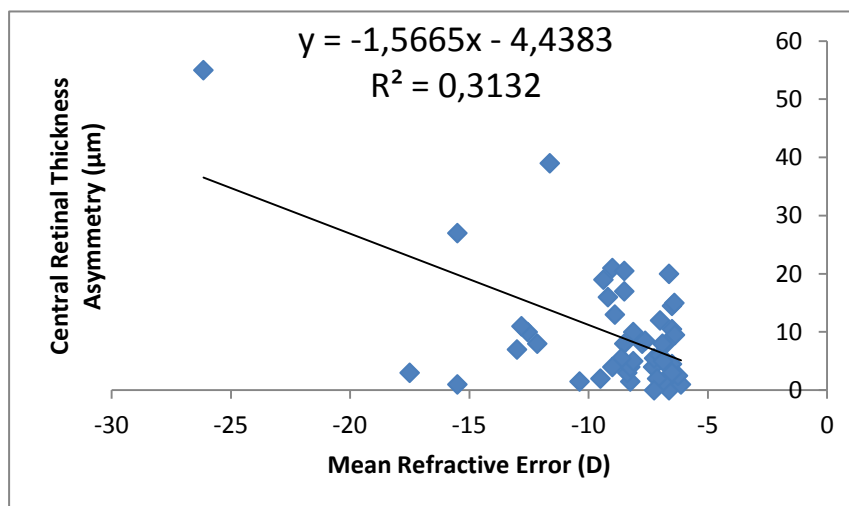


**Figure 6.7** Correlation between absolute inter-ocular asymmetry in central retinal thickness and mean refractive error for the myopia group

*Comparison of retinal parameters between myopia and control groups*

Before comparing retinal, choroidal and retinal sensitivity parameters between myopia and the control group it is important to explore whether these groups were matched in terms of age. A Student t-test for unmatched pairs revealed that differences in age between both groups were not statistically significant ( $t=1.574$ ;  $p=0.120$ ).

The findings from the myopia group were compared with those of the control group. It may be noted that in the comparison of absolute retinal ([Table 6.15](#)) and choroidal parameters between control and myopic groups, differences are not unexpected, given, for example, that both choroidal and retinal parameters have been described to vary with refractive error (Jin et al., 2016; Liu et al., 2015; Zaben et al., 2015). Indeed, the present findings revealed statistically significant differences in thickness of the RNFL of the right eye in both groups at 2 and 3 mm at the superior quadrant, and at 1 mm and 2 mm at the inferior quadrant, as well as, of mean RNFL thickness at 2 mm, macular volume, and mean macular thickness.

In order to explore the differences in inter-ocular asymmetry between both groups, the absolute value of the differences was determined, that is, the comparison refers to asymmetry, without considering which eye had the largest (or smallest) value for each of the parameters under evaluation. Results of this analysis are shown in [Table 6.16](#).

Parameter OD	Myopia		Normal		t	p
	Mean	SD	Mean	SD		
Central RNFL th. ( $\mu\text{m}$ )	192.45	20.69	187.51	17.31	-1.13	0.263
1 mm N RNFL th. ( $\mu\text{m}$ )	312.34	14.68	309.29	37.97	-0.48	0.629
2 mm N RNFL th. ( $\mu\text{m}$ )	284.43	18.32	294.54	26.10	1.96	0.053
3 mm N RNFL th. ( $\mu\text{m}$ )	262.98	36.40	267.94	18.27	0.755	0.465
1 mm T RNFL th. ( $\mu\text{m}$ )	294.71	22.82	291.57	33.84	-0.487	0.627
2 mm T RNFL th. ( $\mu\text{m}$ )	255.40	23.67	263.69	25.95	1.474	0.145
3 mm T RNFL th. ( $\mu\text{m}$ )	231.60	67.18	227.26	14.74	-0.375	0.709
1 mm S RNFL th. ( $\mu\text{m}$ )	310.90	17.71	316.00	22.57	1.119	0.267
2 mm S RNFL th. ( $\mu\text{m}$ )	274.66	17.05	283.31	15.09	2.345	<b>0.022</b>
3 mm S RNFL th. ( $\mu\text{m}$ )	245.16	20.21	256.09	21.43	2.311	<b>0.024</b>
1 mm I RNFL th. ( $\mu\text{m}$ )	298.14	31.07	312.46	18.74	2.393	<b>0.019</b>
2 mm I RNFL th. ( $\mu\text{m}$ )	263.07	25.19	273.20	17.30	2.021	<b>0.047</b>
3 mm I RNFL th. ( $\mu\text{m}$ )	235.15	31.72	239.31	14.79	0.715	0.477
1 mm Mean RNFL th. ( $\mu\text{m}$ )	304.04	17.16	307.36	22.64	0.729	0.468
2 mm Mean RNFL th. ( $\mu\text{m}$ )	269.40	14.78	278.71	16.32	2.633	<b>0.010</b>
3 mm Mean RNFL th. ( $\mu\text{m}$ )	243.75	16.79	247.68	13.52	1.112	0.270
Central macular th. ( $\mu\text{m}$ )	205.20	33.33	200.03	33.36	-0.681	0.498
Macular Vol. ( $\text{mm}^3$ )	7.58	0.47	7.88	0.35	3.087	<b>0.003</b>
Mean macular th. ( $\mu\text{m}$ )	267.57	17.20	277.87	12.98	2.927	<b>0.005</b>

**Table 6.15** Differences in absolute values between myopic and normal eyes in retinal parameters. Data is presented as mean  $\pm$  SD and only the right eye (OD) is shown. The t-test for unmatched pairs was used for statistical analysis (t and p values are shown)

Statistically significant differences were uncovered between myopic and control groups at 1 and 2 mm at the temporal, nasal and inferior quadrants. Interestingly, inter-ocular differences in the myopic group were smaller than those of the control group in the temporal and nasal quadrants, whereas at the inferior quadrant, normal eyes were less asymmetrical than myopic eyes. These different patterns in asymmetry need to be taken into account when examining myopic eyes for possible pathologies.

Parameter differences (Absolute value)	Myopia		Normal		t	p
	Mean	SD	Mean	SD		
Central RNFL th. ( $\mu\text{m}$ )	9.81	10.32	10.63	20.30	0.240	0.811
1 mm N RNFL th. ( $\mu\text{m}$ )	14.67	15.09	23.80	25.97	2.001	<b>0.049</b>
2 mm N RNFL th. ( $\mu\text{m}$ )	20.63	20.88	36.63	20.33	3.471	<b>0.001</b>
3 mm N RNFL th. ( $\mu\text{m}$ )	44.23	31.31	36.60	17.33	-1.471	0.145
1 mm T RNFL th. ( $\mu\text{m}$ )	13.88	17.59	25.97	30.90	2.241	<b>0.028</b>
2 mm T RNFL th. ( $\mu\text{m}$ )	23.46	20.66	38.37	26.92	2.839	<b>0.006</b>
3 mm T RNFL th. ( $\mu\text{m}$ )	53.04	60.72	44.66	14.92	-0.798	0.427
1 mm S RNFL th. ( $\mu\text{m}$ )	14.03	17.89	10.03	12.70	-1.128	0.263
2 mm S RNFL th. ( $\mu\text{m}$ )	15.39	13.06	15.91	29.45	0.108	0.914
3 mm S RNFL th. ( $\mu\text{m}$ )	20.51	26.88	11.86	18.44	-1.637	0.105
1 mm I RNFL th. ( $\mu\text{m}$ )	20.68	28.45	8.91	8.95	-2.358	<b>0.021</b>
2 mm I RNFL th. ( $\mu\text{m}$ )	18.89	19.38	10.71	11.41	-2.224	<b>0.029</b>
3 mm I RNFL th. ( $\mu\text{m}$ )	18.67	24.55	16.86	18.29	-0.367	0.714
1 mm Mean RNFL th. ( $\mu\text{m}$ )	11.40	15.07	8.56	14.01	-0.867	0.389
2 mm Mean RNFL th. ( $\mu\text{m}$ )	9.07	11.32	8.94	14.02	-0.049	0.961
3 mm Mean RNFL th. ( $\mu\text{m}$ )	11.65	17.50	8.20	8.30	-1.077	0.285
Central macular th. ( $\mu\text{m}$ )	20.03	28.70	12.97	18.13	-1.393	0.168
Macular Vol. ( $\text{mm}^3$ )	0.25	0.36	0.16	0.25	-1.277	0.205
Mean macular th. ( $\mu\text{m}$ )	12.10	20.61	6.82	10.23	-1.176	0.243

**Table 6.16** Differences in relative values (inter-ocular asymmetry) between myopic and normal eyes in retinal parameters. Data is presented as in absolute values of (OD-OS) in mean  $\pm$  SD. The t-test for unmatched pairs was used for statistical analysis (t and p values are shown)

### 6.5 Measuring choroidal thickness in patients with high myopia using the enhanced depth imaging (EDI) technique of SD – OCT:

In this section we will present the results of choroidal asymmetry in the group of myopic patients.

First, by following the same presentation order of previous sections, **Table 6.17** displays a summary of the various choroidal parameters for both eyes, including, central choroidal thickness, thickness at each quadrant for each of the three peripheral rings and average thickness of each of these rings.

Parameter	OD		OS		t	p
	Mean	SD	Mean	SD		
Central choroidal th. ( $\mu\text{m}$ )	174.50	62.99	171.67	56.45	0.522	0.604
1 mm N choroidal th. ( $\mu\text{m}$ )	163.93	52.34	153.38	51.96	1.710	0.095
1 mm T choroidal th. ( $\mu\text{m}$ )	187.36	66.10	183.30	51.32	0.580	0.565
1 mm S choroidal th. ( $\mu\text{m}$ )	199.90	62.97	189.59	57.42	1.543	0.130
1 mm I choroidal th. ( $\mu\text{m}$ )	190.20	54.26	188.94	51.22	0.202	0.841
2 mm N choroidal th. ( $\mu\text{m}$ )	128.98	50.82	134.28	67.25	-0.665	0.510
2 mm T choroidal th. ( $\mu\text{m}$ )	183.91	59.61	183.02	52.57	0.108	0.914
2 mm S choroidal th. ( $\mu\text{m}$ )	206.57	57.27	198.56	54.12	1.339	0.188
2 mm I choroidal th. ( $\mu\text{m}$ )	187.93	55.29	188.62	51.96	-0.114	0.909
3 mm N choroidal th. ( $\mu\text{m}$ )	152.65	46.91	210.60	47.72	-7.336	<0.001
3 mm T choroidal th. ( $\mu\text{m}$ )	195.07	44.43	153.49	45.67	4.800	<0.001
3 mm S choroidal th. ( $\mu\text{m}$ )	212.98	48.68	212.00	40.49	0.162	0.872
3 mm I choroidal th. ( $\mu\text{m}$ )	197.98	47.14	199.33	44.76	-0.224	0.824
1 mm mean choroidal th. ( $\mu\text{m}$ )	185.37	54.91	178.83	48.31	1.406	0.167
2 mm mean choroidal th. ( $\mu\text{m}$ )	176.86	46.93	176.15	45.10	0.177	0.860
3 mm mean choroidal th. ( $\mu\text{m}$ )	189.69	31.49	193.88	32.06	-1.168	0.249

**Table 6.17** Summary of choroidal parameters for both eyes for the myopic group. The t-test for matched pairs was used for statistical analysis (t and p values are shown). (th: thickness; OD: right eye; OS: left eye, S: superior; I: inferior; N: nasal; T: temporal)

Statistically significant differences were found between right and left eye in the macular regions away from the centre at 3 mm nasally (mean values of 152.65  $\mu\text{m}$  in OD and 210.60  $\mu\text{m}$  in OS,  $p = <0.001$ ), and 3 mm temporally (mean values

of 195.07  $\mu\text{m}$  in OD and 153.49  $\mu\text{m}$  in OS,  $p = <0.001$ ). No statistically significant differences were found between both eyes in the rest of choroidal parameters under study.

In both eyes, the average of the choroidal thickness was higher at 3 mm (mean values of 189.69  $\mu\text{m}$  in OD and 193.88  $\mu\text{m}$  in OS), followed by 1 mm (mean values of 185.37  $\mu\text{m}$  in OD and 178.83  $\mu\text{m}$  in OS), then 2 mm (mean values of 176.86  $\mu\text{m}$  in OD and 176.15  $\mu\text{m}$  in OS).

Besides, as seen in [Table 6.17](#), the choroid was thicker at 3 mm at the superior quadrant and both eyes, followed by 2 mm at the superior quadrant and right eye, and by 3 mm at the nasal quadrant and left eye, that is, the choroid is thinner towards the centre of the macula and progressively gains thickness towards the periphery. The distribution of choroidal thickness in the four quadrants does follow the same pattern (see [Figure 6.8](#)), within each distance and eye except at 3 mm and left eye: the superior quadrant is thicker, followed by the inferior, temporal and nasal quadrants (SITN). However, the order for the left eye at 3 mm is SINT. It may be observed that the superior quadrant is always thicker, followed by the temporal quadrant, irrespective of the distance from the centre of the macula.

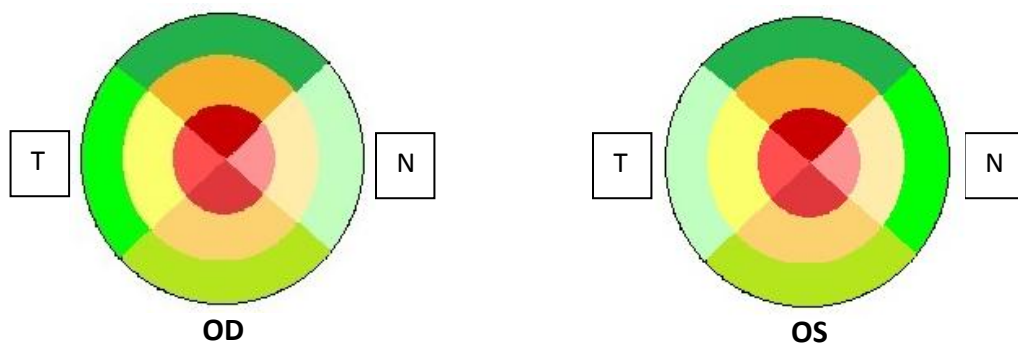


**Figure 6.8** The distribution of choroidal thickness in the four quadrants in myopic group. Within each peripheral ring location, darker colours denote thicker areas.

In agreement with the previous studies reporting the differences in choroidal thickness between the various quadrants (Gupta et al., 2015), our findings revealed thinner values at the temporal than at the nasal quadrant only at 3 mm and left eye.

Statistically significant differences in choroidal thickness were found between right and left eye in the macular regions away from the centre at 3 mm temporally and nasally. Regarding mean choroidal thickness, these findings are in disagreement with previous studies as in the present report the left eye was found to present thicker mean choroidal thickness values than the right eye only at 3 mm in nasal and inferior quadrants, although these differences were statistically significant just for the nasal quadrant (Hayreh and Zimmerman, 2014; Ruiz-Medrano et al., 2015; Sohrab et al., 2012). Also, in the study of Harb et al. (2015), the authors concluded that choroidal thinning occurred mostly in the nasal quadrant ( $191.5 \pm 69.3 \mu\text{m}$ ). Finally, Lee et al (2015) studied the topographical variations of macular choroidal thickness in a group of 85 patients with low myopia using OCT, documenting the order of the choroidal thickness to be (STIN) at 1.5 mm away from the centre of the macula. The authors suggested that these topographical changes might be induced by stretching of the choroid and sclera towards a temporal direction with eyeball elongation in high myopia and myopia progression.

A summary of the inter-ocular differences in choroidal parameters is shown in **Table 6.18**. It may be observed that at the 2 mm ring, particularly in the inferior quadrant, differences between eyes are very small. In contrast, large inter-ocular differences were found at the 3 mm ring, in which the choroid was considerably thicker in the left eye in the nasal quadrant and in the right eye in the temporal quadrant.



Finally, the analysis of the possible association between the absolute values of choroidal inter-ocular asymmetry and the degree of refractive error was explored. Statistically significant correlations were found between mean refractive error and absolute inter-ocular choroidal asymmetry only at the first ring superior quadrant (see [Figure 6.9](#)) ( $r=-0.44$ ;  $p=0.002$ ). These findings suggest that as myopia increases, the level of asymmetry also increases, although this association is not as manifest as that described above for retinal thickness asymmetry.

Parameter differences (OD-OS)	Mean	SD	2.5 <sup>th</sup> perc.	97.5 <sup>th</sup> perc.
Central choroidal th. ( $\mu\text{m}$ )	2.83	35.48	-71.50	70.65
1 mm N choroidal th. ( $\mu\text{m}$ )	10.55	40.46	-65.40	108.05
1 mm T choroidal th. ( $\mu\text{m}$ )	4.06	45.88	-95.60	142.10
1 mm S choroidal th. ( $\mu\text{m}$ )	10.30	43.77	-74.85	188.75
1 mm I choroidal th. ( $\mu\text{m}$ )	1.26	40.68	-84.35	129.85
2 mm N choroidal th. ( $\mu\text{m}$ )	-5.30	52.32	-149.75	94.20
2 mm T choroidal th. ( $\mu\text{m}$ )	0.88	53.61	-120.85	167.30
2 mm S choroidal th. ( $\mu\text{m}$ )	8.01	39.24	-81.95	88.05
2 mm I choroidal th. ( $\mu\text{m}$ )	-0.69	39.34	-73.50	103.85
3 mm N choroidal th. ( $\mu\text{m}$ )	-57.95	51.80	-178.30	43.90
3 mm T choroidal th. ( $\mu\text{m}$ )	41.58	56.81	-95.70	136.30
3 mm S choroidal th. ( $\mu\text{m}$ )	0.98	39.63	-81.10	90.70
3 mm I choroidal th. ( $\mu\text{m}$ )	-1.35	39.46	-86.40	82.20
1 mm mean choroidal th. ( $\mu\text{m}$ )	6.54	30.51	-49.59	75.29
2 mm mean choroidal th. ( $\mu\text{m}$ )	0.73	26.47	-60.25	69.19
3 mm mean choroidal th. ( $\mu\text{m}$ )	-4.18	23.47	-60.40	47.65

**Table 6.18** Inter-ocular difference in choroidal parameters (right eye - left eye) for the myopic group.

Data is presented as mean  $\pm$  SD. Limits of difference are shown as the 2.5<sup>th</sup> and 97.5<sup>th</sup> percentiles. (th:

thickness; OD: right eye; OS: left eye, S: superior; I: inferior; N: nasal; T: temporal)

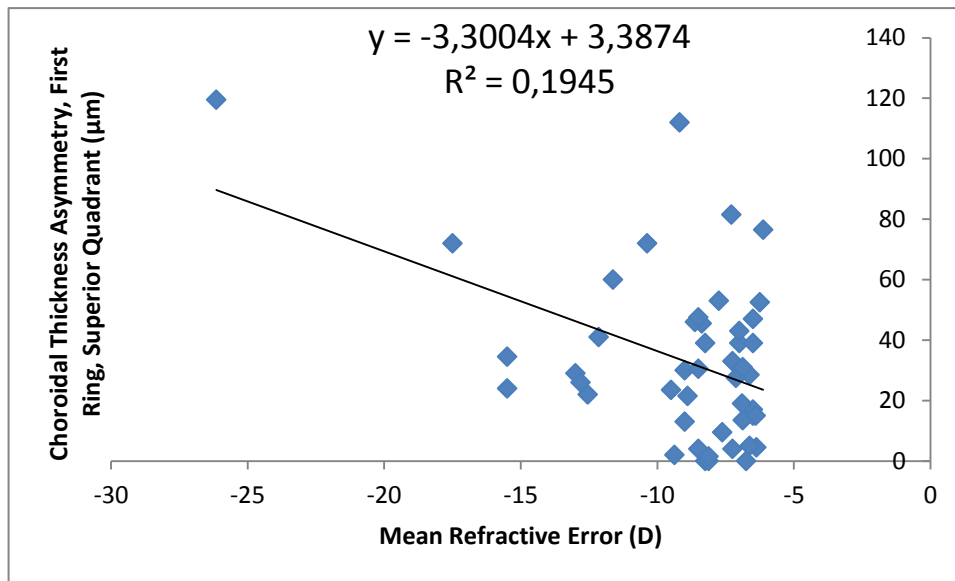


**Figure 6.9** Correlation between absolute inter-ocular asymmetry in choroidal thickness at the first ring superior quadrant and mean refractive error for the myopia group

*Comparison of choroidal parameters between myopia and control groups*

Finally, the findings from the myopia group were compared with those of the control group ([Table 6.19](#) and [Table 6.20](#)). As noted above, of particular interest is the investigation of differences in absolute values of inter-ocular asymmetry between high myopia and normal eyes.

Parameter OD	Myopia		Normal		t	p
	Mean	SD	Mean	SD		
Central choroidal th. ( $\mu\text{m}$ )	174.50	62.99	307.31	13.77	12.225	<0.001
1 mm N choroidal th. ( $\mu\text{m}$ )	163.93	52.34	277.03	13.74	12.426	<0.001
1 mm T choroidal th. ( $\mu\text{m}$ )	187.36	66.10	252.51	16.20	8.679	<0.001
1 mm S choroidal th. ( $\mu\text{m}$ )	199.90	62.97	212.74	19.14	9.157	<0.001
1 mm I choroidal th. ( $\mu\text{m}$ )	190.20	54.26	285.60	11.32	11.279	<0.001
2 mm N choroidal th. ( $\mu\text{m}$ )	128.98	50.82	263.77	10.64	13.808	<0.001
2 mm T choroidal th. ( $\mu\text{m}$ )	183.91	59.61	224.20	14.61	7.817	<0.001
2 mm S choroidal th. ( $\mu\text{m}$ )	206.57	57.27	301.60	20.52	5.275	<0.001
2 mm I choroidal th. ( $\mu\text{m}$ )	187.93	55.29	259.00	14.45	6.981	<0.001
3 mm N choroidal th. ( $\mu\text{m}$ )	152.65	46.91	219.26	17.20	7.105	<0.001
3 mm T choroidal th. ( $\mu\text{m}$ )	195.07	44.43	296.23	13.19	3.715	<0.001
3 mm S choroidal th. ( $\mu\text{m}$ )	212.98	48.68	254.83	13.54	0.727	0.470
3 mm I choroidal th. ( $\mu\text{m}$ )	197.98	47.14	221.63	17.95	2.805	0.006
1 mm mean choroidal th. ( $\mu\text{m}$ )	185.37	54.91	290.14	10.58	11.107	<0.001
2 mm mean choroidal th. ( $\mu\text{m}$ )	176.86	46.93	257.55	8.86	10.012	<0.001
3 mm mean choroidal th. ( $\mu\text{m}$ )	189.69	31.49	219.48	11.61	5.301	<0.001

**Table 6.19** Differences in absolute values between myopic and normal eyes in choroidal parameters. Data is presented as mean  $\pm$  SD and only the right eye (OD) is shown. The t-test for unmatched pairs was used for statistical analysis (t and p values are shown)

Compared with the results of the control group, the present findings revealed that the choroid progressively loses thickness in myopic patients. As noted above, these results are not unexpected, as it has extensively described in the literature that high myopia is associated with choroidal thinning (Harb et al., 2015; Zaben et al., 2015).

Parameter differences (Absolute value)	Myopia		Normal		t	p
	Mean	SD	Mean	SD		
Central choroidal th. ( $\mu\text{m}$ )	28.00	21.37	13.97	15.04	-3.317	<b>0.001</b>
1 mm N choroidal th. ( $\mu\text{m}$ )	31.16	26.64	14.46	13.14	-3.409	<b>0.001</b>
1 mm T choroidal th. ( $\mu\text{m}$ )	36.10	29.10	14.34	12.47	-4.048	<b>&lt;0.001</b>
1 mm S choroidal th. ( $\mu\text{m}$ )	33.40	27.59	18.29	15.01	-2.932	<b>0.004</b>
1 mm I choroidal th. ( $\mu\text{m}$ )	27.74	27.51	17.46	14.08	-2.022	<b>0.047</b>
2 mm N choroidal th. ( $\mu\text{m}$ )	38.30	35.81	18.17	14.53	-3.135	<b>0.002</b>
2 mm T choroidal th. ( $\mu\text{m}$ )	42.40	38.26	14.34	12.47	-4.172	<b>&lt;0.001</b>
2 mm S choroidal th. ( $\mu\text{m}$ )	32.24	23.70	20.00	12.59	-2.776	<b>0.007</b>
2 mm I choroidal th. ( $\mu\text{m}$ )	29.61	24.19	17.91	12.62	-2.605	<b>0.011</b>
3 mm N choroidal th. ( $\mu\text{m}$ )	59.83	46.82	20.51	20.34	-4.646	<b>&lt;0.001</b>
3 mm T choroidal th. ( $\mu\text{m}$ )	54.53	43.20	12.37	11.56	-5.618	<b>&lt;0.001</b>
3 mm S choroidal th. ( $\mu\text{m}$ )	28.11	25.73	16.40	11.68	-2.503	<b>0.014</b>
3 mm I choroidal th. ( $\mu\text{m}$ )	31.55	23.11	16.66	12.36	-3.459	<b>0.001</b>
1 mm mean choroidal th. ( $\mu\text{m}$ )	22.32	19.63	10.91	10.20	-3.133	<b>0.002</b>
2 mm mean choroidal th. ( $\mu\text{m}$ )	21.66	16.64	10.49	7.34	-3.706	<b>&lt;0.001</b>
3 mm mean choroidal th. ( $\mu\text{m}$ )	18.38	13.85	8.51	6.36	-3.912	<b>&lt;0.001</b>

**Table 6.20** Differences in relative values (inter-ocular asymmetry) between myopic and normal eyes in choroidal parameters. Data is presented as in absolute values of (OD-OS) in mean  $\pm$  SD. The t-test for unmatched pairs was used for statistical analysis (t and p values are shown)

Regarding the absolute values of inter-ocular asymmetry, statistically significant differences were found between the control and myopic groups in all locations, as well as in the mean values for each of the rings. It must be noted that in myopia differences between OD and OS are much larger than in the control group. Indeed, these findings are of relevance when exploring inter-ocular asymmetry as an indicator of a pathological condition (the present sample of myopic patients were free of ocular pathologies). Further studies may explore the range of asymmetry in common pathological conditions associated with high myopia. Besides, as noted above, although inter-ocular asymmetry differences were found between both groups, asymmetry does not show a clear increment with refractive error once only the myopic group is considered.

## 6.6 Exploring the inter-ocular asymmetry of macular sensitivity in patients with high myopia:

In this section we will summarize and discuss our findings regarding macular sensitivity, that is, visual function, in patients with high myopia also exploring the normal range of inter-ocular asymmetry in retinal sensitivity.

First, **Table 6.21** displays a summary of the retinal sensitivity parameters for both eyes, including, central sensitivity and sensitivity at each quadrant for each of the three peripheral rings, as well as mean overall sensitivity and mean sensitivity for each of these rings.

Parameter	OD		OS		t	p
	Mean	SD	Mean	SD		
<b>Central sensitivity (dB)</b>	24.84	4.58	26.05	3.60	-2.260	<b>0.029</b>
<b>1 mm N sensitivity (dB)</b>	27.21	4.39	28.76	2.16	-3.150	<b>0.003</b>
<b>1 mm T sensitivity (dB)</b>	26.92	4.89	28.46	2.43	-2.711	<b>0.010</b>
<b>1 mm S sensitivity (dB)</b>	27.64	3.64	28.12	2.93	-1.112	0.272
<b>1 mm I sensitivity (dB)</b>	26.89	3.96	28.03	2.20	-2.193	0.034
<b>2 mm N sensitivity (dB)</b>	27.15	4.84	28.62	2.46	-2.900	<b>0.006</b>
<b>2 mm T sensitivity (dB)</b>	26.77	3.25	27.80	1.99	-3.030	<b>0.004</b>
<b>2 mm S sensitivity (dB)</b>	27.54	2.43	27.88	3.82	-0.847	0.402
<b>2 mm I sensitivity (dB)</b>	27.29	2.85	28.07	2.56	-2.365	<b>0.023</b>
<b>3 mm N sensitivity (dB)</b>	26.31	4.63	27.54	4.38	-3.968	<b>&lt;0.001</b>
<b>3 mm T sensitivity (dB)</b>	26.13	2.95	26.76	2.83	-2.056	<b>0.046</b>
<b>3 mm S sensitivity (dB)</b>	26.96	3.59	27.02	3.57	-0.187	0.853
<b>3 mm I sensitivity (dB)</b>	26.86	2.37	27.38	1.97	-1.649	0.107
<b>1 mm mean sensitivity (dB)</b>	27.18	4.02	28.44	2.12	-2.834	<b>0.007</b>
<b>2 mm mean sensitivity (dB)</b>	27.25	3.15	28.14	2.44	-3.663	<b>0.001</b>
<b>3 mm mean sensitivity (dB)</b>	26.56	3.21	27.30	2.93	-3.084	<b>0.004</b>
<b>Mean Sensitivity (dB)</b>	27.10	3.61	27.91	2.50	-2.472	<b>0.018</b>

**Table 6.21** Summary of retina sensitivity for both eyes for the myopic group. The t-test for matched pairs was used for statistical analysis (t and p values are shown). (OD: right eye; OS: left eye, S: superior; I: inferior; N: nasal; T: temporal)

Several statistically significant differences were found between right and left eye in the macular region (mean values of 27.10 dB in OD and 27.91 dB in OS,  $p = 0.018$ ) and away from the centre at several peripheral locations. In all instances the left eye was found to have higher sensitivity than the right eye (higher values in dB). The mean of macular sensitivity showed gradually decreased values away from the centre for the left eye, with the lower retinal sensitivity at 3 mm temporally away from the macula (mean values 26.13 dB in OD and 26.76 dB in OS), while the higher retinal sensitivity was found at 1 mm in the superior quadrant in the right eye (mean values 27.64 dB), and at 1 mm in the nasal quadrant in left eye (mean values 28.76 dB).

As seen in [Table 6.21](#), the retinal sensitivity in the four quadrants does not follow the same pattern (see [Figure 6.10](#)), within each distance and eye: at 1 mm and at the right eye retinal sensitivity was higher at the superior quadrant, followed by the nasal, temporal and inferior quadrants (SNTI), whereas, at the left eye and at 1, 2 and 3 mm the order was constant (NIST). Contrarily, at 2 and 3 mm retinal sensitivity order at the right eye was SINT. Therefore, the sensitivity is always higher at the superior quadrant in the right eye, as compared with the nasal quadrant in the left eye.

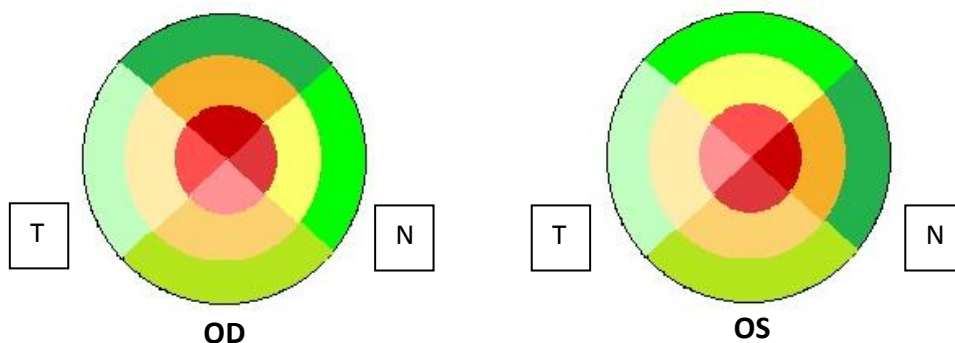


**Figure 6.10** The distribution of retinal sensitivity in the four quadrants in myopic group. Within each peripheral ring location, darker colours denote thicker areas.

Only one study has explored the retinal sensitivity of high myopic patients, and as far as we know there are not studies assessing the asymmetry of retinal sensitivity in subjects affected by high myopia. To cite this study, Zaben et al. (2015) estimated the correlation between the choroidal thickness in the macular area and the retinal sensitivity in high myopia using a MAIA™ microperimeter in a sample of 96 eyes from 77 patients. The authors concluded that mean choroidal thickness was directly, albeit very weakly, correlated with retinal sensitivity ( $r = 0.306$ ;  $p = 0.004$ ) and visual acuity ( $r = 0.431$ ;  $p = 0.001$ ) in these patients, also revealing a negative correlation with spherical equivalent ( $r = -0.306$ ;  $p = 0.003$ ) and age ( $r = -0.507$ ;  $p < 0.001$ ), that is, sensitivity decreased in higher myopes and in elder patients. By comparing [Figure 6.8](#) (retinal sensitivity) and [Figure 6.7](#) (choroidal thickness) it may be observed that our findings are in agreement with those of Zaben et al. (2015), with small discrepancies (particularly at the nasal quadrant in OD, in which high retinal sensitivity was found in a region of low choroidal thickness).

A summary of the inter-ocular differences in retinal sensitivity parameters is shown in [Table 6.22](#).

It may be observed that, overall, inter-ocular differences tend to decrease towards the periphery, with the largest differences occurring at the 1 mm ring, with the exception of the superior quadrant. In addition, the left eye was always found to be present lower average values of retinal sensitivity than the right eye. Although eyes were always examined in a random order, it may be speculated whether some artefact of our measurement methodology or of the instrumentation lead to these differences. Therefore, these findings warrant further investigation.

Parameter differences (OD-OS)	Mean	SD	2.5 <sup>th</sup> perc.	97.5 <sup>th</sup> perc.
Central sensitivity (dB)	-1.21	3.51	-9.80	7.70
1 mm N sensitivity (dB)	-1.55	3.23	-12.16	3.87
1 mm T sensitivity (dB)	-1.55	3.74	-15.89	5.66
1 mm S sensitivity (dB)	-0.49	2.87	-8.84	5.30
1 mm I sensitivity (dB)	-1.14	3.41	-9.80	4.36
2 mm N sensitivity (dB)	-1.47	3.32	-15.06	3.93
2 mm T sensitivity (dB)	-1.03	2.23	-7.11	2.97
2 mm S sensitivity (dB)	-0.34	2.63	-3.94	10.66
2 mm I sensitivity (dB)	-0.78	2.15	-8.00	2.96
3 mm N sensitivity (dB)	-1.23	2.03	-6.97	3.17
3 mm T sensitivity (dB)	-0.63	2.02	-7.67	2.69
3 mm S sensitivity (dB)	-0.05	1.88	-4.57	3.94
3 mm I sensitivity (dB)	-0.52	2.06	-4.56	5.19
1 mm mean sensitivity (dB)	-1.26	2.91	-10.32	3.72
2 mm mean sensitivity (dB)	-0.89	1.60	-4.42	1.50
3 mm mean sensitivity (dB)	-0.74	1.57	-3.98	2.29
Mean Sensitivity (dB)	-0.81	2.15	-4.99	5.50

**Table 6.22** Inter-ocular difference in retinal sensitivity (right eye - left eye) for the myopic group. Data is presented as mean  $\pm$  SD. Limits of difference are shown as the 2.5<sup>th</sup> and 97.5<sup>th</sup> percentiles. (OD: right eye; OS: left eye, S: superior; I: inferior; N: nasal; T: temporal)

Finally, as we did for retinal and choroidal thickness, the correlation between the absolute values of inter-ocular asymmetry and the degree of refractive error was investigated. Statistically significant correlations were found between mean refractive error and absolute inter-ocular asymmetry in retinal sensitivity at most of the locations under study, particularly towards the centre of the retina. Thus, for instance, **Figure 6.11** shows the correlation between mean refractive error and sensitivity asymmetry at the first ring and temporal quadrant ( $r=-0.74$ ;  $p<0.001$ ). Other moderate to strong correlations were found at the first ring nasal quadrant ( $r=-0.58$ ;  $p<0.001$ ), first ring inferior quadrant ( $r=-0.49$ ;  $p<0.001$ ), second ring nasal quadrant ( $r=-0.63$ ;  $p<0.001$ ) and second ring superior quadrant ( $r=-0.50$ ;  $p<0.001$ ). In addition, mean refractive error was also found to present a statistically significant correlation with mean retinal function asymmetry of the first ring ( $r=-0.55$ ;  $p<0.001$ ). These findings point out that with an increase in myopic refractive error, the level of asymmetry in retinal function also increases,



particularly towards central regions. The relevance of these results must be described in the light of determining normalized values of retinal functional asymmetry when exploring patients with high myopia in order to discover possible retinal pathologies. Indeed, as myopia increases, the range of what should be considered normal asymmetry in the absence of pathology is progressively enlarged.

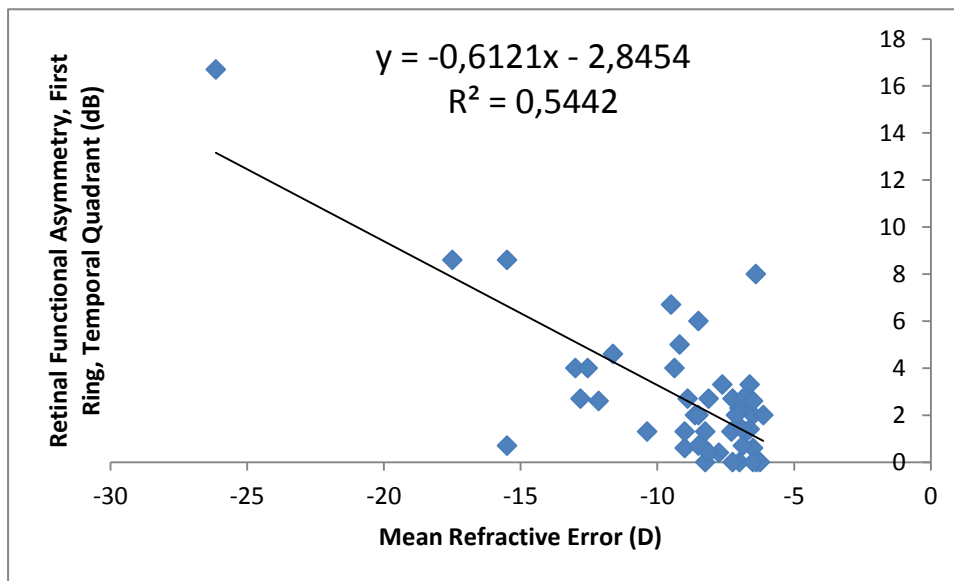


**Figure 6.11** Correlation between absolute inter-ocular asymmetry in central retinal thickness and mean refractive error for the myopia group

#### *Comparison of retinal sensitivity parameters between myopia and control groups*

Finally, the findings from the myopia group were compared with those of the control group ([Table 6.23](#) and [Table 6.24](#)).

The present findings revealed statistically significant differences in retinal sensitivity parameters at the right eye at the centre of the macula (high myopia resulted in less sensitivity). No other statistically significant differences were

found between the high myopia and control groups in retinal sensitivity, although in almost all instances lower sensitivity values may be observed in the myopia group. Indeed, retinal sensitivity values were lower in the myopic at all locations except at 2 mm and 3 mm superiorly, and at 3 mm inferiorly. These findings are in agreement with the work of Zaben and co-workers (2015), in which the authors concluded the retinal sensitivity is reduced in high myopic patients.

Parameter OD	Myopia		Normal		t	p
	Mean	SD	Mean	SD		
<b>Central sensitivity (dB)</b>	24.84	4.58	27.74	2.51	3.36	<b>0.001</b>
<b>1 mm N sensitivity (dB)</b>	27.21	4.39	27.42	1.86	0.267	0.790
<b>1 mm T sensitivity (dB)</b>	26.92	4.89	28.37	1.79	1.669	0.099
<b>1 mm S sensitivity (dB)</b>	27.64	3.64	28.51	2.14	1.251	0.215
<b>1 mm I sensitivity (dB)</b>	26.89	3.96	27.98	1.96	1.485	0.142
<b>2 mm N sensitivity (dB)</b>	27.15	4.84	28.03	2.10	1.003	0.319
<b>2 mm T sensitivity (dB)</b>	26.77	3.25	27.31	1.62	0.899	0.371
<b>2 mm S sensitivity (dB)</b>	27.54	2.43	27.44	2.24	-0.186	0.853
<b>2 mm I sensitivity (dB)</b>	27.29	2.85	27.69	2.10	0.679	0.499
<b>3 mm N sensitivity (dB)</b>	26.31	4.63	26.91	1.79	0.730	0.468
<b>3 mm T sensitivity (dB)</b>	26.13	2.95	26.54	1.92	0.707	0.482
<b>3 mm S sensitivity (dB)</b>	26.96	3.59	26.69	2.07	-0.405	0.687
<b>3 mm I sensitivity (dB)</b>	26.86	2.37	26.84	1.97	-0.050	0.960
<b>1 mm mean sensitivity (dB)</b>	27.18	4.02	28.04	1.71	1.175	0.244
<b>2 mm mean sensitivity (dB)</b>	27.25	3.15	27.72	1.91	0.775	0.441
<b>3 mm mean sensitivity (dB)</b>	26.56	3.21	26.70	1.72	0.189	0.850
<b>Mean Sensitivity (dB)</b>	27.10	3.61	27.50	1.71	0.559	0.578

**Table 6.23** Differences in absolute values between myopic and normal eyes in retinal sensitivity. Data is presented as mean  $\pm$  SD and only the right eye (OD) is shown. The t-test for unmatched pairs was used for statistical analysis (t and p values are shown)

Parameter differences (Absolute value)	Myopia		Normal		t	p
	Mean	SD	Mean	SD		
Central sensitivity (dB)	2.77	2.56	1.89	1.89	-1.717	0.900
1 mm N sensitivity (dB)	2.47	2.59	1.60	1.31	-1.818	0.073
1 mm T sensitivity (dB)	2.72	3.06	1.51	1.10	-2.233	<b>0.028</b>
1 mm S sensitivity (dB)	2.40	2.17	1.57	1.30	-2.013	<b>0.047</b>
1 mm I sensitivity (dB)	2.63	2.56	1.58	1.41	-2.175	<b>0.033</b>
2 mm N sensitivity (dB)	2.71	3.39	1.30	1.26	-2.327	<b>0.023</b>
2 mm T sensitivity (dB)	2.04	1.73	1.38	0.89	-2.069	<b>0.042</b>
2 mm S sensitivity (dB)	2.00	2.30	1.49	1.41	-1.157	0.251
2 mm I sensitivity (dB)	1.97	2.34	1.48	1.24	-1.119	0.266
3 mm N sensitivity (dB)	2.10	2.19	1.29	1.19	-1.982	0.051
3 mm T sensitivity (dB)	1.65	1.58	1.27	1.37	-1.142	0.257
3 mm S sensitivity (dB)	1.51	1.69	1.47	1.37	-0.121	0.904
3 mm I sensitivity (dB)	1.94	1.78	1.30	0.98	-1.939	0.056
1 mm mean sensitivity (dB)	2.33	2.35	1.23	0.99	-2.606	<b>0.011</b>
2 mm mean sensitivity (dB)	1.66	1.82	1.21	0.90	-1.341	0.184
3 mm mean sensitivity (dB)	1.53	1.26	1.13	1.04	-1.527	0.131
Mean Sensitivity (dB)	1.84	1.78	1.07	0.89	-2.371	<b>0.020</b>

**Table 6.24** Differences in relative values (inter-ocular asymmetry) between myopic and normal eyes in retinal sensitivity. Data is presented as in absolute values of (OD-OS) in mean  $\pm$  SD. The t-test for unmatched pairs was used for statistical analysis (t and p values are shown)

Regarding absolute inter-ocular asymmetry, statistically significant differences were found between the control and myopic groups at the 1 and 2 mm rings in several quadrants, as well as in mean values at the 1 mm ring and overall mean values. In all instances, asymmetry values were larger in the myopic group than in the normal group, in agreement with the correlation analysis described above,

in which moderate to strong correlations were found between mean refractive error and asymmetry in retinal function. These findings give support to the need to take into account these large asymmetries in myopic patients without associated pathological conditions when exploring patients for the onset of these pathologies. Indeed, as previously discussed, an interesting addition to this research would be to investigate the values of asymmetry in the presence of unilateral or bilateral typical pathologies related to high myopia such as staphylomas, which have been observed to occur mostly at the inferior quadrant.

### 6.7 Analysing the relationship between structural and functional changes in patients with high myopia:

The aim of this last part of the study was to investigate the association between asymmetry in retinal sensitivity and the corresponding asymmetry in macular and choroidal thickness.

All correlation analyses were performed with the Pearson correlation test ( $r$ ), the outcome of which is a value ranging from -1 (negative correlation) to 1 (positive correlation): values under  $\pm 0.3$  denote lack of correlation; from  $\pm 0.3$  to  $< \pm 0.6$  are weak correlations; from  $\pm 0.6$  to  $< \pm 0.8$ , moderate correlation, and from  $\pm 0.8$  to  $\pm 1$  strong correlation. For a correlation to exist, these values need to be associated with a level of significance  $p < 0.05$ .

Correlations between macular, choroid and retinal sensitivity were explored two-fold, first in healthy participants, and then in myopia. For each group of participants, point-by-point correlations were investigated between macular and retinal sensitivity parameters, as well as between choroidal thickness and retinal sensitivity, that is, the corresponding areas of the retina and choroid (1N, 1T, 1S, 1I, 2N, 2T, 2S, 2I, 3N, 3T, 3S, 3I) were assessed, and the mean values for each of the eccentricity rings and central values. In all instances, absolute values of inter-ocular asymmetry were considered.

#### Control group of healthy participants

Statistical analysis failed to reveal any correlation between macular/choroidal thickness asymmetry and retinal sensitivity asymmetry, with the exception of between retinal thickness asymmetry and choroidal thickness asymmetry at the centre of the retina ( $r=0.627$ ;  $p<0.001$ ) and at the 3 ring, temporal quadrant (3T) ( $r=0.358$ ;  $p=0.035$ ). The first correlation is shown in [Figure 6.12](#), together with the corresponding regression line,  $R^2$  and linear equation.

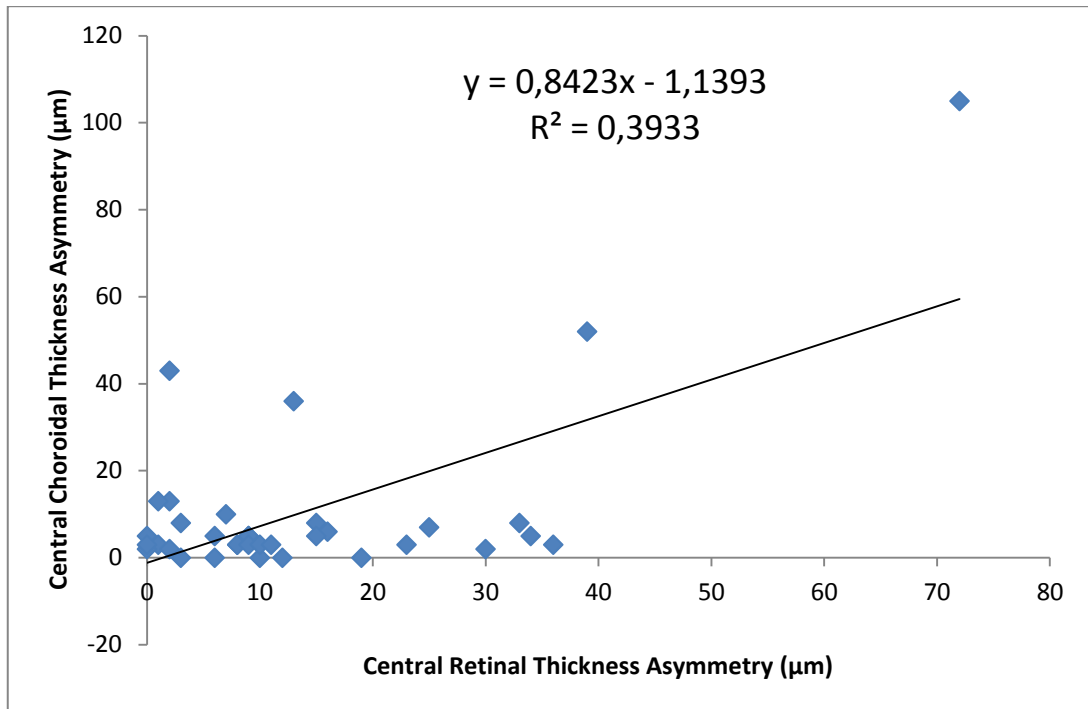


**Figure 6.12** Correlation between inter-ocular differences (absolute values) in retinal and choroidal thickness at the central position for the control group.

It may be observed that, overall, patients with good symmetry in central retinal thickness also display good symmetry in central choroidal thickness (data points near the Cartesian coordinate origin). Similarly, those few instances in which a large retinal asymmetry was found also presented large choroidal asymmetry. However, there are a number of patients with good central choroidal symmetry associated with a certain level of retinal asymmetry, that is, in normal patients, the thickness at the centre of the choroid may be more symmetrical than the corresponding thickness at the retinal centre.

Myopia group

The same analysis in the myopia group revealed several instances of statistically significant correlations:

1) Between retinal sensitivity asymmetry and choroidal thickness asymmetry at the second ring, superior quadrant (2S) ( $r=0.41$ ;  $p=0.005$ ) (**Figure 6.13**).

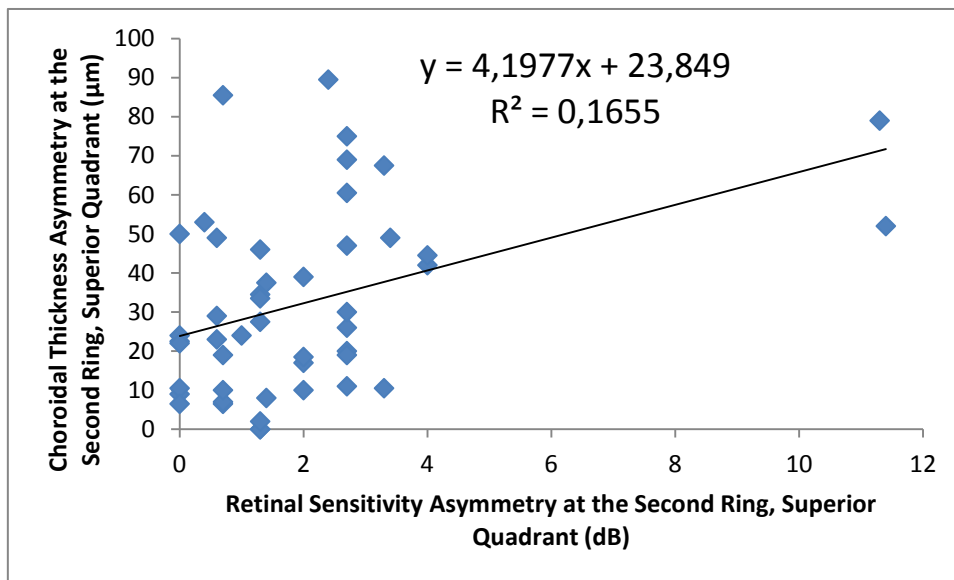


**Figure 6.13** Correlation between absolute inter-ocular difference in retinal sensitivity and absolute asymmetry of choroidal thickness at the 2S position for the myopia group.

2) Between absolute retinal sensitivity asymmetry and absolute retinal thickness asymmetry at the first ring and superior quadrant (1S) ( $r=0.36$ ;  $p=0.012$ ) (**Figure 6.14**), and at the second ring and temporal quadrant (2T) ( $r=0.38$ ;  $p=0.008$ ) (**Figure 6.15**).

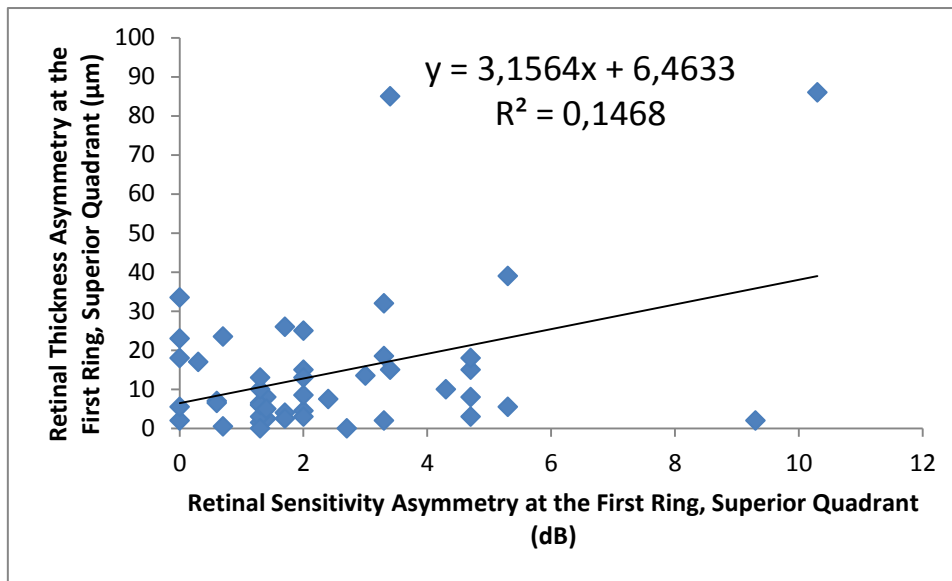


**Figure 6.14** Correlation between absolute inter-ocular difference in retinal sensitivity and absolute asymmetry of retinal thickness at the 1S position for the myopia group.

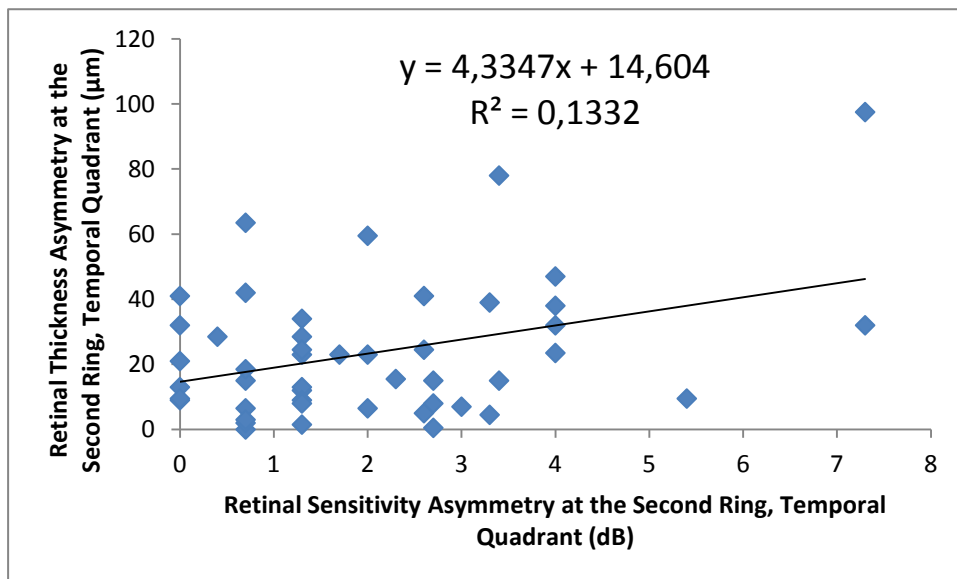


**Figure 6.15** Correlation between absolute inter-ocular difference in retinal sensitivity and absolute asymmetry of retinal thickness at the 2T position for the myopia group.



Therefore, it may be concluded that both in normal patients and in those with high myopia there is a general lack of correlation between anatomical (retinal and choroidal thickness) and functional asymmetry. These findings are in agreement with the pattern previously described when discussing the relationship between asymmetry and mean refractive error. Indeed, whereas a strong association was found between mean refractive error and retinal sensitivity, this association was not as manifest for retinal parameters and even less when choroidal asymmetry was considered. Overall, it may be concluded that retinal functional asymmetry is the most sensitive parameter, as compared to retinal and choroidal thickness asymmetry, to changes in refractive error in high myopia.



## 7. CONCLUSIONS

To the best of our knowledge, this is the first study exploring the inter-ocular asymmetry of the functional/structural profile of the macular area in high myopia. The main findings of the present research may be summarized as follows:

1- **Retinal thickness in normal patients** showed statistically significant differences between right and left eye in the macular regions at 1 mm, 2 mm, 3 mm both in the nasal and temporal quadrant. These results revealed that the inter-ocular asymmetry in retinal thickness may be an effective approach to gain a better understanding of the physiological variations of the macula in normal patients.

2- **Choroidal thickness in normal patients**, assessed with the depth imaging (EDI) technique of the SD – OCT, revealed statistically significant differences between right and left eye in the macular regions away from the centre at 1 mm and 2 mm temporally. Besides, the choroid was thicker at the centre of the macula in both eyes, followed by 2 mm at the superior quadrant and 3 mm at the inferior quadrant at the left eye. These findings suggest that the choroid is a dynamic anatomical structure worth investigating in health and disease.

3- **Retinal (macular) sensitivity differences between both eyes in normal patients** showed that in all instances the left eye had higher sensitivity than the right eye. The mean macular sensitivity values gradually decreased towards the periphery, with the lower retinal sensitivity at the 3 mm ring and temporal quadrant in both eyes, while the higher retinal sensitivity was found at 1 mm in the superior quadrant for both eyes. It is interesting to mention that the

reduction in retinal sensitivity towards the periphery is accompanied with a reduction of the mean retinal thickness as well.

4- Measuring **retinal thickness asymmetry in patients with high myopia** revealed a statistically significant correlation between mean refractive error and central retinal thickness asymmetry ( $r=-0.56$ ;  $p<0.001$ ), that is, asymmetry between both eyes increased with refractive error. In addition, when compared with the control group, statistically significant differences were uncovered at the 1 and 2 mm in most quadrants, thus giving support to the need to take into account these differences in asymmetry when examining myopic eyes for the existence of disease.

5- Measuring **choroidal thickness in patients with high myopia** using the enhanced depth imaging (EDI) technique of the SD – OCT showed that the choroid in high myopia was thinner towards the centre of the macula and progressively gained thickness towards the periphery. Besides, statistically significant differences were found between the control and myopic groups in choroidal parameters in most locations under study, with larger differences between OD and OS in the myopic than in the control group. Interestingly, although inter-ocular asymmetry differences were found between both groups, asymmetry did not increase with refractive error in the myopic group.

6- Exploring **retinal sensitivity in patients with high myopia** revealed that sensitivity gradually decreased away from the centre of the macula. Besides, although in almost all instances lower sensitivity values were observed in the myopia group, these differences were mostly not statistically significant. A relevant finding, however, was that in the myopic group absolute values of inter-ocular asymmetry increased with refractive error. These findings support caution

when investigating inter-ocular asymmetry in retinal function to rule the existence of disease as a larger range of normality needs to be considered in high myopia.

7- Finally, analysing the **relationship between structural and functional parameters** for both the control and myopic group revealed only anecdotal associations, that is, there was a general lack of correlation between anatomical (retinal and choroidal thickness) and functional asymmetry. These findings would suggest a different behaviour/origin for these anatomical and functional asymmetries. Further studies shall explore anatomical and functional asymmetry in the presence of some of the most common pathological conditions associated with high myopia, such as inferior staphyloma.



## 8. Future Research

The present findings evidenced a different level of inter-ocular asymmetry in high myopia that in an age- and gender-matched group of healthy patients. In addition, statistically significant correlations were uncovered between refractive error and inter-ocular asymmetry, albeit not all anatomical and functional parameters displayed this relationship, and results also differed within the same type of measurement (retinal and choroidal thickness and retinal sensitivity). Future research shall aim at understanding this behaviour in the light of myopia development and progression. Indeed, not all patients with high myopia develop pathological changes in their ocular fundi. There is a current lack of understanding of why in certain patients high myopia progresses to pathological or degenerative myopia while in other patients high refractive error is not associated *per se* with severe ocular complications. The study of inter-ocular asymmetry in the absence of disease may provide support to this investigation.

As described in the state of the art, pathological myopia is associated with many severe, potentially visual threatening conditions, mainly related to chorio-retinal vascularisation. Further research using the OCT and MAIA instrumentation may be directed to explore anatomical and functional parameters (both in terms of absolute and relative or inter-ocular values) in those patients with pathological myopia, paying particular attention to those in which pathology is progressing asymmetrically. In effect, in those patients it would be of interest to determine the possible correlation between inter-ocular asymmetry in anatomical and functional parameters and differences in refractive error or differences in pathological progression. Related to this, in the present study anisometropia was strictly controlled to avoid the possibility of confounding variables that may hinder the interpretation of the results. Future research may focus on the association between the difference of refractive error between the eyes and the

corresponding degree of inter-ocular asymmetry in the various anatomical and functional parameters under study.

Of recent interest is the finding that one of the contributing factors leading to the development and progression of myopia could be peripheral hypermetropic defocus, that is, if light rays reaching the periphery of the retina focus behind it, the eye may be compelled to increase its axial length, resulting in myopia progression. It may be relevant to correlate the anatomical and functional characteristics of the periphery of the retina to further understand the mechanisms involved in myopia progression.

Finally, we have noted throughout this thesis that the results we reported were, in most cases, difficult to compare with previous research, due to differences in both instrumentation and study sample characteristics. Given the giant steps being conducted in the development of new instrumentation it is critical that research such as the one performed for this thesis shall be constantly reviewed and revisited as soon as this new instrumentation becomes available. Thus, practitioners need to be aware of the range of normality, both in absolute and relative values, associated with each device in order to improve in their diagnostic proficiency. In addition, specific age groups need to be further explored, according to the lack of published literature, as well as ethnic groups with particular characteristics.

In this regards, we would like to encourage future researchers to use the results described in this thesis as a basis for their own research, and to be very critical with the limitations of our instrumentation, study sample and methodology. It will be our satisfaction to discover how these researchers find ingenious ways to overcome our limitations, thus helping, in our humble way, to scientific progress.



## 9. Works Derived From the Thesis

The research described in the present thesis has been presented in several international meetings and conferences, and has been submitted and accepted (pending publication) to a prestigious journal.

### Articles in peer-reviewed indexed journals

**Alzaben Z**, Cardona G, Zapata MA, Zaben A. Inter-ocular asymmetry in choroidal thickness and retinal sensitivity in high myopia. *Retina*. 2017; Available online 6 July 2017 <http://dx.doi.org/10.1097/IAE.0000000000001756> (**Annex II**)

*Retina (The Journal of Retinal and Vitreous Diseases)* is a journal published by Wolters and Kluwer with a periodicity of 12 issues per year. It currently holds an impact factor of **3.039** and is **9/57** in the **Ophthalmology** Category of the Journal Citation Reports (2015 edition). ISSN: 0275-004X

### Articles in peer-reviewed, non-index journals

Alzaben Z, Cardona G, Zaben A, Zapata MA. Inter - ocular asymmetry of retinal parameters in Caucasian healthy children and young adults measured with optical coherence tomography. *Guoji Yanke Zazhi (International Eye Science)*. 2018;18(1):1-6. <http://dx.doi.org/10.3980/j.issn.1672-5123.2018.1.01> (**Annex III**)

### Abstracts submitted to peer-reviewed meetings and conferences

**Alzaben Z**, Cardona G, Zapata MA, Zaben A. Retinal sensitivity asymmetry in high myopia and its correlation with refractive error. *Association for Research in Vision and Ophthalmology (ARVO)*, Baltimore, Maryland, May 7-11, 2017. (**Annex IV**).

Zaben A, **Alzaben Z**, Zapata MA, Cardona G, Maldonado MJ, Koff D. The choroidal profile in a sample of young Caucasians affected by myopia. 6th Global Ophthalmologists Annual Meeting, Osaka, Japan, 2016 (*J Clin Exp Ophthalmol.* 2016;7(2, Suppl): 87, ISSN: 2155-9570). ([Annex V](#)).

**Alzaben Z**, Cardona G, Zapata MA, Zaben A, Maldonado MJ, Koff D. Functional asymmetry in macular area in patients with pathological myopia using microperimetry. 6th Global Ophthalmologists Annual Meeting, Osaka, Japan, 2016 (*J Clin Exp Ophthalmol.* 2016;7(2, Suppl): 92, ISSN: 2155-9570). ([Annex V](#)).

**Alzaben Z**, Cardona G, Zapata MA, Zaben A, Maldonado MJ, Koff D. Inter-ocular asymmetry of retinal parameters as measured with Ocular Coherence Tomography (OCT) in a sample of healthy young adults. 6th Global Ophthalmologists Annual Meeting, Osaka, Japan, 2016 (*J Clin Exp Ophthalmol.* 2016;7(2, Suppl): 81, ISSN: 2155-9570). ([Annex V](#)).

**Alzaben Z**, Cardona G, Zapata MA, Zaben A, Maldonado MJ, Koff D. Asimetría funcional en area macular en pacientes con miopía patológica usando microperimetría. XXIV Congreso Internacional de Optometría, Contactología y Óptica Oftálmica. Optom2016, Madrid, 2016 (libro de Abstracts, ISBN: 978-84-941966-4-5). ([Annex VI](#)).

**Alzaben Z**, Cardona G, Zaben A, Zapata MA, Koff D. Variación del espesor de la coroides con la longitud axial en la población caucásica con alta miopía. XXIV Congreso Internacional de Optometría, Contactología y Óptica Oftálmica. Optom2016, Madrid, 2016 (libro de Abstracts, ISBN: 978-84-941966-4-5). ([Annex VI](#)).

It is also worth noting that the research described in this thesis received the approval of the **Ethics review Board the Hospital Universitari Mutua de Terrassa, Spain.**

## 10. References

- Adhi, M., Aziz, S., Muhammad, K., Adhi, M.I., 2012. Macular thickness by age and gender in healthy eyes using spectral domain optical coherence tomography. *PLoS ONE* 7(5), e37638.
- Adhi, M., Duker, J.S., 2013. Optical coherence tomography – current and future applications. *Curr. Opin. Ophthalmol.* 24, 213–221.
- Adhi M, Liu JJ, Qavi AH, Grulkowski I, Lu CD, Mohler KJ, Ferrara D, Kraus MF, Baumal CR, Witkin AJ, Waheed NK, Hornegger J, Fujimoto JG, Duker JS, 2014. Choroidal analysis in healthy eyes using swept-source optical coherence tomography compared to spectral domain optical coherence tomography. *Am J Ophthalmol*, 157(6), 1272-1281.e1.
- Aironi, V., Gandage, S., 2009. Pictorial essay: B-scan ultrasonography in ocular abnormalities. *Indian J. Radiol. Imaging* 19, 109–115.
- Alasil, T., Wang, K., Keane, P.A., Lee, H., Baniyadi, N., de Boer, J.F., Chen, T.C., 2013. Analysis of normal retinal nerve fiber layer thickness by age, sex, and race using spectral domain optical coherence tomography. *J. Glaucoma* 22, 532–541.
- Albou-Ganem, C., Lavaud, A., Amar, R., 2015. SMILE: Refractive lenticule extraction for myopic correction. *J. Fr. Ophtalmol.* 38(3), 229-237.
- Alencar, L.M., Medeiros, F.A., 2011. The role of standard automated perimetry and newer functional methods for glaucoma diagnosis and follow-up. *Indian J. Ophthalmol.* 59, S53–S58.
- Alexander, P., Mushtaq, F., Osmond, C., Amoaku, W., 2012. Microperimetric changes in neovascular age-related macular degeneration treated with ranibizumab. *Eye* 26, 678–683.
- Alkabes, M., Padilla, L., Salinas, C., Nucci, P., Vitale, L., Pichi, F., Burès-Jelstrup, A., Mateo, C., 2013. Assessment of OCT measurements as prognostic factors in myopic macular hole surgery without foveoschisis. *Graefes Arch. Clin. Exp. Ophthalmol.* 251, 2521–2527.
- Alluwimi MS, Swanson WH, Malinovsky VE, 2014. Between-subject variability in asymmetry analysis of macular thickness. *Optom Vis Sci*, 91(5), 484-490.
- Altemir I, Oros D, Elía N, Polo V, Larrosa JM, Pueyo V, 2013. Retinal asymmetry in children measured with optical coherence tomography. *Am J Ophthalmol.* 156, 1238–1243.
- Arevalo, J.F., Sanchez, J.G., Garcia, R.A., 2009. Artifacts and Limitations in Time-Domain Optical Coherence Tomography Images, in: FACS, J.F.A.M. (Ed.), *Retinal Angiography and Optical Coherence Tomography*. Springer New York, pp. 375–386.

## Chapter 10. References

Armaly MF, 1967. Genetic determination of cup/disc ratio of the optic nerve. *Arch Ophthalmol.* 78, 35-43.

Atchison, D.A., 2014. Relative peripheral defocus and myopic progression in children. *Graefes Arch. Clin. Exp. Ophthalmol.* 252, 173.

Aygit, E.D., Yilmaz, I., Ozkaya, A., Alkin, Z., Gokyigit, B., Yazici, A.T., Demirok, A., 2015. Choroidal thickness of children's eyes with anisometropic and strabismic amblyopia. *J. AAPOS Off. Publ. Am. Assoc. Pediatr. Ophthalmol. Strabismus Am. Assoc. Pediatr. Ophthalmol. Strabismus* 19, 237–241.

Battaglia Parodi, M., Triolo, G., Morales, M., Borrelli, E., Cicinelli M. V., Cascavilla, M. L., Bandello F., 2015. MP1 and MAIA fundus perimetry in healthy subjects and patients affected by retinal dystrophies. *Retina.* 35, 1662-1669.

Battu R, Khanna A, Hegde B, Berendschot TT, Grover S, Schouten JS, 2015. Correlation of structure and function of the macula in patients with retinitis pigmentosa. *Eye (Lond)*, 29(7), 895-901.

Bell, G.R., 1993. Biomechanical considerations of high myopia: Part II--Biomechanical forces affecting high myopia. *J. Am. Optom. Assoc.* 64, 339–345.

Benavente-Pérez, A., Nour, A., Troilo, D., 2014. Axial eye growth and refractive error development can be modified by exposing the peripheral retina to relative myopic or hyperopic defocus. *Invest. Ophthalmol. Vis. Sci.* 55, 6765–6773.

Benmerzouga Mahfoudi, N., Chaker Harbi, M., Boulaneb Beddiar, F., Chachoua, L., 2015. Bilateral retinal detachment and high myopia: Report of nine cases. *J. Fr. Ophthalmol.* 38, 141–145.

Bentaleb-Machkour, Z., Jouffroy, E., Rabilloud, M., Grange, J.-D., Kodjikian, L., 2012. Comparison of central macular thickness measured by three OCT models and study of interoperator variability. *ScientificWorldJournal*, 842795.

Branchini LA, Adhi M, Regatieri CV, Nandakumar N, Liu JJ, Laver N, Fujimoto JG, Duker JS, 2013. Analysis of choroidal morphologic features and vasculature in healthy eyes using spectral-domain optical coherence tomography. *Ophthalmology*, 120(9), 1901-1908.

Browning, D.J., Lee, C., 2015. Scotoma analysis of 10-2 visual field testing with a white target in screening for hydroxychloroquine retinopathy. *Clin. Ophthalmol.* 9, 943–952.

Budenz DL, 2008. Symmetry between the right and left eyes of the normal retinal nerve fiber layer measured with optical coherence tomography (an AOS thesis). *Trans Am Ophthalmol Soc.* 106, 252–275.

Budenz DL, Anderson DR, Varma R, et al, 2007. Determinants of normal retinal fiber layer thickness measured by Stratus OCT. *Ophthalmology.* 114, 1046-1052.

## Chapter 10. References

- Carmen A., P., 2012. A Brief History of Optical Coherence Tomography: A Personal Perspective. *Ophthalmic Surg. Lasers Imaging Retina* 39, S6–S7.
- Chan A, Duker JS, Ko TH, Fujimoto JG, Schuman JS, 2006. Normal macular thickness measurements in healthy eyes using Stratus optical coherence tomography. *Arch Ophthalmol.* 124, 193–198.
- Chebil, A., Ben Achour, B., Maamouri, R., Ben Abdallah, M., El Matri, L., 2014. Peripapillary changes detected by SD OCT in eyes in high myopia. *J. Fr. Ophtalmol.* 37, 635–639.
- Chebil, A., Maamouri, R., Ben Abdallah, M., Ouderni, M., Chaker, N., El Matri, L., 2015. Foveal choroidal thickness assessment with SD-OCT in high myopic glaucoma. *J. Fr. Ophtalmol.* 38, 440–444.
- Chen, F.K., Patel, P.J., Webster, A.R., Coffey, P.J., Tufail, A., Da Cruz, L., 2011. Nidek MP1 is able to detect subtle decline in function in inherited and age-related atrophic macular disease with stable visual acuity. *Retina* 31, 371–379.
- Chen, F.K., Patel, P.J., Xing, W., Bunce, C., Egan, C., Tufail, A.T., Coffey, P.J., Rubin, G.S., Da Cruz, L., 2009. Test-retest variability of microperimetry using the Nidek MP1 in patients with macular disease. *Invest. Ophthalmol. Vis. Sci.* 50, 3464–3472.
- Chen FK, Yeoh J, Rahman W, Patel PJ, Tufail A, Da Cruz L, 2012. Topographic variation and interocular symmetry of macular choroidal thickness using enhanced depth imaging optical coherence tomography. *Invest Ophthalmol Vis Sci*, 23, 53(2), 975-985.
- Chen, H., Wen, F., Li, H., Zuo, C., Zhang, X., Huang, S., Luo, G., 2012. The types and severity of high myopic maculopathy in Chinese patients. *Ophthalmic Physiol. Opt. J. Br. Coll. Ophthalmic Opt. Optom.* 32, 60–67.
- Chen, W., Wang, Z., Zhou, X., Li, B., Zhang, H., 2012. Choroidal and photoreceptor layer thickness in myopic population. *Eur. J. Ophthalmol.* 22, 590–597.
- Chhablani, J., Deepa, M.J., Tyagi, M., Narayanan, R., Kozak, I., 2015. Fluorescein angiography and optical coherence tomography in myopic choroidal neovascularization. *Eye Lond. Engl.* 29(4), 519-524.
- Chhablani, J., Krishnan, T., Sethi, V., Kozak, I., 2014. Artifacts in optical coherence tomography. *Saudi J. Ophthalmol.* 28, 81–87.
- Chhablani, J., Rao, P.S., Venkata, A., Rao, H.L., Rao, B.S.K., Kumar, U., Narayanan, R., Pappuru, R.R., 2014. Choroidal thickness profile in healthy Indian subjects. *Indian J. Ophthalmol.* 62, 1060–1063.

Choi JA, Kim JS, Park HY, Park H, Park CK, 2014. The foveal position relative to the optic disc and the retinal nerve fiber layer thickness profile in myopia. *Invest Ophthalmol Vis Sci*, 55(3), 1419-1426.

Chui, T.Y.P., VanNasdale, D.A., Elsner, A.E., Burns, S.A., 2014. The association between the foveal avascular zone and retinal thickness. *Invest. Ophthalmol. Vis. Sci.* 55, 6870–6877.

Colombo, L., Sala, B., Montesano, G., Pierrottet, C., De Cillà, S., Maltese, P., Bertelli, M., Rossetti, L., 2015. Choroidal thickness analysis in patients with usher syndrome type 2 using EDI OCT. *J. Ophthalmol.* 189140.

Christina Springer, Stefan Bültmann, Hans E Völcker, Klaus Rohrschneider (2005). Fundus Perimetry with the Micro Perimeter 1 in Normal Individuals: Comparison with Conventional Threshold Perimetry. *Ophthalmology*, 112(5), 848-854.

Crossland, M.D., Jackson, M.-L., Seiple, W.H., 2012. Microperimetry: a review of fundus related perimetry. *Optom. Rep.* 2, 11–15.

Crossland, M.D., Sims, M., Galbraith, R.F., Rubin, G.S., 2004. Evaluation of a new quantitative technique to assess the number and extent of preferred retinal loci in macular disease. *Vision Res.* 44, 1537–1546.

Dagliesh JD, Tariq YM, Burlutsky G, Mitchell P, 2015. Symmetry of retinal parameters measured by spectral-domain OCT in normal young adults. *J Glaucoma*, 24(1), 20-24.

Dave P, Shah J, 2015. Applicability of ISNT and IST rules to the retinal nerve fibre layer using spectral domain optical coherence tomography in early glaucoma. *Br J Ophthalmol.* 99(12), 1713-1717.

Dawczynski J, Koenigsdoerffer E, Augsten R, Strobel J, 2007. Anterior segment optical coherence tomography for evaluation of changes in anterior chamber angle depth after intraocular lens implantation in eyes with glaucoma. *Eur J Ophthalmol.* 17, 363-367.

Dhoot, D.S., Huo, S., Yuan, A., Xu, D., Srivistava, S., Ehlers, J.P., Traboulsi, E., Kaiser, P.K., 2013. Evaluation of choroidal thickness in retinitis pigmentosa using enhanced depth imaging optical coherence tomography. *Br. J. Ophthalmol.* 97, 66–69.

Ding, X., Li, J., Zeng, J., Ma, W., Liu, R., Li, T., Yu, S., Tang, S., 2011. Choroidal thickness in healthy Chinese subjects. *Invest. Ophthalmol. Vis. Sci.* 52, 9555–9560.

Dirani, M., Chamberlain, M., Shekar, S.N., Islam, A.F.M., Garoufalos, P., Chen, C.Y., Guymer, R.H., Baird, P.N., 2006. Heritability of refractive error and ocular biometrics: the Genes in Myopia (GEM) twin study. *Invest. Ophthalmol. Vis. Sci.* 47, 4756–4761.

Drexler W, Fujimoto JG, 2008. State-of-the-art retinal optical coherence tomography. *Prog Retin Eye Res.* 27, 45-48.

## Chapter 10. References

- Dunbar, H.M.P., Crossland, M.D., Rubin, G.S., 2010. Fixation Stability: A Comparison between the Nidek MP-1 and the Rodenstock Scanning Laser Ophthalmoscope in Persons with and without Diabetic Maculopathy. *Invest. Ophthalmol. Vis. Sci.* 51, 4346–4350.
- El-Dairi MA, Asrani SG, Enyedi LB, Freedman SF, 2009. Optical coherence tomography in the eyes of normal children. *Arch Ophthalmol.* 127, 50-58.
- El Matri L, Bouladi M, Chebil A, Kort F, Bouraoui R, Lagueche L, Mghaieth F, 2012. Choroidal thickness measurement in highly myopic eyes using SD-OCT. *Ophthalmic Surg Lasers Imaging*, 43(6 Suppl), S38-43.
- El Matri L, Bouladi M, Chebil A, Kort F, Lagueche L, Mghaieth F, 2013. Macular choroidal thickness assessment with SD-OCT in high myopia with or without choroidal neovascularization. *J Fr Ophtalmol*, 36(8), 687-692.
- Essock EA, Sinai MJ, Fechtner RD, 1999. Interocular symmetry in nerve fiber layer thickness of normal eyes as determined by polarimetry. *J Glaucoma.* 8, 90-98.
- Field MG, Alasil T, Baniyadi N, Que C, Simavli H, Sobeih D, Sola-Del Valle D, Best MJ, Chen TC, 2016. Facilitating Glaucoma Diagnosis With Intereye Retinal Nerve Fiber Layer Asymmetry Using Spectral-Domain Optical Coherence Tomography. *J Glaucoma*, 25(2), 167-176
- Flores-Moreno, I., Lugo, F., Duker, J.S., Ruiz-Moreno, J.M., 2013. The relationship between axial length and choroidal thickness in eyes with high myopia. *Am. J. Ophthalmol.* 155, 314–319.
- Flores-Moreno I, Ruiz-Medrano J, Duker JS, Ruiz-Moreno JM, 2013. The relationship between retinal and choroidal thickness and visual acuity in highly myopic eyes. *Br J Ophthalmol*, 97(8), 1010-1013.
- Fujimoto, G., Pitris, C., Boppart, S., Brezinski, M., 2000. Optical Coherence Tomography: An emerging technology for biomedical imaging and optical biopsy. *Neoplasia*, 2 (1-2), 9-25.
- Fujiwara, A., Shiragami, C., Manabe, S., Izumibata, S., Murata, A., Shiraga, F., 2014. Normal values of retinal sensitivity determined by macular integrity assessment. 118, 15–21.
- Fujiwara, A., Shiragami, C., Shirakata, Y., Manabe, S., Izumibata, S., Shiraga, F., 2012. Enhanced depth imaging spectral-domain optical coherence tomography of subfoveal choroidal thickness in normal Japanese eyes. *Jpn. J. Ophthalmol.* 56, 230–235.
- Fujiwara, T., Imamura, Y., Margolis, R., Slakter, J.S., Spaide, R.F., 2009. Enhanced depth imaging optical coherence tomography of the choroid in highly myopic eyes. *Am. J. Ophthalmol.* 148, 445–450.

## Chapter 10. References

- Gabriele, M.L., Wollstein, G., Ishikawa, H., Kagemann, L., Xu, J., Folio, L.S., Schuman, J.S., 2011. Optical coherence tomography: history, current status, and laboratory work. *Invest. Ophthalmol. Vis. Sci.* 52, 2425–2436.
- Gallego-Pinazo, R., Díaz-Llopis, M., 2011. Redescubriendo la mácula de la miopía magna en el siglo xxi. *Arch. Soc. Esp. Oftalmol.* 86, 135–138.
- García-Ben, A., García-Campos, J.M., Morillo Sanchez, M.J., Figueroa-Ortiz, L.C., 2014. Choriorretinal atrophy after spontaneous resolution of myopic foveoschisis. *Case Rep. Ophthalmol. Med.* 2014, 825906.
- Gaucher, D., Haouchine, B., Tadayoni, R., Massin, P., Erginay, A., Benhamou, N., Gaudric, A., 2007. Long-term follow-up of high myopic foveoschisis: natural course and surgical outcome. *Am. J. Ophthalmol.* 143, 455–462.
- Geiser, M.H., Truffer, F., Evequoz, H., Khayi, H., Mottet, B., Chiquet, C., 2013. Schlieren laser Doppler flowmeter for the human optical nerve head with the flicker stimuli. *J. Biomed. Opt.* 18 (12), 127001.
- Gómez-Resa, M., Burés-Jelstrup, A., Mateo, C., 2014. Myopic traction maculopathy. *Dev. Ophthalmol.* 54, 204–212.
- Gomi, F., Tano, Y., 2008. Polypoidal choroidal vasculopathy and treatments. *Curr. Opin. Ophthalmol.* 19, 208–212.
- Grover, S., Murthy, R.K., Brar, V.S., Chalam, K.V., 2010. Comparison of retinal thickness in normal eyes using Stratus and Spectralis optical coherence tomography. *Invest. Ophthalmol. Vis. Sci.* 51, 2644–2647.
- Gupta, P., Cheung, C.Y.-L., Saw, S.-M., Bhargava, M., Tan, C.S.H., Tan, M., Yang, A., Tey, F., Nah, G., Zhao, P., Wong, T.Y., Cheng, C.-Y., 2015. Peripapillary Choroidal Thickness in Young Asians with High Myopia. *Invest. Ophthalmol. Vis. Sci.* 56 (3), 1475-1481.
- Gupta, P., Saw, S.-M., Cheung, C.Y., Girard, M.J.A., Mari, J.M., Bhargava, M., Tan, C., Tan, M., Yang, A., Tey, F., Nah, G., Zhao, P., Wong, T.Y., Cheng, C.-Y., 2014. Choroidal thickness and high myopia: a case-control study of young Chinese men in Singapore. *Acta Ophthalmol. (Copenh.)*. 93(7), e585-e592.
- Harb, E., Hyman, L., Gwiazda, J., Marsh-Tootle, W., Zhang, Q., Hou, W., Norton, T.T., Weise, K., Dirkes, K., Zangwill, L.M., COMET Study Group, 2015. Choroidal thickness profiles in myopic eyes of young adults in the correction of myopia evaluation trial cohort. *Am. J. Ophthalmol.* 160, 62–71.e2.
- Hayreh, S.S., Zimmerman, M.B., 2014. Amaurosis fugax in ocular vascular occlusive disorders: prevalence and pathogeneses. *Retina* 34, 115–122.



## Chapter 10. References

- Hazel, C.A., Petre, K.L., Armstrong, R.A., Benson, M.T., Frost, N.A., 2000. Visual function and subjective quality of life compared in subjects with acquired macular disease. *Invest. Ophthalmol. Vis. Sci.* 41, 1309–1315.
- Henaine-Berra, A., Zand-Hadas, I.M., Fromow-Guerra, J., García-Aguirre, G., 2013. Prevalence of macular anatomic abnormalities in high myopia. *Ophthalmic Surg. Lasers Imaging Retina* 44, 140–144.
- Herrera, L., Perez-Navarro, I., Sanchez-Cano, A., Perez-Garcia, D., Remon, L., Almenara, C., Caramello, C., Cristóbal, J.A., Pinilla, I., 2015. Choroidal thickness and volume in a healthy pediatric population and its relationship with age, axial length, ametropia, and sex. *Retina*. 35(12), 2574-2583.
- Hirata M, Tsujikawa A, Matsumoto A, Hangai M, Ooto S, Yamashiro K, Akiba M, Yoshimura N, 2011. Macular choroidal thickness and volume in normal subjects measured by swept-source optical coherence tomography. *Invest Ophthalmol Vis Sci*, 52(8), 4971-4978.
- Ho, M., Liu, D.T.L., Chan, V.C.K., Lam, D.S.C., 2013. Choroidal thickness measurement in myopic eyes by enhanced depth optical coherence tomography. *Ophthalmology* 120, 1909–1914.
- Hoffmann EM, Zangwill LM, Crowston JG, Weinreb RN, 2007. Optic Disk Size and Glaucoma. *Surv Ophthalmol.* 52, 32–49
- Hong, S.W., Lee, S.B., Jee, D.-H., Ahn, M.D., 2015. Interocular retinal nerve fiber layer thickness difference in normal adults. *PloS One* 10 (2), e0116313.
- Honjo M, Omodaka K, Ishizaki T, Ohkubo S, Araie M, Nakazawa T, 2015. Retinal Thickness and the Structure/Function Relationship in the Eyes of Older Adults with Glaucoma. *PLoS One*, 10(10), e0141293.
- Huang, D., Swanson, E.A., Lin, C.P., Schuman, J.S., Stinson, W.G., Chang, W., Hee, M.R., Flotte, T., Gregory, K., Puliafito, C.A., 1991. Optical coherence tomography. *Science* 254, 1178–1181.
- Hua, R., Liu, L., Wang, X., Chen, L., 2013. Imaging evidence of diabetic choroidopathy in vivo: angiographic pathoanatomy and choroidal-enhanced depth imaging. *PloS One* 8 (12), e83494.
- Huynh SC, Wang XY, Burlutsky G, Mitchell P, 2007. Symmetry of optical coherence tomography retinal measurements in young children. *Am J Ophthalmol.* 143, 518–520.
- Huynh SC, Wang XY, Rochtchina E, Mitchell P, 2006. Distribution of macular thickness by optical coherence tomography: findings from a population-based study of 6-year-old children. *Invest Ophthalmol Vis Sci.* 47, 2351-2357.

## Chapter 10. References

- Hyman, L., Gwiazda, J., Hussein, M., Norton, T.T., Wang, Y., Marsh-Tootle, W., Everett, D., 2005. Relationship of age, sex, and ethnicity with myopia progression and axial elongation in the correction of myopia evaluation trial. *Arch. Ophthalmol.* 123, 977–987.
- Iester, M., Violanti, S., Borgia, L., 2015. Clinical assessment of retinal changes by spectral-domain OCT. *Eur. J. Ophthalmol.* 25(5), 443-447.
- Ikuno Y, Kawaguchi K, Nouchi T, Yasuno Y (2010). Choroidal thickness in healthy Japanese subjects. *Invest Ophthalmol Vis Sci* 51, 2173–2176.
- Ikuno, Y., Tano, Y., 2009. Retinal and choroidal biometry in highly myopic eyes with spectral-domain optical coherence tomography. *Invest. Ophthalmol. Vis. Sci.* 50, 3876–3880.
- Invernizzi, A., Mapelli, C., Viola, F., Cigada, M., Cimino, L., Ratiglia, R., Staurenghi, G., Gupta, A., 2015. Choroidal granulomas visualized by enhanced depth imaging optical coherence tomography. *Retina* 35, 525–531.
- Ismail, S.A., Sharanjeet-Kaur, Mutalib, H.A., Ngah, N.F., 2015. Macular retinal sensitivity using MP-1 in healthy Malaysian subjects of different ages. *J. Optom.* 8(4), 266-272.
- Jaffe GJ, Caprioli J, 2004. Optical coherence tomography to detect and manage retinal disease and glaucoma. *Am J Ophthalmol.* 137, 156–69.
- Jin P, Zou H, Zhu J, Xu X, Jin J, Chang TC, Lu L, Yuan H, Sun S, Yan B, He J, Wang M, He X, 2016. Choroidal and Retinal Thickness in Children With Different Refractive Status Measured by Swept-Source Optical Coherence Tomography. *Am J Ophthalmol.* 168, 164-176.
- Jirarattanasopa, P., Panon, N., Hiranyachattada, S., Bhurayanontachai, P., 2014. The normal choroidal thickness in southern Thailand. *Clin. Ophthalmol.* 8, 2209–2213.
- Karapetyan A, Ouyang P, Tang LS, Gemilyan M, 2016. Choroidal Thickness in Relation to Ethnicity Measured Using Enhanced Depth Imaging Optical Coherence Tomography. *Retina*, 36(1), 82-90.
- Koyoko Ohno-Matsui, 2016. What is the Fundamental Nature of Pathological Myopia?. *Retina* DOI: 10.1097/IAE.0000000000001348
- Kashani, A.H., Zimmer-Galler, I.E., Shah, S.M., Dustin, L., Do, D.V., Elliott, D., Haller, J.A., Nguyen, Q.D., 2010. Retinal thickness analysis by race, gender, and age using Stratus OCT™. *Am. J. Ophthalmol.* 149, 496–502.e1.
- Kawaguchi C, Nakatani Y, Ohkubo S, Higashide T, Kawaguchi I, Sugiyama K, 2014. Structural and functional assessment by hemispheric asymmetry testing of the macular region in preperimetric glaucoma. *Jpn J Ophthalmol*, 58(2), 197-204.

## Chapter 10. References

- Kee, S.-Y., Lee, S.-Y., Lee, Y.-C., 2006. Thicknesses of the fovea and retinal nerve fiber layer in amblyopic and normal eyes in children. *Korean J. Ophthalmol.* KJO 20, 177–181.
- Khetan, V., Bindu, A., Kamat, P., Kumar, S.K., 2014. Failure of globe conservation in a case of adult onset retinoblastoma. *Middle East Afr. J. Ophthalmol.* 21, 358–360.
- Kim, J.T., Lee, D.H., Joe, S.G., Kim, J.-G., Yoon, Y.H., 2013. Changes in choroidal thickness in relation to the severity of retinopathy and macular edema in type 2 diabetic patients. *Invest. Ophthalmol. Vis. Sci.* 54, 3378–3384.
- Knight, O.J., Girkin, C.A., Budenz, D.L., Durbin, M.K., Feuer, W.J., Cirrus OCT Normative Database Study Group, 2012. Effect of race, age, and axial length on optic nerve head parameters and retinal nerve fiber layer thickness measured by Cirrus HD-OCT. *Arch. Ophthalmol.* 130, 312–318.
- Kochendörfer, L., Bauer, P., Funk, J., Töteberg-Harms, M., 2014. Posterior pole asymmetry analysis with optical coherence tomography. *Klin Monbl Augenheilkd*, 231, 368–373.
- Koh, V.T., Nah, G.K., Chang, L., Yang, A.H.X., Lin, S.T., Ohno-Matsui, K., Wong, T.Y., Saw, S.M., 2013. Pathologic changes in highly myopic eyes of young males in Singapore. *Ann Acad Med Singapore*, 42, 216–224.
- Kojima, A., Ohno-Matsui, K., Teramukai, S., Yoshida, T., Ishihara, Y., Kobayashi, K., Shimada, N., Yasuzumi, K., Futagami, S., Tokoro, T., Mochizuki, M., 2004. Factors associated with the development of chorioretinal atrophy around choroidal neovascularization in pathologic myopia. *Exp. Ophthalmol.* 242, 114–119.
- Krebs, I., Smretschmig, E., Moussa, S., Brannath, W., Womastek, I., Binder, S., 2011. Quality and reproducibility of retinal thickness measurements in two spectral-domain optical coherence tomography machines. *Invest. Ophthalmol. Vis. Sci.* 52, 6925–6933.
- Larsson E, Eriksson U, Alm A, 2011. Retinal nerve fibre layer thickness in full-term children assessed with Heidelberg retinal tomography and optical coherence tomography: normal values and interocular asymmetry. *Acta Ophthalmol (Copenh)*. 89, 151–158.
- Laviers, H., Zambarakji, H., 2014. Enhanced depth imaging-OCT of the choroid: a review of the current literature. *Exp. Ophthalmol.* 252, 1871–1883.
- Lee, J., Lee, H.K., Kim, C.Y., Hong, Y.J., Choe, C.M., You, T.W., Seong, G.J., 2005. Purified high-dose anthocyanoside oligomer administration improves nocturnal vision and clinical symptoms in myopia subjects. *Br. J. Nutr.* 93, 895–899.
- Lee JW, Yau GS, Woo TT, Yick DW, Tam VT, Lai JS (2015). Retinal nerve fiber layer thickness in myopic, emmetropic, and hyperopic children. *Medicine (Baltimore)*. 94(12), e699.

## Chapter 10. References

- Lee, K., Lee, J., Lee, C.S., Park, S.Y., Lee, S.C., Lee, T., 2015. Topographical variation of macular choroidal thickness with myopia. *Acta Ophthalmol. (Copenh.)*, 93(6), e469-e474.
- Lee, S., Han, S.X., Young, M., Beg, M.F., Sarunic, M.V., Mackenzie, P.J., 2014. Optic nerve head and peripapillary morphometrics in myopic glaucoma. *Invest. Ophthalmol. Vis. Sci.* 55, 4378–4393.
- Li, L., Yang, Z., Dong, F., 2012. Choroidal thickness in normal subjects measured by enhanced depth imaging optical coherence tomography. *Zhonghua Yan Ke Za Zhi Chin. J. Ophthalmol.* 48, 819–823.
- Li T, Zhou X, Wang Z, Zhu J, Shen W, Jiang B (2016). Assessment of Retinal and Choroidal Measurements in Chinese School-Age Children with Cirrus-HD Optical Coherence Tomography. *PLoS One*, 11(7), e0158948.
- Lim, C.-S., Parra-Velandia, F.J., Chen, N., Zhang, P., L-M Teo, S., 2014. Optical coherence tomography as a tool for characterization of complex biological surfaces. *J. Microsc.* 255, 150–157.
- Lim HT, Chun BY, 2013. Comparison of OCT measurements between high myopic and low myopic children. *Optom Vis Sci.* 90(12), 1473-1478.
- Lim MC, Hoh ST, Foster PJ, Lim TH, Chew SJ, Seah SK, Aung T (2005). Use of optical coherence tomography to assess variations in macular retinal thickness in myopia. *Invest Ophthalmol Vis Sci.* 46 (3), 974-978.
- Liu, J.J., Grulkowski, I., Kraus, M.F., Potsaid, B., Lu, C.D., Baumann, B., Duker, J.S., Hornegger, J., Fujimoto, J.G., 2013. In vivo imaging of the rodent eye with swept source/Fourier domain OCT. *Biomed. Opt. Express* 4, 351–363.
- Liu, L., Zou, J., Jia, L., Yang, J., Chen, S., 2014. Spectral- and time-domain optical coherence tomography measurements of macular thickness in young myopic eyes. *Diagn. Pathol.* 9, 38.
- Liu, T., Hu, A.Y., Kaines, A., Yu, F., Schwartz, S.D., Hubschman, J.-P., 2011. A pilot study of normative data for macular thickness and volume measurements using cirrus high-definition optical coherence tomography. *Retina.* 31, 1944–1950.
- Liu X, Shen M, Yuan Y, Huang S, Zhu D, Ma Q, Ye X, Lu F (2015). Macular Thickness Profiles of Intraretinal Layers in Myopia Evaluated by Ultrahigh-Resolution Optical Coherence Tomography. *Am J Ophthalmol.* 160 (1), 53-61.
- LoDuca, A.L., Zhang, C., Zelkha, R., Shahidi, M., 2010. Thickness mapping of retinal layers by spectral domain optical coherence tomography. *Am. J. Ophthalmol.* 150, 849–855.

## Chapter 10. References

Maalej, A., Wathek, C., Khallouli, A., Rannen, R., Gabsi, S., 2014. Foveoschisis in highly myopic eyes: clinical and tomographic features. *J. Fr. Ophtalmol.* 37, 42–46.

Maduka Okafor, F.C., Okoye, O.I., Eze, B.I., 2009. Myopia: a review of literature. *Niger. J. Med. J. Natl. Assoc. Resid. Dr. Niger.* 18, 134–138.

Margolis, R., Spaide, R.F., 2009. A pilot study of enhanced depth imaging optical coherence tomography of the choroid in normal eyes. *Am. J. Ophthalmol.* 147, 811–815.

Markowitz, S.N., Reyes, S.V., 2013. Microperimetry and clinical practice: an evidence-based review. *Can. J. Ophthalmol.* 48, 350–357.

Matsuo Y, Sakamoto T, Yamashita T, Tomita M, Shirasawa M, Terasaki H, 2013. Comparisons of choroidal thickness of normal eyes obtained by two different spectral-domain OCT instruments and one swept-source OCT instrument. *Invest Ophthalmol Vis Sci*, 19;54(12), 7630-7636.

Maul, E.A., Friedman, D.S., Chang, D.S., Boland, M.V., Ramulu, P.Y., Jampel, H.D., Quigley, H.A., 2011. Choroidal thickness measured by spectral domain optical coherence tomography: Factors affecting thickness in glaucoma patients. *Ophthalmology* 118, 1571–1579.

Mehreen A., Sumbul A., Kashif M., Mohammad A., 2012. Macular thickness by age and gender in healthy eyes using spectral domain optical coherence tomography. *PloS One*, 7(5), e37638.

Michalewski J, Michalewska Z, Nawrocka Z, Bednarski M, Nawrocki J, 2014. Correlation of choroidal thickness and volume measurements with axial length and age using swept source optical coherence tomography and optical low-coherence reflectometry. *Biomed Res Int.*, 639160.

Mwanza JC, Durbin MK, Budenz DL, 2011. Cirrus OCT Normative Database Study Group. Interocular symmetry in peripapillary retinal nerve fiber layer thickness measured with the Cirrus HD-OCT in healthy eyes. *Am J Ophthalmol.* 151, 514–521.

McBrien, N.A., Jobling, A.I., Gentle, A., 2009. Biomechanics of the sclera in myopia: extracellular and cellular factors. *Optom. Vis. Sci. Off. Publ. Am. Acad. Optom.* 86, E23–E30.

Miyake, Y., Tsunoda, K., 2015. Occult macular dystrophy. *Jpn. J. Ophthalmol.* 59 (2), 71–80.

Morgan, I.G., Ohno-Matsui, K., Saw, S.-M., 2012. Myopia. *The Lancet*, 379, 1739–1748.

Mwanza JC, Hochberg J T, Banitt MR, et al., 2011. Lack of association between glaucoma and macular choroidal thickness measured with enhanced depth-imaging optical coherence tomography. *Invest. Ophthalmol. Vis. Sci.* 52, 3430–3435.

## Chapter 10. References

- Motolko M, Drance SM, 1981. Features of the optic disc in preglaucomatous eyes. *Arch Ophthalmol.* 99, 1992-1994.
- Nagasawa T, Mitamura Y, Katome T, Shinomiya K, Naito T, Nagasato D, Shimizu Y, Tabuchi H, Kiuchi Y, 2013. Macular choroidal thickness and volume in healthy pediatric individuals measured by swept-source optical coherence tomography. *Invest Ophthalmol Vis Sci*, 54(10), 7068-7074.
- Nakagawa, N., Parel, J.M., Murray, T.G., Oshima, K., 2000. Effect of scleral shortening on axial length. *Arch. Ophthalmol.* 118, 965–968.
- Nakano, N., Hangai, M., Noma, H., Nukada, M., Mori, S., Morooka, S., Takayama, K., Kimura, Y., Ikeda, H.O., Akagi, T., Yoshimura, N., 2013. Macular imaging in highly myopic eyes with and without glaucoma. *Am. J. Ophthalmol.* 156, 511–523.e6.
- Neelam, K., Cheung, C.M.G., Ohno-Matsui, K., Lai, T.Y.Y., Wong, T.Y., 2012. Choroidal neovascularization in pathological myopia. *Prog. Retin. Eye Res.* 31, 495–525.
- Nguyen, N.X., Besch, D., Bartz-Schmidt, K., Gelissen, F., Trauzettel-Klosinski, S., 2007. Reading performance with low-vision aids and vision-related quality of life after macular translocation surgery in patients with age-related macular degeneration. *Acta Ophthalmol. Scand.* 85, 877–882.
- Nguyen, N.X., Weismann, M., Trauzettel-Klosinski, S., 2009. Improvement of reading speed after providing of low vision aids in patients with age-related macular degeneration. *Acta Ophthalmol. (Copenh.)* 87, 849–853.
- Nishida Y, Fujiwara T, Imamura Y, Lima LH, Kurosaka D, Spaide RF, 2012. Choroidal thickness and visual acuity in highly myopic eyes. *Retina*, 32(7), 1229-1231.
- Nickla, D.L., Wallman, J., 2010. The multifunctional choroid. *Prog. Retin. Eye Res.* 29, 144–168.
- Nicolò, M., Zoli, D., Musolino, M., Traverso, C.E., 2012. Association between the efficacy of half-dose photodynamic therapy with indocyanine green angiography and optical coherence tomography findings in the treatment of central serous chorioretinopathy. *Am. J. Ophthalmol.* 153, 474–480.e1.
- Ohno-Matsui, K., Kawasaki, R., Jonas, J.B., Gemmy Cheung, C.M., Saw, S.-M., Verhoeven, V.J.M., Klaver, C.C.W., Moriyama, M., Shinohara, K., Kawasaki, Y., Yamazaki, M., Meuer, S., Ishibashi, T., Yasuda, M., Yamashita, H., Sugano, A., Wang, J.J., Mitchell, P., Wong, T.Y., 2015. International photographic classification and grading system for myopic maculopathy. *Am. J. Ophthalmol.* 159 (5), 877-883.e7.
- Ohno-Matsui, K., Yoshida, T., 2004. Myopic choroidal neovascularization: natural course and treatment. *Curr. Opin. Ophthalmol.* 15, 197–202.

## Chapter 10. References

- Ohsugi, H., Ikuno, Y., Oshima, K., Tabuchi, H., 2013. 3-D choroidal thickness maps from EDI-OCT in highly myopic eyes. *Optom. Vis. Sci.* 90, 599–606.
- Ong LS, Mitchell P, Healey PR, Cumming RG, 1999. Asymmetry in optic disc parameters: the Blue Mountains Eye Study. *Invest Ophthalmol Vis Sci.* 40, 849-857.
- Osmanbasoglu, O.A., Alkin, Z., Ozkaya, A., Ozpinar, Y., Yazici, A.T., Demirok, A., 2013. Diurnal choroidal thickness changes in normal eyes of Turkish people measured by spectral domain optical coherence tomography. *J. Ophthalmol.* 687165.
- Ostadimoghaddam, H., Yekta, A.A., Heravian, J., Azimi, A., Hosseini, S.M.A., Vatandoust, S., Sharifi, F., Abolbashari, F., 2014. Prevalence of refractive errors in students with and without color vision deficiency. *J. Ophthalmic Vis. Res.* 9, 484–486.
- Ozdogan Erkul, S., Kapran, Z., Uyar, O.M., 2014. Quantitative analysis of subfoveal choroidal thickness using enhanced depth imaging optical coherence tomography in normal eyes. *Int. Ophthalmol.* 34, 35–40.
- Pagliara MM, Lepore D, Balestrazzi E, 2008. The role of OCT in glaucoma management. *Prog Brain Res.* 173, 139–148.
- Park, H.-Y., Jung, Y., Park, C.K., 2015. Posterior staphyloma is related to optic disc morphology and the location of visual field defect in normal tension glaucoma patients with myopia. *Eye Lond. Engl.* 29 (3), 333-341.
- Park JJ, Oh DR, Hong SP, Lee KW, 2005. Asymmetry analysis of the retinal nerve fiber layer thickness in normal eyes using optical coherence tomography. *Korean J Ophthalmol.* 19, 281–287.
- Park KA, Oh SY, 2013. Choroidal thickness in healthy children. *Retina*, 33(9), 1971-1976.
- Parodi MB, Triolo G, Morales M, Borrelli E, Cicinelli MV, Cascavilla ML, Bandello F (2015). MP1 and MAIA Fundus Perimetry in Healthy Subjects and Patients Affected by Retinal dystrophies. *Retina* 35 (8), 1662-1669.
- Parravano, M., Oddone, F., Boccassini, B., Chiaravalloti, A., Scarinci, F., Sciamanna, M., Boninfante, A., Tedeschi, M., Varano, M., 2013. Functional and structural assessment of lamellar macular holes. *Br. J. Ophthalmol.* 97, 291–296.
- Parravano, M., Oddone, F., Giorno, P., Cacciamani, A., Abbate, R., Caminiti, G., Peiretti, E., Varano, M., 2014. Influence of macular choroidal thickness on visual function in highly myopic eyes. *Ophthalmic Res.* 52, 97–101.
- Phasukkijwatana, N., Thaweerattanasilp, W., Laotaweerungsawat, S., Rodanant, N., Singalavanija, A., Tanterdtham, J., Namatra, C., Trinavarat, A., Thoongsuwan, S., Rattanawarinchai, K., Thongyou, K., 2014. Enhanced depth imaging spectral-domain

optical coherence tomography of the choroid in Thai population. *J. Med. Assoc. Thai.* 97, 947–953.

Qian, J., Jiang, Y.-R., 2010. Anatomic evaluation of macular holes with silicone oil tamponades in highly myopic eyes using optical coherence tomography. *Eur. J. Ophthalmol.* 20, 938–944.

Qin, Y., Zhu, M., Qu, X., Xu, G., Yu, Y., Witt, R.E., Wang, W., 2010. Regional macular light sensitivity changes in myopic Chinese adults: an MP1 study. *Invest. Ophthalmol. Vis. Sci.* 51, 4451–4457.

Rahimy, E., Beardsley, R., Ferrucci, S., Ilsen, P., Sarraf, D., 2013. Optical coherence tomography findings in ocular argyrosis. *Ophthalmic Surg. Lasers Imaging Retina* 44 Online, E20–E22.

Rajavi, Z., Moghadasifar, H., Feizi, M., Haftabadi, N., Hadavand, R., Yaseri, M., Sheibani, K., Norouzi, G., 2014. Macular thickness and amblyopia. *J. Ophthalmic Vis. Res.* 9, 478–483.

Read, S.A., Collins, M.J., Vincent, S.J., Alonso-Caneiro, D., 2013. Choroidal thickness in myopic and nonmyopic children assessed with enhanced depth imaging optical coherence tomography. *Invest. Ophthalmol. Vis. Sci.* 54, 7578–7586.

Regatieri, C.V., Branchini, L., Fujimoto, J.G., Duker, J.S., 2012. Choroidal imaging using spectral-domain optical coherence tomography. *Retina.* 32, 865–876.

Richer, S., Cho, J., Stiles, W., Levin, M., Wrobel, J.S., Sinai, M., Thomas, C., 2012. Retinal spectral domain optical coherence tomography in early atrophic age-related macular degeneration (amd) and a new metric for objective evaluation of the efficacy of ocular nutrition. *Nutrients* 4, 1812–1827.

Riva, C.E., Geiser, M., Petrig, B.L., Beijing 100193, PR China Ocular Blood Flow Research Association, 2010. Ocular blood flow assessment using continuous laser Doppler flowmetry. *Acta Ophthalmol. (Copenh.)* 88, 622–629.

Rohrschneider, K., Bültmann, S., Springer, C., 2008. Use of fundus perimetry (microperimetry) to quantify macular sensitivity. *Prog. Retin. Eye Res.* 27, 536–548.

Rossou E, Abegão Pinto L, Vandewalle E, Cassiman C, Willekens K, Stalmans I, 2014. Choroidal thickness of the papillomacular region in young healthy individuals. *Ophthalmologica*, 232(2), 97-101.

Ruiz-Medrano, J., Flores-Moreno, I., Peña-García, P., Montero, J.A., Duker, J.S., Ruiz-Moreno, J.M., 2015. Asymmetry in macular choroidal thickness profile between both eyes in a healthy population measured by swept-source optical coherence tomography. *Retina.* 35(10), 2067-2073.



## Chapter 10. References

Rydzanicz, M., Nath, S.K., Sun, C., Podfigurna-Musiak, M., Frajdemberg, A., Mrugacz, M., Winters, D., Ratnamala, U., Radhakrishna, U., Bejjani, B.A., Gajecka, M., 2011. Identification of novel suggestive loci for high-grade myopia in Polish families. *Mol. Vis.* 17, 2028–2039.

Sabates FN, Vincent RD, Koulen P, Sabates NR, Gallimore G. (2011). Normative data set identifying properties of the macula across age groups: integration of visual function and retinal structure with microperimetry and spectral-domain optical coherence tomography. *Retina* (7), 1294-1302.

Salchow DJ, Oleynikov YS, Chiang MF, et al, 2006. Retinal nerve fibre layer thickness in normal children measured with optical coherence tomography. *Ophthalmology.* 113, 768-791.

Samarawickrama, C., Mitchell, P., Tong, L., Gazzard, G., Lim, L., Wong, T.-Y., Saw, S.-M., 2011. Myopia-related optic disc and retinal changes in adolescent children from Singapore. *Ophthalmology* 118, 2050–2057.

Saw, S.-M., 2006. How blinding is pathological myopia? *Br. J. Ophthalmol.* 90, 525–526.

Saw, S.-M., Gazzard, G., Shih-Yen, E.C., Chua, W.-H., 2005. Myopia and associated pathological complications. *Ophthalmic Physiol. Opt. J. Br. Coll. Ophthalmic Opt.* 25, 381–391.

Saxena, R., Vashist, P., Tandon, R., Pandey, R.M., Bhardawaj, A., Menon, V., Mani, K., 2015. Prevalence of Myopia and Its Risk Factors in Urban School Children in Delhi: The North India Myopia Study (NIM Study). *PloS One* 10, e0117349.

Scott, R.A., Ezra, E., West, J.F., Gregor, Z.J., 2000. Visual and anatomical results of surgery for long standing macular holes. *Br. J. Ophthalmol.* 84, 150–153.

Seibold, L.K., Mandava, N., Kahook, M.Y., 2010. Comparison of retinal nerve fiber layer thickness in normal eyes using time-domain and spectral-domain optical coherence tomography. *Am. J. Ophthalmol.* 150, 807–814.

Seo, J.H., Kim, T.-W., Weinreb, R.N., Park, K.H., Kim, S.H., Kim, D.M., 2012. Detection of localized retinal nerve fiber layer defects with posterior pole asymmetry analysis of spectral domain optical coherence tomography. *Invest. Ophthalmol. Vis. Sci.* 53, 4347–4353.

Shah, V.A., Chalam, K.V., 2009. Values for macular perimetry using the MP-1 microperimeter in normal subjects. *Ophthalmic Res.* 41, 9–13.

## Chapter 10. References

- Shao, L., Xu, L., Wei, W.B., Chen, C.X., Du, K.F., Li, X.P., Yang, M., Wang, Y.X., You, Q.S., Jonas, J.B., 2014. Visual acuity and subfoveal choroidal thickness: the Beijing Eye Study. *Am. J. Ophthalmol.* 158, 702–709.e1.
- Shen, Z.-M., Zhang, Z.-Y., Zhang, L.-Y., Li, Z.-G., Chu, R.-Y., 2015. Posterior scleral reinforcement combined with patching therapy for pre-school children with unilateral high myopia. *Graefes Arch Clin Exp Ophthalmol.* 253(8), 1391-1395.
- Shin, H.J., Cho, B.J., 2011. Comparison of retinal nerve fiber layer thickness between stratus and spectralis OCT. *Korean J. Ophthalmol.* 25, 166–173.
- Shin, J.W., Shin, Y.U., Cho, H.Y., Lee, B.R., 2012. Measurement of choroidal thickness in normal eyes using 3D OCT-1000 Spectral Domain Optical Coherence Tomography. *Korean J. Ophthalmol.* 26, 255–259.
- Silva, R., 2012. Myopic maculopathy: a review. *Ophthalmol. J. Int. Ophtalmol. Int. J.* 228, 197–213.
- Simunovic, M.P., 2015. Metamorphopsia and its quantification. *Retina.* 35(7), 1285-1291.
- Singh, R., Invernizzi, A., Agarwal, A., Kumari, N., Gupta, A., 2015. Enhanced depth imaging spectral domain optical coherence tomography versus ultrasonography B-scan for measuring retinochoroidal thickness in normal eyes. *Retina.* 35, 250–256.
- Sohrab, M., Wu, K., Fawzi, A.A., 2012. A pilot study of morphometric analysis of choroidal vasculature in vivo, using en face optical coherence tomography. *PLoS One* 7, e48631.
- Sommer A, Katz J, Quigley HA, et al, 1991. Clinically detectable nerve fiber atrophy precedes the onset of glaucomatous field loss. *Arch Ophthalmol.* 109, 77-83.
- Song, A.-P., Wu, X.-Y., Wang, J.-R., Liu, W., Sun, Y., Yu, T., 2014. Measurement of retinal thickness in macular region of high myopic eyes using spectral domain OCT. *Int. J. Ophthalmol.* 7, 122–127.
- Song, W.K., Lee, S.C., Lee, E.S., Kim, C.Y., Kim, S.S., 2010. Macular thickness variations with sex, age, and axial length in healthy subjects: a spectral domain-optical coherence tomography study. *Invest. Ophthalmol. Vis. Sci.* 51, 3913–3918.
- Spaide RF, Koizumi H, Pozzoni MC., 2008. Enhanced depth imaging spectral-domain optical coherence tomography. *Am J Ophthalmol*, 146, 496–500.
- Spaide, R.F., Ohno-Matsui, K., Yannuzzi, L.A., 2014. *Pathologic Myopia.* Springer-Verlag New York.

Storm, T., Heegaard, S., Christensen, E. I., & Nielsen, R. (2014). Megalin-deficiency causes high myopia, retinal pigment epithelium-macro melanosomes and abnormal development of the ciliary body in mice. *Cell Tissue Res*, 358 (1), 99-107

Sull, A.C., Vuong, L.N., Price, L.L., Srinivasan, V.J., Gorczynska, I., Fujimoto, J.G., Schuman, J.S., Duker, J.S., 2010. Comparison of spectral / fourier domain optical coherence tomography instruments for assessment of normal macular thickness. *Retina*. 30(2), 235-245.

Sullivan-Mee, M., Ruegg, C.C., Pensyl, D., Halverson, K., Qualls, C., 2013. Diagnostic precision of retinal nerve fiber layer and macular thickness asymmetry parameters for identifying early primary open-angle glaucoma. *Am. J. Ophthalmol.* 156, 567–577.e1.

Takahashi, A., Ito, Y., Iguchi, Y., Yasuma, T.R., Ishikawa, K., Terasaki, H., 2012. Axial length increases and related changes in highly myopic normal eyes with myopic complications in fellow eyes. *Retina*. 32, 127–133.

Tanabe, H., Ito, Y., Terasaki, H., 2012. Choroid is thinner in inferior region of optic disks of normal eyes. *Retina*. 32, 134–139.

Tanaka, Y., Shimada, N., Ohno-Matsui, K., 2015. Extreme thinning or loss of inner neural retina along the staphyloma edge in eyes with pathologic myopia. *Am. J. Ophthalmol.* 159, 677–682.e2.

Tan, C.S.H., Cheong, K.X., Lim, L.W., Li, K.Z., 2014. Topographic variation of choroidal and retinal thicknesses at the macula in healthy adults. *Br. J. Ophthalmol.* 98, 339–344.

Tan, C.S., Ouyang, Y., Ruiz, H., Sadda, S.R., 2012. Diurnal variation of choroidal thickness in normal, healthy subjects measured by spectral domain optical coherence tomography. *Invest. Ophthalmol. Vis. Sci.* 53, 261–266.

Tano, Y., 2002. Pathologic myopia: where are we now?. *Am. J. Ophthalmol.* 134, 645–660.

Tenlik, A., Gurağaç, F.B., Güler, E., Dervişoğulları, M.S., Totan, Y., 2015. Choroidal thickness measurement in healthy pediatric population using Cirrus HD optical coherence tomography. *Arq. Bras. Oftalmol.* 78, 23–26.

Thorell, M.R., Goldhardt, R., Nunes, R.P., de Amorim Garcia Filho, C.A., Abbey, A.M., Kuriyan, A.E., Modi, Y.S., Gregori, G., Yehoshua, Z., Feuer, W., Sadda, S., Rosenfeld, P.J., 2015. Association between subfoveal choroidal thickness, reticular pseudodrusen, and geographic atrophy in age-related macular degeneration. *Ophthalmic Surg. Lasers Imaging Retina* 46, 513–521.

Toprak, I., Yaylalı, V., Yildirim, C., 2015. Age-based analysis of choroidal thickness and choroidal vessel diameter in primary open-angle glaucoma. *Int. Ophthalmol.* 36(2), 171-177.

## Chapter 10. References

- Tuncer I, Karahan E, Zengin MO, Atalay E, Polat N, 2015. Choroidal thickness in relation to sex, age, refractive error, and axial length in healthy Turkish subjects. *Int. Ophthalmol.* 35(3), 403-410.
- Turalba, A.V., Grosskreutz, C., 2010. A review of current technology used in evaluating visual function in glaucoma. *Semin. Ophthalmol.* 25, 309–316.
- Turan-Vural, E., Yenerel, N., Okutucu, M., Yildiz, E., Dikmen, N., 2015. Measurement of Subfoveal Choroidal Thickness in Pseudoexfoliation Syndrome Using Enhanced Depth Imaging Optical Coherence Tomography. *Ophthalmologica.* 233(3-4), 204-208.
- Turk A, Ceylan OM, Arici C, et al, 2012. Evaluation of the nerve fiber layer and macula in the eyes of healthy children using spectral-domain optical coherence tomography. *Am J Ophthalmol.* 153, 552–559.
- Um TW, Sung KR, Wollstein G, Yun SC, Na JH, Schuman JS, 2012. Asymmetry in hemifield macular thickness as an early indicator of glaucomatous change. *Invest Ophthalmol Vis Sci,* 53(3), 1139-1144.
- Van Bol, L., Rasquin, F., 2014. [Age-related macular degeneration]. *Rev. Médicale Brux.* 35, 265–270.
- Van Velthoven, M.E.J., Faber, D.J., Verbraak, F.D., van Leeuwen, T.G., de Smet, M.D., 2007. Recent developments in optical coherence tomography for imaging the retina. *Prog. Retin. Eye Res.* 26, 57–77.
- Varma, R., Bazzaz, S., Lai, M., 2003. Optical tomography-measured retinal nerve fiber layer thickness in normal latinos. *Invest. Ophthalmol. Vis. Sci.* 44, 3369–3373.
- Vienola, K.V., Braaf, B., Sheehy, C.K., Yang, Q., Tiruveedhula, P., Arathorn, D.W., de Boer, J.F., Roorda, A., 2012. Real-time eye motion compensation for OCT imaging with tracking SLO. *Biomed. Opt. Express* 3, 2950–2963.
- Vincent SJ, Collins MJ, Read SA, Carney LG, 2013. Retinal and choroidal thickness in myopic anisometropia. *Invest Ophthalmol Vis Sci,* 54(4), 2445-2456.
- Virgili, G., Menchini, F., Casazza, G., Hogg, R., Das, R.R., Wang, X., Michelessi, M., 2015. Optical coherence tomography (OCT) for detection of macular oedema in patients with diabetic retinopathy. *Cochrane Database Syst Rev.* Jan 7, 1, CD008081.
- Vizzeri, G., Weinreb, R.N., Gonzalez-Garcia, A.O., Bowd, C., Medeiros, F.A., Sample, P.A., Zangwill, L.M., 2009. Agreement between spectral-domain and time-domain OCT for measuring RNFL thickness. *Br. J. Ophthalmol.* 93, 775–781.
- Vujosevic, S., Pilotto, E., Bottega, E., Benetti, E., Cavarzeran, F., Midena, E., 2008. Retinal fixation impairment in diabetic macular edema. *Retina Phila. Pa* 28, 1443–1450.

## Chapter 10. References

Wang J, Gao X, Huang W, Wang W, Chen S, Du S, Li X, Zhang X, 2015. Swept-source optical coherence tomography imaging of macular retinal and choroidal structures in healthy eyes. *BMC Ophthalmol*, 15, 122.

Wang, X.-G., Peng, Q., Wu, Q., 2012. Comparison of central macular thickness between two spectral-domain optical coherence tomography in elderly non-mydratic eyes. *Int. J. Ophthalmol.* 5, 354–359.

Welfer D, Scharcanski J, Marinho DR, 2011. Fovea center detection based on the retina anatomy and mathematical morphology. *Comput Methods Programs Biomed.* 104, 397–409.

Winter, P.W., York, A.G., Nogare, D.D., Ingaramo, M., Christensen, R., Chitnis, A., Patterson, G.H., Shroff, H., 2014. Two-photon instant structured illumination microscopy improves the depth penetration of super-resolution imaging in thick scattering samples. *Optica* 1, 181–191.

Wolf-Schnurrbusch, U.E.K., Ceklic, L., Brinkmann, C.K., Iliev, M.E., Frey, M., Rothenbuehler, S.P., Enzmann, V., Wolf, S., 2009. Macular thickness measurements in healthy eyes using six different optical coherence tomography instruments. *Invest. Ophthalmol. Vis. Sci.* 50, 3432–3437.

Wong, T.Y., Ferreira, A., Hughes, R., Carter, G., Mitchell, P., 2014. Epidemiology and disease burden of pathologic myopia and myopic choroidal neovascularization: an evidence-based systematic review. *Am. J. Ophthalmol.* 157, 9–25.e12.

Wong, T.Y., Ohno-Matsui, K., Leveziel, N., Holz, F.G., Lai, T.Y., Yu, H.G., Lanzetta, P., Chen, Y., Tufail, A., 2015. Myopic choroidal neovascularisation: current concepts and update on clinical management. *Br. J. Ophthalmol.* 99, 289–296.

Wu, P.-C., Chen, Y.-J., Chen, C.-H., Chen, Y.-H., Shin, S.-J., Yang, H.-J., Kuo, H.-K., 2008. Assessment of macular retinal thickness and volume in normal eyes and highly myopic eyes with third-generation optical coherence tomography. *Eye (Lond)*, 22(4), 551-555.

Wu, Z., Ayton, L.N., Guymer, R.H., Luu, C.D., 2014. Comparison between multifocal electroretinography and microperimetry in age-related macular degeneration. *Invest. Ophthalmol. Vis. Sci.* 55, 6431–6439.

Yamada, H., Hangai, M., Nakano, N., Takayama, K., Kimura, Y., Miyake, M., Akagi, T., Ikeda, H.O., Noma, H., Yoshimura, N., 2014. Asymmetry analysis of macular inner retinal layers for glaucoma diagnosis. *Am. J. Ophthalmol.* 158, 1318–1329.e3.

Yamada, K., Motomura, Y., Matsumoto, C.S., Shinoda, K., Nakatsuka, K., 2009. Optical coherence tomographic evaluation of the outer retinal architecture in Oguchi disease. *Jpn. J. Ophthalmol.* 53, 449–451.

## Chapter 10. References

- Yamashita T, Sakamoto T, Kakiuchi N, Tanaka M, Kii Y, Nakao K, 2014. Posterior pole asymmetry analyses of retinal thickness of upper and lower sectors and their association with peak retinal nerve fiber layer thickness in healthy young eyes. *Invest Ophthalmol Vis Sci*, 55(9), 5673-5678.
- Yang, Q.-H., Chen, B., Peng, G.-H., Li, Z.-H., Huang, Y.-F., 2014. Accuracy of axial length measurements from immersion B-scan ultrasonography in highly myopic eyes. *Int. J. Ophthalmol.* 7, 441–445.
- Yannuzzi, L.A., 2011. Indocyanine green angiography: a perspective on use in the clinical setting. *Am. J. Ophthalmol.* 151, 745–751.e1.
- Yasuo K, Kaori M, Yumi K, et al, 2000. Asymmetries of the retinal nerve fibre layer thickness in normal eyes. *Br J Ophthalmol.* 84, 469-472.
- Young, T.L., 2004. Dissecting the genetics of human high myopia: a molecular biologic approach. *Trans. Am. Ophthalmol. Soc.* 102, 423–445.
- Youssif AR, Ghalwash AZ, Ghoneim AR, 2008. Optic disc detection from normalized digital fundus images by means of a vessels' direction matched filter. *IEEE Trans Med Imaging.* 27, 11–18.
- Xu, L., Wang Y., Wang, S., Wang, Y., & Jonas, J. B., 2007. High myopia and glaucoma susceptibility: the Beijing Eye Study. *Ophthalmology*, 114 (2), 216-220.
- Zaben, A., Zapata, M.Á., Garcia-Arumi, J., 2015. Retinal sensitivity and choroidal thickness in high myopia. *Retina.* 35, 398–406.
- Zeng, J., Liu, R., Zhang, X., Li, J., Chen, X., Pan, J., Tang, S., Ding, X., 2012. Relationship between gender and posterior pole choroidal thickness in normal eyes. *J. Ophthalmol.* 48, 1093–1096.
- Zhao MH, Wu Q, Hu P, Jia LL, 2016. Macular Thickness in Myopia: An OCT Study of Young Chinese Patients. *Curr Eye Res.* 10, 1-6.
- Zheng YF, Pan CW, Chay J, et al, 2013. The economic cost of myopia in adults aged over 40 years in Singapore. *Invest Ophthalmol Vis Sci*, 54, 7532–7537.
- Zhu, Y., Terry, N.G., Wax, A., 2012. Angle-resolved low-coherence interferometry: an optical biopsy technique for clinical detection of dysplasia in Barrett's esophagus. *Expert Rev. Gastroenterol. Hepatol.* 6, 37–41.
- Zhu, Y., Zhang, T., Wang, K., Xu, G., Huang, X., 2015. Changes in choroidal thickness after panretinal photocoagulation in patients with type 2 diabetes. *Retina.* 35, 695–703.
- Ziylan S, Kiziloglu OY, Yenerel NM, Gokce B, Ciftci F, 2015. Macular Thickness in Highly Myopic Children Aged 3 to 7 Years. *J Pediatr Ophthalmol Strabismus.* 52(5), 282-286.

## Chapter 10. References

Zysk, A.M., Nguyen, F.T., Oldenburg, A.L., Marks, D.L., Boppart, S.A., 2007. Optical coherence tomography: a review of clinical development from bench to bedside. *J. Biomed. Opt.* 12, 051403.





## 11. Annexes

### Annex I. Informed Consent

#### HOJA DE CONSENTIMIENTO INFORMADO

En cumplimiento de los artículos 8 y siguientes de la Ley 41/2002, de 14 de noviembre, básica reguladora de la autonomía del paciente y de derechos y obligaciones en materia de información y documentación clínica le ofrecemos por escrito y de manera comprensible la descripción de las características de riesgo y beneficios de participar en el proyecto de investigación cuyo objetivo es **determinar la asimetría de diversos parámetros fisiológicos de la retina mediante tomografía de coherencia óptica (3D OCT - 2000)**.

Nombre del informador: Don. Zeyad Alzaben (MSc) Firma: \_\_\_\_\_

#### Descripción

Este proyecto de investigación está siendo realizado por Zeyad A. Alzaben, estudiante del doctorado de la Facultat d'Òptica i Optometria de Terrassa (Universidad Politécnica de Catalunya), dirigido por el Prof. Genís Cardona y por el Dr. Miguel Angel Zapata del hospital de la Vall d'Hebron.

El propósito de esta investigación es **determinar la asimetría de diversos parámetros fisiológicos de la retina mediante tomografía de coherencia óptica (3D OCT - 2000) y microperimetría**.

Usted es candidato para participar en este proyecto de investigación por tener retinas normales y ojos sanos o por haber sido diagnosticado con alta miopía.

Si acepta participar en este proyecto de investigación se le solicitará la realización de un conjunto de pruebas y la recolección de datos como su **refracción ocular , agudeza visual , parámetros de la retina** mediante la tomografía de coherencia óptica (prueba que permite adquirir, de forma no invasiva para el paciente sin aplicación de ningún colirio para la dilatación pupilar, y visualizar en tiempo real imágenes en alta resolución de la morfología retiniana, de la interfase vitreoretiniana y del segmento anterior). La participación en este estudio le tomará aproximadamente unos 30 min.

### **Riesgos y beneficios**

No existen riesgos a nivel ocular durante la realización de este estudio dado que las pruebas que se realizan son empleadas en las consultas de optometría y oftalmología de manera cotidiana y todas ellas en este caso se realizan de manera NO invasiva.

Los beneficios esperados de esta investigación son su aportación a la ciencia, y la realización de distintas pruebas de tipo optométrico-oftalmológicas sin coste alguno.

### **Confidencialidad**

La identidad del participante será protegida ya que todo este proceso será totalmente anónimo, solo se conocerá la edad y el sexo. Toda información o datos que pueda identificar al participante serán manejados confidencialmente.

Solamente el optometrista de este trabajo y los facultativos implicados en esta investigación tendrán acceso a los datos que puedan identificar directa o indirectamente a un participante, incluyendo esta hoja de consentimiento.

Estos datos serán almacenados en expedientes confidenciales con la finalidad única de esta investigación y se conservarán por un periodo de 2 años máximo después de que concluya este estudio.

### **Derechos**

Si ha leído este documento y ha decidido participar, por favor entienda que su participación es completamente voluntaria y que usted tiene derecho a abstenerse de participar o retirarse del estudio en cualquier momento, sin ninguna penalidad. También tiene derecho a no participar en alguna prueba en particular. Además, tiene derecho a recibir una copia de este documento.

Si tiene alguna pregunta o desea más información sobre esta investigación, por favor comuníquese con XXXX al Tel. 97XXXX

---

## Chapter 11. Annexes

Su firma en este documento significa que ha decidido participar después de haber leído y discutido la información presentada en esta hoja de consentimiento y que ha recibido copia de este documento.

\_\_\_\_\_

Nombre de el/la	participante	Firma	Fecha
-----------------	--------------	-------	-------

Ha discutido el contenido de esta hoja de consentimiento con el/la arriba firmante

\_\_\_\_\_

Nombre de el/la	participante	Firma	Fecha
-----------------	--------------	-------	-------

## **Annex II. Preprint of Paper published in RETINA**

**TITLE:** INTER-OCULAR ASYMMETRY IN CHOROIDDAL THICKNESS AND RETINAL SENSITIVITY IN HIGH MYOPIA

**Short title:** Inter-ocular asymmetry in high myopia

**Authors:** Zeyad Alzaben, MSc<sup>1</sup>  
Genís Cardona, PhD<sup>1</sup>  
Miguel A. Zapata, PhD, MD<sup>2</sup>  
Ahmad Zaben, PhD<sup>3</sup>

<sup>1</sup> Department of Optics and Optometry, Technical University of Catalonia, Terrassa, Spain

<sup>2</sup> Ophthalmology Department, Vall d'Hebron Hospital, Barcelona, Spain

<sup>3</sup> Optipunt Eye Clinic, Figueres, Spain

**Corresponding Author:** Genís Cardona ([genis.cardona@upc.edu](mailto:genis.cardona@upc.edu))  
Terrassa School of Optics and Optometry  
Violinista Vellsolà, 37  
E08222 Terrassa, Catalonia, Spain  
Telephone: +34 93 739 8774

**DISCLOSURE:** The authors report no conflicts of interest and have no proprietary interest in any of the instrumentation mentioned in this article. No funding was received for this work.

**KEY WORDS**

Choroidal Thickness; High Myopia; Inter-ocular Asymmetry; Pathological Myopia;  
Refractive Error; Retinal Sensitivity

**SUMMARY STATEMENT**

When compared with a control group of healthy eyes, patients with high myopia and without retinal abnormalities were found to present larger absolute inter-ocular differences in choroidal thickness and retinal sensitivity. These findings could aid in the early detection and management of pathological conditions associated with high myopia.

## **ABSTRACT**

*Purpose:* To investigate the normal range of inter-ocular asymmetry in choroidal thickness and retinal sensitivity high myopia without ocular fundus manifestations and to determine the relationship between inter-ocular asymmetry and refractive error.

*Methods:* Forty-three patients ( $35.07 \pm 13.31$  years) with high myopia, and 45 healthy participants ( $39.9 \pm 14.1$  years) were administered an ocular coherence tomography and a microperimetry examination to determine choroidal thickness and retinal sensitivity at the foveal region and at 1, 2 and 3 mm, nasally, temporally, superiorly and inferiorly. Absolute inter-ocular differences were calculated to determine the normal range of asymmetry, in 95% confidence intervals.

*Results:* The choroid was thinner in the myopic group at all explored locations (all  $p < 0.05$ ), with larger absolute inter-ocular differences in most of the choroidal locations under evaluation (all  $p < 0.05$ ). Similarly, retinal sensitivity was reduced in the myopic group, although statistically significant differences were only encountered at the subfoveal location ( $p = 0.001$ ). Retinal sensitivity asymmetry was found to increase with refractive error.

*Conclusion:* The expanded range of choroidal thickness and retinal sensitivity asymmetry found in high myopia in the absence of disease is of relevance when exploring these patients for early signs of ocular pathology.

## INTRODUCTION

Pathological myopia is one of the leading causes of blindness in the industrialized world, with significant social and economic impact.<sup>1</sup> The progressive axial elongation associated with pathological myopia has been documented to result in structural changes in the ocular fundus, including thinning of the retina and choroid which, in turn, may derive in a variety of ocular, and vision threatening complications, such as, choroidal neovascularization, posterior staphyloma, lacquer cracks in Bruch's membrane and chorioretinal atrophy.<sup>2-8</sup>

Recent developments in optical coherence tomography (OCT) have provided researchers with high-resolution images and highly reproducible and repeatable measurements of the posterior pole, including the choroid, using the enhanced depth imaging (EDI) technique.<sup>9-20</sup> Examination of the choroid is particularly relevant in high myopia, as the earliest pathological changes appear in this region.<sup>21</sup> Similarly, the widespread use of microperimetry is allowing researchers and clinicians to explore the retinal sensitivity of the macula, as well as, fixation stability and eccentricity, that is, to monitor visual function.<sup>22,23</sup> This device is able to provide a precise retinal sensitivity map over the corresponding fundus image obtained with an infrared camera or a scanning laser ophthalmoscope (SLO). Few researchers have employed microperimetry to assess visual function in high myopia.<sup>24-26</sup> These authors have reported reduced retinal sensitivity in myopic than in emmetropic patients, with a negative correlation between the degree of myopia and the loss of sensitivity. However, the relationship between structural changes and visual function in myopia remains elusive and controversial, and once other confounding variables are considered, only weak correlations are found between choroidal thickness, retinal sensitivity and visual acuity<sup>24,27-30</sup>, albeit there may be a threshold level of choroidal thinning beyond which visual function is compromised<sup>28,29</sup>.

In light of the critical relevance of the prompt detection of any pathological changes associated with high myopia, and given that structural changes in the choroid precede visual manifestations<sup>31</sup>, previous studies have aimed to determine the normal thresholds of inter-ocular asymmetry, whereupon differences in choroidal thickness beyond these thresholds may be suggestive of early stages of choroidal atrophy. However, as far as our literature review has disclosed, these studies have only explored healthy eyes<sup>11,32</sup>. It may be hypothesized that highly-myopic eyes, even in the absence of complications, may present a different range of inter-ocular asymmetry. Therefore, it was the primary objective of the present cross-sectional study to assess the threshold of inter-ocular asymmetry in choroidal thickness, as well as, in retinal sensitivity, in a sample of patients with high myopia without ocular complications and to compare these results with those of an age-matched control group of healthy subjects. As a secondary objective, within the myopic group, the relationship between the degree of structural and functional asymmetry and the level of refractive error was determined.

## **METHODS**

### *Subjects*

Forty-three patients with high myopia participated in this study. Patients were selected consecutively from those attending an optometric practice (Optipunt Figueres, Spain) between April 2014 and June 2016 for routine visual examination. Patients were included if they had a spherical equivalent refractive error  $\geq -6.00$  D, and anisometropia  $\leq 0.50$  D. Only patients without retinal and choroidal complications were included in the study. Therefore, patients were excluded if they presented with any ocular fundus pathology, such as, but not limited to, choroidal neovascularization, foveoschisis, macular hole, diabetic retinopathy, posterior uveitis, drusen or age-related macular degeneration, as were those with a history of ocular trauma, glaucoma, amblyopia, ocular or refractive surgery.

For comparison purposes, an age-matched control group of 45 normal patients was selected from those attending the same centre. Inclusion criteria for the control group were spherical equivalent refraction between  $+4.00$  D and  $-3.00$  D, anisometropia  $\leq 0.50$  D, distance corrected visual acuity (DCVA) of 0.0 logMAR (20/20) or better, and intraocular pressure  $< 21$  mmHg. Patients with a history of ocular trauma or pathology, ocular or refractive surgery, diabetes mellitus or any other systemic disease with potential ocular manifestations, and those with first-degree relatives diagnosed with glaucoma or retinal disease were excluded from the study.

For both the high myopia and control group, patients without clear ocular media or without central fixation were also excluded, as were those failing to understand or cooperate during OCT or microperimetry measurements.

All patients were provided with written information regarding the procedures and the aim of the study and informed consent was obtained from all participants or from a parent or legal guardian in those patients still underage. The study was conducted in accordance with the Declaration of Helsinki tenets of 1975 (as revised in Tokyo in 2004) and received the approval of the Ethics Review Board of the Hospital Universitari Mutua de Terrassa, Spain.

### *Choroidal thickness evaluation*

A spectral-domain 3D-OCT-2000 (Topcon Corporation, Tokyo, Japan) with a 6 X 6 protocol (512 X 128) was used to measure choroidal thickness at the subfoveal region and at 1 mm, 2 mm and 3 mm from the fovea, nasally, temporally, superiorly and inferiorly. Choroidal thickness was defined as the distance between the retinal pigment epithelium and the inner margin of the sclera (choroidal-scleral interface), seen as a hyper-reflective line behind the large vessel layer of the choroid. A calliper was employed to measure this distance manually. All measurements were performed by two



independent experienced examiners (A. Z. and Z. A.), whereupon the average of the two measurements was used for statistical analysis. Measurements were repeated by a third examiner (M.A.Z.) if the difference between the two measurements was over 15%.

#### *Retinal sensitivity evaluation*

Microperimetry was performed with a MAIA microperimeter (Macular Analyzer Integrity Assessment, CenterVue, Padova, Italy). This instrument uses a combination of scanning laser ophthalmoscopy and static perimetry to provide a maximum illumination level of 318.47 cd/m<sup>2</sup>, which may be attenuated up to 36 dB, in 1 dB steps. Results are classified as normal if over 27 dB, suspect when they fall between 26 and 27 dB and anomalous if under 26 dB. Measurements were performed with the “Expert Exam” mode which utilizes a 4-2-1 staircase strategy to present 37 stimuli in three concentric circles of 2, 6 and 10 degrees of diameter, corresponding, approximately, to 1 mm, 2 mm and 3 mm, respectively, from the center of the macula. Duration of the stimulus is 200 ms, with the whole exam lasting about 5 minutes per eye.

The MAIA microperimeter also allows for the evaluation of fixation by using high speed eye trackers (25 Hz) to register the fixation pattern, whereupon the device calculates fixation indexes to determine the percentage of fixation points inside two circles of pre-defined diameter. Fixation data of our sample of patients shall not be presented and discussed in this article.

Contact lenses were employed during microperimetry in those patients with refractive errors > 15.00 D. For those with refractive error less than 15.00 D the device automatically conducts the required range of focus adjustments. All microperimetry examinations were performed in a dim-illuminated room without the need for pupil dilation and only after the patients were comfortable with the procedure and instrumentation.

#### *Procedure*

Following a comprehensive case history, patients underwent a complete optometric examination, including non-contact air-puff tonometry. Non-cycloplegic refraction was performed and monocular DCVA was assessed with the retro-illuminated Early Treatment Diabetic Retinopathy Study (ETDRS) chart (Lighthouse International, NY). The chart was presented at a distance of 4 m and visual acuity values were recorded in logMAR units.

Ocular fundus and cross-sectional macular images were captured with the OCT device and sent to a medical team of retinal experts (OPTretina S.L., Barcelona, Spain) to

identify and exclude patients with retinal pathologies, in accordance with the predefined inclusion/exclusion criteria.

All patients underwent microperimetry and OCT examination consecutively, allowing for rest between examinations and for adaptation to the dim-light prior to microperimetry. In all instances microperimetry was performed before OCT to avoid any unwanted after-image effect of the strong flash of light employed by the OCT for image capture. During each procedure eyes were examined in random order. All measurements were conducted approximately at the same time of day to avoid the possible effect of diurnal variations in choroidal thickness<sup>33</sup>.

### *Data analysis*

Statistical analysis was conducted with the statistical package IBM SPSS, V. 19 (IBM, Inc, USA) for Windows. Data were evaluated for normality with the Kolmogorov-Smirnov test, which revealed that all variables under examination followed a normal distribution. Therefore, descriptive statistics is presented in terms of mean and standard deviation (SD). In addition, the 95% Confidence Interval (95% CI) was calculated to define the thresholds for normal inter-ocular asymmetry of the various anatomical and functional parameters. For this purpose, the absolute values of inter-ocular asymmetry were considered, rather than the relative values. Inferential statistics were conducted with the Student t-test for matched pairs when comparing data from right and left eyes or with the Student t-test for unmatched pairs if data belonged to different study groups (such as control and high myopia groups). Finally, in order to investigate the possible association between absolute inter-ocular differences and refractive error, in the myopia group, the Pearson correlation test was employed. Correlations were defined as weak if  $0.4 \leq r < 0.6$ , moderate if  $0.6 \leq r < 0.8$  and strong if  $r \geq 0.8$ . A p-value  $< 0.05$  was considered as the threshold for statistical significance.

## **RESULTS**

### *Sample demographics*

Forty-three subjects (15 females; 28 males) were enrolled in the myopic group, with an age of  $35.07 \pm 13.31$  years (range from 13 to 60 years). Forty-five subjects (23 females; 22 males) were enrolled in the control group, with an age of  $39.9 \pm 14.1$  years (range from 16 to 68 years). Both in the myopia and control group, no statistically significant inter-ocular differences were found in spherical equivalent and CDVA. Besides, no statistically significant differences in age were encountered between the groups.

*Choroidal thickness evaluation*

**Table 1** displays a summary of mean choroidal thickness at each of the locations and quadrants under examination for both the high myopia and control groups. Results are presented as mean  $\pm$  SD for right (RE) and left (LE) eyes, and the outcome of the Student t-test for matched pairs for each group is also shown to highlight the statistical significance of the encountered inter-ocular differences. In the control group, statistically significant differences between the RE and LE were found only at 1 mm nasally ( $277.03 \pm 13.74 \mu\text{m}$  in RE;  $278.06 \pm 13.97 \mu\text{m}$  in LE;  $p < 0.001$ ) and at 2 mm temporally ( $224.20 \pm 14.61 \mu\text{m}$  in RE;  $231.09 \pm 14.30 \mu\text{m}$  in LE;  $p = 0.013$ ). For both eyes, mean choroidal thickness values were larger subfoveally, and decreased progressively towards the periphery. Conversely, in the high myopia group, statistically significant differences between both eyes were encountered only at 3 mm nasally ( $152.65 \pm 46.91 \mu\text{m}$  in RE;  $210.60 \pm 47.72 \mu\text{m}$  in LE;  $p < 0.001$ ) and at 3 mm temporally ( $195.07 \pm 44.43 \mu\text{m}$  in RE;  $153.49 \pm 45.67 \mu\text{m}$  in LE;  $p < 0.001$ ). For both eyes, mean choroidal thickness values were larger at the 3 mm ring, followed by the 1 mm ring and 2 mm ring. The choroid was thinnest subfoveally. Overall, the choroid was thinner in the myopic than in the control group at all explored locations (all  $p < 0.05$ ).

Absolute inter-ocular differences in choroidal thickness, described as mean  $\pm$  SD (95% CI) are presented in **Table 2**. The non-matched pairs Student t-test was used to analyze the differences between the myopic and control groups in terms of absolute inter-ocular differences. Inter-ocular differences were larger in the myopic group in most of the choroidal locations under evaluation (all  $p < 0.05$ ).

*Retinal sensitivity evaluation*

**Table 3** displays a summary of retinal sensitivity values for both groups. For each eye, results are presented as mean  $\pm$  SD, and the outcome of the Student t-test for matched pairs to explore the statistical significance of the inter-ocular differences is also shown. In the control group, statistically significant differences were found between RE and LE in overall mean sensitivity values ( $27.50 \pm 1.71 \text{ dB}$  in RE;  $28.07 \pm 1.25 \text{ dB}$  in LE;  $p = 0.008$ ), as well as at several peripheral locations. Retinal sensitivity gradually decreased towards the periphery, with the lowest values at 3 mm temporally in both eyes. Similarly, statistically significant inter-ocular differences were found in the myopic group, both in overall mean retinal sensitivity values ( $27.10 \pm 3.61 \text{ dB}$  in RE;  $27.91 \pm 2.50 \text{ dB}$  in LE;  $p = 0.018$ ) and at several central and peripheral locations. In the myopic group, mean retinal sensitivity was lowest at the macula in both eyes, and progressively increased at the 3 mm, 1 mm and 2 mm locations in the RE and at the 3 mm, 2 mm and 1 mm locations in the LE. Overall, albeit retinal sensitivity was better in the control group, differences only reached statistical significance at the central location ( $p = 0.001$ ).

**Table 4** displays a summary of absolute inter-ocular differences in retinal sensitivity for both groups in terms of mean  $\pm$  SD (95% CI). In general, inter-ocular differences were larger in the myopic group than in the control group, although statistically significant differences were only encountered at the central location ( $p = 0.001$ ).

#### *Inter-ocular differences and refractive error*

A Pearson coefficient of correlation test was employed to investigate the association between mean refractive error and absolute inter-ocular differences in both choroidal thickness and retinal sensitivity in the myopic group. The results of this analysis are shown in **Table 5**. No statistically significant correlations were found between choroidal thickness asymmetry at any of the explored locations and refractive error, with the exception of at the 1 mm ring, superiorly. Conversely, statistically significant moderate negative correlations were found between refractive error and absolute inter-ocular differences in retinal sensitivity at most of the locations under examination, particularly towards the centre of the retina, that is, retinal sensitivity asymmetry was found to increase with refractive error.

## **DISCUSSION**

It is estimated that by 2050 approximately 1 billion people worldwide will have high myopia<sup>34</sup>. However, not all patients with high myopia will develop complications leading to pathological myopia. Indeed, in a longitudinal study of 61 months, Vongphanit and co-workers reported that only 17.4% of their 67 eyes with high myopia developed myopic retinopathy<sup>35</sup>. One of the complications of pathological myopia is posterior staphyloma, in which the retina and choroid are abnormally stretched, leading to anatomical damage and visual impairment. Another complication is diffuse atrophy, which presents as a local area of choroidal thinning but relatively intact outer retinal structures, that is, without initial visual involvement. Both complications may appear unilaterally, highlighting the clinical relevance of an early detection through the exploration of choroidal thickness and retinal sensitivity<sup>36</sup>. The main purpose of the present research was to describe the normal range of inter-ocular asymmetry in choroidal thickness and retinal sensitivity in a sample of patients with high myopia without complications, that is, to define the threshold beyond which early signs of pathological myopia complications may be detected and preventive treatment strategies implemented.

Regarding choroidal thickness, the present findings are in agreement with previous reports describing a thinner choroid in high myopia than in healthy eyes, both subfoveally and in different peripheral locations<sup>2,20,29,30,37</sup>. Besides, whereas in the control group the thickest choroid was found subfoveally, in the myopic group this area was the thinnest. Similarly, differences were observed between the myopic and healthy

groups in the distribution of choroidal thickness across the different quadrants and peripheral rings under examination. These findings are also in general agreement with published literature, although differences in sample demographics and range of refractive errors prevent a direct comparison of absolute choroidal thickness values with previous research. In effect, in the Beijing Eye Study of 2011, in which 3468 were examined with spectral-domain OCT, in myopic subjects with refractive error over 1.00 D subfoveal choroidal thickness was found to decrease by 15  $\mu\text{m}$  (95% CI 11.9 to 18.5  $\mu\text{m}$ ) for every further increase in refractive error of 1.00 D<sup>38</sup>.

Interestingly, absolute inter-ocular differences in choroidal thickness were very small for the control group, in agreement with previous reports documenting differences under 10  $\mu\text{m}$  at the subfoveal region<sup>11,32</sup>. Inter-ocular differences were larger in the myopic, particularly at the 3 mm ring, nasally (57.95  $\pm$  51.80  $\mu\text{m}$  in the myopic group versus 2.34  $\pm$  20.19  $\mu\text{m}$  in the control group) and temporally (41.58  $\pm$  56.81  $\mu\text{m}$  in the myopic group versus 0.66  $\pm$  22.62  $\mu\text{m}$  in the control group). Overall, inter-ocular asymmetry was at least twice in myopia than in healthy eyes. Within the myopic group, no statistically significant correlations were found between refractive error and choroidal thickness asymmetry.

In terms of retinal sensitivity, very few studies have explored visual function in high myopia, documenting a reduction in retinal sensitivity, more pronounced with increasing refractive error<sup>24-26</sup>. Reduced retinal sensitivity was found in our sample of myopic patients, when compared with the control group, albeit these differences only reached statistical significance subfoveally, with mean values of 24.84  $\pm$  4.58 dB in RE and 26.05  $\pm$  3.60 dB in LE for the myopic group and 27.74  $\pm$  2.51 dB in RE and 28.09  $\pm$  2.36 dB in LE for the control group. It must be noted that, although many of the locations under study presented suspect retinal sensitivity values (between 26 and 27 dB), only at the subfoveal region in the RE was the mean value of sensitivity anomalous. However, as evidenced by the large inter-subject variability (large SD values), when considering individual rather than mean values, some of the patients had retinal sensitivity values well below the threshold of normality, even in the absence of ocular fundus disease.

Finally, regarding inter-ocular differences in retinal sensitivity, in general a larger asymmetry was encountered in the myopic group, although differences only reached statistical significance at the subfoveal region, with inter-ocular differences decreasing towards the periphery. Overall, in myopia inter-ocular asymmetry was approximately twice that of healthy eyes. Besides, retinal sensitivity asymmetry was found to increase with refractive error, and statistically significant correlations were found at most of the areas under study. These findings give support to the need to consider refractive error not only in the interpretation of retinal sensitivity nomograms<sup>24</sup>, but also when assessing inter-ocular asymmetry.

The present study was not devoid of limitations. Firstly, many potential participants with myopia over -10.00 D had to be excluded due to the observation of ocular fundus

complications characteristic of pathological myopia. Therefore, although all patients in the high myopia group had refractive errors over -6.00 D, most of them were clustered in the range between -6.00 D and -10.00D, that is, they could be considered to represent the low end of high myopia. Secondly, as also noted by previous authors<sup>30</sup>, the use of manual callipers to perform choroidal thickness measurements may not be a very precise approach, particularly when distances are small, as was the case in some myopic eyes. Finally, even though none of the patients included in the study had any abnormality of the ocular fundus, given the cross-sectional design of this study, it can not be ruled out that the larger inter-ocular differences encountered in some of our patients were indicative of earlier stages of disease. Patients from the myopic group were scheduled for follow-up visits to explore the possible onset of pathological myopia in the future.

In conclusion, as far as we know, this is the first study investigating inter-ocular differences in choroidal thickness and retinal sensitivity in high myopia in the absence of ocular complications. The present findings revealed an expanded range of absolute inter-ocular differences in the high myopia group, when compared with the control group and with published literature (when available). Given the critical importance of an early detection and treatment of pathological conditions such as posterior staphyloma and chorioretinal atrophy, we believe these results to be relevant to eye care providers to aid in their diagnosis and to researchers to provide further insight into the fine line separating high from pathological myopia.

## REFERENCES

1. Zheng YF, Pan CW, Chay J, et al. The economic cost of myopia in adults aged over 40 years in Singapore. *Invest Ophthalmol Vis Sci* 2013; 54:7532–7537.
2. Flores-Moreno I, Lugo F, Duker JS, Ruiz-Moreno JM. The relationship between axial length and choroidal thickness in eyes with high myopia. *Am J Ophthalmol* 2013; 155:314–319.e1.
3. Honjo M, Omodaka K, Ishizaki T et al. Retinal thickness and the structure/function relationship in the eyes of older adults with glaucoma. *PLoS One* 2015; 10(10):e0141293.
4. Ikuno Y, Tano Y. Retinal and choroidal biometry in highly myopic eyes with spectral-domain optical coherence tomography. *Invest Ophthalmol Vis Sci* 2009; 50:3876–3880.
5. Kawaguchi C, Nakatani Y, Ohkubo S et al. Structural and functional assessment by hemispheric asymmetry testing of the macular region in preperimetric glaucoma. *Jpn J Ophthalmol* 2014; 58:197-204.

6. Michalewski J, Michalewska Z, Nawrocka Z et al. Correlation of choroidal thickness and volume measurements with axial length and age using swept source optical coherence tomography and optical low-coherence reflectometry. *Biomed Res Int* 2014; 639160.
7. Vincent SJ, Collins MJ, Read SA, Carney LG. Retinal and choroidal thickness in myopic anisometropia. *Invest Ophthalmol Vis Sci* 2013; 54:2445-2456.
8. Takahashi A, Ito Y, Iguchi Y et al. Axial length increases and related changes in highly myopic normal eyes with myopic complications in fellow eyes. *Retina* 2012; 32: 127-133.
9. Spaide RF, Koizumi H, Pozzoni MC. Enhanced depth imaging spectral-domain optical coherence tomography. *Am J Ophthalmol* 2008; 146:496–500.
10. Branchini LA, Adhi M, Regatieri CV et al. Analysis of choroidal morphologic features and vasculature in healthy eyes using spectral-domain optical coherence tomography. *Ophthalmology* 2013; 120:1901-1908.
11. Chen FK, Yeoh J, Rahman W et al. Topographic variation and interocular symmetry of macular choroidal thickness using enhanced depth imaging optical coherence tomography. *Invest Ophthalmol Vis Sci* 2012; 23:975-985.
12. Hirata M, Tsujikawa A, Matsumoto A et al. Macular choroidal thickness and volume in normal subjects measured by swept-source optical coherence tomography. *Invest Ophthalmol Vis Sci* 2011; 52:4971-4978.
13. Karapetyan A, Ouyang P, Tang LS, Gemilyan M. Choroidal thickness in relation to ethnicity measured using enhanced depth imaging optical coherence tomography. *Retina* 2016; 36:82-90.
14. Nagasawa T, Mitamura Y, Katome T et al. Macular choroidal thickness and volume in healthy pediatric individuals measured by swept-source optical coherence tomography. *Invest Ophthalmol Vis Sci* 2013; 54:7068-7074.
15. Park KA, Oh SY. Choroidal thickness in healthy children. *Retina* 2013; 33:1971-1976.
16. Rossou E, Abegão Pinto L, Vandewalle E et al. Choroidal thickness of the papillomacular region in young healthy individuals. *Ophthalmologica* 2014; 232:97-101.
17. Shao L, Xu L, Chen CX et al. Reproducibility of subfoveal choroidal thickness measurements with enhanced depth imaging by spectral-domain optical coherence tomography. *Invest Ophthalmol Vis Sci* 2013; 54:230-233.
18. Rahman W, Chen FK, Yeoh J et al. Repeatability of manual subfoveal choroidal thickness measurements in healthy subjects using the technique of enhanced depth imaging optical coherence tomography. *Invest Ophthalmol Vis Sci* 2011; 52: 2267-2271.

19. Tuncer I, Karahan E, Zengin MO et al. Choroidal thickness in relation to sex, age, refractive error, and axial length in healthy Turkish subjects. *Int Ophthalmol* 2015; 35:403-410.
20. Wang J, Gao X, Huang W et al. Swept-source optical coherence tomography imaging of macular retinal and choroidal structures in healthy eyes. *BMC Ophthalmol* 2015; 15:122.
21. Saw SM, Gazzard G, Shih-Yen EC, Chua WH. Myopia associated pathological complications. *Ophthalmic Physiol Opt* 2005; 25:381-391.
22. Markowitz SN, Reyes SV. Microperimetry and clinical practice: An evidence-based review. *Can J Ophthalmol* 2013; 48: 350-357.
23. Rohrschneider K, Bültmann S, Springer C. Use of fundus perimetry (microperimetry) to qualify macular sensitivity. *Prog Retin Eye Res* 2008; 27: 536-548.
24. Zaben A, Zapata MA, Garcia-Arumi J. Retinal sensitivity and choroidal thickness in high myopia. *Retina* 2015; 35: 398–406.
25. Qin Y, Zhu M, Qu X et al. Regional macular light sensitivity changes in myopic Chinese adults: an MP1 study. *Invest Ophthalmol Vis Sci* 2010; 51: 4451-4457.
26. Gella L, Raman R, Sharma T. Evaluation of in vivo human retinal morphology and function in myopes. *Curr Eye Res* 2011; 36: 943-946.
27. Flores-Moreno I, Ruiz-Medrano J, Duker JS, Ruiz-Moreno JM. The relationship between retinal and choroidal thickness and visual acuity in highly myopic eyes. *Br J Ophthalmol* 2013; 97:1010-1013.
28. Nishida Y, Fujiwara T, Imamura Y et al. Choroidal thickness and visual acuity in highly myopic eyes. *Retina* 2012; 32:1229-1236.
29. Gupta P, Saw SM, Cheung CY et al. Choroidal thickness and high myopia: a case-control study of young Chinese men in Singapore. *Acta Ophthalmol* 2015; 93: e585-592.
30. Gupta P, Cheung CY, Saw SM et al. Choroidal thickness does not predict visual acuity in young high myopes. *Acta Ophthalmol* 2016; doi: 10.1111/aos.13084.
31. Yoshida T, Ohno-Matsui K, Yasuzumi K et al. Myopic choroidal neovascularization: a 10-year follow-up. *Ophthalmology* 2003; 110:1297-1305.
32. Ruiz-Medrano J, Flores-Moreno I, Peña-García P et al. Asymmetry in macular choroidal thickness profile between both eyes in a healthy population measured by swept-source optical coherence tomography. *Retina* 2015; 35:2067-2073.



33. Tan CS, Ouyang U, Ruiz H, Sadda SR. Diurnal variations of choroidal thickness in normal, healthy subjects measured by spectral domain optical coherence tomography. *Invest Ophthalmol Vis Sci* 2012;53:261-266.
34. Holden BA, Fricke TR, Wilson DA et al. Global prevalence of myopia and high myopia and temporal trends from 2000 through 2050. *Ophthalmology* 2016;123:1036-1042.
35. Vongphanit J, Mitchell P, Wang JJ. Prevalence and progression of myopic retinopathy in an older population. *Ophthalmology* 2002;109:704-711.
36. Ohno-Matsui K. What is the fundamental nature of pathological myopia? *Retina* 2016; DOI: [10.1097/IAE.0000000000001348](https://doi.org/10.1097/IAE.0000000000001348)
37. Ohsugi H, Ikuno Y, Oshima K, Tabuchi H. 3-D choroidal thickness maps from EDI-OCT in highly myopic eyes. *Optom Vis Sci* 2013;90:599-606.
38. Wei W, Xu L, Jonas J et al. Subfoveal choroidal thickness: the Beijing eye study. *Ophthalmology* 2012;120:175-180.

**Table 1.** Mean choroidal thickness at each of the locations and quadrants under examination (N: Nasal; T: Temporal; S: Superior; I: Inferior) for myopia and control groups. Results are presented as mean  $\pm$  SD for right (RE) and left (LE) eyes, and the outcome of the Student t-test for matched pairs for each group is also shown. P-values in bold denote statistically significant inter-ocular differences.

Choroidal Thickness ( $\mu\text{m}$ )	CONTROL GROUP					MYOPIA GROUP				
	RE		LE		p	RE		LE		p
	Mean	SD	Mean	SD		Mean	SD	Mean	SD	
<b>Central</b>	307.31	13.77	309.80	18.12	0.478	174.50	62.99	171.67	56.45	0.604
<b>1 mm N</b>	277.03	13.74	278.06	13.97	<b>&lt;0.001</b>	163.93	52.34	153.38	51.96	0.095
<b>1 mm T</b>	252.51	16.20	254.23	17.61	0.668	187.36	66.10	183.30	51.32	0.565
<b>1 mm S</b>	212.74	19.14	214.70	24.13	0.695	199.90	62.97	189.59	57.42	0.130
<b>1 mm I</b>	285.60	11.32	290.71	14.75	0.139	190.20	54.26	188.94	51.22	0.841
<b>2 mm N</b>	263.77	10.64	268.91	15.52	0.108	128.98	50.82	134.28	67.25	0.510
<b>2 mm T</b>	224.20	14.61	231.09	14.30	<b>0.013</b>	183.91	59.61	183.02	52.57	0.914
<b>2 mm S</b>	301.60	20.52	304.40	18.57	0.489	206.57	57.27	198.56	54.12	0.188
<b>2 mm I</b>	259.00	14.45	256.71	18.62	0.573	187.93	55.29	188.62	51.96	0.909
<b>3 mm N</b>	219.26	17.20	221.60	19.55	0.497	152.65	46.91	210.60	47.72	<b>&lt;0.001</b>
<b>3 mm T</b>	296.23	13.19	296.89	17.52	0.865	195.07	44.43	153.49	45.67	<b>&lt;0.001</b>
<b>3 mm S</b>	254.83	13.54	255.66	17.33	0.826	212.98	48.68	212.00	40.49	0.872
<b>3 mm I</b>	221.63	17.95	216.34	13.82	0.132	197.98	47.14	199.33	44.76	0.824
<b>Mean of 1 mm ring</b>	290.14	10.58	292.54	11.60	0.347	185.37	54.91	178.83	48.31	0.167
<b>Mean of 2 mm ring</b>	257.55	8.86	258.90	9.87	0.539	176.86	46.93	176.15	45.10	0.860
<b>Mean of 3 mm ring</b>	219.48	11.61	220.96	13.41	0.417	189.69	31.49	193.88	32.06	0.249

**Table 2.** Absolute inter-ocular differences in choroidal thickness in mean  $\pm$  SD (95% CI) at each of the locations and quadrants under examination (N: Nasal; T: Temporal; S: Superior; I: Inferior) for myopia and control groups. The results of the non-matched pairs Student t-test are shown. P-values in bold denote statistically significant differences between the myopic and control groups in terms of absolute inter-ocular differences.

Absolute inter-ocular difference in choroidal thickness ( $\mu\text{m}$ )	CONTROL GROUP				MYOPIA GROUP				p
	Mean	SD	95% CI		Mean	SD	95% CI		
<b>Central</b>	2.49	20.52	-37.73	42.71	2.83	35.48	-66.71	72.37	<b>0.001</b>
<b>1 mm N</b>	1.03	19.66	-37.50	39.56	10.55	40.46	-68.75	89.85	<b>0.001</b>
<b>1 mm T</b>	1.71	23.41	-44.17	47.59	4.06	45.88	-85.86	93.98	<b>&lt;0.001</b>
<b>1 mm S</b>	1.94	29.03	-54.96	58.84	10.30	43.77	-75.49	96.09	<b>0.004</b>
<b>1 mm I</b>	5.11	19.99	-34.07	44.29	1.26	40.68	-78.47	80.99	<b>0.047</b>
<b>2 mm N</b>	5.14	18.44	-31.00	41.28	5.30	52.32	-97.25	107.85	<b>0.002</b>
<b>2 mm T</b>	6.89	15.57	-23.63	37.41	0.88	53.61	-104.20	105.96	<b>&lt;0.001</b>
<b>2 mm S</b>	2.8	23.70	-43.65	49.25	8.01	39.24	-68.90	84.92	<b>0.007</b>
<b>2 mm I</b>	2.29	23.77	-44.30	48.88	0.69	39.34	-76.42	77.80	<b>0.011</b>
<b>3 mm N</b>	2.34	20.19	-37.23	41.91	57.95	51.8	-43.58	159.48	<b>&lt;0.001</b>
<b>3 mm T</b>	0.66	22.62	-43.68	45.00	41.58	56.81	-69.77	152.93	<b>&lt;0.001</b>
<b>3 mm S</b>	0.83	22.11	-42.51	44.17	0.98	39.63	-76.69	78.65	<b>0.014</b>
<b>3 mm I</b>	5.29	20.24	-34.38	44.96	1.35	39.46	-75.99	78.69	<b>0.001</b>
<b>Mean of 1 mm ring</b>	2.4	14.86	-26.73	31.53	6.54	30.51	-53.26	66.34	<b>0.002</b>
<b>Mean of 2 mm ring</b>	1.35	12.86	-23.86	26.56	0.73	26.47	-51.15	52.61	<b>&lt;0.001</b>
<b>Mean of 3 mm ring</b>	1.47	10.62	-19.35	22.29	4.18	23.47	-41.82	50.18	<b>&lt;0.001</b>

**Table 3.** Mean retinal sensitivity at each of the locations and quadrants under examination (N: Nasal; T: Temporal; S: Superior; I: Inferior) for myopia and control groups. Results are presented as mean  $\pm$  SD for right (RE) and left (LE) eyes. The outcome of the Student t-test for matched pairs for each group is also shown. P-values in bold denote statistically significant inter-ocular differences.

Retinal sensitivity (dB)	CONTROL GROUP					MYOPIA GROUP				
	RE		LE		p	RE		LE		p
	Mean	SD	Mean	SD		Mean	SD	Mean	SD	
Central	27.74	2.51	28.09	2.36	0.452	24.84	4.58	26.05	3.60	<b>0.029</b>
1 mm N	27.42	1.86	28.16	1.64	<b>0.031</b>	27.21	4.39	28.76	2.16	<b>0.003</b>
1 mm T	28.37	1.79	28.78	1.63	0.198	26.92	4.89	28.46	2.43	<b>0.010</b>
1 mm S	28.51	2.14	29.07	1.70	0.098	27.64	3.64	28.12	2.93	0.272
1 mm I	27.98	1.96	28.34	1.55	0.320	26.89	3.96	28.03	2.20	0.034
2 mm N	28.03	2.10	28.48	1.26	0.146	27.15	4.84	28.62	2.46	<b>0.006</b>
2 mm T	27.31	1.62	27.75	1.58	0.112	26.77	3.25	27.80	1.99	<b>0.004</b>
2 mm S	27.44	2.24	28.41	1.52	<b>0.003</b>	27.54	2.43	27.88	3.82	0.402
2 mm I	27.69	2.10	28.30	1.30	0.056	27.29	2.85	28.07	2.56	<b>0.023</b>
3 mm N	26.91	1.79	27.78	1.28	<b>0.002</b>	26.31	4.63	27.54	4.38	<b>&lt;0.001</b>
3 mm T	26.54	1.92	26.74	1.70	0.525	26.13	2.95	26.76	2.83	<b>0.046</b>
3 mm S	26.69	2.07	27.66	1.52	<b>0.002</b>	26.96	3.59	27.02	3.57	0.853
3 mm I	26.84	1.97	27.55	1.71	<b>0.007</b>	26.86	2.37	27.38	1.97	0.107
Mean of 1 mm ring	28.04	1.71	28.56	1.46	<b>0.048</b>	27.18	4.02	28.44	2.12	<b>0.007</b>
Mean of 2 mm ring	27.72	1.91	28.24	1.21	<b>0.041</b>	27.25	3.15	28.14	2.44	<b>0.001</b>
Mean of 3 mm ring	26.70	1.72	27.43	1.29	<b>0.002</b>	26.56	3.21	27.30	2.93	<b>0.004</b>
Overall mean	27.50	1.71	28.07	1.25	<b>0.008</b>	27.10	3.61	27.91	2.50	<b>0.018</b>

**Table 4.** Absolute inter-ocular differences in retinal sensitivity in mean  $\pm$  SD (95% CI) at each of the locations and quadrants under examination (N: Nasal; T: Temporal; S: Superior; I: Inferior) for myopia and control groups. The results of the non-matched pairs Student t-test are shown. P-values in bold denote statistically significant differences between the myopic and control groups in terms of absolute inter-ocular differences.

Absolute inter-ocular difference in retinal sensitivity (dB)	CONTROL GROUP				MYOPIA GROUP				p
	Mean	SD	95% CI		Mean	SD	95% CI		
<b>Central</b>	0.34	2.67	-4.89	5.57	1.21	3.51	-5.67	8.09	<b>0.001</b>
<b>1 mm N</b>	0.74	1.94	-3.06	4.54	1.55	3.23	-4.78	7.88	0.790
<b>1 mm T</b>	0.41	1.84	-3.20	4.02	1.55	3.74	-5.78	8.88	0.099
<b>1 mm S</b>	0.57	1.97	-3.29	4.43	0.49	2.87	-5.14	6.12	0.215
<b>1 mm I</b>	0.36	2.11	-3.78	4.50	1.14	3.41	-5.54	7.82	0.142
<b>2 mm N</b>	0.47	1.77	-3.00	3.94	1.47	3.32	-5.04	7.98	0.319
<b>2 mm T</b>	0.44	1.6	-2.70	3.58	1.03	2.23	-3.34	5.40	0.371
<b>2 mm S</b>	0.97	1.82	-2.60	4.54	0.34	2.63	-4.81	5.49	0.853
<b>2 mm I</b>	0.62	1.84	-2.99	4.23	0.78	2.15	-3.43	4.99	0.499
<b>3 mm N</b>	0.87	1.53	-2.13	3.87	1.23	2.03	-2.75	5.21	0.468
<b>3 mm T</b>	0.2	1.87	-3.47	3.87	0.63	2.02	-3.33	4.59	0.482
<b>3 mm S</b>	0.98	1.76	-2.47	4.43	0.05	1.88	-3.63	3.73	0.687
<b>3 mm I</b>	0.71	1.47	-2.17	3.59	0.52	2.06	-3.52	4.56	0.960
<b>Mean of 1 mm ring</b>	0.52	1.5	-2.42	3.46	1.26	2.91	-4.44	6.96	0.244
<b>Mean of 2 mm ring</b>	0.51	1.43	-2.29	3.31	0.89	1.60	-2.25	4.03	0.441
<b>Mean of 3 mm ring</b>	0.76	1.34	-1.87	3.39	0.74	1.57	-2.34	3.82	0.850
<b>Overall mean</b>	0.6	1.26	-1.87	3.07	0.81	2.15	-3.40	5.02	0.578

**Table 5.** Correlation analysis of the association between mean refractive error and absolute inter-ocular differences in both choroidal thickness and retinal sensitivity in the myopic group. Correlation coefficient (r) and statistical significance (p) are shown), with values in bold denoting statistical significance.

Absolute inter-ocular difference in choroidal thickness ( $\mu\text{m}$ )	r	p	Absolute inter-ocular difference in retinal sensitivity (dB)	r	p
Central	0.189	0.202	Central	<b>-0.345</b>	<b>0.018</b>
1 mm N	0.113	0.448	1 mm N	<b>-0.578</b>	<b>&lt;0.001</b>
1 mm T	-0.111	0.457	1 mm T	<b>-0.738</b>	<b>&lt;0.001</b>
1 mm S	<b>-0.441</b>	<b>0.002</b>	1 mm S	-0.228	0.123
1 mm I	-0.108	0.471	1 mm I	<b>-0.491</b>	<b>&lt;0.001</b>
2 mm N	-0.166	0.265	2 mm N	<b>-0.633</b>	<b>&lt;0.001</b>
2 mm T	0.027	0.856	2 mm T	<b>-0.413</b>	<b>0.004</b>
2 mm S	-0.062	0.681	2 mm S	<b>-0.501</b>	<b>&lt;0.001</b>
2 mm I	0.166	0.264	2 mm I	0.002	0.989
3 mm N	0.164	0.270	3 mm N	-0.120	0.423
3 mm T	-0.276	0.060	3 mm T	-0.074	0.619
3 mm S	-0.223	0.131	3 mm S	0.144	0.334
3 mm I	-0.010	0.949	3 mm I	-0.285	0.052
Mean of 1 mm ring	0.120	0.421	Mean of 1 mm ring	<b>-0.545</b>	<b>&lt;0.001</b>
Mean of 2 mm ring	0.021	0.888	Mean of 2 mm ring	-0.226	0.127
Mean of 3 mm ring	-0.249	0.091	Mean of 3 mm ring	-0.079	0.600
			Overall mean	<b>-0.304</b>	<b>0.038</b>

## Annex III. Preprint of Paper published in International Eye Science

### Inter-ocular asymmetry of retinal parameters in Caucasian healthy children and young adults measured with optical coherence tomography

Zeyad Alzaben<sup>1,2</sup>, Genís Cardona<sup>1</sup>, Ahmad Zaben<sup>3</sup>, Miguel A. Zapata<sup>4</sup>

<sup>1</sup>Department of Optics and Optometry, Universitat Politècnica de Catalunya, BarcelonaTech, Terrassa, E08222, Spain

<sup>2</sup>Opticalia Olot, Olot, E17800, Spain

<sup>3</sup>Optipunt Zaben, Figueres, E17600, Spain

<sup>4</sup>Ophthalmology Department, Vall d'Hebron Hospital, Barcelona, E08035, Spain

**Correspondence to:** Genís Cardona. Terrassa School of Optics and Optometry, Violinista Vellsolà, 37, E08222 Terrassa, Catalonia, Spain. [genis.cardona@upc.edu](mailto:genis.cardona@upc.edu).

#### Abstract

**AIM:** To evaluate retinal parameters in a sample of healthy young Caucasian adults to define the normal or physiological range of inter-ocular asymmetry in this particular age and ethnic group.

**METHODS:** Study sample consisted of 37 Caucasian children and young adults aged between 12 and 23 years (spherical equivalent from -3.00D to +4.00D, anisometropia <0.5D and axial length differences <0.3mm). Normal inter-ocular asymmetry values were determined and 95% inter-ocular difference tolerance values were obtained.

**RESULTS:** Statistically significant inter-ocular differences were found in mean ( $P=0.003$ ) and superior ( $P=0.008$ ) retinal nerve fiber layer (RNFL) thickness, as well as in central macular thickness ( $P=0.039$ ), with larger values in the left eye in all instances, and with tolerance limits of inter-ocular asymmetry of  $-9.00\mu\text{m}$  to  $6.00\mu\text{m}$ ,  $-28.00\mu\text{m}$  to  $9\mu\text{m}$  and  $-39.00\mu\text{m}$  to  $29.00\mu\text{m}$ , respectively. In addition, statistically significant differences were found between males and females in mean thickness of the RNFL in the right eye ( $P=0.020$ ).

**CONCLUSION:** The exploration of the normal asymmetries of the retina may be an effective approach to further understand myopia onset and progression, which is particularly relevant in this age group. Differences in instrumentation and sample characteristics compromise direct comparison with published research and warrant the need for further studies.

**KEYWORDS:** asymmetry; macula; optical coherence tomography; optic nerve; retinal nerve fiber layer; retinal thickness

#### INTRODUCTION

Optical coherence tomography (OCT) is a non-invasive technique that uses low coherence interferometry for real-time *in-vivo* acquisition of retinal images akin to ocular biopsy<sup>[1]</sup>. This technique provides highly reproducible real-time *in-vivo* images of the retina, with an axial resolution of 10 microns or less<sup>[2-3]</sup>. Nowadays, OCT is widely used for the quantitative assessment of optic nerve head parameters, as well as for the measurement of the thickness of the macula and the retinal nerve fiber layer (RNFL)<sup>[4]</sup>. Also, it is the instrument of choice of many eye care providers for the diagnosis and follow-up of patients suffering from retinal and optic nerve alterations such as cystoid macular edema, glaucoma and age-related macular degeneration, among others<sup>[5]</sup>. Various types of OCT models are commercially available with differences in image acquisition time, depth of focus, resolution and other device specifications<sup>[6]</sup>.

Optical coherence tomography has been employed to explore both inter-quadrant<sup>[7]</sup> and inter-ocular differences in retinal parameters. Indeed, a detailed knowledge of physiological retinal asymmetry is very relevant to discard certain unilateral or asymmetrical conditions, such as glaucoma or tumors of the optic nerve<sup>[3,8]</sup>. In addition, myopia onset and progression has been associated with an increase in axial length and with thinning of retinal structures<sup>[9]</sup>. This supports the need for exploration of normal (average or physiological) asymmetry in the absence of inter-ocular differences in refractive error as a means to better understand the changes occurring in myopia, which commonly appears during adolescence and early adulthood, an age range in which inter-ocular asymmetry is not well described in the literature. In particular, subsequent research on patients with different degrees of anisometropia may assist in understanding the development of these retinal alterations. Therefore, although absolute values of retinal parameters have received more attention than inter-ocular asymmetry, some research efforts have been devoted to define normality<sup>[3,10-16]</sup> and to determine which retinal parameter or combination of parameters may yield the best diagnostic sensitivity and specificity for the detection of early stages of a particular condition<sup>[16]</sup>.

Some researchers have documented thicker average values of RNFL in the right than in the left eye<sup>[10-12]</sup>, although other authors have failed to disclose statistically significant inter-ocular differences in average RNFL thickness<sup>[3,13-15]</sup>. Similarly, a quadrant per quadrant analysis has revealed thicker RNFL in the right than in the left eye in the nasal and temporal quadrants, without a consensus in the literature regarding superior and inferior quadrants<sup>[3,10,12,14]</sup>. In turn, macular thickness has been described as a more symmetrical parameter than RNFL thickness<sup>[3,16]</sup>. Finally, good symmetry in disc and rim area, and cup-to-disc ratio (CDR) has also been documented, with reported values of inter-ocular asymmetry of less than 0.02 mm for disc diameter and less than 0.04 mm<sup>2</sup> for rim area<sup>[14]</sup>, and with only between 1% and 6% of healthy adults with CDR asymmetry larger than 0.2<sup>[14]</sup>.

Given the relevance of defining the normal range of inter-ocular asymmetry in the age group at risk of myopia onset and progression (school age, that is, from early puberty to emerging adulthood)<sup>[17]</sup>, a study was designed in which a spectral-domain optical coherence tomographer (3D OCT-2000) was employed to explore several retinal parameters in a sample of healthy Caucasian children and young adults. Inter-ocular differences were determined to define the corresponding thresholds for physiological asymmetry (*i.e.*, the range of normal inter-ocular asymmetry which may be encountered in the absence of significant anisometropia and in the absence of unilateral or asymmetrical pathological conditions) for each parameter under evaluation for this particular age, ethnic group and measurement device. In addition, the possible associations between the various parameters under evaluation were investigated.

## **SUBJECTS AND METHODS**

**Study Sample** Thirty-seven Caucasian patients were recruited from those attending an eye clinic (Optipunt Zaben, Figueres, Spain) between April 2014 and July 2014 for routine visual examination. Inclusion criteria were age from 12 to 23 years, spherical equivalent between +4.00D and -3.00D, best corrected monocular distance visual acuity  $\geq 0.0$  logMAR and intraocular pressure  $< 21$  mmHg. Participants with a history of ocular trauma or pathology, ocular or refractive surgery, diabetes mellitus and those without central fixation were excluded from the study, as were those with anisometropia  $\geq 0.5$ D or axial length differences larger than 0.3 mm. Participants with first-degree relatives diagnosed with glaucoma or retinal disease were also excluded from the sample.

Full explanation of the research was provided, including OCT measurement procedures, and written informed consent was obtained from each patient or from a parent or legal guardian when patients were underage. The study was conducted in accord with the Declaration of Helsinki tenets of 1975 (as revised in Tokyo in 2004) and received the approval of an institutional review board (Department of Optics and Optometry, Universitat Politècnica de Catalunya).



**Instrumentation: The 3D OCT-2000** The spectral-domain 3D OCT-2000, Optical coherence tomography (Topcon Spain, S.A., Barcelona, Spain), was employed for the exploration of the retina. According to the manufacturer, this device incorporates noise reducing algorithms and infrared/3D tracking technology to obtain high resolution scans of the retina. An integrated 16.2 megapixel digital non-mydratic fundus camera with less than 1 millisecond of flash was used for image capture.

A (6×6)mm exploration of the macular area was conducted with the macular cube 512×128 protocol, which performs 128 horizontal scan lines containing 512 A-scans. A thickness map with concentric sectors defining the nine regions of the macular area is generated, whereby the average of all points within the inner 1 mm circle is defined as the central macular thickness. Mean macular thickness and macular volume may also be determined. Similarly, disc parameters including rim area, disc area and CDR were obtained with a (6×6)mm, 512 × 128 protocol with the scan adjusted to the size of the optic disc, as close as possible to the disc margin and without crossing the border of the optic nerve. Finally, average and quadrant per quadrant measurements of RNFL thickness were obtained using the automated software measurement analysis protocol provided by the 3D OCT-2000.

**Procedure** Following a comprehensive case history, all patients underwent a complete optometric examination, including non-contact tonometry, to determine their suitability for the study in accordance to the predefined inclusion/exclusion criteria. Non-dilated pupil refraction in normal illumination conditions was conducted to determine refractive error. Best corrected monocular visual acuity (CDVA) was measured in logMAR with the retro-illuminated ETDRS chart (Lighthouse International, New York, NY), presented at a distance of 4 meters. The health of the ocular structures was explored with a slit-lamp and non-mydratic fundus camera confirmed by an independent experienced ophthalmologist.

All OCT measurements were performed by the same examiner and approximately at the same time of day (mornings). During image acquisition, three consecutive scans were obtained, whereupon the image with the highest signal strength was selected. Scans were considered unacceptable if signal strength was < 7 or if there was any eye movement or blink artifact during image capture. Right and left eyes were examined in random order.

**Data Analysis** Statistical analysis was performed with the IBM SPSS software 19.0 for Windows (IBM Corporation, Armonk, NY). All data were analyzed for normality using the Kolmogorov-Smirnov test, revealing several instances of non-normal distributions, which, given the present sample size, recommended a non-parametric approach. Therefore, descriptive data summarizing results for each eye are presented as median and range (maximum and minimum values), although mean values are also shown to facilitate comparison with previous studies. Inter-ocular differences are shown as mean, median, and 2.5<sup>th</sup> and 97.5<sup>th</sup> percentiles. The Mann-Whitney *U*-test was used to explore the statistical significance of the differences between non-paired data (such as between males and females), whereas the Wilcoxon signed ranks test was used when data was paired (comparing right with left eye). Finally, the Spearman coefficient of correlation test ( $\rho$ ) was used to explore possible associations between the parameters under study. A *P* value of <0.05 was considered to denote statistical significance throughout the study.

## RESULTS

**Study Sample** Thirty-seven Caucasian subjects (23 females; 14 males) participated in this study, with an age of  $17.4 \pm 3.5$  years (mean  $\pm$  SD), ranging from 12 to 23 years. Table 1 shows a summary of spherical equivalent (SE) and distance corrected visual acuity (CDVA) of right (OD) and left (OS) eyes. No statistically significant interocular differences were found in these parameters.

**Table 1** Study sample corrected distance visual acuity and spherical equivalent for right and left eye

Parameters	Mean	Median	Range	Z	P
CDVA OD (logMAR)	-0.025	0.000	0.000, -0.160		
CDVA OS (logMAR)	-0.021	0.000	0.000, -0.160	-1.342	0.180
SE OD (D)	-1.33	-1.00	-3.75, +0.50		
SE OS (D)	-1.23	-1.00	-3.75, +1.00	-1.297	0.195

Data is presented as mean, median and range (minimum, maximum values). The Wilcoxon test was used to assess interocular differences (Z and p values are shown). CDVA: corrected distance visual acuity; SE: spherical equivalent; OD: right eye; OS: left eye.

**Retinal Parameters** Table 2 presents a summary of RNFL, macular and disc parameters for both eyes. Statistically significant differences were found between right and left eye in mean RNFL thickness (median values of 102 $\mu$ m in OD and 104 $\mu$ m in OS,  $P=0.003$ ), superior quadrant RNFL thickness (125 $\mu$ m in OD and 130 $\mu$ m in OS,  $P=0.008$ ) and central macular thickness (183 $\mu$ m in OD and 200 $\mu$ m in OS,  $P=0.039$ ). No statistically significant differences were found between both eyes in the rest of retinal parameters under study. In both eyes, RNFL was thicker in the inferior quadrant, followed by the superior, nasal and temporal quadrants (ISNT). Inter-ocular differences in retinal parameters are shown in Table 3, which also displays the 95% limits of difference in terms of the 2.5<sup>th</sup> and 97.5<sup>th</sup> percentiles. It may be noted that disc parameters were very symmetrical, with a median difference of 0.025mm<sup>2</sup> in disc area, 0.04mm<sup>2</sup> in rim area and 0.02 in CDR.

**Table 2** Retinal parameters for right and left eye

Parameters	Mean	Median	Range	Z	P
Mean RNFL t OD ( $\mu$ m)	102.81	102.00	92.00, 122.00		
Mean RNFL t OS ( $\mu$ m)	104.51	104.00	91.00, 123.00	-2.959	0.003
SQ RNFL t OD ( $\mu$ m)	124.05	125.00	102.00, 146.00		
SQ RNFL t OS ( $\mu$ m)	128.40	130.00	105.00, 149.00	-2.658	0.008
IQ RNFL t OD ( $\mu$ m)	130.18	134.00	110.00, 163.00		
IQ RNFL t OS ( $\mu$ m)	132.75	135.00	108.00, 158.00	-1.528	0.126
NQ RNFL t OD ( $\mu$ m)	82.081	84.00	60.00, 108.00		
NQ RNFL t OS ( $\mu$ m)	82.72	80.00	60.00, 121.00	-0.340	0.734
TQ RNFL t OD ( $\mu$ m)	74.75	75.00	58.00, 87.00		
TQ RNFL t OS ( $\mu$ m)	74.21	73.00	60.00, 96.00	-0.961	0.337
Rim area OD (mm <sup>2</sup> )	1.88	1.89	1.18, 2.64		
Rim area OS (mm <sup>2</sup> )	1.92	1.93	1.25, 1.72	-0.664	0.507
Disc area OD (mm <sup>2</sup> )	2.45	2.49	1.68, 3.52		
Disc area OS (mm <sup>2</sup> )	2.48	2.47	0.12, 3.72	-1.430	0.153
CDR OD	0.22	0.21	0.05, 0.46		
CDR OS	0.24	0.24	0.02, 0.54	-1.318	0.187
Central macular t OD ( $\mu$ m)	194.73	183.00	169.00, 310.00		
Central macular t OS ( $\mu$ m)	200.03	200.00	171.00, 314.00	-2.067	0.039
Macular Vol OD (mm <sup>3</sup> )	7.75	7.72	7.17, 8.52		
Macular Vol OS (mm <sup>3</sup> )	7.75	7.75	7.17, 8.60	-0.574	0.566
Mean macular t OD ( $\mu$ m)	274.21	273.50	253.60, 301.40		
Mean macular t OS ( $\mu$ m)	274.35	274.20	253.50, 304.20	-0.558	0.577

Data is presented as mean, median and range (minimum, maximum values). The Wilcoxon test was used to assess inter-ocular differences (Z and P values are shown). RNFL: retinal nerve fiber layer; t: thickness; SQ: superior quadrant; IQ: inferior quadrant; NQ: nasal quadrant; TQ: temporal quadrant; CDR: cup-to-disc ratio; Vol: volume; OD: right eye; OS: left eye.

**Table 3 Inter-ocular difference in retinal parameters (right eye - left eye).**

Parameter differences (OD-OS)	Mean	Median	Range	2.5 <sup>th</sup> perc.	97.5 <sup>th</sup> perc.
Mean RNFL t ( $\mu\text{m}$ )	-1.70	-1.00	-9.00, 6.00	-9.00	6.00
SQ RNFL t ( $\mu\text{m}$ )	-4.35	-4.00	-28.00, 9.00	-28.00	9.00
IQ RNFL t ( $\mu\text{m}$ )	-2.56	-2.00	-25.00, 14.00	-25.00	14.00
NQ RNFL t ( $\mu\text{m}$ )	-0.64	-2.00	-20.00, 18.00	-20.00	18.00
TQ RNFL t ( $\mu\text{m}$ )	0.54	2.00	-13.00, 12.00	-13.00	12.00
Rim area ( $\text{mm}^2$ )	-0.04	-0.04	-1.01, 0.35	-1.01	0.35
Disc area ( $\text{mm}^2$ )	-0.03	-0.09	-1.20, 2.07	-1.20	2.07
CDR	-0.02	-0.02	-0.28, 0.12	-0.28	0.12
Central macular t ( $\mu\text{m}$ )	-5.30	-9.00	-81.00, 31.00	-39.00	29.00
Macular Vol ( $\text{mm}^3$ )	-0.00	0.00	-0.33, 0.46	-0.33	0.46
Mean macular t ( $\mu\text{m}$ )	-0.13	0.00	-11.80, 16.10	-11.80	16.10

Data is presented as mean, median and range (minimum, maximum values). Limits of difference are shown as the 2.5<sup>th</sup> and 97.5<sup>th</sup> percentiles. RNFL: retinal nerve fiber layer; t: thickness; SQ: superior quadrant; IQ: inferior quadrant; NQ: nasal quadrant; TQ: temporal quadrant; CDR: cup-to-disc ratio; Vol: volume; OD: right eye; OS: left eye.

**Age, Gender and Refractive Error** Statistically significant differences were found between males and females in mean RNFL thickness in the right eye (median of 106 $\mu\text{m}$  in males versus 99 $\mu\text{m}$  in females,  $P=0.020$ ), but not in the left eye.

Statistically significant, albeit weak correlations, were found between spherical equivalent and mean RNFL thickness ( $\rho=0.401$ ;  $P=0.014$  in OD and  $\rho=0.379$ ;  $P=0.021$  in OS), as well as between spherical equivalent and nasal ( $\rho=0.453$ ;  $P=0.005$  in OD and  $\rho=0.514$ ;  $P=0.001$  in OS) and inferior ( $\rho=0.352$ ;  $P=0.033$  in OD and  $\rho=0.421$ ;  $P=0.019$  in OS) RNFL thickness. Overall, however, age was not found to be correlated with neither mean RNFL thickness nor with spherical equivalent.

## DISCUSSION

The main objective of the present study was to determine the limits of normal retinal asymmetry (defined by the 2.5<sup>th</sup> and 97.5<sup>th</sup> percentiles from Table 3) in a sample of Caucasian children and young adults with a spectral-domain OCT. Retinal asymmetry is of relevance for the early detection of retinal conditions and for the study of myopia progression, which commonly manifests during adolescence and early adulthood<sup>[9,17]</sup>. Besides, by exploring asymmetry rather than absolute values, the influence of individual-specific factors such as age, gender or ethnicity on retinal parameters may be minimized. By the same reasoning, however, strict criteria need to be implemented to exclude from the study sample those patients with significant inter-ocular differences in refractive error and/or axial length. Indeed, Budenz *et al*<sup>[18]</sup> described a reduction in RNFL thickness of approximately 2.2  $\mu\text{m}$  (95% CI 1.1-3.4  $\mu\text{m}$ ) for each 1 mm increase in axial length or 0.9  $\mu\text{m}$  (95% CI 0.2-1.6  $\mu\text{m}$ ) for each 1D refractive error change towards greater myopia. Similarly, Park *et al*<sup>[12]</sup> disclosed weak, although statistically significant correlations between refractive error and mean, inferior and nasal quadrant RNFL thickness in both eyes, with increased thickness in hyperopic eyes. In addition, differences in axial length and/or refractive power may also influence actual measurements as a result of ocular magnification<sup>[15]</sup>. In the present study we opted to exclude patients with anisometropia  $\geq 0.5$  D or axial length differences larger than 0.3 mm and to examine eyes in a random order.

Overall, our measured absolute retinal parameter values are in agreement with those reported in previous studies, with small discrepancies accounting for the characteristics of each specific study population (age, ethnicity, etc.) and device employed for retinal exploration (time-domain OCT, spectral-domain OCT), as well as to the actual scan protocol (standard, fast, etc.) that was applied. In particular, in both eyes RNFL thickness follows the

documented ISNT rule, with the thickest and thinner values corresponding to the inferior and temporal quadrants, respectively<sup>[19]</sup>.

Statistically significant differences were found between the right and left eyes in mean and superior quadrant RNFL thickness, with larger thickness values in the left eye in both instances. Regarding mean RNFL thickness, these findings are in disagreement with previous reports in which either no significant inter-ocular difference was found<sup>[3,13-15]</sup> or the right eye was found to present thicker mean RNFL thickness values than the left<sup>[10-12]</sup>. It must be noted that our 2.5<sup>th</sup> and 97.5<sup>th</sup> percentiles of inter-ocular difference limits of -9.00  $\mu\text{m}$  and 6.00  $\mu\text{m}$  are lower than those reported in Caucasian children by Altemir *et al*<sup>[3]</sup> (-12.00 $\mu\text{m}$  and 13.00 $\mu\text{m}$ ) and Huynh *et al*<sup>[14]</sup> (-16.00 $\mu\text{m}$  and 17.00 $\mu\text{m}$ ), and in Korean adults by Park *et al*<sup>[12]</sup> (-19.11 $\mu\text{m}$  and 25.61 $\mu\text{m}$ ), although the latter two studies were conducted with an earlier OCT version. In contrast, our findings are comparable with those of Hong *et al*<sup>[15]</sup> (-8.14 $\mu\text{m}$  and 8.00 $\mu\text{m}$ ), in a sample of adults, also of Korean ethnicity. The narrow range in mean RNFL thickness which was found in the present sample of patients may be explained by our strict inclusion/exclusion criteria with reference to inter-ocular differences in refractive error and/or axial length. In effect, the importance of taking into consideration refractive error differences when assessing physiological asymmetry was evidenced by the statistical significant, albeit weak, correlation which was encountered between refractive error and mean RNFL thickness in both eyes.

Interestingly, statistically significant differences were encountered between males and females in mean RNFL thickness in the right eye. No clear consensus exists in the literature about the actual influence of age and gender on both absolute parameters and inter-ocular asymmetry. Thus, while some authors failed to observe any association between age and retinal parameters<sup>[13,20]</sup>, other authors reported a decrease of 2  $\mu\text{m}$  per decade in mean RNFL thickness<sup>[18]</sup>, resulting in increased inter-ocular asymmetry<sup>[11]</sup>. Similarly, Turk *et al*<sup>[21]</sup> described a statistically significant difference between boys and girls in RNFL in the inferior quadrant, although other authors failed to encounter any influence of gender on retinal parameters<sup>[13,18]</sup>. Therefore, given the aforementioned differences in study sample characteristics and measurement device, inconsistencies with the present investigation must be interpreted with caution.

Discrepancies were more manifest in the quadrant per quadrant RNFL thickness analysis of inter-ocular asymmetry, in which a statistically significant difference between right and left eyes was found in the superior quadrant, with 95% limits of tolerance of -28.00  $\mu\text{m}$  and 9  $\mu\text{m}$ . In effect, whereas previous authors also noted thicker RNFL values in the left eye in the superior quadrant<sup>[3,10,14,15]</sup>, the same authors described other quadrant asymmetries, with nasal and temporal quadrants in the right eye commonly presenting thicker RNFL values than in the left eye. On the contrary, our findings did not reveal significant inter-ocular differences in nasal, temporal and inferior quadrants.

In agreement with previous studies reporting good symmetry for mean macular thickness<sup>[16]</sup>, no statistically significant inter-ocular difference was found in this parameter. In contrast, central macular thickness was found to present with statistically significant inter-ocular differences, with larger values in the left eye and 95% tolerance limits at -39.00  $\mu\text{m}$  and 29.00  $\mu\text{m}$ . Both Altemir *et al*<sup>[3]</sup> and Huynh *et al*<sup>[14]</sup> failed to report significant differences in central macular thickness, although their 95% tolerance limits were not dissimilar to those found in the present research, with values of -17.60  $\mu\text{m}$  and 23.20  $\mu\text{m}$  and of -22.00  $\mu\text{m}$  and 22.00  $\mu\text{m}$ , respectively. It is worth mentioning, to approximate an explanation for this discrepancy, that macular thickness and volume are also highly sensitive to ethnicity, both in adults and in children<sup>[22]</sup>.

Finally, as expected in the light of published reports<sup>[14]</sup>, a high level of symmetry was observed for disc parameters, particularly for CDR, with a median non-statistically significant inter-ocular difference of 0.02 and 95% limits of tolerance of -0.28 and 0.12.

Previous research has noted an association between inter-ocular asymmetry of retinal parameters and changes in retinal and choroidal vasculature morphometry. However, authors also advice that “setting reliable criteria by which to judge the symmetry of the retinal vasculature is challenging” and that there is a lack of detailed knowledge of properties of the

retinal vasculature such as specific path and shape of individual vessels, location of bifurcations and junctions, vessel tortuosity and width, branching angles and geometry, etc. (see, for instance, Cameron *et al*<sup>[231]</sup>).

It must be acknowledged that one of the main limitations of the present study is the size of the sample and the slightly larger percentage of females than males in our group of participants. In consequence, caution is advised in the interpretation of the results, with further research being required to verify our findings. In particular, it may not be ruled out that the encountered differences between males and females originate in the uneven distribution of our sample in terms of gender. Besides, even though no correlation was evidenced between age and retinal parameters, it must be noted that the large age range under study may partially account for the considerable variance encountered in some of the variables under evaluation.

In conclusion, the present findings had a twofold relevance. On the one hand, they agree with published literature in stressing the need to acquire physiological asymmetry data from different populations and with different measurement devices to build a complete description of normality. On the other hand, they give support to the importance of further exploring such retinal parameters as CDR in which age, gender, ethnicity and other study sample characteristics are not so critical in order to consider them as anchor features to better reflect and understand changes occurring in other areas of the retina.

## REFERENCES

1. Gabriele ML, Wollstein G, Ishikawa H, Kagemann L, Xu J, Folio LS, Schuman JS. Optical Coherence tomography: history, current status, and laboratory work. *Invest Ophthalmol Vis Sci* 2011;52(5):2425-2436
2. Regatieri CV, Branchini L, Fujimoto JG, Duker JS. Choroidal imaging using spectral-domain optical coherence tomography. *Retina* 2012;32(5):865-876.
3. Altemir I, Oros D, Elía N, Polo V, Larrosa JM, Pueyo V. Retinal asymmetry in children measured with optical coherence tomography. *Am J Ophthalmol* 2013;156(6):1238–1243.
4. Chan A, Duker JS, Ko TH, Fujimoto JG, Schuman JS. Normal macular thickness measurements in healthy eyes using Stratus optical coherence tomography. *Arch Ophthalmol* 2006;124(2):193–198.
5. Jaffe GJ, Caprioli J. Optical coherence tomography to detect and manage retinal disease and glaucoma. *Am J Ophthalmol* 2004;137(1):156–169.
6. Van Velthoven ME, Faber DJ, Verbraak FD, van Leeuwen TG, de Smet MD. Recent developments in optical coherence tomography for imaging the retina. *Prog Retin Eye Res* 2007;26(1):57–77.
7. Yamada H, Hangai M, Nakano N, Takayama K, Kimura Y, Miyake M, Akagi T, Ikeda HQ, Noma H, Yoshimura N. Asymmetry analysis of macular inner retinal layers for glaucoma diagnosis. *Am J Ophthalmol* 2014;158(6):1318-1329.
8. Pagliara MM, Lepore D, Balestrazzi E. The role of OCT in glaucoma management. *Prog Brain Res* 2008;173(1):139–148.
9. Luo HD, Gazzard G, Fong A, Aung T, Hoh ST, Loon SC, Healey P, Tan DT, Wong TY, Saw SM. Myopia, axial length, and OCT characteristics of the macula in Singaporean children. *Invest Ophthalmol Vis Sci* 2006;47(7):2773-2781.
10. Mwanza JC, Durbin MK, Budenz DL, Cirrus OCT Normative Database Study Group. Interocular symmetry in peripapillary retinal nerve fiber layer thickness measured with the Cirrus HD-OCT in healthy eyes. *Am J Ophthalmol* 2011;151(3):514–521.
11. Budenz DL. Symmetry between the right and left eyes of the normal retinal nerve fiber layer measured with optical coherence tomography (an AOS thesis). *Trans Am Ophthalmol Soc* 2008;106(1):252–275.
12. Park JJ, Oh DR, Hong SP, Lee KW. Asymmetry analysis of the retinal nerve fiber layer thickness in normal eyes using optical coherence tomography. *Korean J Ophthalmol* 2005;19(4):281–287.
13. Larsson E, Eriksson U, Alm A. Retinal nerve fibre layer thickness in full-term children assessed with Heidelberg retinal tomography and optical coherence tomography: normal values and interocular asymmetry. *Acta Ophthalmol (Copenh)* 2011;89(2):151–158.

14. Huynh SC, Wang XY, Burlutsky G, Mitchell P. Symmetry of optical coherence tomography retinal measurements in young children. *Am J Ophthalmol* 2007;143(3):518–520.
15. Hong SW, Lee SB, Jee DH, Ahn MD. Interocular retinal nerve fibre layer thickness difference in normal adults. *PLoS ONE* 2015 Feb 13;10(2):e0116313
16. Sullivan-Mee M, Ruegg CC, Pensyl D, Halverson K, Qualls C. Diagnostic precision of retinal nerve fiber layer and macular thickness asymmetry parameters for identifying early primary open-angle glaucoma. *Am J Ophthalmol* 2013;156(3):567–577.
17. Pärssinen O, Kauppinen M, Viljanen A. The progression of myopia from its onset at age 8-12 to adulthood and the influence of heredity and external factors on myopic progression. A 23-year follow-up study. *Acta Ophthalmol* 2014;92(8):730-739.
18. Budenz DL, Anderson DR, Varma R, Schuman J, Cantor L, Savell J, Greenfield DS, Patella VM, Quigley HA, Tielsch J. Determinants of normal retinal fiber layer thickness measured by Stratus OCT. *Ophthalmology* 2007;114(6):1046-1052.
19. Dave P, Shah J. Applicability of ISNT and IST rules to the retinal nerve fibre layer using spectral domain optical coherence tomography in early glaucoma. *Br J Ophthalmol* 2015;99(12):1713-1717.
20. Salchow DJ, Oleynikov YS, Chiang MF, Kennedy-Salchow SE, Langton K, Tsai JC, Al-Aswad LA. Retinal nerve fibre layer thickness in normal children measured with optical coherence tomography. *Ophthalmology* 2006;113(5):786-791.
21. Turk A, Ceylan OM, Arici C, Keskin S, Erdurman C, Durukan AH, Mutlu FM, Altinsoy HI. Evaluation of the nerve fiber layer and macula in the eyes of healthy children using spectral-domain optical coherence tomography. *Am J Ophthalmol* 2012;153 (3):552–559.
22. El-Dairi MA, Asrani SG, Enyedi LB, Freedman SF. Optical coherence tomography in the eyes of normal children. *Arch Ophthalmol* 2009;127(1):50-58.
23. Cameron JR, Megaw RD, Tatham AJ, McGrory S, MacGillivray TJ, Doubal FN, Wardlaw JM, Trucco E, Chandran S, Dhillon B. Lateral thinking – Interocular symmetry and asymmetry in neurovascular patterning, in health and disease. *Prog Retin Eye Res* 2017;59:131-157.

## Annex IV. ARVO Annual Meeting, Baltimore, USA, 2017

Program Number: 2749 Poster Board Number: A0453

Presentation Time: 8:30 AM–10:15 AM

**Retinal sensitivity asymmetry in high myopia and its correlation with refractive error**

Zeyad A. A. ALzaben<sup>1</sup>, Genis Cardona<sup>1</sup>, Miguel A. Zapata<sup>2</sup>, Ahmad Zaben<sup>3</sup>, Dana N. Koff<sup>4</sup>. <sup>1</sup>Department of Optics and Optometry, Technical University of Catalonia, Olot, Spain; <sup>2</sup>Ophthalmology, Valle de Hebrón Hospital, Barcelona, Spain; <sup>3</sup>Optometry, Optipunt Eye Clinic, Figueres, Spain; <sup>4</sup>Allied Medical Sciences, Jordan University of Science and Technology, Irbid, Jordan.

**Purpose:** High myopia (over -6 D) is characterized with anatomical and functional changes in the retina and choroid. We aimed at examining the normal range of inter-ocular asymmetry in retinal sensitivity and its association with refractive error.

**Methods:** The MAIA microperimeter (Macular Analyzer Integrity Assessment, CenterVue, Padova, Italy) was employed to determine retinal sensitivity in a sample of patients with high myopia without ocular complications (n=43; 15 females; mean age of 35.07 ± 13.31 years) and to compare these results with those of an age-matched control group of healthy subjects (n=45; 23 females; mean age of 39.9 ± 14.1 years). Both in the myopia and control group, no statistically significant inter-ocular differences were found in spherical equivalent and distance corrected visual acuity.

**Results:** A summary of the absolute inter-ocular differences in retinal sensitivity in the myopic and healthy groups is shown in Figure 1. Overall, inter-ocular differences were larger in the myopic group than in the control group, although statistically significant differences were only encountered at the central location (p = 0.001). Statistically significant moderate negative correlations were found between refractive error and absolute inter-ocular differences in retinal sensitivity at most of the locations under examination (Figure 2), particularly towards the center of the retina, that is, retinal sensitivity asymmetry increased with refractive error.

**Conclusions:** Highly-myopic eyes, even in the absence of complications, display a different range of inter-ocular asymmetry than normal eyes, and this asymmetry increases with refractive error. This finding is of relevance for the correct and early diagnosis of unilateral pathological conditions associated with high myopia.

Absolute inter-ocular difference in retinal sensitivity (dB)	CONTROL GROUP			MYOPIA GROUP			p		
	Mean	SD	95% CI	Mean	SD	95% CI			
Central	0.34	2.67	-4.89	5.57	1.21	3.51	-5.67	8.09	0.001
1 mm N	0.74	1.94	-3.06	4.54	1.55	3.23	-4.78	7.88	0.790
1 mm T	0.41	1.84	-3.20	4.02	1.55	3.74	-5.78	8.88	0.099
1 mm S	0.57	1.97	-3.29	4.43	0.49	2.87	-5.14	6.12	0.215
1 mm I	0.36	2.11	-3.78	4.50	1.14	3.41	-5.54	7.82	0.142
2 mm N	0.47	1.77	-3.00	3.94	1.47	3.32	-5.04	7.98	0.319
2 mm T	0.44	1.6	-2.70	3.58	1.03	2.23	-3.34	5.40	0.371
2 mm S	0.97	1.82	-2.60	4.54	0.34	2.63	-4.81	5.49	0.853
2 mm I	0.62	1.84	-2.99	4.23	0.78	2.15	-3.43	4.99	0.499
3 mm N	0.87	1.53	-2.13	3.87	1.23	2.03	-2.75	5.21	0.468
3 mm T	0.2	1.87	-3.47	3.87	0.63	2.02	-3.33	4.59	0.482
3 mm S	0.98	1.76	-2.47	4.43	0.05	1.88	-3.63	3.73	0.687
3 mm I	0.71	1.47	-2.17	3.59	0.52	2.06	-3.52	4.56	0.960
Mean of 1 mm ring	0.52	1.5	-2.42	3.46	1.26	2.91	-4.44	6.96	0.244
Mean of 2 mm ring	0.51	1.43	-2.29	3.31	0.89	1.6	-2.25	4.03	0.441
Mean of 3 mm ring	0.76	1.34	-1.87	3.39	0.74	1.57	-2.34	3.82	0.850
Overall mean	0.6	1.26	-1.87	3.07	0.81	2.15	-3.40	5.02	0.578

Absolute inter-ocular differences in retinal sensitivity in mean ± SD (95% CI) at each of the locations and quadrants under examination (N: Nasal; T: Temporal; S: Superior; I: Inferior) for the myopia and control groups.

## ARVO 2017 Annual Meeting Abstracts

Absolute inter-ocular difference in retinal sensitivity (dB)	r	p
Central	-0.345	0.018
1 mm N	-0.578	<0.001
1 mm T	-0.738	<0.001
1 mm S	-0.228	0.123
1 mm I	-0.491	<0.001
2 mm N	-0.633	<0.001
2 mm T	-0.413	0.004
2 mm S	-0.501	<0.001
2 mm I	0.002	0.989
3 mm N	-0.120	0.423
3 mm T	-0.074	0.619
3 mm S	0.144	0.334
3 mm I	-0.285	0.052
Mean of 1 mm ring	-0.545	<0.001
Mean of 2 mm ring	-0.226	0.127
Mean of 3 mm ring	-0.079	0.600
Overall mean	-0.304	0.038

Correlation analysis of the association between mean refractive error and absolute inter-ocular differences in retinal sensitivity in the myopic group.

Commercial Relationships: Zeyad A. A. ALzaben; Genis Cardona, None; Miguel A. Zapata, None; Ahmad Zaben, None; Dana N. Koff, None

conferenceseries.com

## 6<sup>th</sup> Global Ophthalmologists Annual Meeting

May 16-18, 2016 Osaka, Japan

---

### The choroidal profile in a sample of young Caucasian affected by myopia

Ahmad Zaben<sup>1</sup>, Zeyad A Alzaben<sup>2</sup>, Miguel A Zapata<sup>3</sup>, Genis Cardona<sup>2</sup>, Miguel José Maldonado López<sup>4</sup> and Dana N Koff<sup>5</sup>

<sup>1</sup>Optipunt Eye clinic, Spain

<sup>2</sup>Technical University of Catalonia, Spain

<sup>3</sup>Vall d'Hebron Hospital, Spain

<sup>4</sup>Instituto Oftalmobiología Aplicada, Spain

<sup>5</sup>Jordan University of Science & Technology, Jordan

**Purpose:** To investigate the morphological characteristics of highly myopic eyes through analysing the macular choroidal thickness with respect to the axial length.

**Methods:** A cross-sectional study of patients with high myopia was performed in which the axial length in all patients was measured using Biometry (interferometry laser), and the macular area choroidal thickness was measured using optical coherence tomography. The correlation between the two measurements was analysed.

**Results:** A total of 281 eyes with pathological myopia were included, with a spherical equivalent between -6.00 and -21.00 diopters with an average of  $9.41 \pm 1.722$  SD, and average age was  $43.43 \pm 13.59$  years. The average central choroidal thickness was  $138.00 \pm 40.78$   $\mu$ m. The choroidal thickness was directly correlated with visual acuity ( $r = 0.327$ ,  $p = 0.001$ ) and significantly inversely correlated with axial length ( $r = -0.236$ ,  $p = 0.025$ ), sphere value ( $r = -0.469$ ;  $p < 0.001$ ) and age ( $r = -0.426$ ;  $p < 0.001$ ).

**Conclusions:** The macular choroidal thickness is significantly reduced in patients with pathological myopia, and its value depends on location, spherical equivalent, and age. The axial length in highly near-sighted individuals is inversely correlated with the choroidal thickness. The choroidal thickness in highly near-sighted patients can provide important information on this pathology, as it is highly correlated with functional parameters, age, and spherical equivalent.

#### Biography

Ahmad Zaben received his Bachelor's degree in Optometry (1989) at Universitat Politècnica de Catalunya (UPC), and the first MSc degree in Science of Vision and Optometry (2002) at the Universitat Politècnica de Catalunya (UPC), and the second MSc degree in Visual Rehabilitation (2012) at Universidad de Valladolid (UVA) / Medicine Faculty, and a PhD degree in Science of Vision and Optometry (2015) at Universidad Europea de Madrid. He is currently employed as full-time optometrist at the Department of Low Vision of Optipunt Eye Clinic and a general administrator. He attended a Corporate Program for Management Development/Advanced Program for Optics Management in ESADE Business School in Barcelona (2011).



**conferenceseries.com**

# 6<sup>th</sup> Global Ophthalmologists Annual Meeting

May 16-18, 2016 Osaka, Japan

## Functional asymmetry in macular area in patients with pathological myopia using microperimetry

Zeyad A Alzaben<sup>1</sup>, Genis Cardona<sup>1</sup>, Miguel A Zapata<sup>2</sup>, Ahmad Zaben<sup>3</sup>, Miguel José Maldonado López<sup>4</sup> and Dana N Koff<sup>5</sup>

<sup>1</sup>Technical University of Catalonia, Spain

<sup>2</sup>Vall d'Hebron Hospital, Spain

<sup>3</sup>Optipunt Eye clinic, Spain

<sup>4</sup>Instituto Oftalmobiología Aplicada, Spain

<sup>5</sup>Jordan University of Science & Technology, Jordan

**Introduction:** Microperimetry is a clinical innovation to evaluate the retinal sensitivity. In this study, we explored the inter-ocular retinal variations of retinal sensitivity in the macular area in patients with pathological myopia.

**Methods:** A transversal study was designed in which the macular sensitivity (Expert exam protocol) of MAIATM microperimeter was employed to evaluate the functional variations of 10° in macular areas in patients affected by pathological myopia using 37 points strategy, in a sample of 36 persons aged between 13 and 60 years (spherical equivalent from -6.00 to -16.00 diopters). Inter-ocular asymmetry values were determined and compared with previous published tolerance values by means of a paired t test, and the interocular differences were calculated as the 2.5th and the 97.5th percentiles.

**Results:** The interocular difference tolerance limits for central sensitivity of the macula was 7.28 dB in patients affected by pathological myopia. Statically significant differences were found between males and females in the asymmetry of the central ring and the second ring of retinal sensitivity (SC and S2). There was a significant positive correlation between the retinal sensitivity and the spherical equivalent, and a weak correlation between the retinal sensitivity and the fixation level. Also we encountered significant positive correlation in retinal sensitivity between the central ring and the third ring (SC and S3).

**Conclusions:** A general reduction in the central retinal sensitivity in eyes with pathological myopia is expected to be more marked with increasing ametropia. Considering inter-ocular asymmetry in central retinal sensitivity should help understand better the retinal features of patients with pathological myopia, for which establishing normative percentile values should prove a useful tool.

### Biography

Zeyad A Alzaben received his Bachelor's degree in Optometry (2013) at the Jordan University of Science & Technology (JUST), and the first MSc degree in Science of Vision and Optometry (2014) at the Universitat Politècnica de Catalunya (UPC), and the second MSc degree in Visual Rehabilitation (2014) at Universida de Valladolid (Uva) / Medicine Faculty, and he is a PhD candidate in Optical Engineering doctoral program (2014-2016) at Universitat Politècnica de Catalunya (UPC). He is currently employed as full-time optometrist at the Department of Low Vision of Optipunt Eye Clinic. He has conducted two new researches about normal patients and patients affected by pathological myopia using OCT and MAIA microperimeter, waiting for the acceptance letters to be published. He is a student of Corporate Program for Management Development/Advanced Program for Optics Management in ESADE Business School in Barcelona (2014-2017).

conferenceseries.com

# 6<sup>th</sup> Global Ophthalmologists Annual Meeting

May 16-18, 2016 Osaka, Japan

## Inter-ocular asymmetry of retinal parameters as measured with Ocular Coherence Tomography (OCT) in a sample of healthy young adults

Zeyad A Alzaben<sup>1</sup>, Genis Cardona<sup>1</sup>, Miguel A Zapata<sup>2</sup>, Ahmad Zaben<sup>3</sup>, Miguel José Maldonado López and Dana N Koff<sup>4</sup>

<sup>1</sup>Technical University of Catalonia, Spain

<sup>2</sup>Vall d'Hebron Hospital, Spain

<sup>3</sup>Optipunt Eye Clinic, Figueres, Spain

<sup>4</sup>Instituto Oftalmobiología Aplicada, Spain

<sup>5</sup>Jordan University of Science & Technology, Jordan

Optical coherence tomography (OCT) is a useful non-invasive technique to assess the retina without the need for pupil dilation. In particular, the macular and optic disc areas may be explored in detail and with a high level of spatial resolution. A transversal study was designed in which a spectral-domain 3D-OCT-2000 was employed to evaluate several retinal parameters in a sample of 37 young Caucasian adults aged between 12 and 23 years (spherical equivalent from -3.00 to +4.00 D). Normal inter-ocular asymmetry values were determined and 95% inter-ocular difference tolerance values were obtained. Inter-ocular statistically significant differences were uncovered in mean and superior RNFL thickness, as well as in central macular thickness, with larger values in the left eye in all instances, and with tolerance limits of inter-ocular asymmetry (2.5th and 97.5th percentiles) of -9.00  $\mu\text{m}$  to 6.00  $\mu\text{m}$ , -28.00  $\mu\text{m}$  to 9  $\mu\text{m}$  and -39.00  $\mu\text{m}$  to 29.00  $\mu\text{m}$ , respectively. In addition, statically significant differences were found between males and females in mean thickness of the retinal nerve fiber layer (RNFL) in the right eye. These findings give support to the exploration of the normal asymmetries of the retina as an effective approach for an early detection of pathologies such as glaucoma. Differences in instrumentation and sample characteristics compromise direct comparison with published research and warrant the need for further studies.

### Biography

Zeyad A Alzaben received his Bachelor degree in Optometry (2013) at the Jordan University of Science & Technology (JUST), and the first MSc degree in Science of Vision and Optometry (2014) at the Universitat Politècnica de Catalunya (UPC), and the second MSc degree in Visual Rehabilitation (2014) at Universida de Valladolid (UVA) / Medicine Faculty. He is a PhD candidate in Optical Engineering doctoral program (2014-2016) at Universitat Politècnica de Catalunya (UPC). He is currently employed as full-time optometrist at the Department of Low Vision of Optipunt Eye Clinic ([www.optipunt.com](http://www.optipunt.com)). He has conducted two new researches about normal patients and patients affected by pathological myopia using OCT and MAIA microperimeter, waiting the acceptance letters to be published. He is a student of Corporate Program for Management Development / Advanced Program for Optics Management in ESADE Bussines School in Barcelona (2014-2017). His aim is to utilise his skills to improve his experiences and keep learning more with respect to the challenges about using his valuable assessments.

**Annex VI. 24 Congreso Internacional de Optometría, Contactología y Óptica Oftálmica, Madrid, 2016**



COMUNICACIONES EN PÓSTER

EXPOSITOR N° 44

INVESTIGACIÓN BÁSICA ID:513

► **Asimetría funcional en área macular en pacientes con miopía patológica usando microperimetría.**

**AUTORES:**

Zeyad A. Alzaben<sup>1</sup>, Genís Cardona Torradeflot<sup>2</sup>, Miguel A. Zapata Victor<sup>3</sup>, Ahmad Zaben Omran<sup>4</sup>, Miguel José Maldonado López<sup>5</sup>, Dana N. Koff<sup>6</sup>

<sup>1</sup>Departamento de Optometría, Facultat d'Òptica i Optometria de Terrassa. <sup>2</sup>Departamento de Oftalmología, Hospital de la Vall d'Hebron, Barcelona. <sup>3</sup>Centro Optométrico Optipunt, Figueras. <sup>4</sup>Departamento de Oftalmología, Instituto Oftalmobiología Aplicada (IOBA), Valladolid. <sup>5</sup>Allied Departamento de Ciencias Médicas, Universidad Jordana de Ciencia y Tecnología, Irbid - Jordania

compararon por medio de una prueba t pareada. Además, para establecer los límites de la normalidad, se calcularon las distribuciones porcentuales de las diferencias entre los ojos derecho e izquierdo para los percentiles 2.5% y 97.5%.

**RESULTADOS**

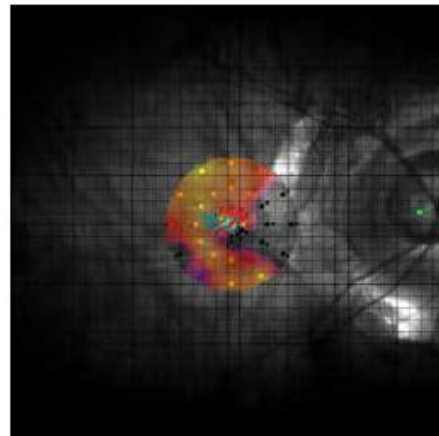
El límite de tolerancia de la diferencia de sensibilidad central de la mácula entre los ojos derechos e izquierdos fue de 7.28 dB en pacientes afectados por miopía patológica. Se encontraron diferencias estadísticamente significativas entre hombres y mujeres, así como asimetría de la sensibilidad retiniana en el anillo central y en el segundo anillo.

**INTRODUCCIÓN**

La microperimetría es una innovación clínica para evaluar la sensibilidad de la retina. En este estudio, se evaluaron las diferencias en la sensibilidad de la retina en el área macular entre ambos ojos en pacientes con miopía patológica. La sensibilidad de la retina en los pacientes con miopía patológica nos puede aportar una mayor información sobre la patología, ya que se correlaciona en mayor medida con parámetros funcionales, con la edad y con el valor esférico de los pacientes.

**MÉTODOS**

Se diseñó un estudio transversal para evaluar la sensibilidad de la retina. En todos los pacientes se midió la sensibilidad retiniana mediante microperimetría MAIA™, utilizando en todos los casos el examen expert test y con una estrategia de 37 puntos dentro de los 10 grados centrales. Se examinó la asimetría inter-ocular funcional en áreas maculares en pacientes con miopía patológica, en una muestra de 36 personas con edades comprendidas entre 13 y 60 años y equivalente esférico entre -6.00 y 16.00 D. Se determinaron los valores de asimetría inter-oculares y se





## COMUNICACIONES EN PÓSTER



Optom  
2016


Existe una correlación negativa significativa entre la sensibilidad de la retina y el equivalente esférico ( $r = -0.50$ ;  $p < 0.001$ ). También encontramos correlación significativa, si bien débil, en la sensibilidad retiniana entre la región central y el tercer anillo ( $r = -0.29$ ;  $p = < 0.012$ ).

### CONCLUSIONES

Hay una reducción general en la sensibilidad retiniana en miopía patológica. En el estudio de las asimetrías entre am-

bos ojos se deben tener en cuenta los valores de los percentiles de la sensibilidad para comprender mejor los límites de normalidad y las características clínicas de la retina en pacientes con miopía patológica.

\*Los autores no tienen ningún interés financiero en este poster





## COMUNICACIONES EN PÓSTER

EXPOSITOR Nº 47

INVESTIGACIÓN BÁSICA ID:571

### ► Variación del espesor de la coroides con la longitud axial en la población caucásica con alta miopía.

#### AUTORES:

Zeyad A. Alzaben<sup>1</sup>, Genís Cardona Torradeflot<sup>1</sup>, Ahmad Zaben<sup>2</sup>, Miguel A. Zapata Victori<sup>3</sup>, Dana N. Koff<sup>4</sup>

<sup>1</sup>Departamento de Óptica y Optometría, Facultat d'Òptica i Optometria de Terrassa. <sup>2</sup>Centro Optomètric Optipunt, Figueras. <sup>3</sup>Departamento de Oftalmología, Hospital de la Vall d'Hebron, Barcelona.

<sup>4</sup>Allied Departamento de Ciencias Médicas, Universidad Jordana de Ciencia y Tecnología, Irbid - Jordania.

#### OBJETIVO

Investigar las características morfológicas de los ojos con miopía alta mediante el análisis del espesor de la coroides en el área macular y explorar la posible relación de este parámetro con la longitud axial del ojo.

#### MÉTODOS

Se diseñó un estudio transversal en pacientes con alta miopía. En todos ellos se midió la longitud axial mediante biometría de interferometría láser y el espesor coroides en el área macular mediante tomografía de coherencia óptica (OCT). Se analizó la correlación entre ambos parámetros, así como entre el espesor de la coroides y la edad, agudeza visual y refracción esférica.

#### RESULTADOS

Se incluyeron 281 ojos con miopía patológica con edad media  $\pm$  SD de  $43.43 \pm 13.59$  años. El equivalente esférico se centró en un intervalo de  $-6.00$  D a  $-20.00$  D, con una media  $\pm$  SD de  $-8.74 \pm 2.73$  D. La media  $\pm$  SD del espesor central de la coroides fue de  $138.00 \pm 40.78$   $\mu$ m. Se halló una correlación débil pero estadísticamente significativa entre el grosor de la coroides y la agudeza visual ( $r = 0.327$ ;  $p = 0.001$ ), así como correlaciones inversas entre el grosor de la coroides y el valor de la esfera ( $r = -0.249$ ;  $p < 0.001$ ) y la edad ( $r = -0.469$ ;  $p < 0.001$ ). No se halló correlación entre el grosor de la coroides y la longitud axial ( $r = -0.163$ ;  $p = 0.006$ ).

#### CONCLUSIONES

El espesor de la coroides en el área macular se reduce significativamente en pacientes con miopía patológica y su valor depende del punto exacto de medida, el valor esférico y la edad. El grosor coroides en los pacientes altos miopes puede aportar una mayor información sobre la patología ya que se correlaciona en mayor medida con parámetros funcionales, con la edad y con el valor de refracción esférica de los pacientes.

\*Los autores no tienen ningún interés financiero en este póster.





